THE UNIVERSITY OF SYDNEY

Developing Translational Tissue Engineering Solutions for Regenerative Medicine

Richard P. Tan

A thesis submitted in fulfilment of the requirements for the degree of Doctor of Philosophy

Faculty of Medicine

University of Sydney

February 12 2019

Abstract

Regenerative medicine is an emerging field that aims to treat injury and disease by harnessing and augmenting the body's innate capacity for tissue regeneration. Many of the strategies developed in this field have relied extensively on the principles of tissue engineering, a set of methods that bring together cells, cellular signals and material scaffolds to repair or replace biological tissue. While the number of novel tissue engineering strategies continues to rapidly expand, the innovations underlying these solutions often fail to consider the key technical, manufacturing, and regulatory barriers that prohibit these technologies from suitable use in humans. As a result, the field of tissue engineering has one of the lowest rates of clinical translation amongst medical research. To address this, this thesis examines each of the prominent components of the tissue engineering practice and develops tools and strategies that enable the development of solutions with high translational potential.

First, using well characterised electrospun polycaprolactone (PCL) scaffolds as an exemplar material, we develop a novel imaging method that allows monitoring of scaffold performance non-invasively and in real-time. Based on bioluminescence imaging, this tool allows us to determine how injected stem cell populations interact with scaffolds after they have been implanted, while also providing an assessment of the functional regenerative outcomes. These findings provide an advantageous new tool for the tissue engineering community that eliminates current trial-and-error methodology, with potential to drastically improve the time and cost constraints of current scaffold design and innovation.

Secondly, using these imaging modalities, we examine some of the unknown effects of novel stem cell sources. Tracking the engraftment behaviour of induced-pluripotent stem cell derived endothelial cells (iPSC-ECs), we demonstrate for the first time that this stem cell phenotype possesses therapeutically relevant tissue regenerative properties, and the extent of these functions are associated with their engraftment behaviour. These findings add fundamental knowledge to the understanding

of iPSCs by highlighting the tissue regenerative capacity of iPSC-ECs, with broader implications for advancing the field of iPSC biology by potentially spurring the investigation of other iPSC lineages for tissue regenerative potential.

Thirdly, to enhance the translation of iPSC-EC therapy as a clinically relevant regenerative medicine approach, we combined them with tissue engineered scaffolds. We fabricated an array of electrospun PCL composite scaffolds containing gelatin blends, and using bioluminescence imaging, to rapidly identify a candidate scaffold which extends iPSC-EC engraftment and function *in vivo*. The findings of this study demonstrate a novel tissue engineering construct capable of tissue revascularisation, demonstrating one of the fundamental mechanisms of tissue regeneration as well as overcoming one the largest challenges of translating tissue engineering solutions.

Lastly, we further emphasize the theme of translation by investigating acellular PCL scaffolds and biofunctionalisation. For the first time, we examine the time and cost-effective plasma surface activation treatment on PCL scaffolds by immobilising the M2 macrophage polarising cytokine IL-4. In this study we show that bioactive coatings of immobilised IL-4 significantly limited the foreign body response and improved the functional performance of implanted scaffolds including vascular grafts. The findings of this study demonstrate a novel off-the-shelf functionalisation method that improves host integration of acellular scaffolds by harnessing the inflammatory influence of macrophage polarisation. These bioactive coatings may have potential applications on a wide range of polymer-based tissue engineering scaffolds, improving both their long-term performance, integration, and clinical translational.

The collective findings of these works propose tools and solutions applicable within the major facets of tissue engineering that may help to lay the groundwork for future therapies with high clinical probability in a number of regenerative medicine applications.

Thesis Presentation

This thesis is presented as 4 published/submitted research manuscripts. Each manuscript describes the methods, results and discussion of the four major projects undertaken in this PhD candidature. Chapter 1 provides a general introduction to the field of regenerative medicine, tissue engineering and the challenges the lay in the path towards clinically translatable therapy, addressed by the main thesis chapters/research articles in Chapters 2-5 where the candidate is the principal author. A general discussion and conclusion about the findings and broader implications of these articles to the field is presented in Chapter 6

Author Contribution Statement

Chapters 2-5 of this thesis were published or submitted for publication as:

Chapter 2: **Tan, R.P.**, Lee, B.S.L., Chan, A.H.P., Yuen, S-C.G., Jin, K., Hung, J., Wise, S.G., Ng, M. K. C. Non-invasive tracking of injected bone marrow mononuclear cells to injury and implanted biomaterials. *Acta Biomaterialia* 53, 378-388 (2017)

Chapter 3: Clayton, Z.E.*, **Tan R.P.*,** Miravet, M.M., Lennartsson, K., Wise, S.G., Patel, S. Induced pluripotent stem cell-derived endothelial cells promote angiogenesis and accelerate wound closure in a murine excisional wound healing model. *Bioscience Reports* (2018) DOI: 10.1042/BSR20180563

***Co-first authors**

Chapter 4: **Tan, R.P.**, Chan, A.H.P., Lee, B.S.L., Ng, M. K. C., Wise, S.G. Integration of induced pluripotent stem cell derived endothelial cells with polycaprolactone/gelatin-based electrospun scaffolds for enhanced therapeutic angiogenesis. *Stem Cell Therapy & Review* 9:70-85 (2018).

Chapter 5: **Tan, R.P.**, Chan, A.H.P., Santos, M., Wei, S., Lee, B.S.L., Filipe, E., Akhavan, B., Xiao, Y., Bilek, M.M., Ng, M.K.C., Wise, S.G. Bioactive Materials Facilitating Targeted Local Modulation of Inflammation. *JACC: Basic to Translational Science*, Under Review

For all publications I designed the study, acquired, analysed and interpreted the data.

Richard Tan

As supervisor for the candidature upon which this thesis is based, I can confirm that the authorship attribution statements above are correct.

Dr. Steven Wise

Full List of Publications Arising During PhD Candidature

1. **Tan, R.P.**, Tong, J., Kosobrodova, E., Bilek, M.M.M., Wise, S.G., Thorn, P.J., Bioactive Encapsulation Device for Beta Cells Transplantation, *Biomaterials*, Submitted.

2. **Tan, R.P.**, Chan, A.H.P., Santos, M., Filipe, E., Lee, B.S.L., Hung, J., Ng, M. K. C., Wise, S.G. Bioactive Materials Facilitating Targeted Local Modulation of Inflammation. *JACC: Basic to Translational Science*, Under Review.

3. Clayton, Z.E.*, **Tan, R.P.***, Miravet, M.M., Lennartsson, K., Wise, S.G., Patel, S. Induced pluripotent stem cell-derived endothelial cells promote angiogenesis and accelerate wound closure in a murine excisional wound healing model. *Bioscience Reports* (2018). DOI: 10.1042/BSR20180563

4. **Tan, R.P.**, Chan, A.H.P., Lee, B.S.L., Ng, M. K. C., Wise, S.G. Integration of induced pluripotent stem cell derived endothelial cells with polycaprolactone/gelatin-based electrospun scaffolds for enhanced therapeutic angiogenesis. *Stem Cell Research & Therapy* 9:70-85 (2018).

5. Santos, M., Michael, P., Filipe, E., Chan, A., Hung, J., **Tan R.P.**, et. al. Plasma Synthesis of Carbon-Based Nanocarriers for Linker-Free Immobilization of Bioactive Cargo. *ACS Applied Nano Materials* 1(2): 580-594 (2018).

6. Santos, M., Waterhouse, A., Lee, B.S.L., Chan, A.H.P., **Tan, R. P.,** et. al. Simple one-step immobilisation of bioactive agents without use of chemicals on plasma activated low thrombogenic stent coatings. Wall, J. Gerard. In Functionalised Cardiovascular Stents, Podbielska, H.; Wawrzyńska, M., Eds. Woodhead Publishing: 2018; pp 211-228.

7. **Tan, R.P.**, Lee, B.S.L., Chan, A.H.P., Yuen, S-C.G., Jin, K., Hung, J., Wise, S.G., Ng, M. K. C. Non-invasive tracking of injected bone marrow mononuclear cells to injury and implanted biomaterials. *Acta Biomaterialia* 53, 378-388 (2017).

8. Chan, A.H.P.**, Tan R.P.**, Michael, P. L.; Lee, B. S.; Vanags, L. Z.; Ng, M. K.; Bursill, C. A.; Wise, S. G. Evaluation of Synthetic Vascular Grafts in a Mouse Carotid Grafting Model. *PloS One* 12 e0174773 (2017).

Conference Proceedings During PhD Candidature

1. **Tan, R.P.**, Chan, A.H.P., Lee, B.S.L., Hung, J., Yuen, S.C.G., Clayton, Z.E., Miravet, M.M., Lennartsson, K., Cooke, J.P., Bursill, C.A., Patel, S., Wise, S.G. (2018) Developing biomaterial-based therapeutic applications for induced pluripotent stem cell derived-endothelial cells using non-invasive bioluminescence imaging. Tissue Engineering and Regenerative Medicine International Society, TERMIS (World Congress), Kyoto, Japan, September 4-7. ***Oral Presentation/Student and Young Investigator Prize Finalist***

2. **Tan, R.P.**, Tong, J., Kosobrodova, E., Bilek, M.M.M., Thorn, P.J., Wise, S.G. (2018) Dual Functionalised Encapsulation Platform for Beta-Cell Transplantation, Australasian Society for Biomaterials and Tissue Engineering (ASBTE), Freemantle, Australia. April 3-5. ***Oral Presentation***

3. **Tan, R.P.**, Chan, A.H.P., Lennartsson, K., Miravet, M.M., Lee, B.S.L., Clayton, Z.E., Cooke, J.P., Ng, M.K.C., Patel, S., Wise, S.G. (2017) 3D Cell Seeded Patches for Therapeutic Angiogenesis, Sydney Cardiovascular Symposium, Darlinghurst, Australia. December 6-8. ***Oral Presentation***

4. **Tan, R.P.**, Chan, A.H.P., Santos, M., Filipe, E., Lee, B.S.L., Bilek, M.M.M., Ng, M.K.C., Wise, S.G. (2017) A Novel Bioactive Interleukin-4 Functionalised Vascular Graft that Modulates Inflammation and Inhibits Neointimal Hyperplasia, European Society of Biomaterials (ESB), Athens, Greece. September 4-8. ***Oral Presentation***

5. **Tan, R.P.**, Chan, A.H.P., Santos, M., Filipe, E., Lee, B.S.L., Bilek, M.M.M., Ng, M.K.C., Wise, S.G. (2017) A Novel Bioactive Interleukin-4 Functionalised Vascular Graft that Modulates

Inflammation and Inhibits Neointimal Hyperplasia, Australian Society of Medical Research (ASMR), Sydney, Australia. June 2. ***Oral Presentation/Best Postgraduate Talk Award Winner***

6. **Tan, R.P.**, Chan, A.H.P., Santos, M., Filipe, E., Lee, B.S.L., Bilek, M.M.M., Ng, M.K.C., Wise, S.G. (2017) A Novel Bioactive Interleukin-4 Functionalised Vascular Graft that Modulates Inflammation and Inhibits Neointimal Hyperplasia, Australasian Society for Biomaterials and Tissue Engineering (ABSTE), Canberra, Australia. April 18-20. ***Oral Presentation***

7. **Tan, R.P.**, Lee, B.S.L., Chan, A.H.P., Yuen, S-C.G., Jin, K., Hung, J., Wise, S.G., Ng, M. K. C. (2016) Non-invasive tracking of bone marrow mononuclear cell engraftment to implanted biomaterial scaffolds, Cardiac Society of Australia and New Zealand (CSANZ), Adelaide, Australia. November 13-16. ***Oral Presentation/ISHR Prize Finalist***

8. **Tan, R.P.**, Lee, B.S.L., Yuen, S-C.G., Jin, K., Hung, J., Wise, S.G., Ng, M. K. C. (2016) Non-Invasive Tracking of Bone Marrow Mononuclear Cell Homing and Engraftment to Implanted Biomaterials. Tissue Engineering and Regenerative Medicine International Society, TERMIS (European Meeting), Uppsala, Sweden. June 28-July 1. ***Oral Presentation***

9. **Tan, R.P.**, Lee, B.S.L., Yuen, S-C.G., Jin, K., Hung, J., Wise, S.G., Ng, M. K. C. (2016) Non-Invasive Tracking of Bone Marrow Mononuclear Cell Homing and Engraftment to Implanted Biomaterials. Australian Society of Medical Research (ASMR), Sydney, Australia. June 6. ***Oral Presentation***

Awards & Achievements During PhD Candidature

2018

Channel 9 Evening News Story

Tissue Engineering and Regenerative Medicine International Society - Young Scientist Prize Finalist

University of Sydney Post-Graduate Research Support Scheme – Travel Grant

2017

Heart Research Institute Illuminate Award – Best Publication

International Society of Heart Research Award – Best Student Publication

Australian Society of Medical Research Conference Award – Best Postgraduate Presentation

Australian Society of Medical Research Press Article

The *Daily Telegraph* Press Article

University of Sydney Post-Graduate Research Support Scheme – Travel Grant

2016

Heart Research Institute Illuminate Award – Best International Presentation

University of Sydney Post-Graduate Research Support Scheme – Travel Grant

Heart Research Institute Conference Travel Grant

Australian Society of Medical Research Press Article

Cardiac Society of Australia and New Zealand ISHR - Student Prize Finalist

2015

University of Sydney Scholarship Merit Top-Up Award

University of Sydney Australian Post-Graduate Award (APA)

Statement of Authentication

The studies presented in this thesis are the results of original research carried out while the author was enrolled as a candidate for the degree of Doctor of Philosophy in the Sydney Medical School, University of Sydney. These studies were conducted between January 2015 and July 2018 at the Heart Research Institute, Sydney.

All experimental work carried out for this thesis is entirely my own original work except where stated otherwise in the text. The work presented in this thesis has not been submitted for a degree or a diploma in any other university.

Richard Tan

July 12, 2018

Acknowledgements

I would firstly like to thank my primary supervisor, Dr. Steven Wise for his continued direction and support throughout my PhD candidature. It is very rare opportunity to work for a supervisor that you can put your utmost faith in, let alone consider them to be a good friend. Thank you for your guidance in teaching me to harness and nurture my inner "beastmode" and allowing me to sneak through the past three and half years with my lacklustre attitude towards "optimisation". I would also like to thank you personally for all the privileges and allowances you have granted me throughout my PhD which have allowed me to be a better husband and father to my family.

I would also like to extend special gratitude to Assoc. Prof. Martin Ng, to whom I attribute the highly successful first year of my PhD candidature. Your encouragement to always "think bigger" has remained a continual source of motivation upon which I have strived to achieve the numerous accomplishments throughout my candidature.

None of the work done in this thesis could have been done without my (past and present) lab mates, Chien, Bob, Elysse, Miguel, Joy, and Eric. The highlight of working with you all was being able to bring to life the culture of the Power of Friendship. May you always remember and continue to live life through its three pillars: Faith, Beastmode, and Friendship. Special gratitude goes to the Ho Pang Chan man, Alex, for always being my reliable source for getting tasks done whenever I couldn't get them done myself during family-days off and/or extreme check-out phases.

I would also like to extend my acknowledgements to all my co-collaborators who helped me complete the work presented in this thesis. Special thanks to Zoe, Maria, Katarina, and Dr. Sanjay Patel from the Cell Therapeutics Group as well as Behnam and Professor Marcela Bilek from the Applied and Plasma Physics Group.

Above all else, I would like to thank my proud family for their undying support, encouragement and love throughout this journey. Thank you, Mom, Dad, Kris, Kelly, and Miles, for always being the first ones to celebrate my accomplishments. Making you proud has been the largest source of inspiration that has helped push me along the path. I would also like to thank my sons, Harley and Roman. You two were unquestionably the single greatest achievements during my PhD. The joy and laughter you gave me coming home from the lab every single day gave me the necessary perspective to remain grounded and never lose sight of my purpose. And lastly, I would like to thank my wife Justyna for her unconditional love and putting up with me always being “switched on”. Not to mention the financial burden you agreed to take when I first started, essentially signing on to support a third child. Thank you for allowing me the opportunity to better myself, supporting and growing with me along the way, and being the best mother to our boys over the past three and a half years.

Table of Contents

List of Figures

Abbreviations

BM-MNC = bone marrow mononuclear cell

CD206 = cluster of differentiation 206/mannose receptor

DC = direct current

EDC = 1-Ethyl-3-(3-dimethylaminopropyl)carbodiimide

EPC = endothelial progenitor/precursor cells

FBGC = foreign body giant cell

FTIR = fourier-transform infrared spectroscopy

H&E = hematoxylin & eosin

HSC = hematopoietic stem cell

IL-1β = interleukin-1 beta

IL-10 = interleukin-10

IL-4 = interleukin-4

IPSC-EC = induce pluripotent stem cell derived endothelial cells

kV = kilovolt

LPS = lipopolysaccharide

MCP-1 = monocyte chemoattractant protein-1

MHCII = major histocompatibility complex II

miRNA = micro ribonucleic acid

MIP-1α = macrophage inflammatory protein-1 alpha

MMP = metallomatrixproteinase

MRI = magnetic resonance imaging

MSC = mesenchymal stem cell

NHS = N-hydroxysuccinimide

PCL = polycaprolactone

SEM = scanning electron microscopy

TGF-β = transforming growth factor-beta

TIMP = tissue inhibitor of metalloproteinase

TNF-α = tumour necrosis factor-alpha

VEGF = vascular endothelial growth factor

Chapter 1

General Introduction

1. Introduction

1.1. Regenerative Medicine

One of the fastest growing biomedical practices in the world is regenerative medicine, an emerging field of medical science that aims to treat injury and disease by harnessing the body's capacity for regeneration [1]. In cases where the body cannot heal itself, this also includes the possibility of utilizing facilities and methods to grow tissue and organs outside the body for implantation [2]. The numerous studies within this field encompass a large body of work that focuses on the replacment or regeneration of human cells, tissues and organs to restore normal function. While there are many biomedical approaches currently being explored, these strategies often rely on the use of stem cells as the key cellular components that facilitate functional repair. Currently, stem cells and their numerous differentiated lineages are being exploited therapeutically for a number of mechanistic approaches including: 1) cell therapy, involving direct injection into injured and/or diseased tissue [3] 2) immunomodulation therapy, where biologically active molecules secreted by stem cells are used to enhance tissue regeneration [4] and 3) tissue engineering, where stem cells are used as building blocks to grow/engineer organs and tissues *ex vivo* in combination with biomaterials for transplantation [5] (Figure 1). While the use and function of stem cells continue to be essential to regenerative medicine, the future development of therapies that may ultimately reach patients relies

on a deeper understanding of the mechanisms which regulate their stimulation, enhancement, and/or replacement of the human body's innate tissue regenerative capabilities.

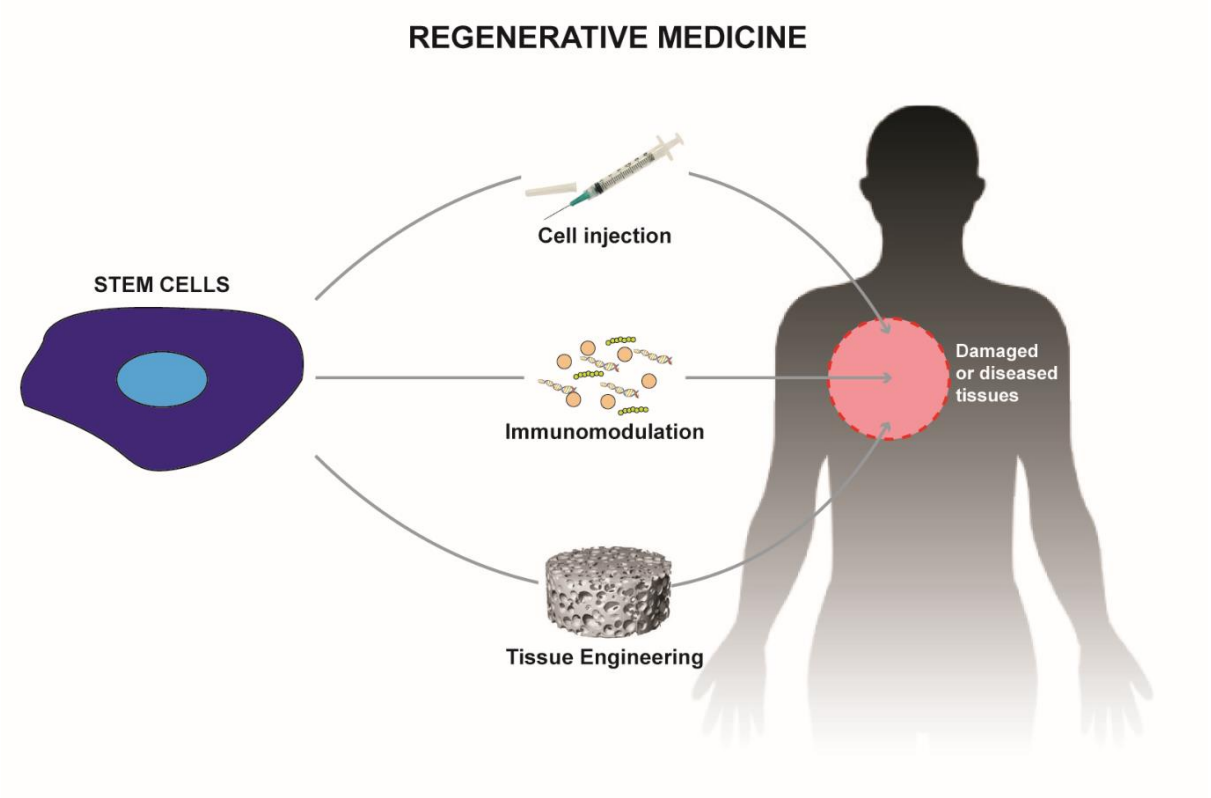

Figure 1 – Stem Cells in Regenerative Medicine

The contribution of stem cells towards the goals of regenerative medicine involve three main pathways. Stems are currently used as direct injection therapies to alleviate and cure symptoms within injured/disease organs and tissue. Their secreted factors are also isolated and used to influence the body's innate capacity for tissue regeneration. In combination with material scaffolds, tissue engineered constructs can potentially replace whole tissue, restoring loss of organ function.

1.1.1. Innate healing/tissue regenerative mechanisms

Inadequate tissue regeneration following traumatic injury, acute illness, or chronic disease affects millions of people worldwide every year [6]. This deficit is the consequence of dysfunctional elements of the normal tissue repair response, which include inflammation, angiogenesis, matrix deposition

and cell recruitment. Although underlying medical conditions such as vascular disease and diabetes are linked to the aggravated dysfunction of these elements, the human body's natural capacity for regeneration is also inherently limited. Typically, the body's response following injury involves the formation of scar tissue, rather than fully regenerating the organ back to its original state, with the exception of a few tissues such as the liver and endometrium [7, 8]. However, advances in research are studying the various elements of innate tissue repair and have enabled the development of breakthrough strategies capable of induced regeneration of many more tissues and organs than originally thought possible. Below, we examine each of the key processes of tissue regeneration in detail (Figure 2).

1.1.1.1. Inflammation

Inflammation is the most crucial biological process of regeneration as it not only initiates but is actively involved in all stages of tissue repair. As a by-product of injured tissue, dying cells release various inflammatory mediators that exist to protect the body by eliminating or sequestering degenerative stimuli. These can include damage associated molecular patterns (DAMPs) [9], lipid mediators [10], oxygen and nitrogen radicals [11], chemokines and cytokines [12] which work in concert to trigger a local inflammatory response by recruiting inflammatory cells of the innate immune system through the circulation. This can occur as a single event such as immediately following a traumatic injury or a gradual release over a period of time from chronically diseased tissue.

In most tissue, subsets of leukocytes, a white blood cell group evolved to protect the body from both infectious disease and foreign pathogens, are the predominant first responders migrating to sites of inflammation [13]. These leukocytes include cells such as neutrophils, monocytes, and monocyte-derived macrophages. Endowed with potent phagocytic and antimicrobial abilities which allow them to appropriately dispense of the inciting stimuli, these cells also actively participate in the controlled degeneration of injured tissue through the sustained and localised secretion of inflammatory

mediators, including matrix metalloproteinases (MMPs) [13]. In healthy tissue, the continued recruitment of immune cells will eventually lead to elimination of the initiating stimulus, appropriate destruction and remodelling of the injured tissue, and finally inflammatory resolution.

The resolution of inflammation is a highly coordinated process controlled by many distinct mechanisms. While it is known that the production of many pro-inflammatory cytokines is transient and the half-life of the mRNAs encoding these cytokines are generally short, it is becoming increasingly accepted that depletion of pro-inflammatory mediators alone is insufficient to halt inflammation [14]. Equally important, the removal of leukocytes and their secretion products is also required. The primary mechanism controlling the local elimination of immune cells is through programmed apoptosis and subsequent removal via macrophage phagocytosis. This process stimulates macrophage release of cytokines such as transforming growth factor-β (TGF-β) and interleukin-10 (IL-10), which contribute to the resolution of inflammation by triggering further leukocyte apoptosis, while also stimulating the next stages of healing, angiogenesis and tissue remodelling [13].

When these immunomodulatory feedback processes are intact, inflammation is self-restricting, and the inflammatory process yields no unnecessary tissue damage. Dysfunction of these resolution mechanisms leads to states of chronic inflammation and consequent tissue injury. Contributing factors to persistent immune responses include inefficient revascularisation processes and subsequently inadequate recruitment of stem and progenitor cells to rebuild tissue. Numerous chronic inflammatory disorders including rheumatoid arthritis, inflammatory bowel disease, type I diabetes, and even atherosclerosis are currently being addressed through regenerative medicine approaches [15]. These strategies aim to replace the body's loss functions of immune resolution allowing for the next stages of repair to occur. Many of these approaches are based on anti-inflammatory drugs. Although inflammation is not as prominent during the late stages of repair, numerous studies suggest that the

events during the inflammatory stage have drastic impacts on the ensuing tissue remodelling phases and ultimately the final regenerative outcome of the injured tissue [13].

1.1.1.2. Revascularisation

In forms of tissue injury where blood vessel walls are damaged, blood loss is initially curtailed by the formation of a haemostatic plug. Collagen fibers exposed in the damaged vessel wall adhere platelets in the blood stream [16]. As platelets attach to the injured vessel, they rapidly upregulate binding integrins that mediate further platelet aggregation forming the haemostatic plug. After binding, platelets activate and degranulate, stimulating the release of procoagulant factors that trigger the formation of a fibrin clot to prevent further blood loss. Platelet degranulation also results in the release of signalling factors such as TGF-β and vascular endothelial growth factor (VEGF) which contribute to the chemoattractant gradient within the tissue injury that is responsible for the recruitment of inflammatory and reparative cells [17]. In doing so, endogenous revascularisation mechanisms are activated which are tasked with the establishing the local vascular network from the injured pre-existing vasculature.

Endothelial cells that line the inner surface of local blood vessels are activated by low oxygen/hypoxic conditions resulting from injury as well as increases in local secretion of pro-angiogenic factors from platelets and macrophages, including VEGF. In response, endothelial cells degrade their surrounding extracellular matrix and begin migrating and proliferating, and re-establishing cell-cell contacts forming new capillaries. An additional and more profound form of tissue revascularisation is vasculogenesis, which relies on the mobilisation of endothelial progenitor cells (EPCs) from the bone marrow to form large diameter arterioles [18]. Over time, the overabundance of newly formed capillaries and arterioles regress, resulting in a normal vascular density.

Angiogenesis is an indispensable process to tissue regeneration and is reliant on several facets of the regenerative process [18]. Macrophages, fibroblasts and new blood vessels simultaneously invade the

injured tissue as a unit and exhibit high interdependence. Macrophages provide a continuing source of pro-angiogenic factors while also releasing cytokines that stimulate fibroblast migration and deposition of new extracellular matrix required for cell ingrowth [13]. Cells repopulating injured tissue are inherently dependent on their local vasculature to supply critical nutrients and remove waste products. It is generally accepted that impaired wound revascularisation can impede healing as inadequate blood perfusion is often a hallmark of chronic wounds. Current regenerative medicine approaches to address tissue revascularisation have spurred a research field known as therapeutic angiogenesis that aims to augment the body's innate angiogenesis mechanisms during tissue repair [19]. However, the cellular events required for angiogenesis are often not readily addressed through the administration of single factors alone [19], but rather involve a highly dynamic and complex interaction between endothelial cells, immune cells, and, perhaps more importantly, the surrounding tissue environment consisting of a highly dynamic turnover of extracellular matrix proteins.

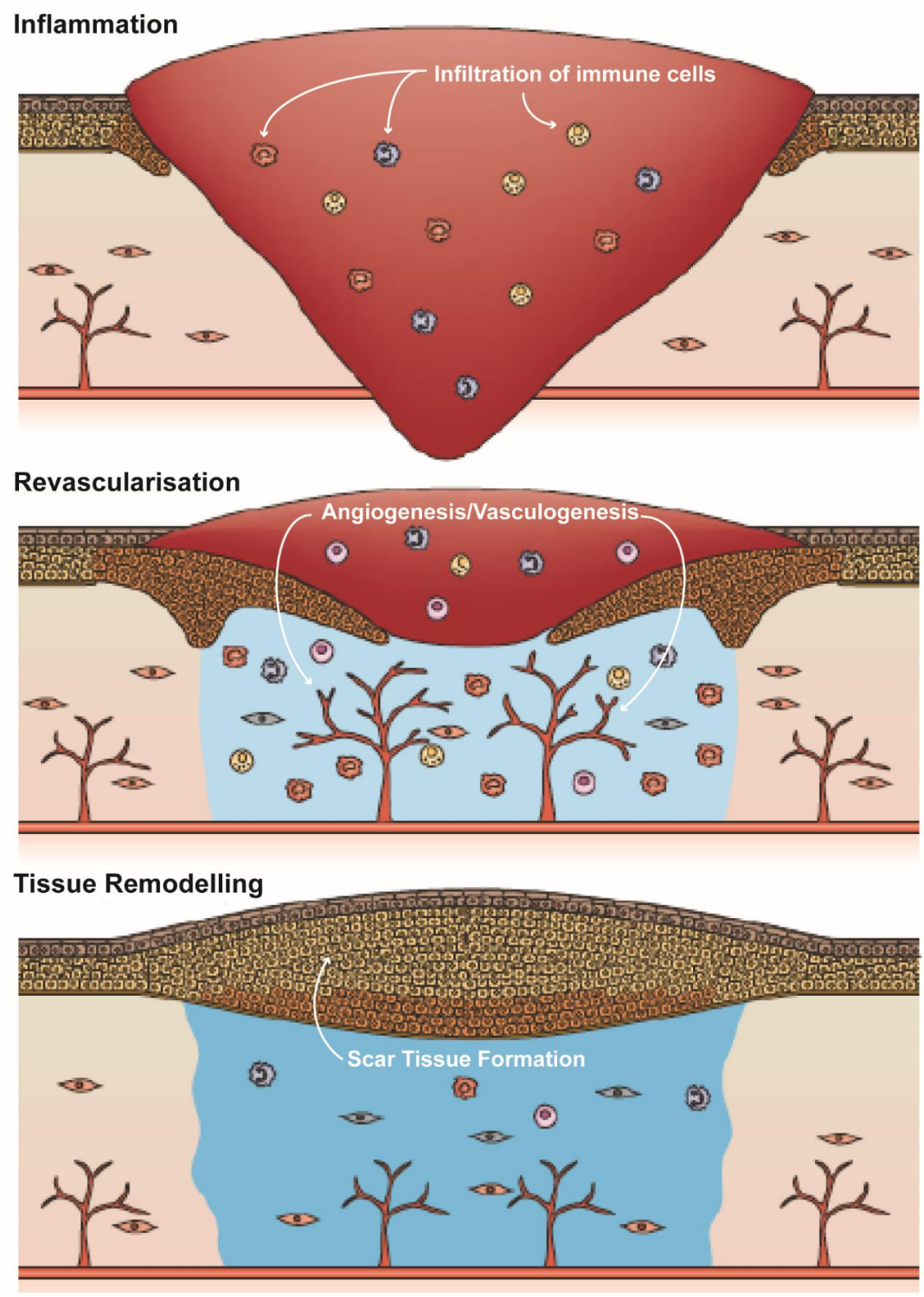

Figure 2 – Stages of Wound Healing

Three major stages of wound healing involve inflammation, revascularisation, and tissue remodelling. Immune cells invade the wound bed to clear necrotic tissue and cells, allowing wound

regeneration responses to occur. These include angiogenesis to re-establish the vasculature which leads to the migration of tissue remodelling cells to close the wound.

1.1.1.3. Tissue remodelling

The last stages of tissue regeneration predominantly involve remodelling of the extracellular matrix. This process requires an intricate balance of matrix protein synthesis and degradation. Some of the key mediators in this process are MMPs and their inhibitors, tissue inhibitors of metalloproteinases (TIMPs) [20]. During the peak of the inflammatory phase, leukocytes facilitate the removal of damaged matrix proteins through the release of tissue-specific MMPs. Amongst the numerous mediators released by macrophages during immune resolution, TIMPs are essential to halt MMP degradation and stimulate the infiltration and function of fibroblasts [20]. The primary role of fibroblasts, regulated by macrophage secreted molecules such as fibroblast growth factor-2 (FGF-2), are to synthesize new extracellular matrix and collagen. Its initial role in tissue injury is to facilitate the formation of granulation tissue, a provisional matrix through which angiogenesis can occur and provide temporary structural support for the ingrowth and differentiation of new cells [21]. Following closure of the wound, the fibers of the provisional matrix are realigned and cross-linked. The process of collagen alignment differentiates remodelled tissue following injury from normal healthy tissue, which consists primarily of randomised collagen fibers. Remodelled tissued often also confers inferior functional quality to healthy tissue and visually appears as what we know as scar tissue [22].

Within most human organs, the natural regenerative outcome to injury or disease is some degree of scar tissue formation, also known as fibrosis. Fibrotic scar tissue is excess fibrous connective tissue comprised of the same protein (usually collagen) as the tissue it replaces. The increased speed at which scar tissue formation occurs in relation to complete tissue regeneration has, evolutionarily, been the reason why the body's regenerative capacities are naturally limited [23]. The body's initial response favours isolation/sealing of the injury site from the outside environment and possible infection, and this occurs at the expense of optimal tissue regeneration. As such, fibrosis negatively

affects organs and tissues by masking their underlying architecture and function. The consequence of all traumatic injury and organ failure is the presence of scar tissue. Restoration of functional ability to a tissue or organ is often determined by tipping the balance in favour of tissue regeneration over scar tissue formation.

Regenerative medicine aims to assist in this endeavour through approaches that include favourable manipulation of innate healing responses and/or augmentation of tissue regenerative mechanisms. Often found at the centre of these research efforts is a vast range of stem cell applications. Stem cells or their secreted products are being trialled as direct injections and cell therapies for numerous diseases such as stroke [24], heart attack [25], diabetes [26], and neurodegeneration [27]. Intensive research focus is also on the study of stem cell behaviour and function during foetal development, as tissue regeneration has been observed to be more prominent than fibrosis in the foetuses of humans and many other species. It is becoming increasingly apparent that stem cell function, origin, and application will become vital to the development of the next generation of regenerative medicine solutions.

1.1.2. Stem Cells

Following the first reporting of stem cell isolations in the early 1960s [28], it was not long before interest into their regenerative functions would emerge. Today this interest dominates current tissue regeneration strategies as aging and disease are linked to reduced regenerative capacity and dysfunction of endogenous stem cell reserves [29-31]. This has highlighted them as a primary focus of many regenerative medicine applications and, given their extensive ability to self-renew and generate numerous cell lineages, they are continually under invesigation for their broad therapeutic potential. The most common therapeutic treatments involve transplanting patients with their own stem cells or stem cell-differentiated lineages. It has been long believed that stem cells for transplantation could be harvested only from accessible tissues such as the blood or skin. However, recent advances allow

directed stem cell differentiation into inaccessible or rare cell types that potentially can replace any cell in the body [28]. From this technology, alternative methods to cell transplantation have been developed that attempt to manipulate stem cell behaviour and function *in vivo*. Despite the enormous potential underlying stem cell research, the development of clinical therapies since their discovery has been limited by controversy surrounding their origins and lack of consensus on the methods to control their behaviour *in vivo* [28]. Adding to these challenges are the difficulties of stem-cell isolation and expansion due to their extensive heterogeneity. Marker-based identification of stem cells is often complicated by the changing nature of their surface markers. Numerous stem cell populations have been shown to maintain stem cell-like properties long after losing marker expression. Complicating this further is the severity of the disease, associated pre-existing conditions, and age which can not only alter the expression of stem cell surface markers, but also drastically impact the overall number of stem cells expressing a particular marker. This has made sourcing the appropriate stem cell population in adequate numbers elusive. To date, three main sources of stem cells each with varying levels of potency, meaning their potential to divide into numerous cell lineages, have been identified and are largely debated on which are the most suitable for regenerative therapy.

1.1.2.1. Stem cell sources and potency

1.1.1.1.1 Adult stem cells

Adult stem cells, or resident stem cells, are undifferentiated cells found in adult tissue throughout life and are responsible for every day tissue maintenance (Figure 3). These cells are largely present in tissue that have rapid turnover rates such as bone marrow/blood, skin, and gut [32]. Since these cells are native to individual tissues they are often characterised as having multipotency, meaning they give rise to multiple cells types of only a single organ. Adult stem cells divide asymmetrically, meaning they divide into a single stem cell to maintain their numbers while also giving rise to a cell of committed lineage. However, the renewal capacity of adult stem cells is limited and decreases with aging. In general, adult stem cells are required to divide quite rarely, however under the appropriate

stimulus, such as an increased demand for cells in regeneration of tissue injury, they are capable of readily proliferating and differentiating. Two common examples are epidermal stem cells in regenerating skin wounds [23] or the release of haematopoietic stem cells from the bone marrow into the blood when inflammation is activated [33]. Since adult stem cells are functioning components of the body's innate mechanisms of healing, regenerative medicine approaches have been designed to manipulate their behaviour both *in vivo* for *in situ* regeneration [34] and *in vitro* for transplantation [35]. Minimal cell numbers resident within adult tissue have been the primary barrier to these approaches as large cell amounts are often needed to therapeutically enhance native repair mechanisms. This need has spurred the advent of other stem cell sources possessing higher proliferative capacities, the first discovered being embryonic stem cells.

1.1.2.1.1. Embryonic stem cells

Embryonic stem cells are derived in culture from fertilized pre-implantation embryos and possess pluripotency, meaning they can differentiate into any cell type within the body. Unlike adult stem cells, embryonic stem cells divide symmetrically, meaning a single cell can give rise to two new pluripotent stem cells [36, 37]. This pluripotency and their indefinite renewal capacity are the main features that distinguish them from adult stem cells. Under defined conditions, embryonic stem cells are capable of replicating indefinitely and have thus been equally employed as a research tool as they have been explored for therapeutic potential [38]. Studying the ways embryonic stem cells develop into mature cells have aided researchers in better understanding how those cells function as well as what goes wrong when they are diseased. As previously discussed, the tissue regenerative capacity of foetal cells vastly outpaces that of mature cells, and insight into cell and tissue healing during development may potentially be linked to the therapeutic possibilities of embryonic stem cells [38]. Previous regenerative medicine approaches employing embryonic stem cells aimed to develop strategies that were capable of extending this enhanced embryonic regenerative capacity into the later stages of life. However, the requirements of fertilized human embryos to extract and culture embryonic stem cells

clouded their clinical use in ethical debate [38]. As a result, the studies investigating the extensive regenerative potential of embryonic stem cells became secondary to finding less controversial sources possessing the same pluripotency and self-renewal features.

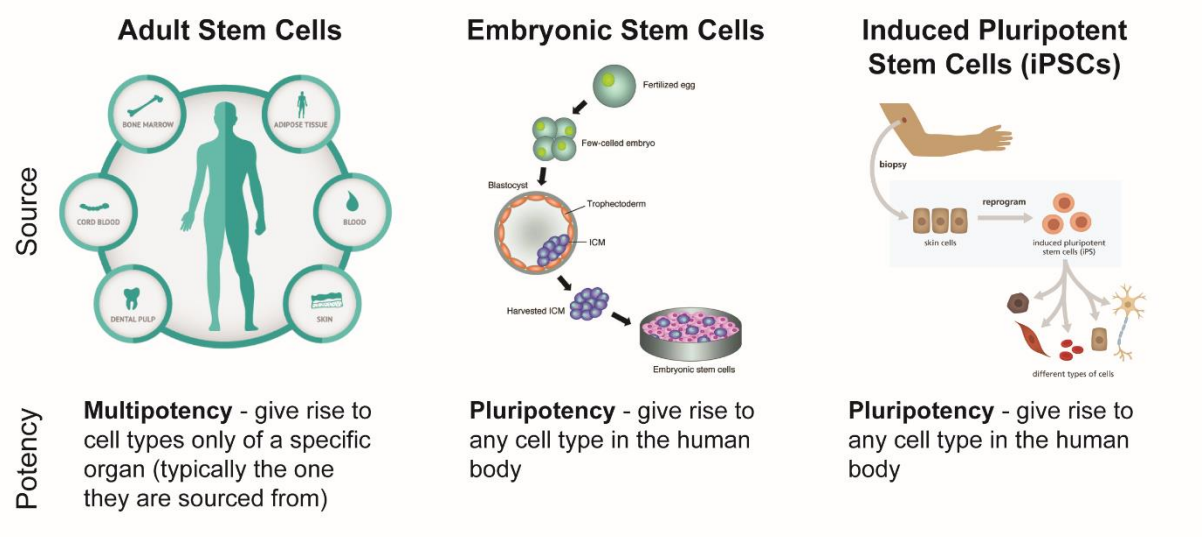

Figure 3 – Current Stem Cell Sources

The three main sources of stem cells are grouped into adult stem cells, embryonic stem cells, and induced pluripotent stem cells. Each stem cell source involves separate methods of derivation and give rise to stem cells with varying levels of potency which define their capacity to differentiate into various cell types within the body.

1.1.2.1.2. Induced pluripotent stem cells

In this manner, induced pluripotent stem cells (iPSCs) have revolutionised modern day stem cell research. Originating from any adult cell, iPSCs are generated by being reprogrammed to embryonic stem cell-like states using four transcription factors known as the Yamanaka factors (Oct4, Sox2, Klf4, and c-Myc) [39]. Because the ethical issues surrounding embryonic stem cells do not apply to iPSCs, the idea that a patient's own tissues could potentially provide them pluripotent stem cells for self-regeneration has become an increasingly possible reality. The ability to induce abundant, readily

accessible cells to pluripotency eliminates the search for rare tissue-resident stem cells while also providing the scalability of culturing clinically relevant quantities of stem cells. Additionally, while embryonic stem cells can only be derived from embryos, iPSCs offer patient-matched stem cells, overcoming the translational challenges of immune-rejection. The numerous benefits of iPSC technology have made it currently the most widely used approach for studying disease modelling [40] and gene therapy [41]. Although these studies are ongoing, the current literature surrounding iPSCs focuses mainly on characterising their pluripotency in comparison to embryonic stem cells and most importantly, defining the conditions necessary to generate all the individual cell types within the human body as conceptually theorized. Still in its infancy, a yet to be explored area of iPSC research is their potential to facilitate tissue regeneration through endogenous stem cell repair mechanisms.

1.1.2.2. Stem cell mechanisms of regeneration: transdifferentiation vs paracrine

Since the discovery of stem cell pluripotency, it is generally accepted that the therapeutic potential of stem cells resides in their ability to replace damaged cells within injured tissue on a cell by cell basis [42, 43]. This method of stem-cell mediated regeneration, known as transdifferentiation assumes that cell transplantation can overcome the inherent limitations of human regeneration by enhancing the overall numbers of stem cells or their lineages within injured tissue in attempts to overwhelm and speed up the repair process in order to ultimately curb fibrosis. For example, new cardiomyocytes identified following heart injury have been shown to express markers of transplanted cardiac stem cells [44]. Additionally, mesenchymal stem cells transplanted into wounds have differentiated into fibroblasts [45]. However, while some beneficial effects in research models have been reported, no solid clinical evidence in humans has shown that these approaches are capable of regenerating damaged solid organs or giving rise to significant organ-specific cell populations, such as functional cardiomyocytes in the heart or beta cells in the pancreas [46]. As a result, this concept of stem cell transdifferentiation has been routinely challenged and positive effects following transplantation therapies have been explained by alternative mechanisms (Figure 4).

There is mounting evidence that stem cells secrete a variety of growth factors [47], chemokines/cytokines [48], and bioactive lipids [49]. In particular, it has been shown these factors are secreted from activated stem cells removed from their physiological niches. It is logical that these factors participate in alternative mechanisms of stem-cell guided regeneration based on paracrine effects. Distinct sets of paracrine factors specific to individual stem cell types have been shown to play a crucial role in regeneration of a variety damaged tissues [50]. Recent data shows that harvested conditioned media containing these factors from stem cell populations such as haematopoietic (HSCs) or adult stem cells can even replace intact cells in cellular therapies [51]. Conditioned media of mesenchymal stem cells (MSCs) derived in culture express pro-angiogenic growth factors such as VEGF and FGF-2, inflammatory chemokines such as macrophage inflammatory protein-1α (MIP-1α) and monocyte chemotactic protein-1 (MCP-1), as well as inflammatory cytokines including TGF-β and IL-10 [52]. The vast array of soluble factors released by stem cells are well known to the mechanisms of innate tissue regeneration and it is widely demonstrated that stem cells and their conditioned media can influence all stages of healing [51].

In addition to soluble factors, activated stem cells also secrete spherical microvesicles from their membranes that significantly inhibit apoptosis of cells residing in damaged tissues, stimulate their proliferation and facilitate vascularisation [53]. In addition to containing small packages of soluble factors, these microvesicles transfer mRNA or regulatory microRNA (miRNA) essential to their pro-regenerative properties. Bone marrow derived-HSCs are capable of changing cell phenotypes to lung cells through delivery of lung-tissue derived microvesicles [54]. Similar transfer mechanisms of organ-specific mRNA into bone marrow cells have been demonstrated from microvesicles derived from brain, heart, and liver, suggesting that microvesicle-mediated changes in phenotype can occur universally throughout the body [54]. These findings report an additional mechanism by which stem cell microvesicle release can drastically affect the phenotype and biology of neighbouring target cells following transplantation.

As the growing evidence suggests, stem cells have the potential to regulate the entirety of the body's natural healing response. While it was originally believed that their role in tissue regenerative therapies would be to serve as the building blocks in the reconstruction of damaged tissue, it has become more apparent that their functions of coordinating regeneration may play a more dominant role. Further understanding of these mechanisms will lead to the development of improved stem cell therapies currently being used in regenerative medicine. Today, the mechanisms of stem-cell guided tissue regeneration are applied in numerous research and clinical studies. However, the transfer of many of these methods to the clinic is still met with a range of translational uncertainties which have largely hindered their widespread use to date.

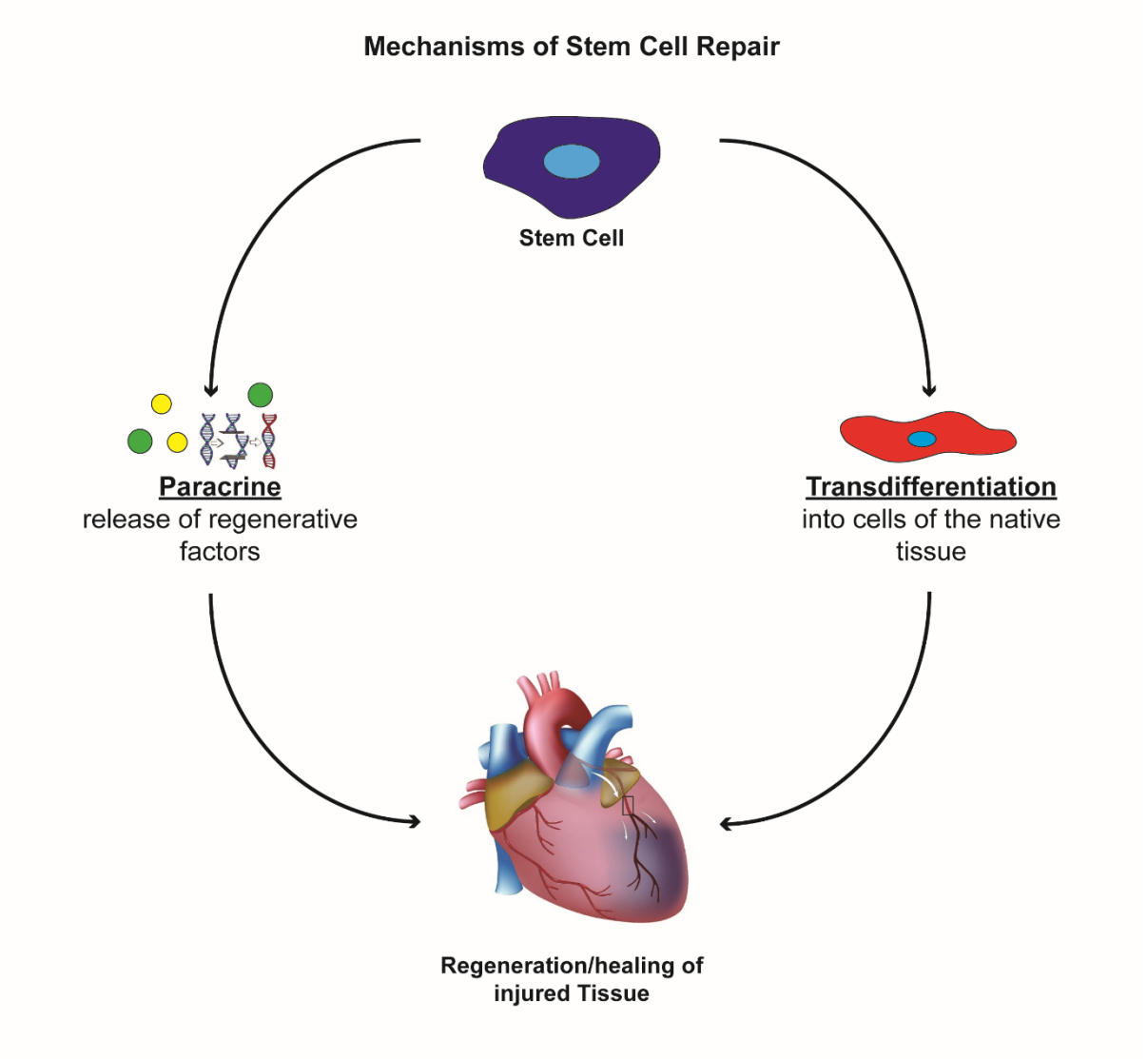

Figure 4 – Mechanisms of Stem Cell Repair

The two generally accepted mechanisms of stem cell tissue repair are through paracrine effects which rely on secreted regenerative factors that drive innate tissue healing and/or transdifferentiation which describes the direct differentiation of stem cells into the dysfunctional or loss cell type of the injured tissue/organ.

1.1.2.3. Current applications and clinical shortcomings

In the past decade, there has been a rapid surge in clinical trials involving stem cell therapies [55]. Currently, one of the most well-established and widely used stem cell populations are those found within the bone marrow. Transplantation of bone marrow HSCs is a common treatment for blood and immune system disorders as well as the current standard for restoring the blood system following cancer treatments [56]. MSCs harvested from the bone marrow are currently being tested in over five hundred clinical trials for a very wide range of repair applications including cartilage, liver, kidney, lung, cardiovascular, bone, brain/nerves, as well as graft-versus-host and autoimmune diseases which exploit MSC's immunosuppressive properties [57]. The majority of these trials are in Phase I (safety studies), Phase II (proof of concept for efficacy in human patients), or a mixture of Phase I/II. Recently discovered in the bone marrow, endothelial progenitor cells (EPCs) are highly effective at stimulating angiogenesis and are a top focus of cardiovascular diseases. While efficacy in preclinical and Phase I trials have been demonstrated, patient benefit over placebo-controlled trials has yet to be obtained in Phase II [58]. Overall, clinical trials on the use of stem cells are well underway for a wide variety of conditions with a particular emphasis on the use of bone marrow stem cell populations. While safety has been consistently demonstrated, sustained functional benefits have yet to be consistently obtained. Nevertheless, progress towards using stem cells for therapeutic benefit is increasing. A strong indication of the confidence in stem cell therapy is the growing participation of large pharmaceutical companies in stem cell research and funding of clinical trials [59]. With increased financial backing, the optimization of future stem cell based regenerative medicine approaches will be more readily achieved.

However, despite the growing enthusiasm for therapeutic application, stem cells are burdened by several challenges observed in the clinic. Their intrinsic features of pluripotency and self-renewal are properties also inherent to cancer cells, and growing concerns about regulating stem cell behaviour *in vivo* to prevent tumour formation are continually discussed. In particular, iPSCs have shown

sizeable genetic and epigenetic abnormalities and there is a clear need to determine their biological significance before they are taken to clinical trial [59]. Additionally, while the technology to induce pluripotency is now available, the logistical yields are still quite inefficient as will be discussed later. In cases where enough stem cells of a particular lineage can be generated, transplantation is still burdened by poor survival and subsequent transient benefits.

Injured tissue is a difficult milieu for cell engraftment and survival due to lack of oxygen and nutrients, a dysfunctional extracellular matrix, and altered biochemical environments. As observed within the stem cell niche, certain signalling factors can have an impact on stem cell engraftment. For example, MSC engraftment is hindered by signals found within the hostile microenvironment of injured tissue that are derived from the highly inflammatory and cytotoxic processes occurring during the stages of healing [60]. Another common lesson from engraftment studies is that transplantation of stem cells requires intact structural networks for survival. Interactions between the extracellular matrix and MSCs have shown that inadequate binding induces an apoptotic process known as anoikis [61]. Preventing anoikis involves activation of integrin receptors through matrix binding which then signal cell survival pathways. One of the established methods to address this issue is the use of artificial three-dimensional matrices to provide temporary structural support and biochemical cues, including integrin activation, to enhance cell survival.

From extensive research and clinical findings, it appears that more needs to be understood about what regulates stem cell engraftment *in vivo* in hopes of translating their regenerative potential. This need has spurred the development of strategies which aim to augment stem cell engraftment to extend their functional benefits by providing adequate structural support following transplantation and/or ensuring that the necessary biomolecules are present to favourably enhance their survival. Today, an entire field within regenerate medicine exists to investigate engraftment solutions to appropriately fulfil this need.

1.2. Tissue Engineering

Developing efficacious solutions to address the complexity of stem cell behaviour requires an interdisciplinary field combining the principles of engineering and life sciences towards achieving the goals of regenerative medicine. Representing that field today is Tissue Engineering, a set of research approaches that employ scaffold matrices to deliver growth factors and/or cells that have the ability to form tissues within the body upon transplantation. Interaction and integration with native tissues and cells are an underlying principle of tissue engineering which is why functionalisation of scaffolds with modifying factors such as biologically active proteins or DNA are critical to their success. Additionally, the target tissues involved usually require certain structural and mechanical properties essential to their function. Thus, the challenges in designing scaffolds with the appropriate biological and mechanical properties become increasingly overwhelming as the scale of the target tissue becomes more complex. Currently tissue engineering plays a relatively small role in patient treatment. The more successful procedures involve small scale repairs such as injection of cartilage forming chondrocytes for damaged cartilage [62] or grafting of skin cell sheets for damaged skin [63]. Strategies to engineer supplemental bladders, arteries, kidneys, and lungs for example are still perceived as a long way from being fully reproducible and ready to implant into patients. However, despite the trials that lay ahead, the development of future successful strategies will rely on the same basic elements of current and past tissue engineering approaches.

1.2.1. Tissue Engineering Paradigm

Tissue engineering methods broadly utilise components of three essential pillars of what has become a common paradigm of the tissue engineering field (Figure 5). Tissue engineering strategies exploit numerous cell sources including autologous, allogenic, and stem cells. These cells are often utilized in combination with exogenous biochemical or biomechanical stimulation to regulate and/or augment their function *in vivo*. Meanwhile, scaffold matrices are used as growth and/or delivery platforms

containing both elements. Tissue engineering strategies typically exist and are categorized as various permutations of these pillars. Common examples are cell-seeded scaffolds, acellular scaffolds functionalised with biomolecules, biochemically enhanced cell populations, or functionalised scaffolds containing cell populations [64]. While the use of various cell types and the biomolecule factors that dictate their function are also largely studied in regenerative medicine, tissue engineering seeks to develop approaches capable of translating their regenerative benefits to the patient's bedside, primarily through the integration of biomaterial scaffolds.

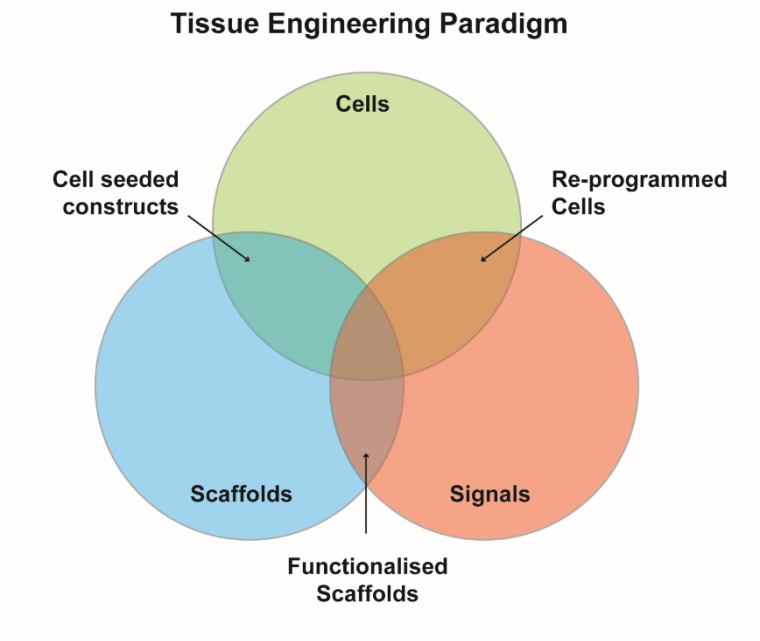

Figure 5 – The Tissue Engineering Paradigm

The three major facets of tissue engineering; cells, scaffolds, and signals, that work in various combinations with one another to form the basis of the tissue engineering paradigm that underlies the development of all tissue engineering solutions.

1.2.2. Scaffolds

Tissue engineering relies extensively on the use of 3D matrices known as scaffolds to provide the appropriate environment for tissue and organ regeneration. Acting primarily as a template for tissue formation, scaffolds are typically seeded with cells and/or growth factors. In some applications, these scaffolds are then subjected to biophysical stimuli within a form of 'bioreactor', a device or system which applies various mechanical and/or chemical stimuli to cells. Scaffolds are either cultured *in vitro* to synthesize tissues (often called a 'tissue engineered construct') which can then be implanted to an injury site, or are implanted directly into the injury site, using the body as a natural bioreactor to induce tissue and organ regeneration *in vivo*. Currently, scaffolds are manufactured from a wide range of biomaterials using a plethora of fabrication techniques, dictated largely by its application and target tissue [65]. However, regardless of these variations in scaffold design, a few key considerations are essential to determining the scaffold's suitability for use in tissue engineering (Figure 6).

1.2.2.1. Essential scaffold features

1.2.2.1.1. Tissue Compatability

One of the first criteria for a tissue engineering scaffold is that it must demonstrate a positive interaction with cells. This property, known as tissue compatibility, determines the extent to which the body tolerates the scaffold. Cells must be able to adhere, maintain function, and proliferate on and throughout the scaffold before laying down new extracellular matrix. Following implantation, the scaffold or tissue engineered construct must also elicit a minimal immune reaction to prevent severe inflammatory responses which may impair healing and/or cause rejection by the body. Over time, the biocompatibility of an implant will help to determine the degree to which it seamlessly integrates with the target tissue.

1.2.2.1.2. Biodegradability

The rate of scaffold integration is also closely linked to the scaffold's replacement with the body's own cells over time. Typically, scaffolds and constructs are not intended to function as permanent implants and must therefore exhibit properties of degradability. While the timing is difficult to accurately match, ideally, the scaffold would degrade at an equal rate to which cells are producing new extracellular matrix. The features of 'bio'degrability would also require that the by-products of this degradation would be non-toxic and able to leave the body without negatively affecting other organs. As scaffolds and constructs have begun to be considered for use in clinical practice, it is becoming increasingly observed that allowing degradation to occur in tandem with tissue formation relies on the controlled infiltration of immune cells such as macrophages capable of facilitating degradation and tissue synthesis [66].

1.2.2.1.3. Mechanical

Another clinical perspective on scaffold requirements focuses on its mechanical properties. The scaffold must be strong enough to withstand surgical handling during implantation, while ideally, also possessing mechanical properties consistent with the anatomical site into which it is being implanted. Combined with degradability requirements, this is especially challenging for load bearing environments such as in cardiovascular and orthopaedic applications [67]. The implanted scaffold must maintain sufficient mechanical integrity to function from the time of implantation to the completion of the regeneration process. As healing rates vary with age and medical condition, this becomes even more difficult to determine. Furthermore, while manufacturing current scaffolds with good mechanical properties is readily achievable, it is often at the expense of adequate scaffold porosity, a feature essential to the vascularisation and thus integration of the scaffold. It has become clear that although the architectural features of any scaffold are closely associated with its mechanical properties, they are equally important to its overall goals of successful tissue replacement.

1.2.2.1.4. Scaffold Architecture

Scaffolds come in many shapes and sizes ranging from flat nanofibrous matrices to amorphous hydrogels. Typically, the intended application of a scaffold will dictate its required architecture. Scaffolds in sheet form may confront problems related to nutrient supply by limiting diffusional distances, while injectable matrices can tackle problems of surgical invasiveness. For example, a nanofibrous sheet would be more suitable for tissue layer regeneration applications such as skin, whereas a hydrogel would benefit injuries with more irregular architecture such as brain or heart injury. While the overall architecture of many scaffolds used in tissue engineering may vary, high porosity remains an architectural feature crucial to the success of any scaffold [68]. An ideal scaffold would have an interconnected pore structure allowing cell penetration and subsequent exchange of nutrients and waste, achievable primarily through the stimulation of angiogenesis throughout the scaffold pores. Pore distribution and diameter are adjustable architectural parameters to help regulate new matrix deposition and scaffold degradation. Therefore, depending upon the cell type used and target tissue being engineered, a critical range of porosity properties must exist within the scaffold.

These essential scaffold features are critical to success in tissue engineering applications and are closely associated with one another in determining their outcomes [69]. However, one criteria upon which all the required properties listed above are dependent upon is the choice of biomaterial from which the scaffold is fabricated.

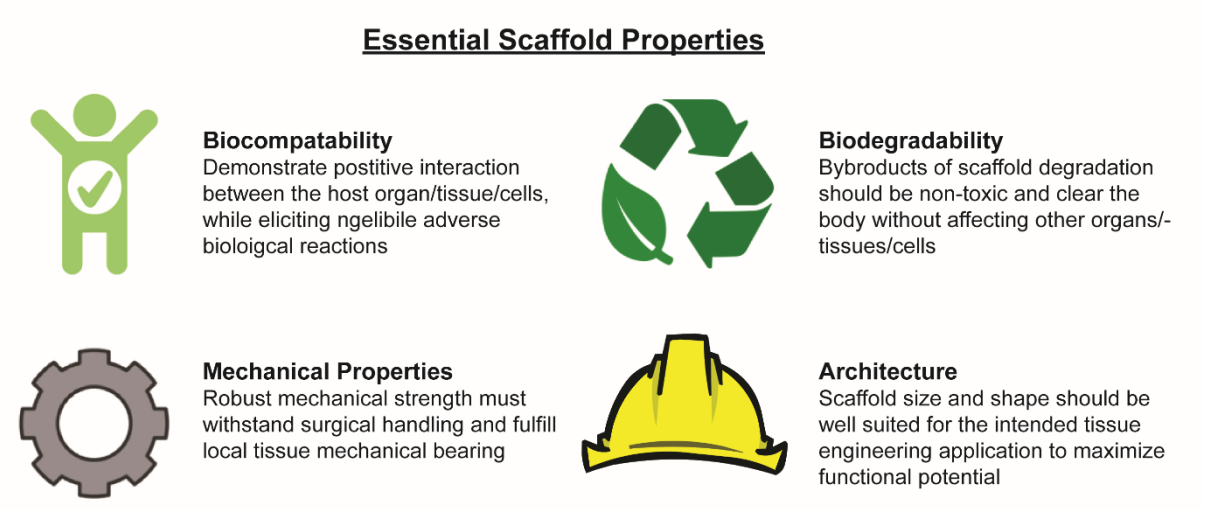

Figure 6 – Biomaterial Scaffold Properties

The essential properties of biomaterial scaffolds taken into consideration when designing scaffolds for tissue engineering

1.2.2.2. Biomaterials

As the field of tissue engineering grows, scaffold materials continue to evolve from merely interacting with the body to influencing biological processes that facilitate tissue regeneration. Scaffolds are typically manufactured from three groups of biomaterials: ceramics, synthetic polymers, and natural polymers (Figure 7).

1.2.2.2.1. Ceramics

Most commonly used for hard tissue bone applications are ceramic scaffolds [70]. Ceramic scaffolds are typically known for high mechanical stiffness (Young's modulus), very low elasticity, and hard brittle surfaces. For bone applications, ceramics intrinsically exhibit excellent biocompatibility with osteogenic cells, cells involved in bone formation. This is due to their closeness to the mineral phases of native bone in both chemical and structural similarity. Various ceramics are used directly in dental and orthopaedic surgery to fill bone defects as well as for coatings of metal implants to improve

implant integration with native bone. However, widespread use in tissue engineering applications have been limited due to their brittleness, difficulty in shaping, and challenges in controlling degradation rate in relation to new bone formation [71]. As previously discussed, porosity greatly compromises the mechanical integrity of ceramics and often the mechanical loads in bone environments cause ceramic scaffolds to fracture. Improved control of mechanical properties is a heavily researched area of ceramic manufacturing. This has led to the popularity of alternative materials such as synthetic polymers which offer more tuneable mechanical features.

1.2.2.2.2. Synthetic Polymers

To date, a vast range of synthetic polymers have been researched for their potential use in both soft and hard tissue applications, including polypropylene (PP), polyethylene (PE), polystyrene (PS), nylon, and polyurethane (PU). The popularity of these synthetic polymers for tissue engineering scaffolds stem from their ease of fabrication with tailored and reproducible architecture, mechanical properties, and degradation by simply varying the polymer itself or composition of the individual polymer [72]. However, concerns exist about the biodegradation of some synthetic polymers which produce acidic by-products and carbon dioxide which can lower local tissue pH leading to cell and tissue necrosis. For example, Poly(lactic-co-glycolic acid) (PLGA) is a commonly used synthetic polymer for a range of tissue engineering applications from stem cell-loaded contructs to bone applications. However, their use has been associated with an increase in localised acidic pH at the site of implantation that instigates inflammation and subsequent fibrosis [73]. While these features are readily tuneable, mechanical properties are often compromised early during degradation, thus polymer selection is limited to distinct applications. At the foremost, these materials are also known to exhibit poor biocompatibility and have an increased risk of rejection by the body. For instance, expanded polytetrafluoroethylene (ePTFE), currently the most widely used polymer for synthetic vascular graft shows poor endothelial cell attachment both *in vitro* and *in vivo* due to their high hydrophobicity [74]. The exchange of biocompatibility for increased control over scaffold mechanical

properties requires additional methods to functionalise scaffold surfaces with cell compatible binding domains like the Asp-Gly-Asp (RGD) motif found in native matrix proteins [75]. To avoid these additional fabrication processes, alternative approaches utilize native biological materials.

1.2.2.2.3. Natural Polymers

Biological polymers found in nature and have been extracted from a range of biological species including rodents, crustaceans, insects, plants, and bacteria [76, 77]. Natural polymers typically consist of components found in the native extracellular matrix, which unlike synthetic polymers, make them inherently biological active, capable of promoting excellent cell adhesion and proliferation. For example, collagen is one of the most widely used and researched natural polymers for biomedical applications and has been extracted from numerous sources including bovine skin and tendons, porcine skin, intestine, and bladder mucosa, and rat tail. As a native component of the extracellular matrix (ECM), collagen electrospun grafts supports the infiltration of fibroblasts for appropriate heart tissue remodelling following myocardial infarction [78]. Additionally, natural polymers are biodegradable with non-toxic by-products, allowing host cells to produce their own extracellular matrix and replace the scaffold over time as it degrades. For instance, one commonly investigated polymer for wound dressings is alginate, a polysaccharide derived from brown seaweed. Alginate polymers biodegrade naturally into non-toxic byproducts and thus have shown minimal inflammatory and foreign body reactions in wound healing studies [79]. However, fabrication of natural polymer-based scaffolds with homogenous and reproducible architectures remains challenging [77]. This is mainly due to variability of processing of the raw material which often results in changes to polymer structure. For example, chitosan, a heavily researched polymer for cartilage, nerve, and tissue engineering, exhibits poor mechanical weakness due to the disruption of its native molecular weight distribution and/or degree of acetylation during its extraction from the exoskeleton of shellfish [80]. The inefficient processability of natural polymers also contributes to their generally poor mechanical properties which often limits their use in load-bearing applications, which has spurred the

investigation of another class of materials incorporating blends of both synthetic and natural polymers.

1.2.2.2.4. Composite scaffolds

The increasing trend of tissue engineering applications is the use of composite scaffolds which rely on the combination of biomaterials to appropriately balance their individual advantages and disadvantages. Typical composite scaffolds are those comprised of blends of synthetic and natural polymers, to provide appropriate mechanical properties while improving biocompatibility, respectively [81]. For example, blends of PCL with collagen (PCL/Collagen) for use in vascular tissue engineering have been demonstrated to enhance smooth muscle cell proliferation and growth while also increasing overall scaffold tensile strength [82]. Designing composite scaffolds of two or more materials often presents itself with increased complexity when attempting to regulate scaffold properties such as biocompatibility and/or biodegradation. Determining the appropriate amount of each composite constituent remains an ongoing challenge of scaffold design and involves mostly trial-and-error methodology. For example, recent work developing an ideal composite alginate/hydroxyapatite scaffold for bone ingrowth required an array of manufacturing parameters, most notably the investigation of a wide range of hydroxyapatite concentrations [83]. This process painstakingly investigated individual hydroxyapatite concentrations from 5-20% (w/v), in order to fabricate a suitable scaffold to study osteoblast compatibility [83].Further accentuating this challenge of scaffold design is the need for biomolecules to be incorporated into the scaffold architecture.

Common Scaffold Biomaterials			
Ceramics	**Synthetic Polymers**	**Natural Polymers**	**Composites**
Alumina	Polycaprolactone (PCL)	Collagen	PCL/Collagen
Zirconia	Polytetrafluoroethylene (PTFE)	Alginate	PCL/Chitosan
Hydroxyapatite	Poly(lactic-coglycolic acid) (PLGA)	Chitosan	Hydroxyapatite/ Alginate
Calcium Phosphate		Hyaluronan	

Figure 7 – Common Scaffold Biomaterials

Table of common classes of materials used in biomaterial scaffold fabrication and examples of the most commonly researched materials

1.2.3. Scaffold functionalisation

A considerable research area within scaffold design has been the adaptation of modification techniques aimed at improving scaffold properties such as biocompatibility and/or regulating biological processes, such as stimulating vascularisation. Today, the most promising scaffolds are typically comprised of synthetic materials that lack cell recognition sites. Therefore, the introduction of functional groups onto the scaffold surface is crucial and can serve as cell recognition sites or focal points for additional modifications with bioactive molecules. Surface functionalisation can be beneficial in regulating cell behaviour *in vitro* and *in vivo*, as well as provide favourable control over biological responses to the scaffold or construct following implantation. The study of biomolecular functionalisation will lead to promising bioactive materials with the ability to dynamically adapt to native tissue microenvironments meanwhile directing cellular function towards tissue regenerative outcomes.

1.2.3.1. Surface chemistry modification

Scaffold surface chemistry properties including hydrophobicity, surface charge density, micro-topography, and specific chemical groups can all impact a range of cellular behaviour including

adhesion, growth, migration, differentiation, matrix synthesis, and tissue morphogenesis [84]. Functional modifications of surface chemistry are thus crucial to inhibiting unfavourable cell effects while enhancing beneficial cell behaviour. Various modification methods are currently exploited to alter surface chemistry, impacting cell behaviour directly, or indirectly by providing functional groups to be used for the conjugation of bioactive molecules.

1.2.3.1.1. Wet chemistry approaches

A commonly practiced method of surface chemistry modification is by incubating scaffolds in aqueous chemical solutions for extended periods of time. Alkaline solutions have been shown to impart rough hydrophilic surfaces to biodegradable polymers which associates to improved cell morphology and viability. These wet approaches catalyse the cleavage of polymer backbones through accelerated hydrolysis, exposing organic chemical groups, such as carboxylic acid and hydroxyl groups, more readily recognizable to cells. Hydrolysis a simple and frequently used method of chemical functionalisation, however it is lengthy, highly pH dependent and leads to some degree of unwanted degradation of the polymer surface, negatively impacting bulk scaffold properties such as mechanical integrity.

Additionally, carboxylic acid groups require further 'activation' by turning the acid into a more active derivative or through chemical linkers for biomolecule conjugation. This is most commonly achieved through incubation in 1-ethyl-3-(3-dimethylaminopropyl) carbodiimide (EDC) and N-hydroxysuccinimide (NHS) buffered aqueous solutions that react with primary amines on proteins side chains and increase their coupling efficiency to the exposed carboxyl groups [85]. However, concerns about facilitating the same reactions between carboxyls and amine groups on proteins may result in unwanted crosslinking, folding, and/or aggregation of the molecules. Covalent linkages using chemical linkers have thus been developed to form more specific bridges within molecules through chemical groups such as thiols or amino acids such as cysteines [86]. However, the use of

linker-chemistry approaches is also limited because they are effective only on surfaces pre-treated with distinct functional groups, as well as rely heavily on wet chemistry reactions that are often complex, possess unwanted side-reactions, yield high variability, and often involve toxic solvents. These challenges highlight the need of alternative functionalisation methods.

1.2.3.1.2. Plasma immersion ion implantation

Functionalisation of scaffold surfaces through plasma treatment is becoming increasingly popular due to its simplicity and efficiency. Plasmas are generated by ionising a neutral gas, such as nitrogen, to a strong electromagnetic field. Incubation of biomaterial surfaces in plasma leads to chemical and physical modifications through electrons, ions, and radicals. Studies into plasma functionalisation have revealed that the energetic ion bombardment of the scaffold surface can yield radicals embedded in carbon rich surface layers. This functionalisation method, known as plasma immersion ion implantation (PIII), has been demonstrated to facilitate the covalent immobilisation of numerous biomolecules to a range of polymeric surfaces, all while retaining their biological function [87](Figure 8). Biomolecule immobilisation occurs in a single step directly from solution in native 3D conformations retaining their bioactivity. In these studies, covalent immobilisation was demonstrated by showing that immobilisation biomolecule surface layers were resistant to aggressive detergent washing protocols. Additionally, PIII treatment can be applied to any underlying material without affecting bulk scaffold properties [87]. This alternative approach simplifies the process of decorating scaffold surfaces with favourable biomolecules by delivering the strength and stability of covalent attachment, while eliminating the requirements and drawbacks of multi-step wet chemistry.

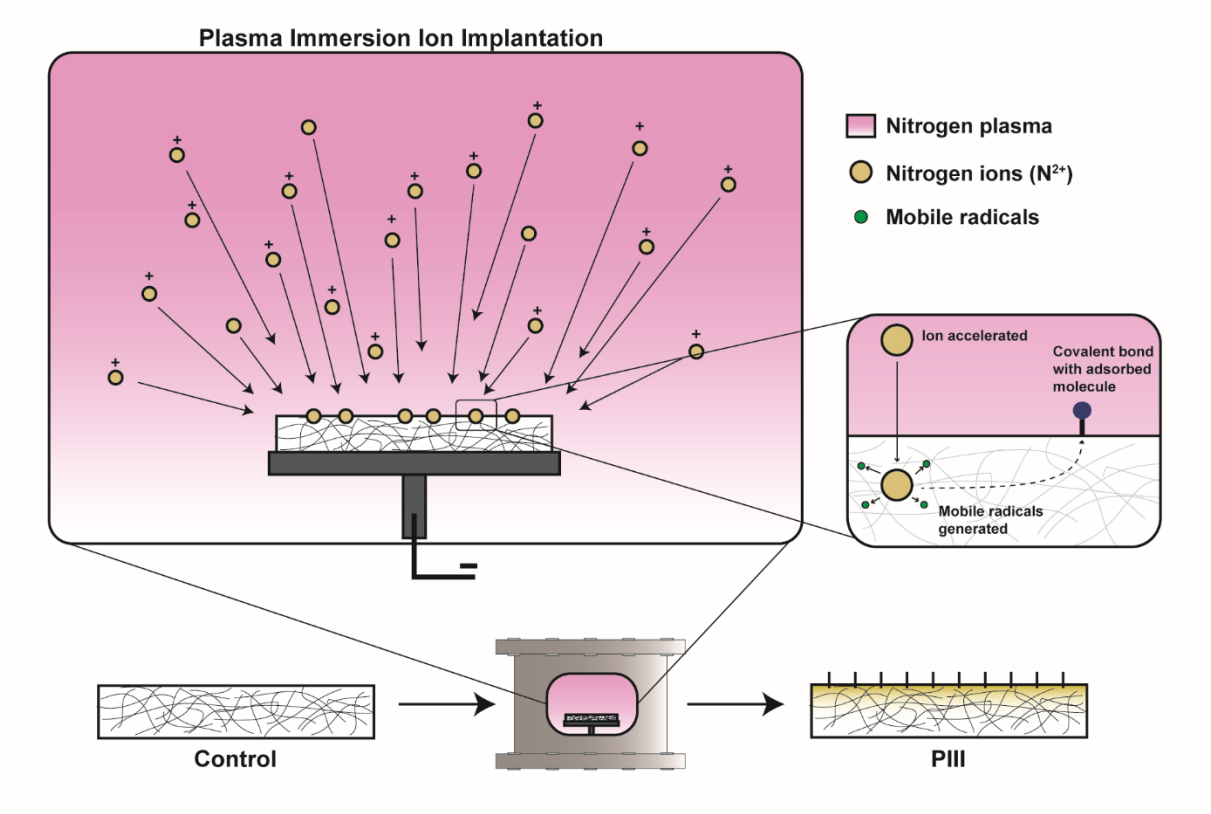

Figure 8 – Plasma immersion ion implantation (PIII)

PIII surface functionalisation involves the ionizing of a nitrogen gas to impart mobile radicals into the surface of an underlying polymer. Polymer substrates are placed into a plasma chamber and following PIII treatment, are capable of single-step surface immobilisation of biomolecules directly from solution.

1.2.3.2. Bioactive molecule incorporation

Unlocking the full potential of regenerative medicine and tissue engineering relies on controlling the delivery of biomolecules into the cellular microenvironment. Typically, this has been investigated through bioengineered materials and/or cells capable of spatiotemporal modulation of biomolecules release and presentation. The types of biomolecules incorporated into scaffolds can function either from the outside-in through the delivery of soluble and insoluble factors, such as proteins and cytokines, which signal by binding receptors on the outside of cells, or from the inside-out through the transfer of reprogramming genes. Although the biomolecules chosen are well-known to the target

tissue application and desired biological responses, it often the delivery and presentation methods which are crucial to their effectiveness in tissue engineering.

1.2.3.2.1. Release strategies

The simplest method of generating scaffolds containing functional biomolecules is by allowing the biomolecules to diffuse into and/or absorb into the scaffold. For example, porous scaffolds seeded with cells *ex vivo* are incubated in bioreactors with growth factor-rich media which infiltrate the scaffold through convection and diffusion [88]. In an effort to better mimic native physiologically environments, growth factors have been incorporated into matrices such as hydrogels, which release their loaded cargo during degradation [89]. In these cases, wet chemistry conjugations are often used to bind growth factors to polymer backbones. An alternative method is to utilize particulate delivery systems for controlled release. Micro- and nanoparticles fabricated from polymers incorporate therapeutic agents through the particle on loaded in their cores [90]. This prevents the cargo from biological degradation and clearance from the body, extending their functional bioactivity. Another advantage is the controlled release of the encapsulated cargo over time.

While numerous biomolecule release strategies exist, regenerative medicine applications typically require the synergistic functions of numerous factors and thus the temporally controlled sequential delivery of multiple biomolecules can often be challenging. Furthermore, although the rate of factor delivery may be regulated, the spatial localisation of the cargo is subjected to passive diffusion away from the implant site. This is more evident in dynamic flow environments such as in the cardiovasculature. Limited control over where soluble factors localise following delivery can often hinder the targeting of desired biological responses.

1.2.3.2.2. Covalent immobilisation

In covalent surface immobilisation, biomolecules are chemically bonded to the scaffold surface, resulting in a more efficient coating with longer retention compared to adsorption/release strategies.

As previously discussed, this can be achieved through linker or linker-free functionalisation treatments. Immobilisation results in a layer coating of biomolecules providing cues to facilitate target biological responses originating at the scaffold surface. For example, metallic stents have been immobilised with the antibodies specific for endothelial cells to facilitate increased endothelial cell covered on the stent surface [91]. As demonstrated in these studies, immobilisation can retain biological activity in high flow/dynamic environments.

While immobilisation strategies offer more control over the localisation of biomolecule delivery, these approaches possess their own set of drawbacks. Achieving the temporal presentation of multiple factors is not possible as they will exist as a cohesive layer on the exposed surfaces of the scaffold. Furthermore, the dosages of immobilised factors are limited by the surface area of the scaffold and can be significantly less in magnitude to the amount capable of being loaded in release delivery systems. Therefore, biomolecules for covalent immobilisation should be chosen as potent signalling factors capable of acting on multiple cell types and/or stimulating self-sustaining biological responses. Because the available surface area of the scaffold dictates the amount of biomolecule that can be presented through immobilisation, utilisation of this functionalisation method is often associated with the process of scaffold fabrication and the resulting scaffold architecture.

1.2.4. Electrospinning

Over the past decade, one of the fastest growing scaffold fabrication methods in research and commercial attention has been electrospinning [92]. Electrospinning is an electrostatic fabrication technique which produces polymer fibers ranging from nanometres to micrometres. Due to the common research goals of tissue engineering, the popularity of electrospun scaffolds has increased as their intrinsic nanofibrous topography is seen as a close working template to mimicking the native extracellular matrix. The general acceptance of electrospinning in the field of tissue engineering is evident by the fact that hundreds of universities and research institutes worldwide are investigating

the various aspects of the electrospinning method, and this is matched closely to the number of patents for electrospinning-based applications.

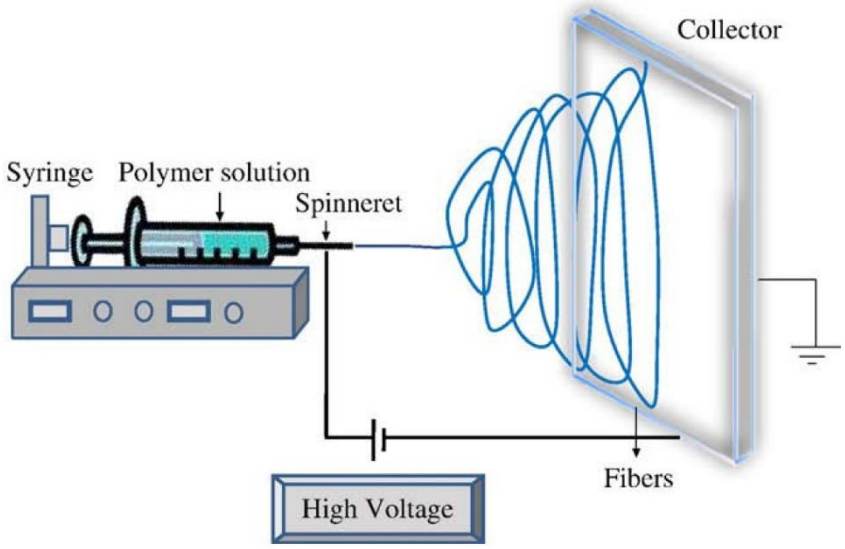

Figure 9 – Electrospinning Apparatus

Electrospinning is a fiber production method that uses electric force to draw charged threads of polymer solution into fiber diameters in the order of hundreds of nanometres. Adapted from [92]

1.2.4.1. Basic principles

Using electrostatic forces, electrospinning produces fine fibers from polymer solutions, both natural and synthetic [92]. The typical electrospinning apparatus utilizes three main components: a high voltage power supply, a spinneret, and a grounded metal collecting target (usually a screen, plate, or rotating mandrel) (Figure 9). Before the electrospinning process, polymers are dissolved in solvents to form polymer solutions. Because some polymer may emit unpleasant or harmful odours, electrospinning is often conducted within ventilated chambers. Direct current (DC) voltages in the range of tens of kilovolts (kVs) are required to generate electrostatic forces which charge the polymer solutions to a critical value where the electrical forces on the liquid overcomes the surface tension in the polymer.

This extrudes the polymer to form a Taylor cone, after which an unstable and rapid whipping of the solution jet occurs. During this process the diameter of the polymer solution decreases due to solvent evaporation. Once reaching the collection target, the polymer solution will have transitioned into a solid phase forming an individual fiber. Continual collection of these fibers form multilayered fibrous structures.

1.2.4.2. Fabrication parameters

The electrospinning process and the architecture of the resulting fibrous scaffolds are governed by numerous process parameters, including applied electric field, distance from tip to collecting target, and solution flow rate. Appropriate manipulation of these parameters produces nanofibers of desired diameter and morphology which then relay bulk scaffold properties such as porosity. One of the most systemically studied processing parameter on scaffold architecture is flow rate [93].

Flow rate influences the solution velocity from the syringe. A lower feed rate is more desirable for allowing solvent evaporation to occur before reaching the collection target. Numerous studies have confirmed that fiber and pore diameter of electrospun scaffolds increase with polymer flow rate [93]. Larger fibers typically yield increased surface area, scaffold features that become important for cell-scaffold contact as well as biomolecule immobilisation. However, at significantly high flow rates, even fiber morphology is lost as beaded fibers are observed because polymer solutions are not allowed to evaporate properly being reaching the collection target [94].

The expanding use of electrospun scaffolds in tissue engineering applications stems from easily tuneable scaffold parameters. Some of these advantages include high surface-to-volume ratio, porosity, wide range of three dimensional conformations, and limitless combinations of nanofiber composition. Scaffold characteristics can be tailored by simply changing single processing parameters such as flow rate. The conformations of electrospun scaffolds are determined by the type of collection target and have previously been spun into sheets, tubes, blocks and even biologically

inspired tissues such as heart valves. Furthermore, scaffold composition is determined simply by the polymer or polymer blends that are loaded into the syringe. In addition to fiber morphology, fiber composition also plays a role in determining essential scaffold features such as mechanical properties and degradation.

1.2.4.3. Application in tissue engineering

The intrinsic fibrous topography of electrospun scaffolds is viewed as essential for cell seeding, invasion, proliferation, and differentiation prior to the regeneration of biologically functional tissue or extracellular matrix. Numerous studies investigating a wide variety of cell types have reported that these scaffolds positively promote cell-matrix and cell-cell interactions, with cells maintaining normal phenotypes, morphologies, and gene expression [95-97]. The diameter of electrospun fibers can be fabricated in similar size to that fibrils of the extracellular matrix, and with the versatility of spinning natural polymers such as collagen, mimicking the native tissue environment becomes more attainable and increases the likelihood of improving cellular behaviour such as engraftment. Additionally, functionalisation treatments with biomolecules can improve these features even further. Electrospun scaffolds have been utilized in numerous tissue engineering applications include, cartilage [98], dermal tissue [99], arterial blood vessels [100], heart [101], and nerves [102].

1.2.4.4. PCL electrospun scaffolds

Of the many polymers currently used for electrospinning, poly(ε-caprolactone) (PCL) is the most widely researched polymer in tissue engineering [103]. PCL has good biocompatibility, excellent biodegradability, exhibits slow degradation rates (2-4 years depending upon the starting molecular weight) and has suitable mechanical properties for a variety of tissue engineering applications. Supporting its popularity is a history of use dating back to 1980 and FDA approval as a medical material for slow release drug delivery devices and sutures. However, one of the main disadvantages of PCL is its hydrophobicity, resulting in poor wettability, lack of cell attachment and uncontrolled

biological interactions. Surfaces with increase hydrophobicity generally lead to the poor absorption of proteins and subsequent unfolding and therefore poor cell attachment. This issue is largely addressed through the incorporation of biologically active components using two previously discussed methods. The first is by blending PCL with appropriate amounts of natural polymers like collagen. The second is through surface functionalisation of bioactive molecules.

However, while PCL serves as an excellent starting template for the development of many tissue engineering scaffolds, there remains an ongoing challenge in tailoring them for specific tissue engineering applications. The design parameters to choose from include limitless copolymer blends and ratios, functionalised biomolecules, and mechanical dimensions. These are also separate to the *in vivo* challenges of inflammatory foreign body responses which can impair scaffold function following implantation. Raising these concerns highlights some of the translational challenges which must be overcome before these scaffolds can be considered for clinical use.

1.3. Translational Scaffold Design Challenges

Tissue engineering scaffolds are subject to numerous design constraints which demand specific features previously discussed, including vascularisation, degradation, mechanical properties, and biocompatibility. While these properties are often exemplified in research studies, the manufacturing of these scaffolds must also occur within clinically relevant timelines with appropriate assurances of safety, sterility, stability, and cost-efficiency. Developing tissue engineering scaffolds for clinically relevant application requires a delicate balance between efficacious scaffolds and robust, scalable, and affordable production methods. The commercialisation of tissue engineering solutions also requires off-the-shelf properties which determine the levels of practicality for therapeutic intervention. It is often the case that promising findings in research studies are either too complicated to produce and/or do not consider the range of clinical challenges arising along the path of scaffold development, implementation, and integration. In this regard, while many of the beneficial effects of

current scaffolds and constructs are often reported, the need for tissue engineered solutions that can wholly integrate with the human body still exists. As previously discussed, tissue engineering solutions for creating complete and functioning full organs are still not achievable. Even for smaller applications, implants that last the lifetime of the patient are rare. The ability to integrate with the human body over time is the first step towards efficacious design and translation of the beneficial properties of tissue engineering solutions.

1.3.1. Host integration

As tissue engineering and regenerative medicine are considered for use in the medical care setting, the integration of these solutions with the surrounding natural tissue environment of treated patients is of paramount importance. Although certain stem cell types have achieved short-term success as therapies for various diseases, it is still unclear whether they are capable of forming whole new tissues themselves or stimulate local cells to regenerate. In either case, the resulting outcome is typically poorly connected to the surrounding tissue environment and functionality of the tissue engineered scaffold/construct is drastically impaired after a few months. Genuine integration can be achieved by designing bioactive materials that not only act as scaffolds for cells to adhere to and form new tissue, but also provide cues and signals that regulate the innate biological responses that are crucial to and/or hinder integration.

1.3.1.1. Mass transport through vascularisation

Several techniques exist for the creation of cellularised scaffolds, but constructs that match the cellular density of native tissue and organs remains a challenge in tissue engineering. Increased cell density requires an increased demand for infrastructure capable of mass transport, such as oxygen and nutrients exchange with cell products and waste. As previously discussed in close association with scaffold porosity, mass transport is an important aspect of scaffold integration. Diffusion is an inadequate method of mass transport when it comes to the scale of full tissue and organ regeneration.

This is particularly the case in regards to scaffolds and constructs that seek to replace organs with endocrine functions [104]. Cells must have close proximity to a functioning and stable blood supply in order to sense physiological indicators and respond appropriately, while also allowing access to nutrients necessary to their survival.

Strategies to address mass transport include promoting pre-vascularisation of the scaffold or construct prior to implantation, or guide *in situ* vascularisation once the material has been implanted. Pre-formation of vasculature has been explored through the seeding of endothelial cells as part of cell-laden constructs [105]. In combination with porous structures, tubular structures can be formed *in vitro* which can then form functional vascular elements or fuse with native vessels once implanted [106]. Guided vascularisation *in vivo* is primarily achieved through recruitment of host cells through the scaffold to participate in angiogenesis. Potential targets include leveraging the pro-angiogenic function of macrophages, along with the engineered delivery of pro-angiogenic factors such as VEGF and FGF-2 [107]. Such strategies rely on continual interactions with the surrounding biological environment, and thus ensuring these interactions are able to take place is a crucial factor to long-term tissue integration and eventual regeneration.

1.3.1.2. Foreign body response

One of the first host reactions towards an implanted biomaterial is the activation of a foreign body response [108] (Figure 10). Foreign body responses are inflammatory driven processes conserved as protective mechanisms to defend the body from foreign pathogens. The outcomes of the foreign body response are isolation of the implant, preventing biological interaction with the surrounding microenvironment. Without intervention the foreign body response can severely impact the function of scaffolds serving as structural support, drug delivery vehicles, sensory devices, electrical devices or constructs containing proteins, cells, and other biological components [108]. Consideration of the foreign body response when designing the scaffolds for tissue engineering is essential to improving

its long-term biocompatibility, safety, and function. Mitigating the foreign body response involves a deeper understanding of the biological process which regulate its activation in order to identify suitable target cells and/or signalling factors.

1.3.1.2.1. Innate immune response

The implantation of a biomaterial activates the same mechanisms of wound healing with one of the primary stages being the activation of the innate immune response. However, the extent and degree of inflammatory activation is determined by the extent of injury during the implantation procedure, the tissue or organ into which the biomaterial is being implanted, and the size of the implant/provisional matrix formation. As previously discussed, monocyte-derived macrophages facilitate numerous roles throughout the innate wound healing process. In response to biomaterial-mediated immune responses, macrophages play an even larger role in facilitating inflammation [109]. When macrophages arrive at the surface of an implant, they initiate phagocytotic functions in an attempt to engulf the implant. When the implant is too large, the formation of an adherent layer of inflammatory macrophages results on the implant surface. In normal wound healing mechanisms, acute inflammation is generally followed by immune resolution through the degranulation of leukocytes, signalling apoptosis and anti-inflammatory cytokine release from macrophages. However, in response to biomaterials, because macrophages are unable to phagocytose the implant, chronic inflammation occurs, involving the further recruitment of inflammatory cells, and macrophages fuse to form foreign body giant cells (FBGC). Through the release of inflammatory mediators, reactive oxygen species and enzyme production, macrophages and FBGC create a low-pH microenvironment at the implant surface that acts synergistically with its secreted factors to damage the material surface through degradation mechanisms such as oxidative chain cleavage, hydrolysis, or stress cracking. Degradation leads to compromises in structural integrity, function, and ultimately safety of the implant.

1.3.1.2.2. Fibrotic capsule formation

Once chronic inflammatory responses have determined the material cannot be engulfed, it is effectively walled off from the local tissue environment by fibrous encapsulation. The thickness of the fibrous capsule around the material is often used as an assessment of a material's biocompatibility. Collagen is the main constituent of fibrous capsules, synthesised by fibroblasts in concentric layers around the implant. The capsule creates a physical barrier between the material and the local biological environment. As a result, mass transport from the scaffold is significantly reduced. In biosensing devices, the fibrous capsule induces significant delays if not complete loss in measurements of desired analytes [110]. In drug delivery systems and cell seeded constructs, it obstructs the therapeutic effects of the drug and biomolecule release, as diffusion through the capsule towards adjacent target tissue is limited or absent.

1.3.1.2.3. Macrophage polarisation

Macrophage activation is a central inflammatory theme of both innate healing mechanisms and foreign body responses. The phenotypes of macrophages exist along a spectrum of polarisation states related to their functional diversity. At one end of the spectrum are pro-inflammatory "M1", and at the other end are anti-inflammatory "M2". In the context of biomaterial implantation, M1 macrophages express inflammatory antigens such as major histocompatibility complex class 2 (MHC Class II) and initiate immune response that leads to the recruitment of inflammatory cells through the production and release of inflammatory cytokines such as interleukin-1β (IL-1β) and tumour necrosis factor-α (TNF-α) [111]. M2 anti-inflammatory macrophages consistently express mannose receptors (CD206) and release anti-inflammatory cytokines such as IL-10 and TGF-β [111]. The presence of such anti-inflammatory cytokines within the tissue remodelling process has been reported to aid in the vascularisation of numerous biomaterials.

Unlike terminally differentiated cells, macrophages are capable of switching polarisation states in response to their microenvironment, and this transitory nature is often related to their paracrine signalling functions. For example, the induction of pro-inflammatory cytokine release following lipopolysaccharide (LPS) stimulation of macrophages can be significantly dampened in the presence of interleukin-4 (IL-4), a M2 polarising cytokine released by nearby M2 macrophages and other leukocytes [112]. This suggests that the presence of macrophages in different polarisation states within the same microenvironment can potentially be harnessed. As a result, well-established M2 polarising cytokines such as IL-4 are highlighted as potential therapeutic biomolecules to minimize inflammatory responses and induce constructive modelling.

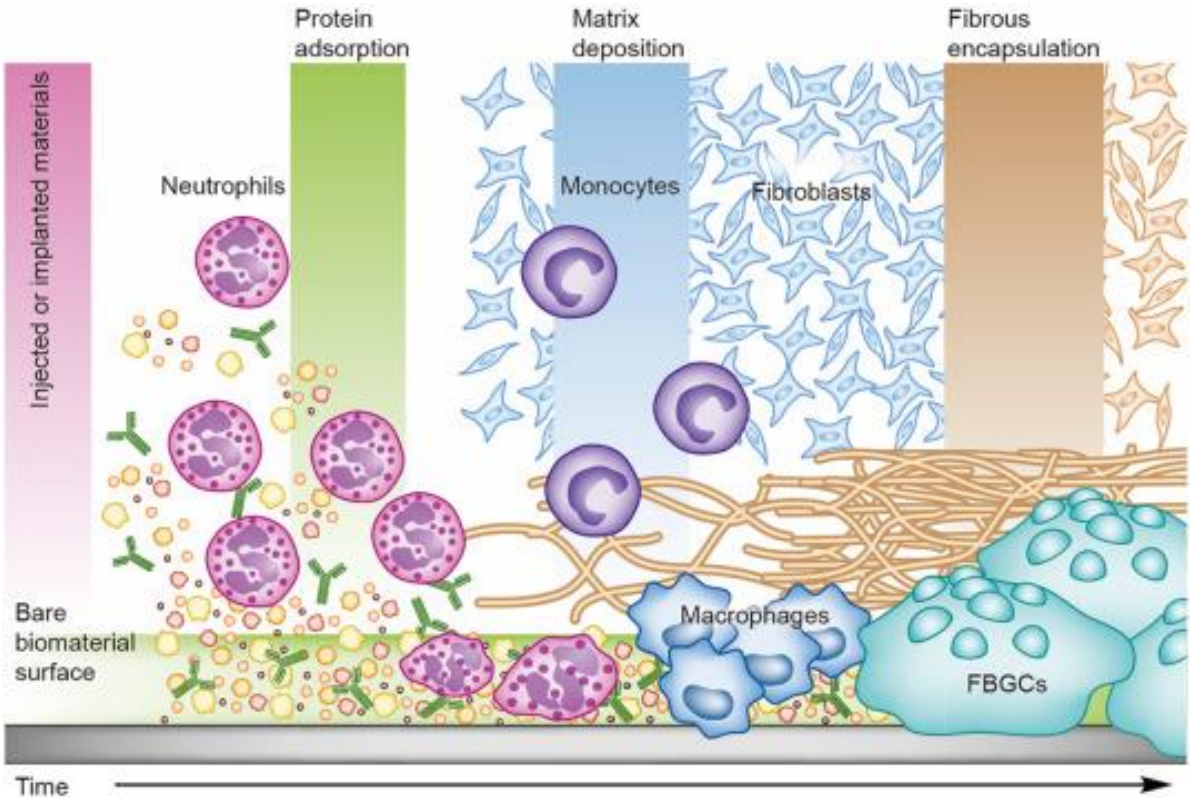

Figure 10 – Foreign Body Response (FBR)

The FBR is a biological response to any foreign material implanted into the tissue characterised mainly by the accumulation of inflammatory cells of the innate immune system on the surface of the implant which then leads to the encapsulation of the implant in a fibrotic capsule that serves to isolate

it from the surrounding biological tissue. The foreign body response hinders the efficacy and safety of any medical device implanted into the body.

1.3.2. Time and cost constraints

Besides demonstrating numerous biological benefits, the clinical and commercial success of tissue engineering products relies on its time and cost-effectiveness, highlighting an additional challenge in balancing sophistication and ease of production. The time required to produced full-sized tissue replacements depends on the manufacturing of the scaffold and/or generation of sufficient quantities of therapeutic cells. More specifically the required time to prepare tissue engineering solutions is a large determinant of their clinical translation as is often referred to as its "off-the-shelf" property. Characterisation as off-the-shelf requires that fabrication time frames match those of the clinical need of the patient. Additionally, more time and complexity associated with fabricating the scaffold or preparing it for implantation translates to higher costs. Several advancements have been made in areas of rapid or high-throughput manufacturing of biomaterial scaffolds, such as in-line production methods and automated printing [69]. However, the pace of producing therapeutic cell types remains an ongoing challenge.

1.3.2.1. Cellular vs acellular approaches

Bioreactor systems have been developed to generate large quantities of stem cells, however the capability of reliably producing fully differentiated cells in clinically relevant timeframes remains an unmet need [113]. Once sufficient numbers of cells are generated, primary cells have limited time windows for use, as they become senescent in later passages [114]. In applications where they may be required to repeatedly proliferate, this may present a problem. However, this does not really affect applications where their paracrine effects are needed for a relatively short amount of times, enough to stimulate biological processes such as angiogenesis. Additionally, the cell source of constructs presents an additional bottleneck in manufacturing. Because of possible immune rejection and the

requirement of life-long immunosuppressive treatment, the increasing trend of cell-based tissue engineering therapies is moving towards re-engineered allogenic or xenogeneic stem cell sources that can potentially evade host detection. However, these traits also lay the potential foundation for cancer cells and tumour formation. Alternatively, with constructs based on autologous cells, tissue samples must first be harvested from patients individually, followed then by isolation, expansion and seeding. This production chain represents batch processing methods rather than continuous processing extending both time and costs. Improving the scalability and efficiency of stem cell production relies on advances in stem cell biology. Concurrent to these research studies, tissue engineering approaches using acellular scaffolds are also be investigated and their translational challenges considered.

Some of the obvious challenges to large-scale manufacturing of biomaterial scaffolds is the requirement to be specifically tailored to individual patients. A “one size fits all” mentality towards tissue engineering is unrealistic considering that the anatomy, physiology, and regenerative capacities differ within patients and amongst disease states. Relying on the endogenous healing potential of individuals, especially when comparing healthy to diseased patients, may require different doses of functionalised biomolecules, which are crucial to the biological function of acellular scaffolds. Additionally, as the behaviour of infiltrating cells are determined by the surface chemistry and composition of the scaffold, manufacturing considerations of scaffolds should also be considered.

1.3.2.2. Scaffold manufacturing

Scaffold composition determines the types of materials required and thus related time and costs of manufacturing. When blends of both synthetic and natural materials are balanced for purposes of achieving desired scaffold properties, such as biocompatibility or biodegradation, manufacturing considerations must also be taken to factor in costs and feasibility of preparation. Synthetic materials like PCL are typically cheap to produce and can be manufactured in large batches with high reproducibility. On the other hand, natural materials such as collagen are often expensive to derive,

and processing methods typically have small yields with high variability between batches. To overcome this, cheaper derivatives such as gelatin (a low-cost denaturation product of collagen) are typically employed, although higher percentages are often required within the composite to account for diminished biological properties [115]. Adding considerations of time and cost-effectiveness of materials chosen for scaffold fabrication poses additional hurdles within the challenges of scaffold design.

In addition to creating scaffolds with multiple materials, the need for controlled architectures and multiple deliverable biomolecules is almost impossible with a single-step fabrication process. The processes contributing major delays to fabrication are conventional functionalisation methods which typically involve multiple steps in the time scale of days [65]. Pre-functionalisation of implants would also exhibit very poor off-the-shelf properties as the decorated biomolecules outside of reconstitution buffers would most likely possess minimal shelf-lives. Thus, biomolecule functionalisation would have to occur on-demand requiring increased preparation times prior to implantation. However, with the advent of plasma surface treatments such as PIII, some of the translational time constraints of conventional functionalisation methods would be drastically reduced to a single step process. Furthermore, the shelf-life of the functional groups imparted by PIII have been previously validated to last up to one year, meaning pre-functionalised implants could sit on the shelf and rapid functionalisation conducted prior to surgery with minimal preparation time.

1.3.3. Identifying candidate scaffolds

Given the many current challenges of scaffold design, both biological and translational, the identification, optimisation, and translation of the next generation of tissue engineering scaffolds would undoubtedly benefit from design tools that could potentially simplify the design process. Current biomaterials research traditionally adopts a trial-and-error approach, by altering previous design iterations based on *in vitro* and/or *in vivo* experimental findings. However repeated

experimentation is costly, and time consuming, and often *in vitro* findings correlate poorly to *in vivo* processes. A beneficial feature in scaffold design would be the ability monitor tissue and scaffold performance over the lifetime of the implant. Real-time monitoring of scaffolds, through the development of advanced imaging strategies, would enable tissue engineering products to be fine-tuned using an analytics-based approach to modify design iterations.

1.3.3.1. Real-time scaffold monitoring

Currently, magnetic resonance imaging (MRI) [116], positron emission tomography (PET) [117] and multiphoton imaging techniques [118] are being trialled to facilitate the tracking of cells within scaffolds, however the sensitivity and resolution of these techniques are still not clinically relevant. Additionally, these imaging methods often require the introduction of tracer agents into cells and have been reported to alter native cell function. For this reason, the imaging modalities of bioluminescence have become increasingly popular. Bioluminescence is a form of chemiluminescence where photon emission is based on a natural enzymatic biochemical reaction of the firefly luciferase enzyme and the luciferin substrate [119]. Bioluminescence chemistries have become a widely preferred method of quantitative bioanalysis because they can deliver up to 10- to 1000-fold higher sensitivity than traditional fluorescence assays. Bioluminescent reporters have been demonstrated to be stably transfected into practically any cell type and form transgenic mouse strains (Figure 11), allowing for imaging in many applications. Furthermore, catalysing bioluminescence reactions have been shown to not affect native cell function and can be conducted repeatedly within the same cells over time [119, 120]. Nevertheless, combining real-time monitoring within tissue engineering products by leveraging advanced imaging techniques could potentially simplify the scaffold design process by permitting the timelier identification of candidate scaffolds for numerous tissue engineering applications.

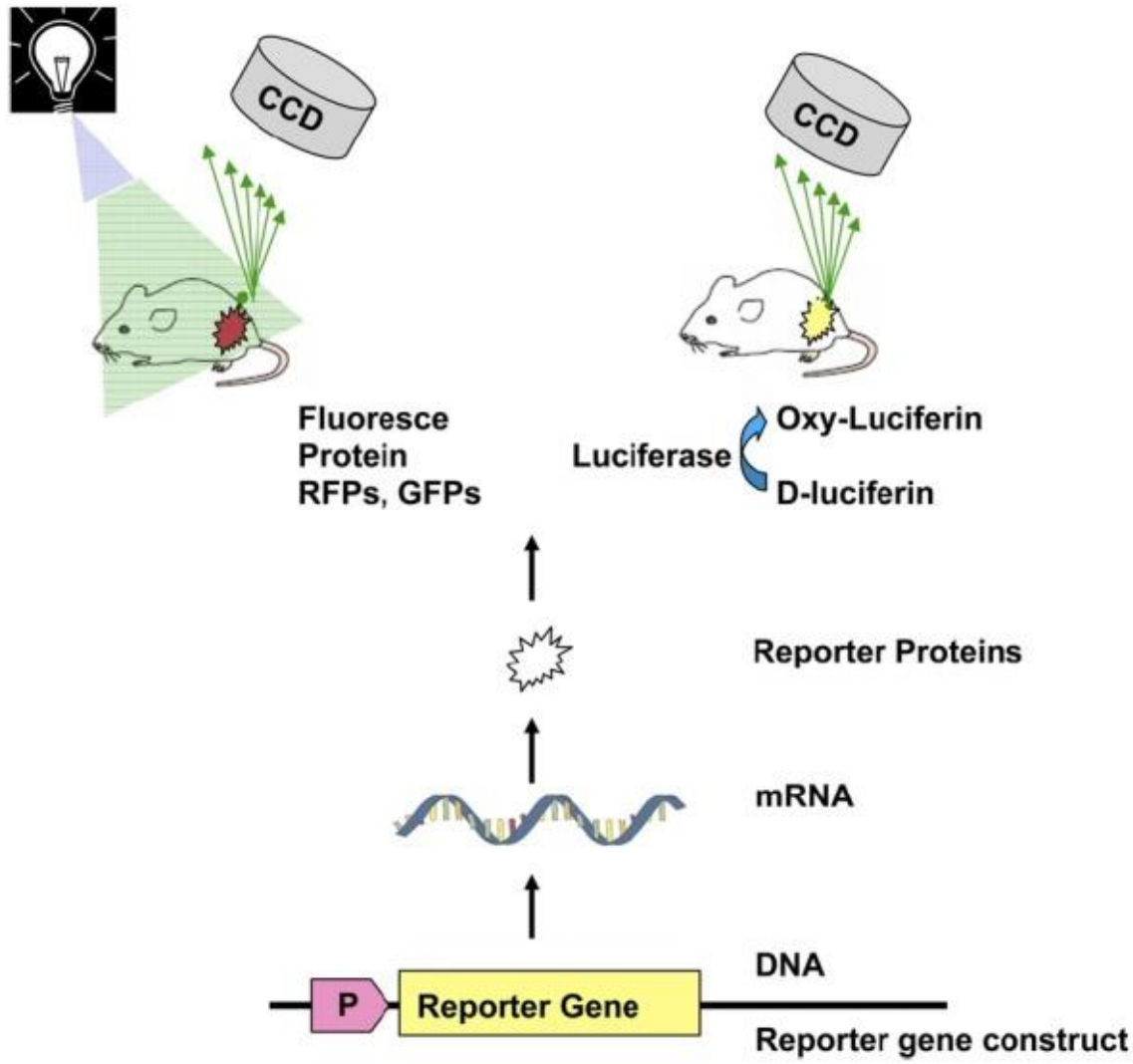

Figure 11 – Transgenic Dual-Reporter Mice

The strategy of promoter (P)-reporter gene constructs for non-invasive imaging and tracking of cells. Encoded reporter proteins include fluorescence proteins and/or bioluminescent enzymes such as luciferase. These reporters can be stably transfected into cells or genetically encoded into transgenic mice to enable real-time monitoring of cell behaviour. Adapted from [119].

1.4. Aims

There is a considerable deficiency in the development of translational tissue engineering solutions for regenerative medicine. In this chapter, we identify inadequacies within the three major components of the tissue engineering field that contribute to this deficiency:

1. Inefficiency of conventional trial-and-error scaffold design processes
2. Lack of suitable stem cell sources with regard to appropriate sources, numbers, and production
3. Lack of functionalisation strategies with translational features necessary for patient use

As such, the overarching aims of this thesis will focus on addressing these inadequacies to improve the development of translationally relevant tissue engineering solutions for regenerative medicine. These include:

1. Develop a high throughput model for scaffold monitoring to increase the efficiency of scaffold design for specific tissue engineering applications.

2. Investigate novel stem cell sources, with high availability and unlimited renewal, for tissue regenerative potential.

3. Develop scaffold functionalisation strategies that possess both translational features and maintain biological function.

Chapter 2

Non-Invasive Tracking of Bone Marrow Mononuclear Cells to Injury and Implanted Biomaterials

Acta Biomaterialia 53 (2017) 378–388

Contents lists available at ScienceDirect

Acta Biomaterialia

journal homepage: www.elsevier.com/locate/actabiomat

Full length article

Non-invasive tracking of injected bone marrow mononuclear cells to injury and implanted biomaterials

Richard P. Tan [a,b], Bob S.L. Lee [a], Alex H.P. Chan [a,b], Sui Ching G. Yuen [a], Juichien Hung [a], Steven G. Wise [a,b,c,*], Martin K.C. Ng [a,c,d,*]

[a] The Heart Research Institute, Sydney, NSW 2042, Australia
[b] Sydney Medical School, University of Sydney, NSW 2006, Australia
[c] School of Life & Environmental Science, University of Sydney, NSW 2006, Australia
[d] Royal Prince Alfred Hospital, Sydney, NSW 2042, Australia

ARTICLE INFO

Article history:
Received 31 October 2016
Received in revised form 31 January 2017
Accepted 1 February 2017
Available online 3 February 2017

Keywords:
Bone marrow mononuclear cells
Subcutaneous implant
Bioluminescence
Tissue regeneration

ABSTRACT

Biomaterial scaffolds enhancing the engraftment of transplanted bone marrow mononuclear cells (BM MNC) have enormous potential for tissue regeneration applications. However, development of appropriate materials is challenging given the precise microenvironments required to support BM MNC engraftment and function. In this study, we have developed a non invasive, real time tracking model of injected BM MNC engraftment to wounds and implanted biomaterial scaffolds. BM MNCs, encoded with firefly luciferase and enhanced GFP reporter genes, were tail vein injected into subcutaneously wounded mice. Luciferase dependent cell bioluminescence curves revealed our injected BM MNCs homed to and engrafted within subcutaneous wound sites over the course of 21 days. Further immunohistochemical characterization showed that these engrafted cells drove functional changes by increasing the number of immune cells present at early time points and remodelling cell phenotypes at later time points. Using this model, we subcutaneously implanted electrospun polycaprolactone (PCL) and PCL/Collagen scaffolds, to determine differences in exogenous BM MNC response to these materials. Following BM MNC injection, immunohistochemical analysis revealed a high exogenous BM MNC density around the periphery of PCL scaffolds consistent with a classical foreign body response. In contrast, transplanted BM MNCs engrafted throughout PCL/Collagen scaffolds indicating an improved biological response. Importantly, these differences were closely correlated with the real time bioluminescence curves, with PCL/Collagen scaffolds exhibiting a ~2 fold increase in maximum bioluminescence compared with PCL scaffolds. Collectively, these results demonstrate a new longitudinal cell tracking model that can non invasively determine transplanted BM MNC homing and engraftment to biomaterials, providing a valuable tool to inform the design scaffolds that help augment current BM MNC tissue engineering strategies.

Statement of Significance

Tracking the dynamic behaviour of transplanted bone marrow mononuclear cells (BM MNCs) is a long standing research goal. Conventional methods involving contrast and tracer agents interfere with cellular function while also yielding false signals. The use of bioluminescence addresses these shortcomings while allowing for real time non invasive tracking *in vivo*. Given the failures of transplanted BM MNCs to engraft into injured tissue, biomaterial scaffolds capable of attracting and enhancing BM MNC engraftment at sites of injury are highly sought in numerous tissue engineering applications. To this end, the results from this study demonstrate a new longitudinal tracking model that can non invasively determine exogenous BM MNC homing and engraftment to biomaterials, providing a valuable tool to inform the design of scaffolds with implications for countless tissue engineering applications.

* Corresponding authors at: Applied Materials Group, The Heart Research Institute, NSW 2042, Australia (S.G. Wise). Department of Cardiology, Royal Prince Alfred Hospital, Missenden Rd, University of Sydney, NSW, 2050, Australia (M.K.C. Ng).
E-mail addresses: Steve.Wise@hri.org.au (S.G. Wise), mkcng@med.usyd.edu.au (M.K.C. Ng).

http://dx.doi.org/10.1016/j.actbio.2017.02.002
1742-7061/

1. Introduction

One of the most widely used cell therapies for tissue regenera tive applications are the transplantation of exogenous bone mar row mononuclear cells (BM MNC), having been employed as treatments for various medical conditions including myocardial infarction [1,2], limb ischemia [3] and traumatic brain injury [4]. The demonstrated tissue regenerative effects of BM MNC are thought to arise from three major classes of stem cells that exist within the BM MNC fraction: hematopoietic stem cells (HSCs), mesenchymal stem cells (MSCs), and endothelial progenitor cells (EPCs) [5]. However, BM MNC therapy has not yet met expectations for clinical efficacy due to their poor survival and engraftment at sites of injury following transplantation [6]. Indeed, BM MNC function is closely related to their local microenviron ment niche, which provides both mechanical and chemical cues that support growth and control differentiation. Importantly, necrotic tissue at sites of injury are largely void of these cues, accentuating the challenge of effective therapy [7]. Tissue engi neering aims to provide artificial microenvironments using bioma terial scaffolds which better regulate BM MNC behaviour and survival [8].

The physical and mechanical properties of implanted biomate rials largely determine the nature of ensuing BM MNC responses. More closely mimicking the native bone marrow niche *in vivo* through tailoring of scaffold parameters including material compo sition, dynamic control of soluble and surface bound cytokines, and physicochemical cues is a favoured approach [8]. However, appropriate mimicry of the extracellular matrix and BM MNC niche is complex and elusive [7]. In combination with an optimal blend of mechanical properties and signalling cues, candidate scaf folds would ideally be available off the shelf to make them clini cally applicable. The most effective current strategies involve pre seeding of BM MNC subpopulations onto scaffolds prior to implantation [9]. However, this severely diminishes the feasibility of clinical application, due to lengthy time requirements for cell harvest, culture, and seeding and the high regulatory burden and cost. Additionally, *ex vivo* expanded BM MNC subpopulations often display altered signalling responses, function and phenotype [10]. Together, these shortcomings have prompted investigation into the cellularization of scaffolds by endogenous recruitment of BM MNC cells *in vivo*, an approach known as *in situ* tissue engineering [11]. Similarly, approaches combining exogenous BM MNC injec tions with implanted scaffolds tuned to recruit and engraft BM MNCs at the site of injury hold significant promise [12].

The model application for *in situ* tissue engineering strategies would see biomaterial scaffolds implanted prior to BM MNC injec tion, serving structural functions in the short term, then facilitate recruitment of injected BM MNCs in the midterm, and eventually lead to long term remodelling and being entirely replaced by new functional tissue. However, as previously mentioned, bioma terial scaffolds possessing appropriate parameters that favourably regulate BM MNC function must first be developed. To more read ily achieve this, *in vivo* responses of transplanted BM MNC popula tions towards these biomaterials must first be better understood.

In this study, we developed a model which tracks the temporal and spatial distribution of intravenously injected BM MNCs, specifically their homing and engraftment. By measuring the luciferase induced bioluminescence of these cells in real time, we were initially able to model injected BM MNC engraftment responses to injury. In addition we show, through immunohisto chemical analysis, that engraftment of these cells leads to func tional effects by elevating the presence of cell phenotypes known to participate in the native response to injury. Extending the utility of this model, we further examined its ability to distinguish *in vivo* engraftment of injected BM MNC to two model scaffolds. We demonstrate the bioluminescent curve of each scaffold closely relates to the ensuing BM MNC engraftment responses towards the scaffold post implantation. Furthermore, we reveal that differ ing engraftment responses elicit distinct scaffold remodelling changes. These findings represent an effective tool to determine, in real time, biomaterial scaffolds more favourable to injectable BM MNC therapies.

2. Materials and methods

2.1. Reagents

D luciferin potassium salt was purchased from Cayman Chem icals (Ann Arbor, MI, USA). Lympholyte® M cell separation media was purchased from Cedarlane Labs (Burlington, ON, CA). Endothe lial Basal Media (phenol red free) was purchased from Lonza (Switzerland). Polycaprolactone (PCL) polymer and 1,1,1,3,3,3 hex afluoro 2 proponal (HFP) solvent were purchased from Sigma Aldrich (St. Louis, MO, USA). Purified, soluble ovine collagen was obtained from CollTech (Osborne Park, WA, Australia) and lyophi lised as previously described [13]. Multiple Stain Solution (MSS) and JB 4 resin were purchased from Polysciences Inc. (Warrington, PA, USA).

2.2. FVB L2G mice

Donor firefly luciferase and enhanced green fluorescent protein (eGFP) co expressing transgenic mouse strains (FVB L2G) were purchased from Jackson Laboratories (Bar Harbor, ME, USA) (FVB/NJ Tg(Hspa1a luc, EGFP)2Chco/J, stock no. 012370) [14,15]. Recipient FVB neutral wildtype (WT) mice were purchased from Australian BioResources (Moss Vale, NSW, Australia).

2.3. Density gradient isolation of BM MNCs

Female FVB L2G mice, aged 7 8 weeks, were anaesthetised under 2% methoxyfluorane and sacrificed by cervical dislocation. To collect the bone marrow, tibias and femurs were explanted and flushed using a 21 gauged needle with sterile PBS. The bone marrow was then layered on top of Lympholyte® M cell separation media (6 ml per one pair of tibia and femur) and centrifuged at 1250×*g* for 25 min with deceleration off. The resulting buffy coat was aspirated and washed three times in sterile PBS: 800×*g* for 10 min, 50×*g* for 10 min, and 200×*g* for 10 min. Following the last wash, the pellet of BM MNC was resuspended in EBM (phenol free) to desired cell concentrations [6].

2.4. Bioluminescence imaging

D luciferin was reconstituted at a concentration of 40 mg/ml. Binding of the luciferin substrate to the luciferase enzyme results in bioluminescence, quantified using the IVIS Series pre clinical *in vivo* imaging system apparatus (Perkin Elmer). To induce biolu minescence, luciferin was given at a total volume of 50 µl for cells and 200 µl (intra peritoneal) for mice. Bioluminescence was mea sured in units of radiance (photos/s/cm^2/steradian). All biolumi nescence measurements were calculated within a pre defined region of interest (ROI). The mean radiance values within an ROI were recorded. For BM MNC tracking to wounds, the mean radi ance for each of the four wound ROIs were averaged to give a single bioluminescence value for each mouse. Bioluminescent profiles represent average measurements of n = 6 mice per group per time point. For BM MNC tracking to scaffolds, mean radiance measure

ments for each scaffold ROI were averaged amongst an n = 6 per group per timepoint.

2.5. Electrospinning

Polycaprolactone (PCL) was dissolved at 10% (w/v) in 1,1,1,3,3, 3 hexafluoro 2 propanol (HFP). PCL/Collagen blends were made by dissolving PCL and collagen simultaneously in a 10% (w/v) HFP solution comprising 90% PCL and 10% collagen. Solutions were loaded into a syringe and fed through a 0.6 mm diameter needle at a flow rate of 4 ml/h using a syringe pump. The needle was con nected to a 20 kV positive power supply and directed at a grounded parallel plate collector at a distance of 20 cm. Scaffolds were then cut into circular discs using a 1 cm diameter biopsy punch. Before implantation, scaffolds were sterilized by UV light for 30 min and washed three times with and stored in sterile PBS.

2.6. Scaffold characterization

Scaffold surfaces were imaged under a 15 kV scanning electron microscope (SEM) at 4000x magnification under high vacuum con ditions. Images were taken for n = 5 scaffolds/group then n = 30 fibers were measured for each sample. For porosity measurements, scaffolds were embedded in JB 4 resin and cut in 5 μm cross sections. Cross sections were stained using Multiple Stain Solution and imaged at 40x magnification. Cross section images were then converted to 8 bit grayscale and the percentage of white (pores) vs black (scaffold) were quantified as porosity.

2.7. Mouse subcutaneous homing and engraftment model

Study approval was obtained from Sydney Local Heath District Animal Welfare Committee (protocol number 2013/050). Experi ments were conducted in accordance with the Australian Code of Practice for the Care and Use of Animals for Scientific Purpose. Under 2% methoxyfluorane anaesthesia, mice had their dorsal sur faces shaved, sterilized with betadine solution, and washed clean with sterile PBS. Four 1.5 cm incisions (two rows side by side) were then cut through the skin to create four subcutaneous pockets [16]. For scaffold experiments, PCL or PCL/Collagen scaffolds were inserted into each incision. Each mouse received two PCL and two PCL/Collagen scaffolds. The wounds were closed with 6 0 silk sutures. While still under anaesthesia, mice were then tail vein injected with 200 μl of isolated BM MNC in EBM (phenol free) solution (1.5×10^7 cells/ml). Mice were then allowed to recover for at least 1 h. Mice underwent IVIS imaging over the course of 21 days in parallel to groups of mice that were sacrificed for skin wound biopsies alone or together with scaffold implants at defined histological time points.

2.8. Histology and immunohistochemistry

Skin biopsies were fixed in 4% paraformaldehyde for up to 4 h at room temperature then changed to 70% ethanol for at least 24 h. Following dehydration overnight in a tissue processor, biopsies were embedded in paraffin. Tissue samples were cut into 5 μm thick transverse sections using a rotary microtome, deparaffinised, and stained. For histology stains, standard H&E was used to assess total cell infiltration. For immunohistochemistry analysis, paraffin sections were stained with primary antibodies including anti neutrophil elastase (NE) (Abcam, USA) for neutrophils, anti CD68 (Abcam, USA) for macrophages, anti vimentin (Abcam, USA) for fibroblasts, and anti CD31 (Abcam, USA) for endothelial cells. Flu orescence microscopy was then used to visualise cell markers using Alexa Fluor 594 conjugated secondary antibodies. All eGFP staining was done using cryosectioning. Briefly, tissue was fixed in 4% paraformaldehyde for up to 4 h at room temperature then changed to 30% sucrose for at least 24 h. Tissue was then fixed in optimum cutting temperature (OCT) compound and kept at −80 °C until cryosectioning. Samples were sectioned into 40 μm thick transverse sections and dropped into PBS in order for the residual O.C.T. to dissolve. Sections were then stained using stan dard free floating techniques with an FITC conjugated anti GFP antibody (GeneTex). Both paraffin and cyrosections were then mounted and coverslipped with DAPI containing mounting media (VECTASHIELD).

2.9. Quantitative image analysis

Quantification of bioluminescence images was performed using LivingImage 4.5 (Perkin Elmer) software. Histological and immunohistochemical sections were imaged using a Zeiss Upright Olympus fluorescence multi channel microscope, captured with a Nikon DP Controller 2.2 (Olympus, Japan). Immunohistochemical and histopathological analysis was done using ImageJ. Briefly, 1×1 mm image fields were taken at the wound or scaffold site. For neutrophils, macrophages, fibroblasts, and endothelial cells, positive staining was quantified as individual particles counted based on a common threshold intensity. All cell types were quan tified from an n = 6 sections per group per time point.

2.10. Statistical analysis

Data are expressed as mean ± SEM and indicated in figures as $^{*}p < 0.05$, $^{**}p < 0.01$. The data were compared using ANOVA fol lowed by Bonferoni's post hoc test using GraphPad Prism version 5.00 (Graphpad Software, San Diego, California) for PC.

3. Results

3.1. Luciferase induced BM MNC bioluminescence

BM MNCs were isolated from the hind limbs of FVB L2G trans genic mice constitutively expressing the firefly luciferase (Fluc) and eGFP reporter genes. These cells were visualised through bio luminescence (IVIS) imaging after administration of the Fluc sub strate, luciferin (Fig. 1A). The resulting bioluminescence signal was directly proportional to BM MNC concentration (R^2: 0.98) (Fig. 1B). Therefore, greater bioluminescence measured in a partic ular region of interest represented higher numbers of these cells in that area.

3.2. Phenotype characterisation of the BM MNC fraction

Flow cytometry analysis was conducted to characterise the sub populations present in isolated BM MNCs. Half (51.4 ± 1.9%) of the BM MNC fraction was comprised of classical immune cell markers ($CD11b^+$, $CD45^+$). Amongst the stem/progenitor cell phenotypes, MSCs ($CD105^+$, $CD90.1^+$, $CD44^+$, $CD45^-$), HSCs (Sca 1^+, c kit^+, $CD45^+$, $CD133^+$), and EPCs ($CD31^+$, $CD34^+$, $CD45^+$) made up 1.2 ± 0.1%, 0.9 ± 0.3%, and 0.6 ± 0.1% of the BM MNC fraction, respectively (Fig. 2). These results indicate that isolated BM MNC fractions are a largely heterogeneous cell population, consistent with previous literature [17].

3.3. Model of BM MNC homing & engraftment tracking

FVB/n mice were given subcutaneous dorsal wounds. Isolated BM MNCs were then diluted to a working concentration of 1.5×10^7 cells/ml. This concentration allowed for the delivery of 3×10^6 cells in a bolus injection volume of 200 μl through the tail

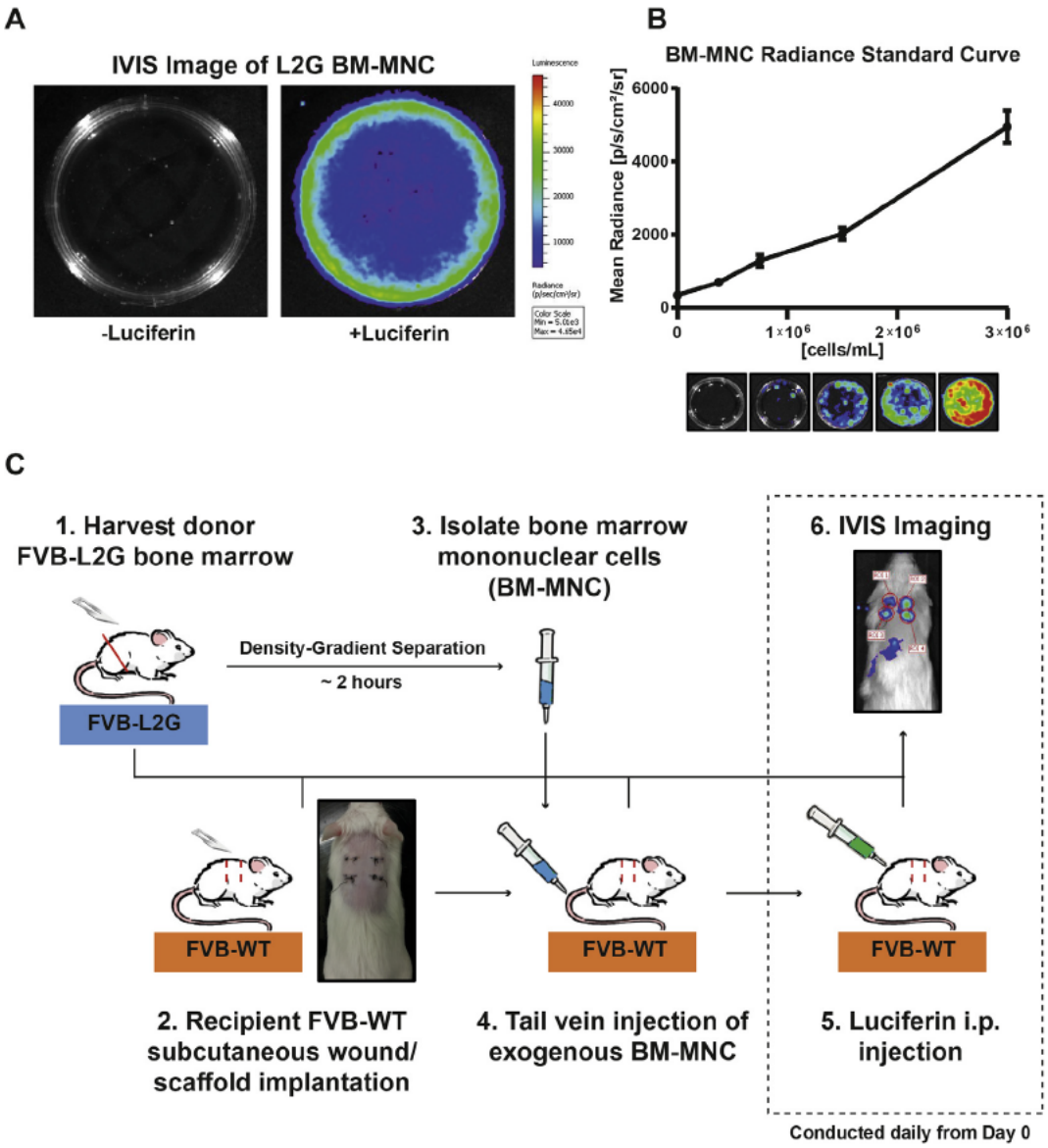

Fig. 1. Bioluminescence tracking model of *in vivo* BM-MNC. A) Luciferin-dependent bioluminescence activation of L2 G BM-MNC. B) Standard curve correlation between BM-MNC bioluminescence and cell density. C) Experimental protocol of BM-MNC bioluminescence tracking model.

vein of wounded WT mice (Fig. 1C). Additionally, it was consis tently found that injections of less than 3×10^6 total cells could not be visualised *in vivo*. IVIS imaging was conducted on the same cohort of mice over 21 days with separate groups for tissue harvest at Days 2, 5, 8, 11, & 21.

3.4. Temporal and spatial tracking of BM MNC homing/engraftment

Bioluminescence curves of wounds in mice treated with BM MNCs displayed a 3 fold greater area under the curve compared to wounds alone (9.69×10^4 vs 3.29×10^4 p/s/cm^2/sr day, Fig. 3A). Control groups included mice receiving wounds alone, BM MNC alone, or neither wounds nor BM MNC (control). Further, this bioluminescence curve peaked at day 11 returning to baseline control levels by day 21. BM MNCs were observed to be localised to the wound sites as well as within the spleen (Fig. 2B). BM MNC distribution within the spleen were also observed in control mice receiving BM MNC but no wounds (Supp. Fig. 1). Additionally, it was confirmed that BM MNCs were engrafted within the wound site by histological staining of the green fluorescent protein marker (Fig. 3C). Analysis of bioluminescence signal as a function of wound location showed that levels of BM MNC homing and engraftment was equal at all four wound locations (Supp. Fig. 2).

3.5. Histological analysis of BM MNC induced cell presence at subcutaneous wounds

The engraftment of BM MNCs at the wound site led to a series of cellular changes within the injured tissue. This was shown through the quantification of classical immune and remodelling cell phenotypes including neutrophils, macrophages, fibroblasts, and endothelial cells.

3.5.1. Neutrophils within subcutaneous wounds

Neutrophils are an essential cell type to innate immune responses [18]. Neutrophil presence at the wound site was quanti fied by staining of the neutrophil elastase (NE$^+$) cytoskeletal mar ker. In wounds alone, neutrophil presence peaked at day 2 and gradually decreased over time, returning to baseline by day 11. Similarly, wounds in mice injected with BM MNC peaked in

A

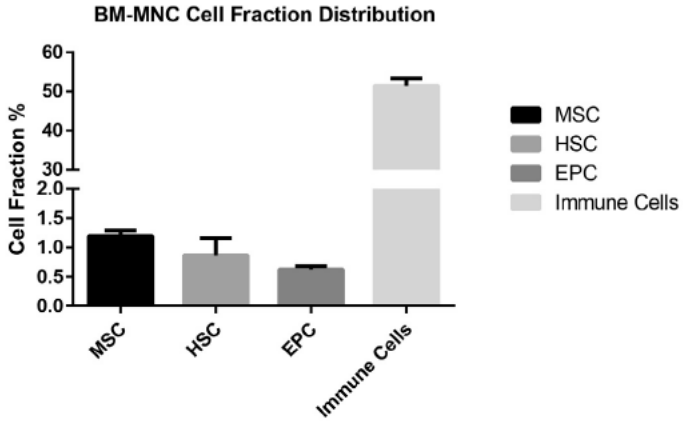

B

BM-MNC Fraction Marker Panel

Mesenchymal Stem Cells (MSCs)	Hematopoietic Stem Cells (HSCs)	Endothelial Precursor Cells (EPCs)	Immune Cells
CD105	Sca-1	CD31	CD11b
CD90.1	c-kit	CD34	CD45
CD29	CD45	CD45	
CD45-	CD133		

Fig. 2. BM-MNC fraction cell phenotyping. A) Subpopulation cell percentages of MSC, HSC, EPC, and Immune cells within isolated BM-MNC fractions. B) Cell markers identifying four classes of BM-MNC subpopulations.

neutrophil presence at day 2, however, this occurred at a 3.3 fold greater magnitude (1029 ± 78 vs 315 ± 120 counts/100 μm^2, $p < 0.05$, Fig. 4A).

3.5.2. Macrophages within subcutaneous wounds

Macrophages are multi functional cell types known to partici pate in immune responses as well as initiate phases of tissue remodelling [19]. Macrophage presence at the wound site was quantified through positive CD68 staining. In wounds alone, macrophage presence reached peak levels by day 8 (971 ± 226 counts/100 μm^2) followed by a decrease by day 11 and return to baseline by day 21. However, in mice injected with BM MNC, macrophage presence was highest by day 2 (1162 ± 296 counts/100 μm^2) and exhibited gradual decreases over subsequent days to baseline by day 21. Day 2 represented the lar gest difference in macrophage presence with BM MNC engrafted wounds displaying a 2.4 fold increase compared to wounds alone (1162 ± 296 vs 477 ± 83 counts/100 μm^2, $p < 0.05$, Fig. 4B). Injec tion of BM MNC drove an earlier macrophage presence at a greater magnitude at the wound site.

3.5.3. Fibroblasts within subcutaneous wounds

Fibroblasts are the classical remodelling cell phenotype as they produce new extracellular matrix proteins essential for the regen eration of tissue [20]. Fibroblast presence at the wound site was quantified through its cytoskeleton marker Vimentin (Vim^+). In wounds alone, fibroblast presence gradually increased to maxi mum by day 8 (1516 ± 480 counts/100 μm^2), followed by a decrease at day 11 and a progressive return to baseline by day 21. In mice injected with BM MNC, this pattern of fibroblast pres ence was significantly enhanced at days 5, 8, and 11 by 3.09 , 1.95 , and 2.59 fold compared to wounds alone, respectively (2849 ± 648 vs 923 ± 109, 2948 ± 449 vs 1516 ± 480, 2516 ± 538 vs 972 ± 293 counts/100 μm^2, $p < 0.05$, Fig. 5A).

3.5.4. Endothelial cells within subcutaneous wounds

Angiogenesis, the generation of new vasculature, is another cru cial process in tissue remodelling [21]. Endothelial cells directly participate in this process and are commonly identified by the CD31 marker. Significant differences in endothelial cells were observed at days 11 and 21. Wounds in mice injected with BM MNC displayed a 2.2 fold ($27 + 6$ vs 12 ± 6 counts/100 μm^2, $p < 0.05$) and 3.5 fold increase (21 ± 4 vs 6 ± 2 counts/100 μm^2, $p < 0.05$) in endothelial cell presence, respectively, when compared to wounds alone (Fig. 5B).

3.6. Tracking of BM MNCs to PCL vs PCL/collagen scaffolds

Electrospun PCL or PCL/Collagen scaffolds (Fig. 6A inset) were subcutaneously implanted into mice subsequently tail vein injected with BM MNCs. For histological controls, a separate cohort of mice was similarly implanted with PCL and PCL/Collagen scaf folds but received no BM MNC injection. Bioluminescence was measured for 21 days within ROIs around the scaffold areas in mice injected with BM MNC. PCL/Collagen scaffolds bioluminescence exhibited a 1.6 fold greater area under the curve compared to PCL scaffolds (max: 38.20×10^4 vs 24.49×10^4 p/s/cm^2/sr, $p < 0.05$, Fig. 6A). Significant differences in bioluminescence began from day 9 and were sustained up to day 21. Immunohistochem istry analysis of the GFP marker indicated that BM MNC engraft ment was isolated to the periphery of PCL scaffolds whereas, in PCL/Collagen, engraftment was observed in the body of the scaffold (Fig. 6B). Scaffold characterization experiments examining fiber width and porosity showed no significant structural differences between scaffolds that would be expected to influence cell migra tion (Supp. Fig. 3). Auto fluorescence effects were accounted for through control PCL and PCL/Collagen scaffolds receiving no trans planted BM MNCs (Supp. Fig. 5). Neither scaffold showed auto fluorescence around or within the scaffold.

3.7. BM MNC remodelling of implanted PCL and PCL/collagen scaffolds

Significant differences between BM MNC engraftment responses to PCL and PCL/Collagen scaffolds were associated with distinct cellular remodelling changes within each scaffold. This was observed through quantification of the cell phenotypes found

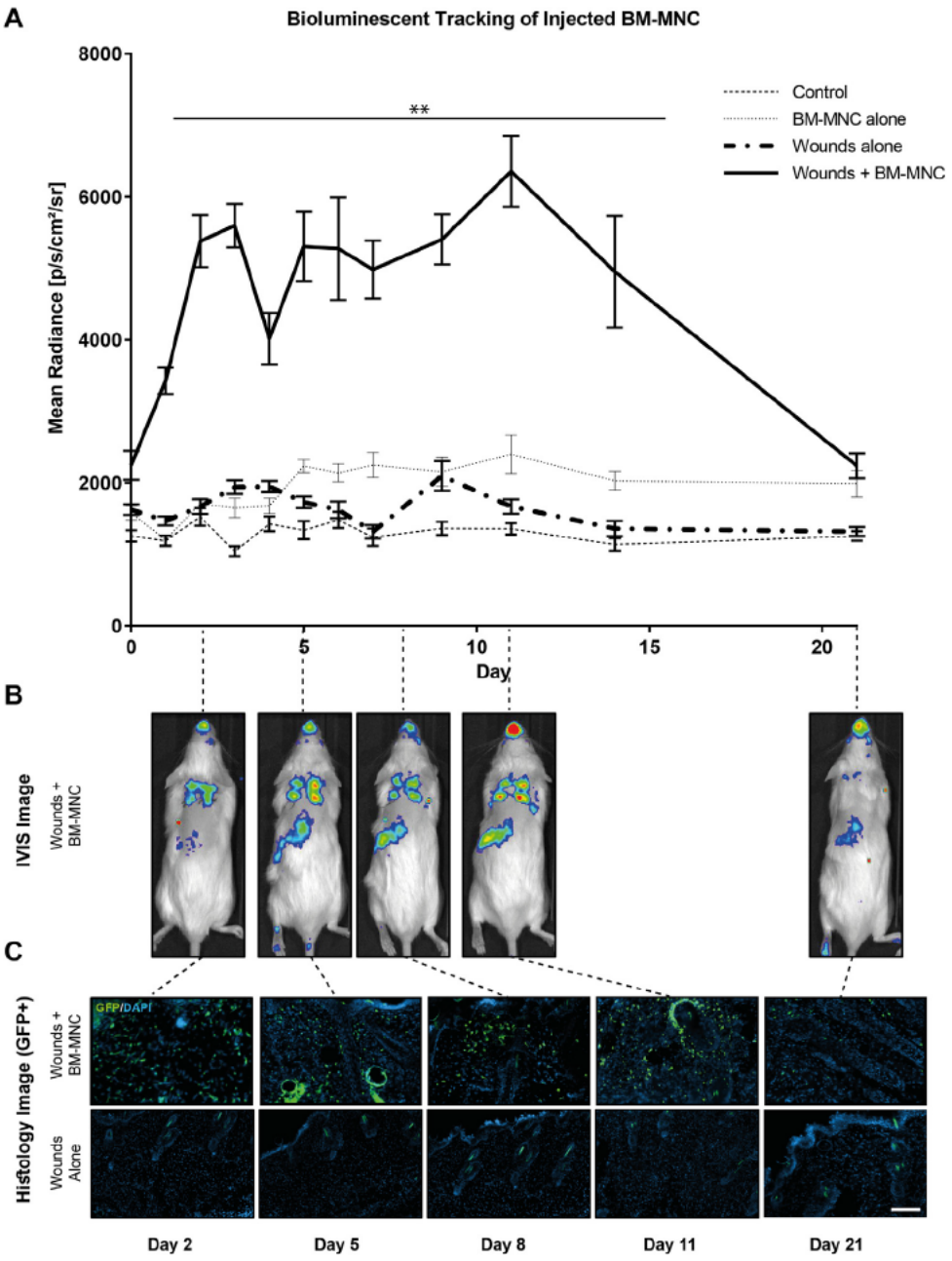

Fig. 3. Tracking BM-MNC homing and engraftment to subcutaneous wounds for 21 days. A) Bioluminescence measurements of wounded mice treated with BM-MNC compared to controls over 21 days. B) Representative IVIS images of wounded mice treated with BM-MNC. C) GFP⁺ BM-MNC engraftment in wounded mice treated with BM-MNC. Data expressed as mean ± SEM and analysed using AUC analysis, n = 6 animals/group, $^{**}p < 0.01$ compared to control, scale bar represents 200 μm.

to be altered by BM MNC engraftment in our previous wounds only experiments: neutrophils, macrophages, fibroblasts, and endothelial cells.

3.7.1. Neutrophils within implanted scaffolds

In all scaffold groups, neutrophil presence peaked at day 3, fol lowed by a gradual decline to baseline by day 21. No significant dif ferences in neutrophil presence were observed between scaffold groups (Fig. 7A).

3.7.2. Macrophages within implanted scaffolds

Macrophage presence within control PCL and PCL/Collagen scaf folds (no BM MNC) both reached peak levels at day 11 followed by decreases at day 21. In BM MNC engrafted PCL and PCL/Collagen scaffolds, respective macrophage presence peaked at day 21. At day 21, BM MNC engrafted PCL/Collagen scaffolds showed a sig nificant 1.9 fold (13,973 ± 3296 vs 7429 ± 1458 and 7448 ± 951) increase in macrophages compared to BM MNC engrafted PCL scaf folds and PCL/collagen control scaffolds, in addition to a 3.2 fold (13,973 ± 3296 vs 4181 ± 1271) increase over PCL control scaffolds (Fig. 7B).

3.7.3. Fibroblasts within implanted scaffolds

Peak fibroblast presence within all scaffold groups occurred at day 21. In BM MNC engrafted PCL/Collagen scaffolds, fibroblast presence showed a 1.8 fold (10,427 ± 1168 vs 5115 ± 995 and 5827 ± 1133) increase compared to BM MNC engrafted PCL scaf folds and PCL/Collagen control scaffolds, in addition to a 3.3 fold

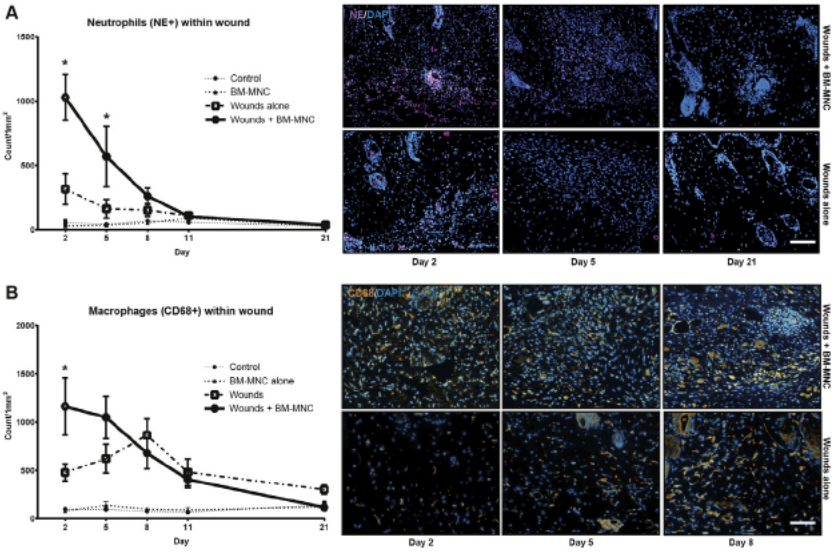

Fig. 4. Histological time course profile analysis of classical immune cell phenotypes at 2, 5, 8, & 11 days post-injury A) Neutrophil (Neutrophil Elastase$^+$) cell quantification and representative images at days 2, 5, & 21 post-injury in wounds with and without BM-MNC. B) Macrophage (CD68$^+$) cell quantification and representative images at days 2, 5, & 8 post-injury in wounds with and without BM-MNC. Data expressed as mean ± SEM and analysed using one-way ANOVA, n = 6 wound sections/group, $^*p < 0.05$ compared to wounds alone, scale bar represents 200 μm.

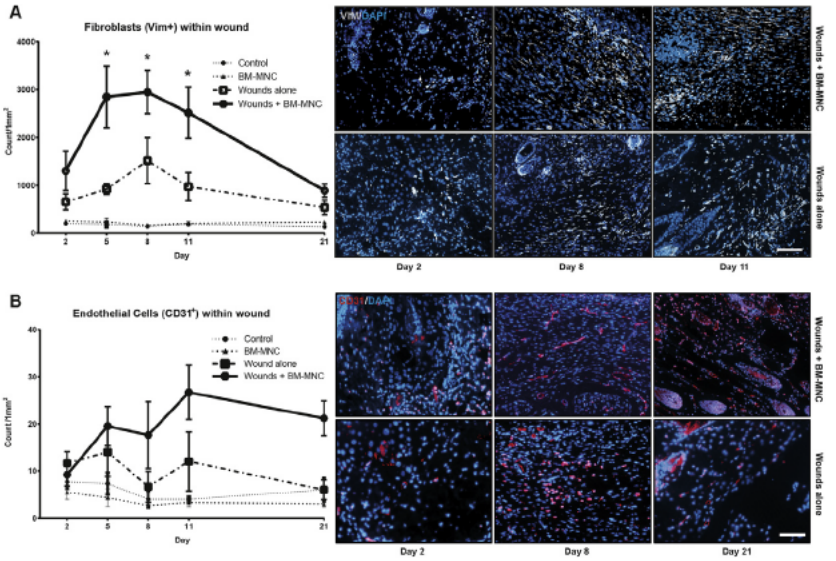

Fig. 5. Histological time course profile analysis of classical remodelling cell phenotypes at 2, 5, 8, 11, & 21 days post-injury A) Fibroblast (Vimentin$^+$) cell quantification and representative images at days 2, 8, & 11 post-injury in wounds with and without BM-MNC. B) Endothelial (CD31$^+$) cell quantification and representative images at days 2, 8, & 21 post-injury in wounds with and without BM-MNC. Data expressed as mean ± SEM and analysed using one-way ANOVA, n = 6 wound sections/group, $^*p < 0.05$ compared to wounds alone, scale bar represents 200 μm.

(10,427 ± 1168 vs 3292 ± 609) increase over PCL control (no cells) scaffolds (Fig. 8A).

3.7.4. *Endothelial cells within implanted scaffolds*

Endothelial cells in control PCL and PCL/Collagen scaffolds remained at constant levels over 21 days. In BM MNC engrafted PCL scaffolds, endothelial cells peaked at day 11. Meanwhile, in BM MNC engrafted PCL/Collagen scaffolds, peak endothelial cell presence was observed at day 21 and occurs at significant levels ~10 to 20 fold (80 ± 17 vs 4 ± 2 and 8 ± 4 and 7 ± 3) greater than all other scaffold groups at day 21 as well as 6.7 fold (80 ± 17 vs 12 ± 2) greater than peak endothelial cells presence in BM MNC engrafted PCL scaffolds at day 11 (Fig. 8B).

4. Discussion

In this study, we developed a model that non invasively tracks the response of injected BM MNC to injury and implantable cell scaffolds *in vivo*. Given their vital functions in tissue regeneration, tracking the dynamic behaviour of BM MNCs following injection has been a long standing research goal [22 24]. In contrast to post mortem immunohistochemistry, bioluminescent molecular imaging is non invasive and enables repeated assessment, thereby providing unparalleled information into cell location and magni tude in real time. Conventional tracking methods of BM MNCs *in vivo* involves imaging techniques reliant upon the cellular uptake of contrast and/or tracer agents that often interfere with normal cellular function [25]. Additionally, these agents elicit

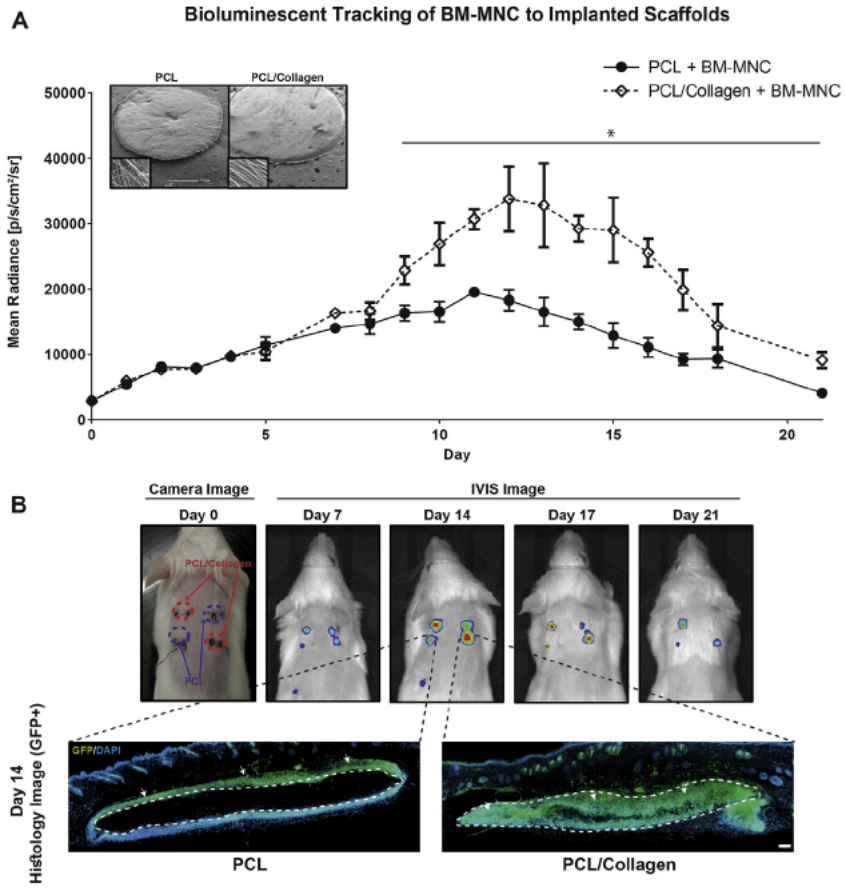

Fig. 6. Tracking BM-MNC to electrospun implantable cellular scaffolds for 21 days. A) Bioluminescence measurements of PCL vs PCL/Collagen subcutaneously implanted scaffolds. Inset images show representative SEM photos of each electrospun scaffold. B) Representative camera and IVIS images of mice implanted with PCL and PCL/Collagen scaffolds. Inset images show difference in GFP⁺ BM-MNC localisation within each scaffold. Dotted lines represent the edges of the scaffold. Arrows point out the localisation of GFP⁺ BM-MNCs. Data expressed as mean ± SEM and analysed using one-way ANOVA, n = 6 scaffolds/group, $^{*}p < 0.05$, scale bar represents 200 μm.

confounding long term imaging results due to either their retention in tissue even after the engrafted cells have died, yielding false positive signals (contrast agents) [24], or their decay over time, yielding false negative signals (tracer agents) [26]. The use of genetically engineered bioluminescence eliminates the use of such agents [27].

In our subcutaneous wound model, daily BM MNC bioluminescence measurements at sites of subcutaneous injury resulted in 21 day bioluminescence curves. These curves revealed that injected BM MNCs, in the absence of scaffolds, homed to and engrafted within sites of subcutaneous injury, and importantly, provided quantification of homing and engraftment of transplanted BM MNCs to subcutaneous injury alone. Furthermore, long term engraftment resulted in cellular remodelling effects, seen through immunohistochemical quantification of four key cell phenotypes present at the wound site over time. At early time points, exogenous BM MNC engraftment elevated immune cell populations, indicated by increased presence of neutrophils and macrophages at the wound site. At later time points, exogenous BM MNC engraftment enhanced the presence of post injury tissue regenerative cell phenotypes represented by increased fibroblast and endothelial cell presence. These results demonstrated that our injected BM MNCs maintained their well documented functional effects associated with their engraftment in injured tissue, most notably increases in fibroblast and endothelial cells [28 30]. With the current data set, we are unable to conclude that injected BM MNCs are differentiating at the wound site, as it is equally likely that paracrine effects of engrafted BM MNCs drive changes in native cell behaviour including migration [31]. Further studies will investigate the key underlying molecules and individual cell phenotypes within the injected BM MNC fraction that drive their engraftment and function, and determine the contribution of local and exogenous cell populations. Additional experiments in models of wound healing and injury could also importantly determine whether these changes drive functional benefits and whether bioluminescent imaging remains well correlated to these effects. This comprehensive insight into exogenous BM MNC therapy will help guide biomaterial development by incorporating these potential findings into the design of candidate biomaterial scaffolds.

Biomaterial scaffolds capable of eliciting favourable BM MNC responses possess significant therapeutic potential in augmenting current BM MNC therapies. However, identifying and testing the appropriate combination of scaffold parameters that will achieve this is highly complex and challenging. To address this, we utilized our model to identify BM MNC supportive scaffolds that may enhance the engraftment and function of transplanted BM MNCs. Electrospinning creates microfiber meshes which aim to mimic the physical nature of the native extracellular matrix. PCL is a non toxic, degradable synthetic polymer widely used in tissue engineering [32], but is limited by a lack of key cell binding motifs to encourage cell attachment and proliferation. Conversely, type I collagen is a natural matrix protein found abundantly in the native extracellular matrix and a common material for biomaterial engineering, especially for dermal and vascular applications [33]. These materials were chosen as they are common representatives of major classes of biomaterials that would be expected to elicit

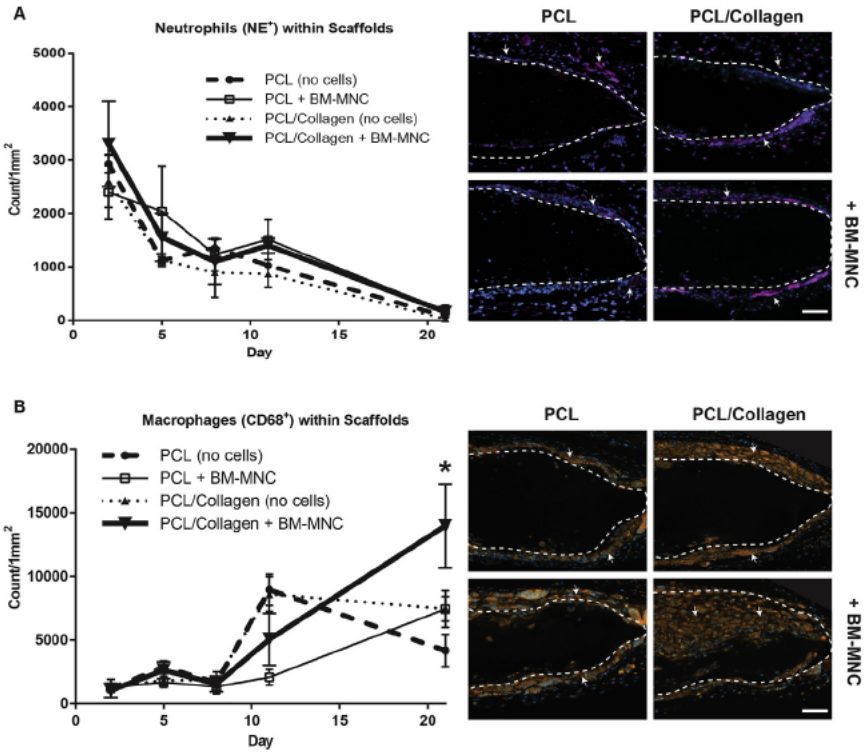

Fig. 7. Scaffold immune cell remodelling time course through quantification of classical immune cells, neutrophils and macrophages within PCL and PCL/Collagen control (no BM-MNC) and BM-MNC engrafted-PCL and PCL/Collagen scaffolds A) Neutrophil (Neutrophil Elastase$^+$) cell quantification and representative images at day 21 post-implantation B) Macrophage (CD68$^+$) cell quantification and representative images at day 21 post-implantation. Dotted lines represent the edges of the scaffold. Arrows point out the localisation of quantified immune cells. Data expressed as mean ± SEM and analysed using one-way ANOVA, n = 6 wound sections/group, $^*p < 0.05$ compared to BM-MNC engrafted-PCL scaffolds, scale bar represents 200 μm.

distinct responses with exogenous BM MNCs following implantation. Scaffolds comprised of either PCL or a PCL/Collagen blend were subcutaneously implanted in wound sites of mice injected with BM MNC and without (control). Bioluminescence measurements at implanted scaffolds, in BM MNC injected mice, over a 21 day period revealed that significant bioluminescence differences occurred 9 days after implantation. This suggested changes in long term engraftment of transplanted BM MNCs within each scaffold. Histological analysis confirmed clear differences in the number of engrafted BM MNCs and their overall distribution within the scaffolds. Engraftment occurred throughout the body of PCL/collagen scaffolds, whereas in PCL scaffolds, engraftment was limited to the scaffold periphery.

Improved engraftment of transplanted BM MNCs in PCL/Collagen scaffolds after day 9 was also associated with increasing macrophages, fibroblasts and endothelial cells within the scaffold from day 11 to significant levels by day 21, when compared to PCL scaffolds and both control scaffolds. Remodelling of scaffolds through increased cellularization remains an important goal in tissue engineering, as it presents a regenerative medicine strategy for organ replacement and tissue regeneration [34]. Neutrophil accumulation initiates immune responses to implantable scaffolds [17]. Neutrophil presence was equivalent for all scaffold groups, possibly due to the enhanced neutrophil response initiated by the implantation of a foreign body for all four conditions. Meanwhile, macrophage infiltration into tissue engineered scaffolds is crucial to scaffold remodelling and neotissue formation [35,36]. Macrophages in PCL and PCL/Collagen control scaffolds were resolving from days 11 to 21, however in both PCL and PCL/Collagen scaffolds engrafted with exogenous BM MNCs, macrophage infiltration was increasing, suggesting that the engraftment of transplanted BM MNC was driving altered scaffold remodelling. Between scaffolds engrafted with exogenous BM MNC, this was further highlighted by significant infiltration of macrophages into PCL/Collagen scaffolds correlating with its enhanced engraftment of exogenous BM MNC compared to PCL scaffolds. This increased presence of macrophages may in part be driven by the antigenic properties of ovine collagen used in PCL/Collagen scaffolds, however, given the equivalent neutrophil response between scaffolds, this does not appear to be a dominant effect. Further investigation into the mechanism behind improved engraftment and remodelling of exogenous BM MNC towards PCL/Collagen scaffolds used in this study are warranted. Augmented remodelling effects in PCL/Collagen scaffolds were further supported by significant fibroblast infiltration, a cellular event preceding new extracellular matrix deposition and facilitated by macrophage derived signalling molecules [28,37]. More significantly, these PCL/Collagen scaffolds exhibited substantial levels of angiogenesis indicating scaffold vascularization, a prevalent challenge of tissue engineering that is essential to the regeneration of tissue/organ specific resident cells [38,39]. Collectively, these results demonstrate that improved engraftment of i.v. injected BM MNC within electrospun scaffolds correlates with well known cellular hallmarks of enhanced scaffold remodelling. More broadly, these results demonstrated that observed engraftment differences of transplanted BM MNCs between PCL and PCL/Collagen scaffolds associated with two distinct scaffold remodelling responses that were non invasively determined by their respective bioluminescent curves.

The combined findings of our experiments showed that the presence of a scaffold drastically enhanced the engraftment response of transplanted BM MNCs at the injury site. This was highlighted by the approximately 4 fold increase in maximum bioluminescence when either scaffold was present, compared to wounds alone (Supp. Fig. 4). Furthermore, the peak engraftment of macrophages within scaffolds occurred at later time points, compared with injured tissue alone. This further suggested altered

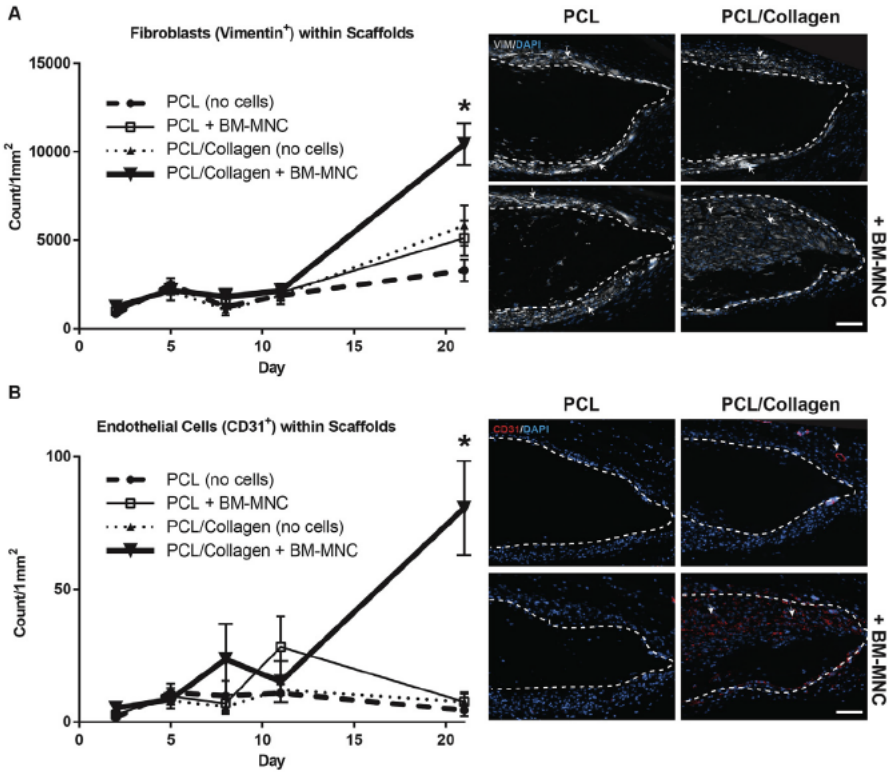

Fig. 8. Scaffold cellular remodelling time course through quantification of classical remodelling cell phenotypes, fibroblasts and endothelial cells within PCL and PCL/Collagen control (no BM-MNC) and BM-MNC engrafted-PCL and PCL/Collagen scaffolds A) Fibroblasts (Vimentin$^+$) cell quantification and representative images at day 21 post-implantation B) Endothelial (CD31$^+$) cell quantification and representative images at day 21 post-implantation. Dotted lines represent the edges of the scaffold. Arrows point out the localisation of quantified fibroblasts and endothelial cells. Data expressed as mean ± SEM and analysed using one-way ANOVA, n = 6 wound sections/group, $^*p < 0.05$ compared to BM-MNC engrafted-PCL scaffolds, scale bar represents 200 μm.

cellular remodelling responses of transplanted BM MNCs due to scaffold presence. However, the specific properties of implanted biomaterial scaffolds determine the extent of the ensuing engraft ment and function of transplanted BM MNCs. In our electrospun scaffolds, the addition of collagen significantly enhanced exoge nous BM MNC responses. Collagen and other ECM based scaffolds are chemoattractive for bone marrow derived progenitor cells, dri ven by peptides and cleavage products formed during scaffold degradation of ECM components [40,41]. Thus, varying scaffolds with diverse material compositions are often utilized to enhance engraftment [42]. Additionally, scaffold functionalization with an array of classical biochemical signals from the bone marrow niche, including homing chemokines (e.g. SDF 1) that facilitate endoge nous BM MNC recruitment and/or growth factors that drive cell differentiation (e.g. VEGF, TGF β), is also common in tissue engi neering to elicit positive responses from transplanted BM MNCs [43,44]. Scaffolds utilizing these approaches would also be of par ticular interest to test in our model. Our model tracking trans planted BM MNCs to subcutaneous injury alone can help narrow the field of biochemical signals to those that elicit positive effects of transplanted BM MNCs at sites of injury. Translating these potential findings to biomaterial development, our future work will develop scaffolds with enhanced capacity to recruit and prop agate injected BM MNCs. Collectively, our model provides a unique tool to advance biomaterial development aimed at enhancing the therapeutic efficacy of current BM MNC therapy.

5. Conclusion

By utilising bioluminescent molecular imaging, we describe an animal model that enables the temporal and spatial tracking of comprehensive cellular engraftment responses to BM MNC trans plantation therapy following injury. This can be used to non invasively and accurately distinguish the *in situ* responses of exogenous BM MNCs to implanted biomaterial scaffolds as they occur in real time. Using this model has implications for the high throughput *in vivo* screening of candidate molecules and cell phenotypes underlying the therapeutic effects of BM MNC trans plant following injury for the informed development of candidate biomaterials that augment current BM MNC therapy and tissue regeneration applications.

Acknowledgements

This work was supported by a grant from the National Health and Medical Research Council (APP1066174; MKCN). R.P.T is the recipient of an Australian Postgraduate Scholarship. We have no competing interests.

Appendix A. Supplementary data

Supplementary data associated with this article can be found, in the online version, at http://dx.doi.org/10.1016/j.actbio.2017.02.002.

References

[1] B. Assmus, S. Alakmeh, S. De Rosa, H. Bönig, E. Hermann, W.C. Levy, S. Dimmeler, A.M. Zeiher, Improved outcome with repeated intracoronary injection of bone marrow-derived cells within a registry: rationale for the randomized outcome trial REPEAT, Eur. Heart J. 37 (2016) 1659–1666.

[2] D. Sürder, R. Manka, V. Lo Cicero, T. Moccetti, K. Rufibach, S. Soncin, L. Turchetto, M. Radrizzani, G. Astori, J. Schwitter, P. Erne, M. Zuber, C. Auf der Maur, P. Jamshidi, O. Gaemperli, S. Windecker, A. Moschovitis, A. Wahl, I. Bühler, C. Wyss, S. Kozerke, U. Landmesser, T.F. Lüscher, R. Corti, Intracoronary injection of bone marrow-derived mononuclear cells early or late after acute

myocardial infarction: effects on global left ventricular function, Circulation 127 (2013) 1968–1979.
[3] Y. Higashi, M. Kimura, K. Hara, K. Noma, D. Jitsuiki, K. Nakagawa, T. Oshima, K. Chayama, T. Sueda, C. Goto, H. Matsubara, T. Murohara, M. Yoshizumi, Autologous bone-marrow mononuclear cell implantation improves endothelium-dependent vasodilation in patients with limb ischemia, Circulation 109 (2004) 1215–1218.
[4] C.S.J. Cox, J.E. Baumgartner, M.T. Harting, L.L. Worth, P.A. Walker, S.K. Shah, L. Ewing-Cobbs, K.M. Hasan, M.-C. Day, D. Lee, F. Jimenez, A. Gee, Autologous bone marrow mononuclear cell therapy for severe traumatic brain injury in children, Neurosurgery 68 (2011) 588–600.
[5] D. Henrich, R. Verboket, A. Schaible, K. Kontradowitz, E. Oppermann, J.C. Brune, C. Nau, S. Meier, H. Bonig, I. Marzi, C. Seebach, Characterization of bone marrow mononuclear cells on biomaterials for bone tissue engineering in vitro, Biomed. Res. Int. 2015 (2015) 762407.
[6] A.Y. Sheikh, B.C. Huber, K.H. Narsinh, J.M. Spin, K. van der Bogt, P.E. de Almeida, K.J. Ransohoff, D.L. Kraft, G. Fajardo, D. Ardigo, J. Ransohoff, D. Bernstein, M.P. Fischbein, R.C. Robbins, J.C. Wu, In vivo functional and transcriptional profiling of bone marrow stem cells after transplantation into ischemic myocardium, Arterioscler. Thromb. Vasc. Biol. 32 (2012) 92–102.
[7] S. Gobaa, S. Hoehnel, M. Roccio, A. Negro, S. Kobel, M.P. Lutolf, Artificial niche microarrays for probing single stem cell fate in high throughput, Nat. Methods 8 (2011) 949–955.
[8] S. Martino, F. D'Angelo, I. Armentano, J.M. Kenny, A. Orlacchio, Stem cell-biomaterial interactions for regenerative medicine, Biotechnol. Adv. 30 (2012) 338–351.
[9] A.-L. Leblond, J. O'Sullivan, N. Caplice, Bone marrow mononuclear stem cells: potential in the treatment of myocardial infarction, Stem Cells Cloning 2 (2009) 11–19.
[10] C.C. Zhang, H.F. Lodish, Murine hematopoietic stem cells change their surface phenotype during ex vivo expansion, Blood 105 (2005) 4314–4320.
[11] F.-M. Chen, L.-A. Wu, M. Zhang, R. Zhang, H.-H. Sun, Homing of endogenous stem/progenitor cells for in situ tissue regeneration: promises, strategies, and translational perspectives, Biomaterials 32 (2011) 3189–3209.
[12] P. Thevenot, A. Nair, J. Shen, P. Lotfi, C.Y. Ko, L. Tang, The effect of incorporation of SDF-1α into PLGA scaffolds on stem cell recruitment and the inflammatory response, Biomaterials 31 (2010) 3997–4008.
[13] J. Rnjak-Kovacina, S.G. Wise, Z. Li, P.K.M. Maitz, C.J. Young, Y. Wang, A.S. Weiss, Electrospun synthetic human elastin:collagen composite scaffolds for dermal tissue engineering, Acta Biomater. 8 (2012) 3714–3722.
[14] G.J. Wilmink, S.R. Opalenik, J.T. Beckham, M.A. Mackanos, L.B. Nanney, C.H. Contag, J.M. Davidson, E.D. Jansen, In-vivo optical imaging of hsp70 expression to assess collateral tissue damage associated with infrared laser ablation of skin, J. Biomed. Opt. 13 (2008) 054066.
[15] C.E. O'Connell-Rodwell, M.A. Mackanos, D. Simanovskii, Y.-A. Cao, M.H. Bachmann, H.A. Schwettman, C.H. Contag, In vivo analysis of heat-shock-protein-70 induction following pulsed laser irradiation in a transgenic reporter mouse, J. Biomed. Opt. 13 (2008) 030501.
[16] H. Liu, S.G. Wise, J. Rnjak-Kovacina, D.L. Kaplan, M.M.M. Bilek, A.S. Weiss, J. Fei, S. Bao, Biocompatibility of silk-tropoelastin protein polymers, Biomaterials 35 (2014) 5138–5147.
[17] K.E.A. van der Bogt, A.A. Hellingman, M.A. Lijkwan, E.-J. Bos, M.R. de Vries, M.P. Fischbein, P.H. Quax, R.C. Robbins, J.F. Hamming, J.C. Wu, Molecular imaging of bone marrow mononuclear cell survival and homing in murine peripheral artery disease, JACC Cardiovasc. Imaging 5 (2012) 46–55.
[18] T.A. Wilgus, S. Roy, J.C. McDaniel, Neutrophils and wound repair: positive actions and negative reactions, Adv. Wound Care 2 (2013) 379–388.
[19] T.J. Koh, L.A. DiPietro, Inflammation and wound healing: the role of the macrophage, Expert Rev. Mol. Med. 13 (2011) e23.
[20] P. Bainbridge, Wound healing and the role of fibroblasts, J. Wound Care 22 (2013) 407–412.
[21] S.A. Eming, B. Brachvogel, T. Odorisio, M. Koch, Regulation of angiogenesis: wound healing as a model, Prog. Histochem. Cytochem. 42 (2007) 115–170.
[22] Y. Zhao, A.J. Bower, B.W. Graf, M.D. Boppart, S.A. Boppart, Imaging and tracking of bone marrow-derived immune and stem cells, Methods Mol. Biol. 1052 (2013) 57–76.
[23] M.K. Scott, O. Akinduro, C. Lo Celso, In Vivo 4-dimensional tracking of hematopoietic stem and progenitor cells in adult mouse calvarial bone marrow, J Vis. Exp. 91 (2014) e51683.
[24] A. Sohni, C.M. Verfaillie, Mesenchymal stem cells migration homing and tracking, Stem Cells Int. 2013 (2013) 130763.
[25] A. Crabbe, C. Vandeputte, T. Dresselaers, A.A. Sacido, J.M.G. Verdugo, J. Eyckmans, F.P. Luyten, K. Van Laere, C.M. Verfaillie, U. Himmelreich, Effects of MRI contrast agents on the stem cell phenotype, Cell Transplant. 19 (2010) 919–936.
[26] C. Caracó, L. Aloj, L.-Y. Chen, J.Y. Chou, W.C. Eckelman, Cellular release of [18F] 2-fluoro-2-deoxyglucose as a function of the glucose-6-phosphatase enzyme system, J. Biol. Chem. 275 (2000) 18489–18494.
[27] P.E. de Almeida, J.R.M. van Rappard, J.C. Wu, In vivo bioluminescence for tracking cell fate and function, Am. J. Physiol. Heart Circ. Physiol. 301 (2011) H663–H671.
[28] H. Kurobe, M.W. Maxfield, C.K. Breuer, T. Shinoka, Concise review: tissue-engineered vascular grafts for cardiac surgery: past, present, and future, Stem Cells Transl. Med. 1 (2012) 566–571.
[29] C.J. Li, R.L. Gao, Y.J. Yang, F.H. Hu, W.X. Yang, S.J. You, L.F. Song, Y.M. Ruan, S.B. Qiao, J.L. Chen, J.J. Li, Implantation of autologous bone marrow mononuclear cells into ischemic myocardium enhances coronary capillaries and systolic function in miniswine, Chin. Med. Sci. J. 23 (2008) 234–238.
[30] H. Zhang, N. Zhang, M. Li, H. Feng, W. Jin, H. Zhao, X. Chen, L. Tian, Therapeutic angiogenesis of bone marrow mononuclear cells (MNCs) and peripheral blood MNCs: transplantation for ischemic hindlimb, Ann. Vasc. Surg. 22 (2008) 238–247.
[31] H.F. Tse, C.W. Siu, S.G. Zhu, L. Songyan, Q.Y. Zhang, W.H. Lai, Y.L. Kwong, J. Nicholls, C.P. Lau, Paracrine effects of direct intramyocardial implantation of bone marrow derived cells to enhance neovascularization in chronic ischaemic myocardium, Eur. J. Heart Fail. 9 (2007) 747–753.
[32] Q.P. Pham, U. Sharma, A.G. Mikos, Electrospun poly(ε-caprolactone) microfiber and multilayer nanofiber/microfiber scaffolds: characterization of scaffolds and measurement of cellular infiltration, Biomacromolecules 7 (2006) 2796–2805.
[33] L. Steinstraesser, M. Wehner, G. Trust, M. Sorkin, D. Bao, T. Hirsch, H. Sudhoff, A. Daigeler, I. Stricker, H.-U. Steinau, F. Jacobsen, Laser-mediated fixation of collagen-based scaffolds to dermal wounds, Lasers Surg. Med. 42 (2010) 141–149.
[34] L. Teodori, A. Costa, R. Marzio, B. Perniconi, D. Coletti, S. Adamo, B. Gupta, A. Tarnok, Native extracellular matrix: a new scaffolding platform for repair of damaged muscle, Front. Physiol. 5 (2014) 218.
[35] N. Hibino, T. Yi, D.R. Duncan, A. Rathore, E. Dean, Y. Naito, A. Dardik, T. Kyriakides, J. Madri, J.S. Pober, T. Shinoka, C.K. Breuer, A critical role for macrophages in neovessel formation and the development of stenosis in tissue-engineered vascular grafts, FASEB J. 25 (2011) 4253–4263.
[36] J.D. Roh, R. Sawh-Martinez, M.P. Brennan, S.M. Jay, L. Devine, D.A. Rao, T. Yi, T.L. Mirensky, A. Nalbandian, B. Udelsman, N. Hibino, T. Shinoka, W.M. Saltzman, E. Snyder, T.R. Kyriakides, J.S. Pober, C.K. Breuer, Tissue-engineered vascular grafts transform into mature blood vessels via an inflammation-mediated process of vascular remodeling, Proc. Natl. Acad. Sci. U.S.A. 107 (2010) 4669–4674.
[37] T.A. Wynn, L. Barron, Macrophages: master regulators of inflammation and fibrosis, Semin. Liver Dis. 30 (2010) 245–257.
[38] H. Bramfeldt, G. Sabra, V. Centis, P. Vermette, Scaffold vascularization: a challenge for three-dimensional tissue engineering, Curr. Med. Chem. 17 (2010) 3944–3967.
[39] M. Lovett, K. Lee, A. Edwards, D.L. Kaplan, Vascularization strategies for tissue engineering, Tissue Eng. Part B Rev. 15 (2009) 353–370.
[40] F. Li, W. Li, S. Johnson, D. Ingram, M. Yoder, S. Badylak, Low-molecular-weight peptides derived from extracellular matrix as chemoattractants for primary endothelial cells, Endothelium 11 (2004) 199–206.
[41] S.F. Badylak, K. Park, N. Peppas, G. McCabe, M. Yoder, Marrow-derived cells populate scaffolds composed of xenogeneic extracellular matrix, Exp. Hematol. 29 (2001) 1310–1318.
[42] F.J. O'Brien, Biomaterials & scaffolds for tissue engineering, Mater. Today 14 (2011) 88–95.
[43] S. Amadesi, C. Reni, R. Katare, M. Meloni, A. Oikawa, A.P. Beltrami, E. Avolio, D. Cesselli, O. Fortunato, G. Spinetti, R. Ascione, E. Cangiano, M. Valgimigli, S.P. Hunt, C. Emanueli, P. Madeddu, Role for substance P-based nociceptive signaling in progenitor cell activation and angiogenesis during ischemia in mice and in human subjects, Circulation 125 (2012) 1719–1774.
[44] I. Petit, M. Szyper-Kravitz, A. Nagler, M. Lahav, A. Peled, L. Habler, T. Ponomaryov, R.S. Taichman, F. Arenzana-Seisdedos, N. Fujii, J. Sandbank, D. Zipori, T. Lapidot, G-CSF induces stem cell mobilization by decreasing bone marrow SDF-1 and up-regulating CXCR4, Nat. Immunol. 3 (2002) 687–694.

Chapter 3

Induced Pluripotent Stem-Cell Derived Endothelial Cells Promote Angiogenesis and Accelerate Wound Closure in a Murine Excisional Wound Healing Model

Bioscience Reports (2018) **38** BSR20180563
https://doi.org/10.1042/BSR20180563

PORTLAND PRESS

Research Article

Induced pluripotent stem cell-derived endothelial cells promote angiogenesis and accelerate wound closure in a murine excisional wound healing model

Zoë E. Clayton[1,*], Richard P. Tan[1,2,*], Maria M. Miravet[1,3], Katarina Lennartsson[1,3], John P. Cooke[4], Christina A. Bursill[1], Steven G. Wise[1] and Sanjay Patel[1,2]

[1]Cell Therapeutics and Applied Materials Groups, Heart Research Institute, 7 Eliza Street, Newtown NSW 2042, Australia; [2]Sydney Medical School, University of Sydney, Camperdown NSW 2050, Australia; [3]Faculty of Medicine and Health Sciences, Linköping University, Linköping 581 83, Sweden; [4]Department of Cardiovascular Sciences, Houston Methodist Research Institute, 6670 Bertner Ave, Houston, TX 77030, U.S.A.

Correspondence: Sanjay Patel (sanjay.patel@hri.org.au)

Chronic wounds are a major complication in patients with cardiovascular diseases. Cell therapies have shown potential to stimulate wound healing, but clinical trials using adult stem cells have been tempered by limited numbers of cells and invasive procurement procedures. Induced pluripotent stem cells (iPSCs) have several advantages of other cell types, for example they can be generated in abundance from patients' somatic cells (autologous) or those from a matched donor. iPSCs can be efficiently differentiated to functional endothelial cells (iPSC-ECs). Here, we used a murine excisional wound model to test the pro-angiogenic properties of iPSC-ECs in wound healing. Two full-thickness wounds were made on the dorsum of NOD-SCID mice and splinted. iPSC-ECs (5×10^5) were topically applied to one wound, with the other serving as a control. Treatment with iPSC-ECs significantly increased wound perfusion and accelerated wound closure. Expression of endothelial cell (EC) surface marker, platelet endothelial cell adhesion molecule (PECAM-1) (CD31), and pro-angiogenic EC receptor, Tie1, mRNA was up-regulated in iPSC-EC treated wounds at 7 days post-wounding. Histological analysis of wound sections showed increased capillary density in iPSC-EC wounds at days 7 and 14 post-wounding, and increased collagen content at day 14. Anti-GFP fluorescence confirmed presence of iPSC-ECs in the wounds. Bioluminescent imaging (BLI) showed progressive decline of iPSC-ECs over time, suggesting that iPSC-ECs are acting primarily through short-term paracrine effects. These results highlight the pro-regenerative effects of iPSC-ECs and demonstrate that they are a promising potential therapy for intractable wounds.

Introduction

Due to poor circulation and prolonged tissue ischaemia, many patients with peripheral arterial disease (PAD) develop chronic wounds or ulcers on their lower limbs, which can become infected and often necessitate amputation of the affected foot or leg. The complications associated with infection and amputation also lead to increased mortality in these patients, particularly in diabetics. Revascularization therapies improve wound healing in patients with critical limb ischaemia, yet chronic wounds remain a major individual and societal burden, with estimated global cost of care in excess of US$ 22 billion each year [1,2]. Current treatments for chronic wounds are largely focused on cleaning, infection control and debridement of dead tissue. The gold-standard in chronic wound care is the split-thickness autograft, which is a patch of skin taken from a healthy region and grafted on to the wound [3]. Other treatment options include bioactive dressings and donor keratinocytes, but these have limitations and additional therapies are

*These authors contributed equally to this work.

Received: 22 January 2018
Revised: 04 June 2018
Accepted: 04 July 2018

Accepted Manuscript Online: 05 July 2018
Version of Record published: 31 July 2018

Bioscience Reports (2018) **38** BSR20180563
https://doi.org/10.1042/BSR20180563

required to better address the microvascular deficiency, which underlies the development of these wounds and contributes to their persistence and re-occurrence.

Acute wound healing comprises four overlapping stages; haemostasis, inflammation, proliferation and remodelling [4]. The inflammation and cellular proliferation phases take place from hours to several weeks after an injury and involve the recruitment of inflammatory cells to the wound site, formation of extracellular matrix (ECM) proteins and granulation tissue, keratinocyte migration, contraction and wound closure. Angiogenesis, the growth of new blood vessel networks, is a vital component of these processes and is dependent upon pro-angiogenic growth factors released by supporting cells, proliferation and migration of local endothelial cells into the wound bed, and recruitment of bone marrow-derived stem cells/endothelial progenitor cells (EPCs) [4-7]. The pathophysiology of chronic wounds is complex and disordered, but can be largely attributed to persistent inflammation and a lack of adequate tissue perfusion in the region, exacerbated by failure of ischaemia-mediated angiogenesis in the wound. Collagen deposition is also reduced in diabetic/PAD patient wounds and the collagen that is present is often glycated, which impairs the adherence of new keratinocytes to the ECM [8]. Inflammation is also known to be the primary driving force behind excessive scar formation when a wound does eventually heal [9]. Meanwhile, the inability of EPCs and supporting cells to form new blood vessel networks to clear necrotic debris and deliver oxygen and nutrients to the granulation tissue maintains the wound's inflammatory status. Therapies that can effectively resolve either or both pathological processes are key to breaking the vicious cycle of failed healing in chronic wounds.

Stem cell therapy is a promising strategy to enhance angiogenesis and promote healing of chronic wounds. Adult stem and progenitor cells have been studied extensively in animal models of wound healing and appear to exert their beneficial effects via multiple mechanisms, including recruitment of other cells types, such as keratinocytes, macrophages and EPCs [10-12]. They have also been shown to produce collagen types I and III, which are critical for regeneration of the ECM and are the source of structural integrity and tensile strength in the healing tissue [13]. Clinical trials with bone marrow-derived stem cells are underway and there are a handful of published studies in both acute (surgical) and chronic (venous insufficiency and diabetic) wounds, which have reported consistent decreases in wound size, particularly with repeat treatments [14-17]. EPCs and embryonic stem cell derived endothelial cells have also been tested in animal models and improve wound healing via increased vascularization [18,19]. Indeed, a common beneficial feature of all stem cell therapies seems to be their pro-angiogenic effect.

Induced pluripotent stem cells (iPSCs) are derived by reprogramming somatic cells, such as dermal fibroblasts. They have unlimited self-renewal capacity and are therefore an abundant potential source of autologous or donor matched cells for therapy and may be more clinically translatable than other stem cell types. iPSCs can be differentiated to functional endothelial cells (iPSC-ECs) with high efficiency and reproducibility. We have shown previously that iPSC-ECs enhance angiogenesis and improve perfusion recovery in a mouse model of peripheral arterial disease [20,21]. The objective of the current study was to determine whether the pro-angiogenic properties of iPSC-ECs can be harnessed to promote wound healing. We demonstrate for the first time that iPSC-ECs enhance wound angiogenesis and perfusion, promote physiological collagen deposition and accelerate wound closure in a murine excisional wound healing model. These findings suggest that iPSC-ECs have potential as a treatment for chronic wounds and support further development of clinical grade iPSC-ECs for therapeutic angiogenesis.

Methods

iPSC reprogramming and differentiation to iPSC-ECs

Human iPSCs were generated via retroviral overexpression of Oct4, Klf4, Sox2, and c-Myc (OKSM) transcription factors in human dermal fibroblasts derived from healthy subjects. The iPSCs were differentiated to endothelial cells using previously described methods [20-23] (Supplementary Figure S1). The cells were transduced with a double fusion reporter construct encoding GFP and firefly luciferase, to enable *in vivo* fluorescence and bioluminescent imaging (BLI).

Wound healing procedure

The wounding procedure was adapted from that previously described by Galiano et al. [24] and Dunn et al. [25]. Male NOD/SCID mice were used at 8–10 weeks of age. The operative region of the mouse's back was prepared by removing the fur with clippers and a light depilatory cream, and two wound outlines were made, using a sterilized 5-mm biopsy punch. The skin in the middle of the outline was lifted using serrated forceps and full-thickness wounds were cut and excised using iris scissors. Silicone splints (approximately 10 mm diameter) were used to prevent wound closure via contraction. An adhesive was applied sparingly to one side of the splint and the splints were centred over the wounds. The splints were then secured in place using interrupted 6-0 PROLENE^{TM} sutures (8805H, Ethicon LLC, San Lorenzo,

Puerto Rico). After splinting, the mice were scanned with a laser Doppler (MOOR-LMD V192, Moor Instruments, U.K.) for wound perfusion measurement. They were placed on a heat mat in the prone position and the wound area was scanned three times per mouse per time point. Doppler scans were performed on alternate days post-wounding, up to and including day 14. Subsequent to the initial Doppler scan, cell treatments (5×10^5 iPSC-ECs suspended in vehicle containing a 1:1 ratio of endothelial basal medium to growth factor reduced Matrigel) were injected into the wounds and the wounds were covered with adhesive Opsite^{TM} dressings (66000041, Smith & Nephew, London, U.K.). All wound healing experiments and associated procedures were conducted in accordance with National Health and Medical Research Council (NHMRC) guidelines for the care and use of animals for scientific purposes and were approved by the Sydney Local Health District Animal Welfare Committee, Protocol #2014-004A.

BLI

BLI was used for longitudinal tracking of iPSC-EC survival *in vivo* and was performed with an IVIS Lumina XRMS and Living Image software (version 4.5, PerkinElmer, Waltham, MA 02451, U.S.A.). The mice were anaesthetized with 2% isoflurane and D-luciferin (100 µl, 375 mg/kg) was administered by subcutaneous injection in a medial position immediately inferior to the wound sites. Bioluminescence intensity was calculated as the maximum mean radiance (photons/second/cm^2/steradian) recorded in pre-defined ROI centred over the wounds. BLI was performed on alternate days post-wounding, up to and including day 14.

Histological analysis of explanted wounds

Wound explants were fixed in 4% paraformaldehyde for up to 4 h at room temperature, then changed to 70% ethanol for at least 24 h. Paraffin infiltration was performed overnight by an automated tissue processor (Leica TP1020, Leica Biosystems Nussloch GmbH, Heidelberger Straße 17-19 69226 Nussloch, Germany). The infiltrated samples were then embedded in paraffin blocks for sectioning. Tissue samples were cut into 5-µm thick transverse sections using a rotary microtome, deparaffinized, and stained. Milligan's Trichrome stain was performed to visualize collagen content. For immunohistochemistry analysis, paraffin sections were stained using immunohistochemistry techniques with primary antibodies anti-CD31 (Abcam, U.S.A.) for endothelial cells and anti-CD68 (Abcam, U.S.A.) for macrophages. Fluorescence microscopy was then used to visualize cell markers using Alexa Fluor 594 conjugated secondary antibodies. Anti-GFP staining was done using cryosectioning. Briefly, tissue was fixed in 4% paraformaldehyde for up to 4 h at room temperature then changed to 30% sucrose for at least 24 h. Tissue was then fixed in optimum cutting temperature (OCT) compound and kept at −80°C until cryosectioning. Samples were sectioned into 40-µm thick transverse sections and dropped into PBS in order for the residual O.C.T. to dissolve. Sections were then stained using standard free-floating techniques with a FITC-conjugated anti-GFP antibody (GeneTex). Both paraffin and cyrosections were then mounted and coverslipped with DAPI-containing mounting media (Vectashield, Vector Laboratories Inc., CA, U.S.A.).

Analysis of host angiogenic gene expression in wounds

Total RNA was isolated from explanted control and iPSC-EC treated wounds with TRIzol reagent. Real-time quantitative PCR analysis was performed to evaluate the expression of murine vascular endothelial cadherin (VE-cadherin; sense: 5′-TCCTCTGCATCCTCACTATCACA-3′, antisense: 5′-GTAAGTGACCAACTGCTCGTGAAT-3′) , vascular endothelial growth factor receptor-1 (Flt-1; sense: 5′-GAGGAGGATGAGGGTGTCTATAGGT-3′, antisense: 5′- GTGATCAGCTCCAGGTTTGACTT-3′), vascular endothelial growth factor receptor-2 (KDR; sense 5′-CCCTGCTGTGGTCTCACTAC-3′, antisense: 5′-CAAAGCATTGCCCATTCGAT-3′), platelet endothelial cell adhesion molecule (PECAM-1; sense: 5′-GAGCCCAATCACGTTTCAGTTT-3′, antisense: 5′-TCCTTCCTGCTTCTTGCTAGCT-3′), tyrosine kinase with Ig-like and EGF-like domains-1 (Tie-1; sense: 5′-CAAGGTCACACACACGGTGAA-3′, antisense: 5′-GCCAGTCTAGGGTATTGAAGTAGGA-3′), and vascular endothelial growth factor (VEGF; sense: 5′-TGCCAAGTGGTCCCAG-3′, antisense: 5′-GTGAGGTCTTGATCCG-3′). Glyceraldehyde-3-phosphate dehydrogenase (GAPDH; sense: 5′-GGGGCTCTCTGCTCCTCCCTGT-3′, antisense: 5′-CGGCCAAATCCGTTCACACCGA-3′) was used as a loading control. Relative gene expression was calculated as fold change compared with paired control wounds.

Quantificative analysis of bioluminescence and histological images

Quantification of bioluminescence images was performed using LivingImage 4.5 (PerkinElmer) software. Histological and immunohistochemical sections were imaged using a Zeiss Upright Olympus fluorescence multichannel microscope, captured with a Nikon DP Controller 2.2 (Olympus, Japan). Immunohistochemical and histopathological

Bioscience Reports (2018) **38** BSR20180563
https://doi.org/10.1042/BSR20180563

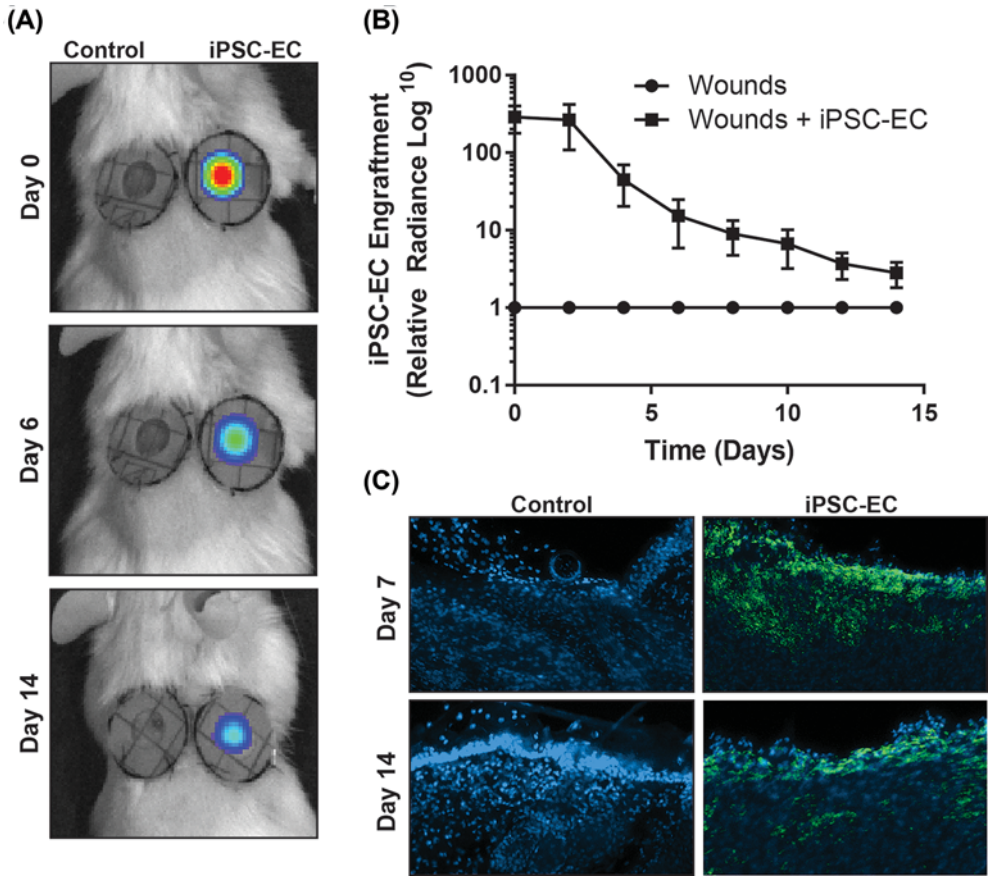

Figure 1. iPSC-EC engraftment in wounds

iIPSC-ECs were transduced with a double fusion reporter construct encoding GFP for fluorescence imaging and firefly luciferase for BLI. (**A**) Representative IVIS images, showing bioluminescent signal present in iPSC-EC-treated wounds (right) on days 0, 6 and 14 post-wounding. (**B**) Declining bioluminescent signal in wounds over time, relative to control wound background signal. (**C**) GFP staining (green) with DAPI nuclear stain (blue) in control and iPSC-EC treated wounds at on days 7 and 14 post-wounding (n=6 per treatment group).

analyses were done using ImageJ. Briefly, regions of interest (ROIs) were drawn around the wound site. For endothelial cells and fibroblasts, positive staining was quantified as individual particles counted based on a common threshold intensity. All cell types were quantified from n=6 sections per group per time point.

Statistics

Data are expressed as mean ± S.E.M. and indicated in figures as $^{*}P<0.05$, $^{**}P<0.01$. The data were compared using paired Student's t tests followed by Bonferoni's post-hoc test using GraphPad Prism version 5.00 (GraphPad Software, San Diego, CA) for PC. IPSC-EC experimental samples were paired to control wounds within the same mouse.

Results

Engraftment of iPSC-ECs within wounds decreases following transplantation

BLI was used to quantify the levels of iPSC-EC engraftment within wounds over time. Transfection of iPSC-ECs with a dual-report construct containing both the enhanced GFP (eGFP) and the firefly luciferase enzyme enabled visualization and quantification of transplanted iPSC-ECs. Intramuscular injection of D-luciferin substrate catalysed a bioluminescent reaction through the firefly luciferase enzyme within viable iPSC-ECs that could be visualized and quantified using the IVIS apparatus (Figure 1A). Bioluminescence quantification over 14 days showed that iPSC-EC presence in wounds decreases steadily over time (Day 0: $1.39 \times 10^{7} \pm 5.61 \times 10^{6}$ compared with Day 14: $4.04 \times$

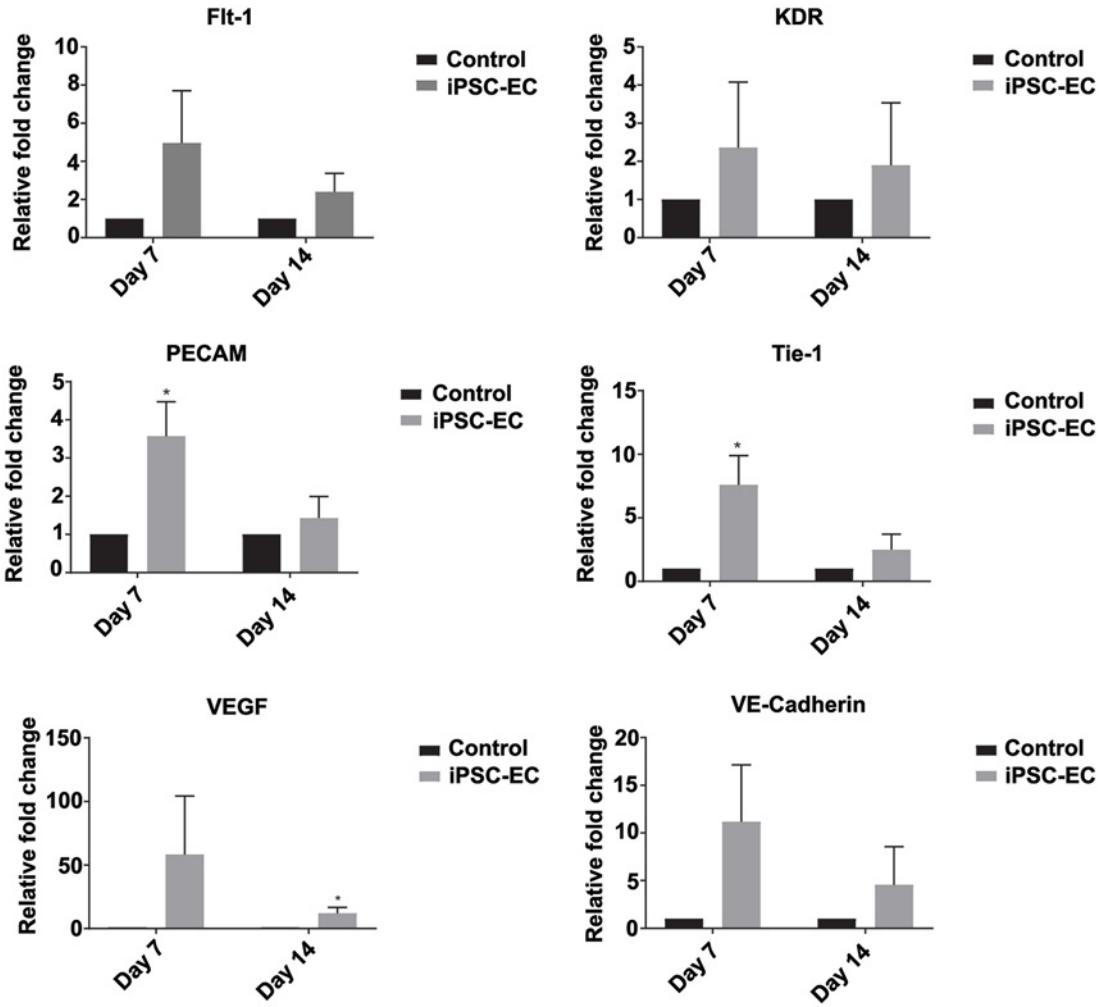

Figure 2. iPSC-EC treatment increases expression of pro-angiogenic genes

qPCR analysis of wound mRNA revealed a significant up-regulation of PECAM (CD31) and endothelial cell receptor, Tie-1, expression in iPSC-EC wounds on day 7 post-wounding. This was resolved by day 14. No significant differences in endothelial cell surface marker VE-cadherin (CD144), VEGF, VEGF receptor 1 (Flt1) or VEGF receptor 2 (KDR) expression were measured (*$P<0.05$ compared with controls, $n=6$ per treatment group).

$10^4 \pm 1.53 \times 10^4$ photons/cm^2/s/steradian). The largest decrease in bioluminescence occurred between days 2 and 4 (Day 2: $8.36 \times 10^6 \pm 5.44 \times 10^6$ compared with Day 4: $7.66 \times 10^5 \pm 3.65 \times 10^5$ photons/cm^2/s/steradian, Figure 1B). Immunohistochemistry staining of the eGFP marker identified iPSC-ECs engrafted within the wound site at day 7, and a smaller proportion remaining at 14 days post-transplantation (Figure 1C).

Engraftment of iPSC-ECs correlates with up-regulation of host angiogenic gene expression

Functional angiogenesis is a complex process regulated by numerous cells types and growth factors. Ischaemic/injured tissues undergoing revascularization processes are often identified by the up-regulation of key angiogenic genes including VE-cadherin, VEGF, Flt-1, KDR, PECAM, and Tie-1. Wounds were explanted at days 7 and 14 for qPCR analysis to determine levels of these classical angiogenic genes. Increasing trends were observed in the expression of VE-cadherin, Flt-1, and KDR in iPSC-EC treated wounds when compared with control wounds at both time points, however no statistical significance was obtained. At day 7, *PECAM* and *Tie-1* genes were found to be significantly u-regulated by 350 ± 89 and 534 ± 134% in iPSC-EC treated wounds compared with control wounds (Figure 2).

Bioscience Reports (2018) **38** BSR20180563
https://doi.org/10.1042/BSR20180563

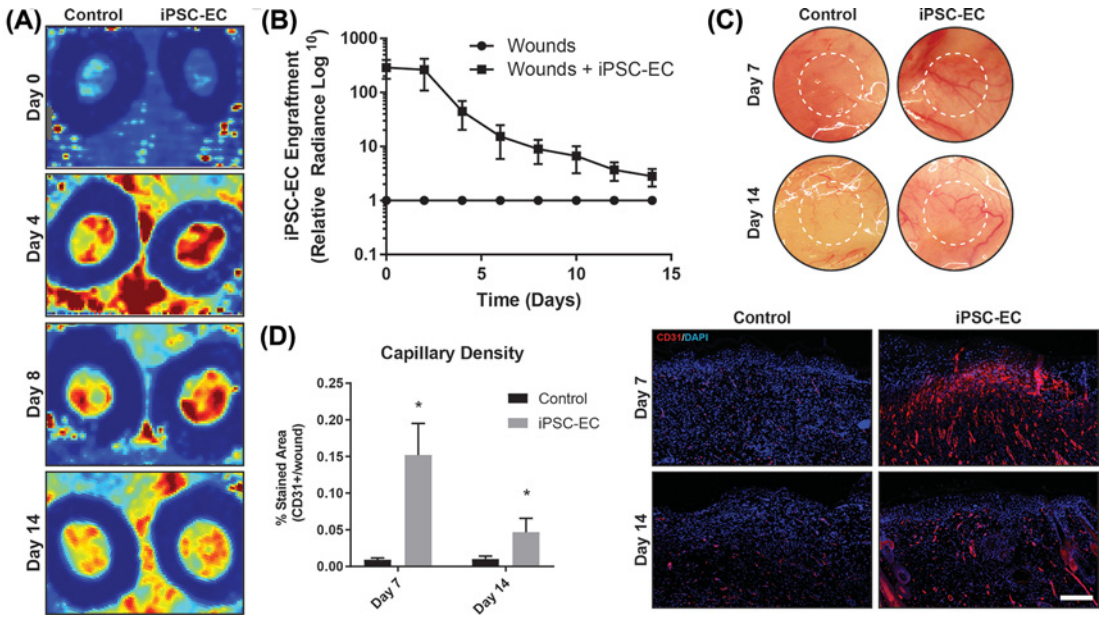

Figure 3. iPSC-EC treatment increases vascular density and wound perfusion

(**A**) Representative laser Doppler images, showing perfusion in control and iPSC-EC treated wounds on days 0, 4, 8 and 18 post–wounding. (**B**) Wound perfusion in iPSC-EC treated wounds, relative to their respective control wounds. Increased perfusion in iPSC-EC treated wounds was most pronounced during the first week of healing. (**C**) Representative photomicrographs of wounds, showing increased neo-vessel formation in iPSC-EC wounds relative to controls. (**D**) Capillary density, as measured by CD31+ staining, was significantly increased in iPSC-EC wounds at both early and late time points (*$P<0.05$, $n=6$ per treatment group).

At day 14, VEGF expression was significantly up-regulated by 12 ± 4% in iPSC-EC treated wounds compared with controls (Figure 2).

Wounds treated with iPSC-ECs exhibit increased angiogenesis

The anatomical hallmarks of angiogenesis include increased blood perfusion and high density of neo-capillary formation. Non-invasive IR laser Doppler imaging was conducted at the wound sites over 14 days to visualize and quantify levels of blood perfusion for the duration of wound healing (Figure 3A). Laser Doppler analysis revealed a maximum of two-fold increase in wound perfusion compared with control within the first 4 days following treatment in iPSC-EC treated wounds compared with control (Figure 3B). This gradually decreased back to baseline control wound perfusion levels by day 10. The subcutaneous layers of iPSC-EC treated, and control wounds were photographed following explant. A higher density of observable blood vessels was observed in iPSC-EC treated wounds compared with control (Figure 3C). To assess neo-capillary formation, cross-sections of wound explants were stained using the CD31 endothelial cell marker. At day 7, iPSC-EC treated wounds showed a 16-fold increase in capillary density compared with control wounds, which decreased to a four-fold increase by day 14 (Figure 3D).

iPSC-EC treatment enhances the native wound healing process

Native wound healing processes involve numerous cell phenotypes responsible for rebuilding the tissue architecture necessary for cell repopulation. Of these cell types, fibroblasts are largely implicated as essential matrix remodelling cells which facilitate neo-collagen deposition as a temporary matrix for cell growth and tissue regeneration. Using trichrome staining, wound cross-sections were quantified for levels of collagen deposition. iPSC-EC treated wounds showed a 20 ± 4% increase in collagen deposition at day 14 compared with control wounds (Figure 4B). Similar trends were observed with macrophage infiltration. At day 14, iPSC-EC treated wounds showed a 174 ± 6% increase in macrophage numbers compared with control wounds (Figure 5). The functional outcomes of wound healing were measured by taking three diameter measurements of wounds over 14 days and represented as percentage of total wound closure. iPSC-EC treated wounds show accelerated wound closure from day 2, which was significant on days 4 and 10 post-wounding and achieved complete wound closure 4 days earlier than control wounds (Figure 4A).

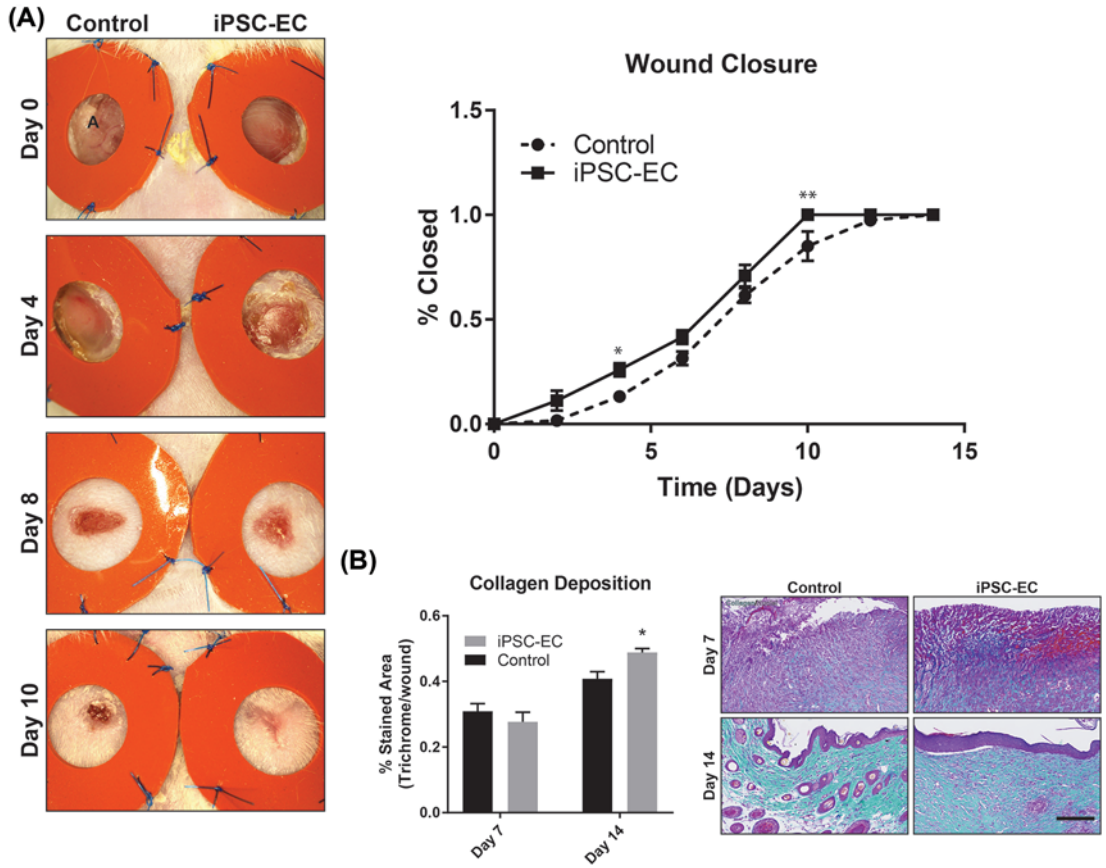

Figure 4. iPSC-EC treatment increases collagen deposition and accelerates wound closure

(**A**) Representative photomicrographs, showing progressive wound closure over a 14-day period. Rate of closure was significantly increased in iPSC-EC treated wounds compared with controls. (**B**) Milligan's Trichrome staining for collagen content. No differences were observed on day 7; by day 14 iPSC-EC treated wounds had significantly higher collagen content (*$P<0.05$, **$P<0.01$, $n=6$ per treatment group).

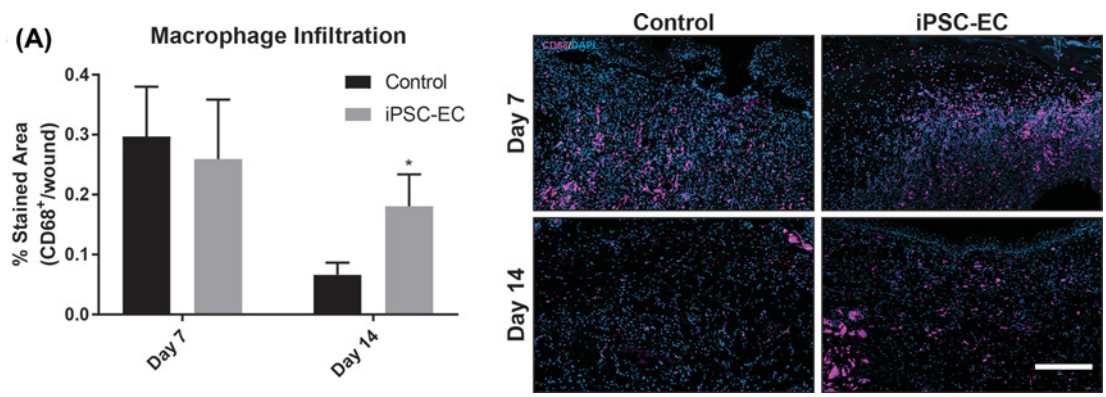

Figure 5. iPSC-EC treatment increases macrophage infiltration

(**A**) Anti-CD68 staining for macrophage infiltration. No differences were observed on day 7; by day 14 iPSC-EC treated wounds had significantly macrophage infiltration (*$P<0.05$, $n=6$ per treatment group).

Discussion

Chronic wounds and ulcers persist in a state of pathological inflammation, characterized by increased proteolytic activity, increased production of reactive oxygen species (ROS), senescent or dysfunctional fibroblasts, neutrophils and

Bioscience Reports (2018) **38** BSR20180563
https://doi.org/10.1042/BSR20180563

macrophages, and reduced pro-angiogenic growth factors and cytokines [4,7]. The aetiology of chronic wound formation in diabetes and peripheral arterial disease is multifactorial, but a major cause is underlying vasculopathy and diminished angiogenesis. The angiogenic response to ischaemia declines naturally with age and is further impaired in patients with vascular disease, who have reduced number and functionality of circulating EPCs [26-30]. The importance of angiogenesis in wound healing has been highlighted by interventional studies, which have shown that topical application of pro-angiogenic factors, such as VEGF or bFGF, is beneficial in accelerating diabetic wound healing in mice, while neutralizing them has the opposite effect [31-33]. However, clinical trials using single growth factors to boost angiogenesis have been largely unsuccessful, which likely reflects the complex regulation of angiogenesis *in vivo* and the need for a multifactorial approach [34].

Bone marrow and adipose tissue derived MSCs and EPCs have been in development for therapeutic angiogenesis for the past two decades, and have shown promise in promoting wound healing , however limited availability of healthy adult stem cells, and invasive aspiration procedures have tempered their use. iPSCs and their derivatives have several advantages, such as their relatively abundant supply, their non-controversial origins and the lack of immunogenicity if used for autologous transplantation [35]. Furthermore, the development of iPSC banking, the creation of multiple iPSC lines representing commonly present HLA allele combinations, means that patients could receive non-autologous cells without evoking an immune rejection, increasing the throughput while simultaneously reducing the time, cost and invasiveness of pluripotent cell therapies [36].

Here, we demonstrate the pro-angiogenic and wound healing capabilities of iPSC-ECs in a murine excisional wound model. Angiogenesis is vital for the formation and maintenance of granulation tissue in the first 2–4 days post-wounding. Neo-vessel formation typically begins around this time, peaking around day 7 before giving way to remodelling and maturation of the newly formed vasculature. We observed significantly accelerated wound closure in iPSC-EC treated wounds, as well as increased wound perfusion in the first week of healing, which was associated with a significant increase in endothelial cell surface marker PECAM-1 (CD31) staining in the wounds at both 7 and 14 days post-wounding. Consistent with previously described temporal patterns of angiogenesis in wound healing, absolute laser Doppler perfusion measurements decreased in both groups during the second week, approaching those of the surrounding healthy skin, as new dermis progressively covered exposed capillaries at the wound surface. Expression of *PECAM-1* and *Tie-1* mRNA was significantly up-regulated in iPSC-EC wounds on day 7 but was similar to expression in control wounds by day 14. Tie 1 is an endothelial cell specific orphan receptor, which has been shown to promote sprouting angiogenesis via regulation of Tie 2 receptor signalling [37].

iPSC-EC treatment also increased wound collagen deposition; sections from wounds treated with iPSC-ECs had significantly higher collagen content than the control wounds on day 14. Collagen deposition is vital for healthy wound healing, but the implication of increased collagen depends on the stage of healing as well as the types of collagen present; in the proliferative stage of healing collagen provides a matrix to support inflammatory and vascular cells as well as forming a stronger barrier than the fibrin clot [38]. In the late stages (remodelling), a reduction in collagen content is desirable to limit scarring. Collagen deposition begins within the first 24 h after wounding and peaks between 1 and 3 weeks later, depending on the wound site and size. As these wounds were still actively healing and in the proliferative phase at day 14, the observation of increased collagen is most likely indicative of a more advanced stage of healing compared with the controls, rather than excessive scarring. We also observed increased macrophage infiltration in iPSC-EC treated wounds at day 14 post-wounding, as evidenced by significantly increased CD68+ staining. In normal wound healing, macrophage infiltration peaks during the inflammatory phase (day 1–3 post-wounding) before subsiding. We observed no difference in CD68+ staining between control and iPSC-EC treated wounds at 7 days post-wounding. However, by day 14 iPSC-EC treated wounds had significantly greater CD68+ staining compared with their respective controls, suggesting sustained macrophage activity. This observation may be due to increased recruitment of macrophages in response to iPSC-ECs.

Poor cell survival and engraftment remains a major limitation to the long-term efficacy of cell therapies and therefore their suitability for clinical use. Most cells are lost within the first 48 h after administration, due to poor retention and cell death due to excessive inflammation, ischaemia or anoikis, the programmed death that occurs in endothelial cells and other anchorage-dependent cell types when they lose their interaction with ECM [39]. Very few previous wound healing studies included longitudinal tracking of the implanted cells to determine their eventual fate and those that did reported low rates of engraftment [40,41]. We used a firefly luciferase reporter gene construct and BLI for longitudinal tracking of iPSC-EC survival *in vivo* and although iPSC-EC fluorescent and bioluminescent signal was still detectable in the wounds 14 days post-treatment, we observed a substantial and progressive decline over the 2-week period. These data are consistent with previous *in vivo* survival of iPSC-ECs and suggest that the pro-angiogenic and pro-healing effects of our cells were primarily mediated via secretion of paracrine factors rather than engraftment or proliferation of the cells themselves [42]. Despite low rates of engraftment, stem cell treatments consistently evoke a

beneficial response. This suggests that even small increases in retention could translate to sizeable improvements in tissue regeneration and long-term recovery and we are conducting further studies seeding iPSC-ECs on biomaterial scaffolds to determine if this can increase their *in vivo* longevity and potentiate their beneficial effects.

Limitations

NOD/SCID mice are widely used in human haematopoietic cell studies and are an ideal strain for human cell transplantation because they lack functional B and T lymphocytes, lack the ability to mount an antibody-mediated response and additional deficiencies in their innate immune system allow for increased donor cell engraftment [43]. However, the blunted immune response to the cells creates a somewhat artificial environment in comparison with the situation in an immune competent organism. That being said, it is not possible to conduct pre-clinical, mechanistic investigations using human cells in other species without modulating the immune response. It is anticipated that the use of autologous or donor matched cells clinically would also mitigate the effects of immune rejection of the engrafted cells by the recipient, therefore we considered the NOD/SCID mouse to be the most suitable and appropriate model for these studies. It should also be noted that these mice are neither aged nor diabetic, so most innate wound healing capabilities are intact. This means that treatment effects are more difficult to detect, thus we anticipate an even more pronounced improvement after iPSC-EC treatment if we were able to use these cells in such a model.

Finally, we acknowledge that the iPSC-ECs used in the present study were differentiated from iPSCs that were generated using integrating viral vectors. These cells may not be suitable for use in a clinical setting because of the possibility of foreign DNA integrating into the host genome. However, the development of reprogramming protocols using small molecules means that iPSC-ECs for clinical applications can be generated without the use of viral vectors.

Conclusion

In the present study, we have demonstrated for the first time that human iPSC-ECs have pro-angiogenic functionality in wound healing, promote fibroblast infiltration and collagen deposition and accelerate wound closure. Longitudinal tracking of iPSC-ECs *in vivo* revealed a progressive decline in surviving iPSC-ECs over time, indicating that the cells are acting primarily through short-term paracrine effects. These findings have provoked further studies optimising iPSC-EC delivery to improve *in vivo* survival and engraftment rates, and also make a strong case for the development of clinical grade iPSCs and their derivatives for therapeutic angiogenesis in patients with vascular diseases.

Perspectives

(i) Ischaemia-mediated angiogenesis is impaired in patients with cardiovascular disease and diabetes, which leads to the development of intractable wounds and ulcers.

(ii) Here, we show that human iPSC-derived endothelial cells (iPSC-ECs) promote angiogenesis, increase collagen deposition and accelerate healing in a murine wound healing model.

(iii) Further development of human iPSC-ECs for therapeutic angiogenesis is a promising strategy to reduce the burden of chronic wounds in patients with peripheral arterial disease and diabetes.

Funding

This work was supported by the National Health and Medical Research Council (NHMRC) Early Career Fellowship [grant number GNT0633283 (to S.P.)].

Author contribution

Z.E.C. and R.P.T. contributed significantly and equally to the design and execution of the present study. Z.E.C. conceived and designed the study, developed the research plan, performed experiments, assisted with data analysis, and wrote the manuscript. R.P.T. conducted all *in vivo* and histology experiments, performed data analysis, and contributed to manuscript writing. M.M.M. and K.L. performed histological staining and quantitative PCR preparation and analysis. C.A.B. provided guidance on wound healing procedures. C.A.B., J.P.C., S.G.W., and S.P. supervised the project. All authors discussed the results, gave feedback, and approved the final manuscript.

Competing interests

The authors declare that there are no competing interests associated with the manuscript.

Abbreviations

bFGF, basic fibroblast growth factor; BLI, bioluminescent imaging; ECM, extracellular matrix; EGF, epidermal growth factor; eGFP, enhanced GFP; EPC, endothelial progenitor cell; iPSC, induced pluripotent stem cell; iPSC-EC, iPSC-derived endothelial cell; MSC, mesenchymal stem cell; NOD-SCID, non-obese diabetic - severe combined immunodeficiency; OCT, optimal cutting temperature; PAD, peripheral arterial disease; PECAM-1, platelet endothelial cell adhesion molecule; ROI, regions of interest; Tie-1, tyrosine kinase with Ig-like and EGF-like domains-1; VEGF, vascular endothelial growth factor; VE-cadherin, vascular endothelial cadherin.

References

1 Leavitt, T., Hu, M.S., Marshall, C.D., Barnes, L.A., Longaker, M.T. and Lorenz, H.P. (2016) Stem cells and chronic wound healing: state of the art. *Chronic Wound Care Management Res.* **3**, 7–27

2 Hinchliffe, R.J., Brownrigg, J.R.W., Andros, G., Apelqvist, J., Boyko, E.J., Fitridge, R. et al. (2016) Effectiveness of revascularization of the ulcerated foot in patients with diabetes and peripheral artery disease: a systematic review. *Diabetes Metab. Res. Rev.* **32**, 136–144, https://doi.org/10.1002/dmrr.2705

3 Dreifke, M.B., Jayasuriya, A.A. and Jayasuriya, A.C. (2015) Current wound healing procedures and potential care. *Mater. Sci. Eng. C Mater. Biol. Appl.* **48**, 651–662, https://doi.org/10.1016/j.msec.2014.12.068

4 Greaves, N.S., Ashcroft, K.J., Baguneid, M. and Bayat, A. (2013) Current understanding of molecular and cellular mechanisms in fibroplasia and angiogenesis during acute wound healing. *J. Dermatol. Sci.* **72**, 206–217, https://doi.org/10.1016/j.jdermsci.2013.07.008

5 Asahara, T., Masuda, H., Takahashi, T., Kalka, C., Pastore, C., Silver, M. et al. (1999) Bone marrow origin of endothelial progenitor cells responsible for postnatal vasculogenesis in physiological and pathological neovascularization. *Circ. Res.* **85**, 221–228, https://doi.org/10.1161/01.RES.85.3.221

6 Ishida, Y., Kimura, A., Kuninaka, Y., Inui, M., Matsushima, K., Mukaida, N. et al. Pivotal role of the CCL5/CCR5 interaction for recruitment of endothelial progenitor cells in mouse wound healing. *J. Clin. Invest.* **122**, 711–721, https://doi.org/10.1172/JCI43027

7 Falanga, V. Wound healing and its impairment in the diabetic foot. *Lancet North Am. Ed.* **366**, 1736–1743, https://doi.org/10.1016/S0140-6736(05)67700-8

8 Schultz, G.S. and Wysocki, A. (2009) Interactions between extracellular matrix and growth factors in wound healing. *Wound Repair Regen.* **17**, 153–162, https://doi.org/10.1111/j.1524-475X.2009.00466.x

9 Martin, P. and Nunan, R. (2015) Cellular and molecular mechanisms of repair in acute and chronic wound healing. *Br. J. Dermatol.* **173**, 370–378, https://doi.org/10.1111/bjd.13954

10 Kim, S.-W., Zhang, H.-Z., Guo, L., Kim, J.-M. and Kim, M.H. (2012) Amniotic mesenchymal stem cells enhance wound healing in diabetic NOD/SCID mice through high angiogenic and engraftment capabilities. *PLoS ONE* **7**, e41105, https://doi.org/10.1371/journal.pone.0041105

11 Jackson, W.M., Nesti, L.J. and Tuan, R.S. (2012) Concise review: clinical translation of wound healing therapies based on mesenchymal stem cells. *Stem Cells Transl. Med.* **1**, 44–50, https://doi.org/10.5966/sctm.2011-0024

12 Nie, C., Yang, D., Xu, J., Si, Z., Jin, X. and Zhang, J. (2011) Locally administered adipose-derived stem cells accelerate wound healing through differentiation and vasculogenesis. *Cell Transplant.* **20**, 205–216, https://doi.org/10.3727/096368910X520065

13 Fathke, C., Wilson, L., Hutter, J., Kapoor, V., Smith, A., Hocking, A. et al. (2004) Contribution of bone marrow–derived cells to skin: collagen deposition and wound repair. *Stem Cells* **22**, 812–822, https://doi.org/10.1634/stemcells.22-5-812

14 Badiavas, E.V. and Falanga, V. (2003) Treatment of chronic wounds with bone marrow–derived cells. *Arch. Dermatol.* **139**, 510–516, https://doi.org/10.1001/archderm.139.4.510

15 Dash, N.R., Dash, S.N., Routray, P., Mohapatra, S. and Mohapatra, P.C. (2009) Targeting nonhealing ulcers of lower extremity in human through autologous bone marrow-derived mesenchymal stem cells. *Rejuv. Res.* **12**, 359–366, https://doi.org/10.1089/rej.2009.0872

16 Isakson, M., de Blacam, C., Whelan, D., McArdle, A. and Clover, A.J.P. (2015) Mesenchymal stem cells and cutaneous wound healing: current evidence and future potential. *Stem Cells Int.* **2015**, 831095, https://doi.org/10.1155/2015/831095

17 Marino, G., Moraci, M., Armenia, E., Orabona, C., Sergio, R., De Sena, G. et al. (2013) Therapy with autologous adipose-derived regenerative cells for the care of chronic ulcer of lower limbs in patients with peripheral arterial disease. *J. Surg. Res.* **185**, 36–44, https://doi.org/10.1016/j.jss.2013.05.024

18 Asai, J., Takenaka, H., Ii, M., Asahi, M., Kishimoto, S., Katoh, N. et al. (2013) Topical application of *ex vivo* expanded endothelial progenitor cells promotes vascularisation and wound healing in diabetic mice. *Int. Wound J.* **10**, 527–533, https://doi.org/10.1111/j.1742-481X.2012.01010.x

19 Park, S.-J., Moon, S.-H., Lee, H.-J., Lim, J.-J., Kim, J.-M., Seo, J. et al. (2013) A comparison of human cord blood- and embryonic stem cell-derived endothelial progenitor cells in the treatment of chronic wounds. *Biomaterials* **34**, 995–1003, https://doi.org/10.1016/j.biomaterials.2012.10.039

20 Rufaihah, A.J., Huang, N.F., Jame, S., Lee, J.C., Nguyen, H.N., Byers, B. et al. (2011) Endothelial cells derived from human iPSCS increase capillary density and improve perfusion in a mouse model of peripheral arterial disease. *Arterioscler Thromb. Vasc. Biol.* **31**, e72–9, https://doi.org/10.1161/ATVBAHA.111.230938

21 Clayton, Z.E., Yuen, G.S., Sadeghipour, S., Hywood, J.D., Wong, J.W., Huang, N.F. et al. (2017) A comparison of the pro-angiogenic potential of human induced pluripotent stem cell derived endothelial cells and induced endothelial cells in a murine model of peripheral arterial disease. *Int. J. Cardiol.* **234**, 81–89, https://doi.org/10.1016/j.ijcard.2017.01.125

22 Takahashi, K., Tanabe, K., Ohnuki, M., Narita, M., Ichisaka, T., Tomoda, K. et al. (2007) Induction of pluripotent stem cells from adult human fibroblasts by defined factors. *Cell* **131**, 861–872, https://doi.org/10.1016/j.cell.2007.11.019
23 Rufaihah, A.J., Huang, N.F., Kim, J., Herold, J., Volz, K.S., Park, T.S. et al. (2013) Human induced pluripotent stem cell-derived endothelial cells exhibit functional heterogeneity. *Am. J. Transl. Res.* **5**, 21–35
24 Galiano, R.D., Michaels, V.J., Dobryansky, M., Levine, J.P. and Gurtner, G.C. (2004) Quantitative and reproducible murine model of excisional wound healing. *Wound Rep. Regen.* **12**, 485–492, https://doi.org/10.1111/j.1067-1927.2004.12404.x
25 Dunn, L., Prosser, H.C.G., Tan, J.T.M., Vanags, L.Z., Ng, M.K.C. and Bursill, C.A. (2013) Murine model of wound healing. *J. Vis. Exp.* **2013**, e50265
26 Loh, S.A., Chang, E.I., Galvez, M.G., Thangarajah, H., El-ftesi, S., Vial, I.N. et al. (2009) SDF-1α expression during wound healing in the aged is HIF dependent. *Plast. Reconstr. Surg.* **123**, 65S–75S, https://doi.org/10.1097/PRS.0b013e318191bdf4
27 Takahashi, T., Kalka, C., Masuda, H., Chen, D., Silver, M., Kearney, M. et al. (1999) Ischemia- and cytokine-induced mobilization of bone marrow-derived endothelial progenitor cells for neovascularization. *Nat. Med.* **5**, 434–438, https://doi.org/10.1038/7434
28 Shintani, S., Murohara, T., Ikeda, H., Ueno, T., Honma, T., Katoh, A. et al. (2001) Mobilization of endothelial progenitor cells in patients with acute myocardial infarction. *Circulation* **103**, 2776–2779, https://doi.org/10.1161/hc2301.092122
29 Vasa, M., Fichtlscherer, S., Aicher, A., Adler, K., Urbich, C., Martin, H. et al. (2001) Number and migratory activity of circulating endothelial progenitor cells inversely correlate with risk factors for coronary artery disease. *Circ. Res.* **89**, e1–e7, https://doi.org/10.1161/hh1301.093953
30 Schmidt-Lucke, C., Rössig, L., Fichtlscherer, S., Vasa, M., Britten, M., Kämper, U. et al. (2005) Reduced number of circulating endothelial progenitor cells predicts future cardiovascular events: proof of concept for the clinical importance of endogenous vascular repair. *Circulation* **111**, 2981–2987, https://doi.org/10.1161/CIRCULATIONAHA.104.504340
31 Galiano, R.D., Tepper, O.M., Pelo, C.R., Bhatt, K.A., Callaghan, M., Bastidas, N. et al. (2004) Topical vascular endothelial growth factor accelerates diabetic wound healing through increased angiogenesis and by mobilizing and recruiting bone marrow-derived cells. *Am. J. Pathol.* **164**, 1935–1947, https://doi.org/10.1016/S0002-9440(10)63754-6
32 Gurtner, G.C., Werner, S., Barrandon, Y. and Longaker, M.T. (2008) Wound repair and regeneration. *Nature* **453**, 314–321, https://doi.org/10.1038/nature07039
33 Yoshida, S., Yamaguchi, Y., Itami, S., Yoshikawa, K., Tabata, Y., Matsumoto, K. et al. (2003) Neutralization of hepatocyte growth factor leads to retarded cutaneous wound healing associated with decreased neovascularization and granulation tissue formation. *J. Invest. Dermatol.* **120**, 335–343, https://doi.org/10.1046/j.1523-1747.2003.12039.x
34 Henry, T.D., Annex, B.H., McKendall, G.R., Azrin, M.A., Lopez, J.J., Giordano, F.J. et al. (2003) The VIVA Trial: vascular endothelial growth factor in ischemia for vascular angiogenesis. *Circulation* **107**, 1359–1365, https://doi.org/10.1161/01.CIR.0000061911.47710.8A
35 Leeper, N.J., Hunter, A.L. and Cooke, J.P. (2010) Stem cell therapy for vascular regeneration: adult, embryonic, and induced pluripotent stem cells. *Circulation* **122**, 517–526, https://doi.org/10.1161/CIRCULATIONAHA.109.881441
36 Solomon, S., Pitossi, F. and Rao, M.S. (2015) Banking on iPSC- is it doable and is it worthwhile. *Stem Cell Rev. Rep.* **11**, 1–10, https://doi.org/10.1007/s12015-014-9574-4
37 Chong, J.J.H., Reinecke, H., Iwata, M., Torok-Storb, B., Stempien-Otero, A. and Murry, C.E. (2013) Progenitor cells identified by PDGFR-alpha expression in the developing and diseased human heart. *Stem Cells Dev.* **22**, 1932–1943, https://doi.org/10.1089/scd.2012.0542
38 Martin, P. (1997) Wound healing–aiming for perfect skin regeneration. *Science* **276**, 75–81, https://doi.org/10.1126/science.276.5309.75
39 Li, X., Tamama, K., Xie, X. and Guan, J. (2016) Improving cell engraftment in cardiac stem cell therapy. *Stem Cells Int.* **2016**, 11, https://doi.org/10.1155/2016/7168797
40 Wu, Y., Chen, L., Scott, P.G. and Tredget, E.E. (2007) Mesenchymal stem cells enhance wound healing through differentiation and angiogenesis. *Stem Cells* **25**, 2648–2659, https://doi.org/10.1634/stemcells.2007-0226
41 Lee, K.B., Choi, J., Cho, S.B., Chung, J.Y., Moon, E.S. and Kim, N.S. (2011) Topical embryonic stem cells enhance wound healing in diabetic rats. *J. Orthop. Res.* **29**, 1554–1562, https://doi.org/10.1002/jor.21385
42 Park, S.-R., Kim, J.-W., Jun, H.-S., Roh, J.Y., Lee, H.-Y. and Hong, I.-S. (2018) Stem cell secretome and its effect on cellular mechanisms relevant to wound healing. *Mol. Ther.* **26**, 606–617, https://doi.org/10.1016/j.ymthe.2017.09.023
43 Shultz, L.D., Ishikawa, F. and Greiner, D.L. (2007) Humanized mice in translational biomedical research. *Nat. Rev. Immunol.* **7**, 118–130, https://doi.org/10.1038/nri2017

Chapter 4

Integration of Induced Pluripotent Stem Cell Derived Endothelial Cells with Polycaprolactone/Gelatin-Based Electrospun Scaffolds for Enhanced Therapeutic Angiogenesis

Tan et al. Stem Cell Research & Therapy (2018) 9:70
https://doi.org/10.1186/s13287 018 0824 2

Stem Cell Research & Therapy

RESEARCH Open Access

Integration of induced pluripotent stem cell-derived endothelial cells with polycaprolactone/gelatin-based electrospun scaffolds for enhanced therapeutic angiogenesis

Richard P. Tan[1,2*], Alex H. P. Chan[1,2], Katarina Lennartsson[1], Maria M. Miravet[1], Bob S. L. Lee[1,2], Jelena Rnjak Kovacina[5], Zoe E. Clayton[1], John P. Cooke[4], Martin K. C. Ng[1,3], Sanjay Patel[1,3] and Steven G. Wise[1,2]

Abstract

Background: Induced pluripotent stem cell derived endothelial cells (iPSC ECs) can be generated from any somatic cell and their iPSC sources possess unlimited self renewal. Previous demonstration of their proangiogenic activity makes them a promising cell type for treatment of ischemic injury. As with many other stem cell approaches, the low rate of in vivo survival has been a major limitation to the efficacy of iPSC ECs to date. In this study, we aimed to increase the in vivo lifetime of iPSC ECs by culturing them on electrospun polycaprolactone (PCL)/gelatin scaffolds, before quantifying the subsequent impact on their proangiogenic function.

Methods: iPSC ECs were isolated and stably transfected with a luciferase reporter to facilitate quantification of cell numbers and non invasive imaging in vivo PCL/gelatin scaffolds were engineered using electrospinning to obtain woven meshes of nanofibers. iPSC ECs were cultured on scaffolds for 7 days. Subsequently, cell growth and function were assessed in vitro followed by implantation in a mouseback subcutaneous model for 7 days.

Results: Using a matrix of conditions, we found that scaffold blends with ratios of PCL:gelatin of 70:30 (PG73) spun at high flow rates supported the greatest levels of iPSC EC growth, retention of phenotype, and function in vitro. Implanting iPSC ECs seeded on PG73 scaffolds in vivo improved their survival up to 3 days, compared to cells directly injected into control wounds, which were no longer observable within 1 h. Enhanced engraftment improved blood perfusion, observed through non invasive laser Doppler imaging. Immunohistochemistry revealed a corresponding increase in host angiogenic mechanisms characterized by the enhanced recruitment of macrophages and the elevated expression of proangiogenic cytokines vascular endothelial growth factor and placental growth factor.

Conclusions: Knowledge of these mechanisms combined with a deeper understanding of the scaffold parameters influencing this function provides the groundwork for optimizing future iPSC EC therapies utilizing engraftment platforms. The development of combined scaffold and iPSC EC therapies could ultimately improve therapeutic angiogenesis and the treatment of ischemic injury.

Keywords: Induced pluripotent stem cells, Endothelial cells, Biomaterial scaffolds, Angiogenesis, Regenerative medicine

* Correspondence: richard.tan@hri.org.au
[1]The Heart Research Institute, Sydney, NSW 2042, Australia
[2]Sydney Medical School, University of Sydney, Sydney, NSW 2006, Australia
Full list of author information is available at the end of the article

Background

Ischemic injury is one of the key biological events underlying the tissue pathology of some of the most debilitating diseases, including myocardial infarction, acute kidney failure, and stroke [1]. Ischemia, caused by the complete or even partial occlusion of the blood vessel network in the affected organ, results in drastic levels of nutrient and oxygen depletion (hypoxia) as well as inadequate removal of metabolic waste. Without timely and robust intervention, ischemia progresses to tissue necrosis and, in highly sensitive organs such as the brain or heart, can lead to immediate death [2, 3]. Responding to tissue ischemia, the body activates innate healing mechanisms that attempt to restore blood flow through the formation of new blood vessel networks, a process known as angiogenesis. However, these native revascularization systems often occur too slowly and/or are inadequate in magnitude to overcome large-scale ischemic injury [4]. This shortcoming has inspired a field of regenerative medicine that aims to augment and control the host angiogenic response to revascularize ischemic tissue, known as therapeutic angiogenesis.

While individual growth factors and genes regulating angiogenesis have been well characterized, their translation to therapeutic angiogenesis in vivo has been underwhelming, demonstrated by several inconclusive or negative clinical trials [5, 6]. For example, single agents such as vascular endothelial growth factor (VEGF) aiming to promote increased peripheral angiogenesis are promising in preclinical studies, but perform poorly in human trials [7]. As a result, it has become increasingly accepted that modulation of angiogenesis involves the activation of a complex network of events not readily addressed by a single growth factor or gene therapy. Thought to represent a more extensive and comprehensive control over angiogenesis, stem/progenitor cell-based therapy has gained attention due to the cells' intrinsic characteristics as hypoxia-responsive multiparacrine release vehicles. While stem cell therapy has traditionally been plagued by inadequate cell numbers and ethical concerns regarding their origin, in recent years the advent of induced pluripotent stem cells (iPSCs) has overcome some of these barriers [8]. iPSCs can be generated from any somatic cell and possess unlimited self-renewal and differentiation potential [8]. Of the numerous iPSC-derived cell phenotypes extensively studied for proangiogenic function, iPSC-derived endothelial cells (iPSC-ECs) appear to be most promising for therapeutic angiogenesis [9–11]. However, translational challenges for iPSC-ECs common to traditional stem cell therapy remain; in particular, low levels of in-vivo engraftment and short-term viability [12]. iPSC-ECs fail to integrate with the host tissue and gradually die after delivery [9, 10, 13], highlighting an essential need for engraftment strategies capable of extending their in-vivo lifetime and potentially augmenting their proangiogenic function.

Synthetic biomaterial scaffolds have made a tremendous impact in regenerative medicine by allowing researchers to provide functional platforms containing the biophysical and chemical cues necessary to sustain stem cell behavior and function [14] that are often absent at sites of ischemic injury and necrotic tissue. The employment of biomaterial scaffolds to enhance engraftment of iPSC-ECs in vivo is a promising approach to improve therapeutic angiogenesis. However, literature surrounding iPSC-ECs combined with biomaterial scaffolds in vivo is limited, with only a few publications to date investigating this concept [15, 16]. While demonstrating enhanced angiogenic effects, these studies are conducted in immunodeficient mice that do not represent native engraftment conditions following exogenous cell injections. Additionally, the functional mechanisms underlying scaffold-mediated enhancement of iPSC-EC proangiogenic function in vivo have not yet been defined. Insight into these mechanisms is important for future optimization of combined iPSC-EC scaffold strategies and for defining the practical guidelines necessary for their improved translation.

In this study, we conduct a comprehensive analysis of electrospun polycaprolactone (PCL)/gelatin scaffolds and their potential to enhance the engraftment and proangiogenic function of iPSC-ECs in vitro and in vivo. Through tailoring of material composition and structural properties, we identify candidate scaffolds best able to support iPSC-EC growth and function in vitro. Using these scaffolds as engraftment platforms, we assess their potential to augment the proangiogenic effects of iPSC-ECs following implantation in vivo. Through gene expression and immunohistochemical analysis, we identify some of the key drivers of scaffold-mediated enhancement of iPSC-EC angiogenic function, while defining important benchmarks of scaffold performance that relate to these effects. The findings of this study provide mechanistic knowledge essential to the future development of optimized therapies combining iPSC-ECs with biomaterial scaffolds, which may ultimately improve the translation of iPSC-ECs for therapeutic angiogenesis.

Methods

Reagents

D-Luciferin potassium salt was purchased from Cayman Chemicals (Ann Arbor, MI, USA). Lympholyte®-M cell separation medium was purchased from Cedarlane Labs (Burlington, ON, CA). Endothelial Basal Medium (phenol red free) was purchased from Lonza (Switzerland). Polycaprolactone (PCL) polymer, gelatin, and 1,1,1,3,3,3-hexafluoro-2-proponal (HFP) solvent were purchased from

Sigma-Aldrich (St. Louis, MO, USA). Purified, soluble ovine collagen was obtained from CollTech (Osborne Park, WA, Australia) and lyophilized as described previously. Multiple Stain Solution (MSS) and JB-4 resin were purchased from Polysciences Inc. (Warrington, PA, USA).

Electrospinning

PCL and gelatin were dissolved at a total of 10% (*w/v*) in HFP in varying ratios. Solutions were loaded into a syringe and fed through a 0.6-mm-diameter needle at a flow rate of either 8 ml/h or 16 ml/h using a syringe pump. The needle was connected to a 20-kV positive power supply and directed at a grounded parallel plate collector at a distance of 20 cm. Scaffolds were then cut into circular discs using a 6-mm-diameter biopsy punch. Before cell seeding and implantation, scaffolds were sterilized by UV light for 30 min and washed three times with and stored in sterile PBS.

Scaffold characterization

Scaffold surfaces were imaged under a 15-kV scanning electron microscope at 4000× magnification under high vacuum conditions. Images were taken for $n = 5$ scaffolds/group and then $n = 100$ fibers were measured for each sample. For porosity measurements, scaffolds were embedded in JB-4 resin and cut into 5-μm cross-sections. The cross-sections were stained using Multiple Stain Solution and imaged at 40× magnification. Cross-section images were then converted to 8-bit grayscale and the percentage of white (pores) vs black (scaffold) was quantified as porosity. For scaffold wetting experiments, scaffolds were soaked in PBS for 7 days at 37 °C. Scaffolds were then completely dried overnight in a fume hood at RT prior to scanning electron microscopy (SEM) imaging.

Mechanical testing of the electrospun scaffolds was performed on an Instron Tensile Machine (Instron 5543). Briefly, scaffolds were cut into strips of 0.5 cm × 3.5 cm and clamped into the Instron. A constant pull of 3 mm/min was applied and the force measured by a 50-N load cell. Wet samples were incubated in PBS at 37 °C for 1 h and dried prior to measurement. The elastic modulus was obtained from the linear region of the stress/strain curve. Ultimate tensile strength was defined as the maximum force at break.

Degradation testing of electrospun scaffolds was performed by immersing scaffold samples in a 1 U/ml Protease XIV (Sigma) solution at 37 °C for 4 days. Samples were preweighed prior to immersion and were allowed to dry prior to reweighing. Degradation was expressed as the percentage of initial weight remaining per day.

iPSC-EC derivation and culture

iPSC-ECs were fully differentiated and characterized, as described previously [17], prior to use in experiments. Briefly, iPSCs were generated via retroviral overexpression of Oct4, SOX2, KLF4, and c-Myc in adult human dermal fibroblasts and differentiated into endothelial cells using previously described methods [9, 18]. On day 14 of differentiation, iPSC-ECs were purified using FACS to sort for $CD31^+$ cells (Anti-human CD31-PE; eBioscience Inc., San Diego, CA, USA) as described previously [19]. iPSC-ECs were also stably transfected with a reporter expression system encoding the firefly luciferase enzyme as an imaging modality. iPSC-ECs were cultured in EGM-2MV media (CC3202; Lonza Group Ltd) and seeded on PCL/gelatin scaffolds at a concentration of 1×10^5 cells/scaffold in a total media volume of 200 μl. After 24 h, scaffolds were placed into fresh EGM-2MV and the media changed every other day for 7 days (Fig. 1b). For hypoxia experiments, iPSC-ECs were cultured in 1% O_2 for 24 h prior to RNA extraction and subsequent qPCR analysis. Prior to implantation, iPSC-EC-seeded scaffolds and iPSC-ECs alone were washed and suspended in basal EGM to remove all endothelial growth factors from the media.

Angiogenic gene expression in vitro

Quantitative PCR was performed using iQ SYBR-Green Supermix and the iCycler Real-time PCR Detection System (Bio-Rad). Gene expression was calculated using primers for vascular endothelial growth factor (VEGF) (forward, 5′-TGCCAAGTGGTCCCAG–3′; reverse, 5′-GTGAGGTCT TGATCCG-3′), epidermal growth factor (EGF) (forward, 5′-GAGGAGCACGGGAAAAGAA-3′; reverse, 5′-CCGG AGCTCCTTCACATATT-3′), and placental growth factor (PlGF) (forward, 5′-GTTCAGCCCATCCTGTGTCT-3′; reverse, 5′-TTAGGAGCTGCATGGTGACA-3′), with *B2M* as a housekeeping gene.

Mouse subcutaneous implantation

Study approval was obtained from Sydney Local Heath District Animal Welfare Committee (protocol number 2013/050). Experiments were conducted in accordance with the Australian Code of Practice for the Care and Use of Animals for Scientific Purpose. Under 2% methoxyfluorane anesthesia, wild-type FVB/n mice had their dorsal surfaces shaved, sterilized with betadine solution, and washed clean with sterile PBS. Four 1.5-cm incisions (two rows side by side) were then cut through the skin to create four subcutaneous pockets [20]. Within each wound, control EBM media, iPSC-ECs, iPSC-EC-seeded scaffolds, or scaffold alone were transplanted. The wounds were closed with 6–0 silk sutures. Mice were then allowed to recover for at least 1 h. Mice underwent IVIS imaging over the course of 9 days when bioluminescent signals from iPSC-ECs were no longer observed. Skin wound biopsies were taken at defined histological time points.

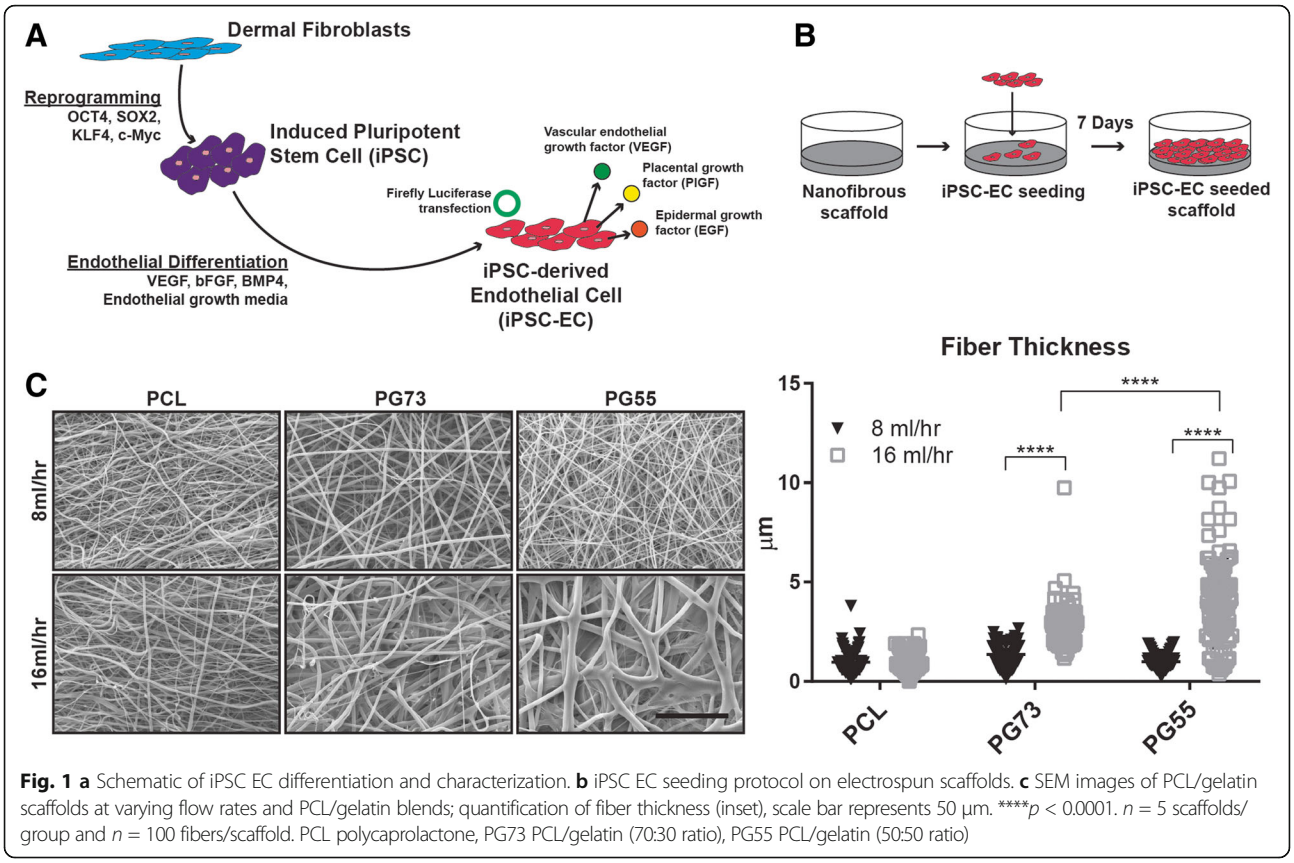

Fig. 1 **a** Schematic of iPSC EC differentiation and characterization. **b** iPSC EC seeding protocol on electrospun scaffolds. **c** SEM images of PCL/gelatin scaffolds at varying flow rates and PCL/gelatin blends; quantification of fiber thickness (inset), scale bar represents 50 μm. ****$p < 0.0001$. $n = 5$ scaffolds/group and $n = 100$ fibers/scaffold. PCL polycaprolactone, PG73 PCL/gelatin (70:30 ratio), PG55 PCL/gelatin (50:50 ratio)

Bioluminescence imaging

D-Luciferin was reconstituted at a concentration of 40 mg/ml. Binding of the luciferin substrate to the luciferase enzyme results in bioluminescence, quantified using the IVIS Series preclinical in-vivo imaging system apparatus (Perkin Elmer). To induce bioluminescence, luciferin was given at a total volume of 100 μl through intramuscular administration at the implantation site. Bioluminescence was measured in units of radiance (photons/s/cm^2/sr). All bioluminescence measurements were calculated as mean radiance within a predefined region of interest (ROI). Mean radiance measurements for each ROI were averaged amongst $n = 5$ per group using repeated measurement of the same subjects over time.

Perfusion Doppler imaging and analysis

Post surgery, perfusion at the implantation site was measured by laser Doppler MOOR-LMD V192 (Moor Instruments, UK). Mice were anesthetized prior to imaging and the anesthetic removed during imaging. Three repeat Doppler measurements were taken after removal of the anesthetic to prevent perfusion data being affected by variations in depth of anesthesia. Doppler recordings were taken of the entire mouse back in a scan area of 6 cm × 8 cm at a scan rate of 10 px/s. Doppler measurements ($n = 5$ per group) were quantified by drawing equal areas with the surgical wound of the implantation site located in the middle of the quantification area.

Histology and immunohistochemistry

Histology and immunohistochemistry analysis was conducted as described previously [20]. Briefly, for histology stains, standard H&E was used to assess total cell infiltration. For immunohistochemistry analysis, sections were stained with primary antibodies including anti-VEGFA (Abcam, USA) for vascular endothelial growth factor expression, anti-PlGF (Abcam, USA) for placental growth factor expression, anti-NE (neutrophil elastase) (Abcam, USA) for neutrophils, anti-CD68 (Abcam, USA) for macrophages, anti-CD31 (Abcam, USA) for endothelial cells, anti-vimentin (Abcam, USA) for fibroblasts, and anti-SMC-α actin (Abcam, USA) for smooth muscle cells. Fluorescence microscopy was then used to visualize cell markers using Alexa Fluor 594-conjugated secondary antibodies. Sections were mounted with DAPI-containing mounting media (VECTASHIELD).

Quantitative image analysis

Quantification of bioluminescence images was performed using LivingImage 4.5 (Perkin Elmer) software. Histological and immunohistochemical sections were imaged using a Zeiss Upright Olympus fluorescence

multichannel microscope, captured with a Nikon DP Controller 2.2 (Olympus, Japan). Immunohistochemical and histopathological analysis was done using ImageJ. For immunohistochemical analysis, marker expression was expressed as the positive stained area determined by a common threshold intensity divided by the tissue area of measurement. All markers were quantified from $n = 6$ sections per group per time point.

Statistical analysis

Data are expressed as mean ± SEM and statistical significance indicated as either $p < 0.05$, $p < 0.01$, $p < 0.001$, or $p < 0.0001$. The data were compared using one-way ANOVA followed by Bonferroni's post-hoc test or two-way ANOVA followed by Tukey's post-hoc test using GraphPad Prism version 5.00 (GraphPad Software, San Diego, CA, USA) for PC.

Results

Scaffold characterization

Solutions of pure PCL and blends of PCL and gelatin at ratios of 70:30 (PG73) and 50:50 (PG55) were electrospun at low (8 ml/h) and high (16 ml/h) flow rates. SEM analysis of scaffold surfaces showed that the fiber width increased at high flow rates in gelatin-containing blends only (1.35 ± 0.53 vs 2.63 ± 1.04 μm in PG73, $p < 0.0001$; 0.98 ± 0.38 vs 3.95 ± 2.27 μm in PG55, $p < 0.0001$) (Fig. 1b). High flow rate fibers were largest in PG55 blends followed by PG73 (3.95 ± 2.27 vs 2.63 ± 1.04 μm, $p < 0.0001$; Fig. 1b). However, PG55 scaffolds had a larger distribution of fiber widths compared to PG73. SEM analysis of high flow rate PG73 and PG55 scaffolds after 7 days of wetting in PBS showed that PG55 fibers appeared to be more structurally compromised compared to PG73 fibers, indicated by a loss of fiber morphology (Additional file 1: Figure S1A).

To further examine the physical stability of PG73 scaffolds, mechanical testing and degradation experiments were conducted. Mechanical testing of PG73 scaffolds showed that wetting of the scaffold did not compromise structural integrity, indicated by no significant changes in ultimate tensile strength (UTS) and Young's modulus before and after wetting (Additional file 2: Figure S2B, C). Additionally, under accelerated degradation conditions in a Protease XIV solution at 37 °C for 4 days, PG73 scaffolds showed similar degradation profiles as pure PCL (Additional file 2: Figure S2D).

Cross-sectional imaging revealed the internal structure of scaffolds, allowing for an estimation of pore size. No significant differences were observed between scaffold groups; however, pore size tended to be reduced with both higher flow rates and increasing gelatin content (Additional file 1: Figure S1B).

iPSC-EC growth and phenotype on scaffolds

iPSC-ECs were seeded on scaffolds and cell growth was quantified using a transfected bioluminescence reporter. Generation of a standard curve demonstrated a linear correlation of bioluminescence intensity to iPSC-EC number (Fig. 2a). The detectable range of iPSC-EC bioluminescence was found to be between 1×10^3 and 1×10^6 cells/well (Additional file 3: Figure S3). Concentrations of iPSC-ECs less than 1×10^3 cells/well were not significantly different from background signals, while those greater than 1×10^6 cells/well saturated the bioluminescence reading capacity of the IVIS imaging apparatus.

At day 3 in culture, the highest cell numbers were observed on PG73 and PG55 scaffolds at high flow rates (1.44 ± 0.45 and 1.45 ± 0.28 × 10^5 cells, respectively; Fig. 2b). By day 7, these conditions were both significantly increased compared to all scaffold groups (3.12 ± 0.73 and 2.69 ± 1.02 × 10^5 cells, respectively, $p < 0.001$ and $p < 0.01$; Fig. 2b).

Immunofluorescence analysis using the CD31 endothelial cell marker at day 7 in culture revealed the highest CD31 expression for iPSC-ECs seeded on PG73 scaffolds at high flow rate (3.49 ± 0.11%, $p < 0.01$; Fig. 2c), followed by PG55 scaffolds at high flow rate (2.68 ± 0.41%, $p < 0.05$; Fig. 2c), when compared to PCL.

Cross-sectional staining of seeded scaffolds using DAPI nuclei counterstain revealed no differences in infiltration of iPSC-ECs into the scaffolds, irrespective of fiber size or composition at day 7 in culture (Additional file 2: Figure S2).

The elevated growth rates and high CD31 expression suggested an advantage for using PG73 high flow rate scaffolds as candidate engraftment platforms for subsequent in-vivo studies.

Preimplantation characterization of iPSC-EC-seeded PG73 scaffolds

To assess functional changes of iPSC-ECs seeded on PG73 scaffolds after 7 days in culture, we analyzed hypoxia-induced gene expression and scaffold remodeling effects. When grown on tissue culture plastic under hypoxic conditions, iPSC-ECs upregulated the expression of epidermal growth factor (EGF) and placental growth factor (PlGF), while vascular endothelial growth factor (VEGF) upregulation was highly variable. However, when cultured on PG73 scaffolds under similar hypoxic conditions, this upregulation was further enhanced by 1.8-fold, 3.17-fold, and 1.17-fold, respectively (4.86 ± 0.85 vs 2.67 ± 0.89-fold, 6.24 ± 2.01 vs 1.97 ± 0.86-fold, and 20.25 ± 4.28 vs 17.24 ± 10.87-fold, respectively, $p < 0.05$, $p < 0.01$; Fig. 3a). The hypoxia-responsive function of iPSC-ECs on PG73 scaffolds was enhanced compared to normal tissue culture conditions.

To assess dedifferentiation of iPSC-ECs back to dermal fibroblast phenotypes, iPSC-EC cultures on PG73 and PCL scaffolds were assessed for fibroblast phenotypes

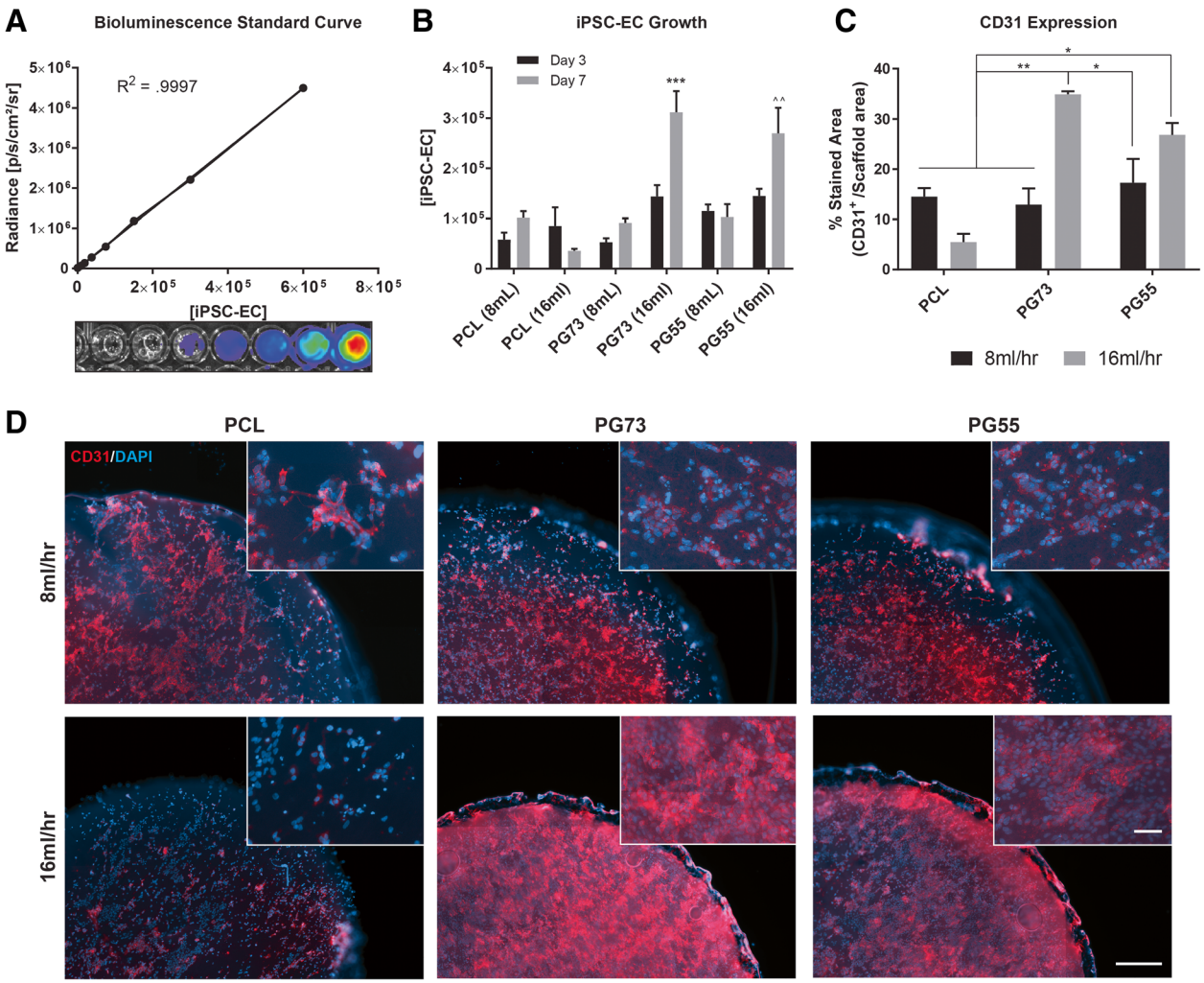

Fig. 2 a Bioluminescence standard curve of iPSC EC cell number, representative cell bioluminescence images (inset). **b** iPSC EC growth at 3 and 7 days on electrospun scaffolds of varying flow rate and PCL/gelatin blends. ***$p < 0.001$, **$p < 0.01$ compared to PCL (8 ml/h) control scaffolds within the same time point. $n = 5$ scaffolds/group. **c** CD31 quantification of iPSC EC cultures on scaffolds at 7 days *in vitro*. *$p < 0.05$, **$p < 0.01$. $n = 5$ scaffolds/group. **d** Representative photographs of iPSC EC cultures stained with CD31 (red) and counterstained with DAPI (blue) at 5×; magnified images at 10× (inset). Scale bar represents 100 μm, inset scale bar represents 10 μm. iPSC EC induced pluripotent stem cell derived endothelial cell, PCL polycaprolactone, PG73 PCL/gelatin (70:30 ratio), PG55 PCL/gelatin (50:50 ratio), DAPI 4',6 diamidino 2 phenylindole

compared to human dermal fibroblasts (Additional file 4: Figure S4). Endothelial and fibroblast phenotypes were assessed using the CD31 and Vimentin markers, respectively. iPSC-ECs cultured on PCL scaffolds showed a 4.1-fold decrease in CD31 expression (Additional file 4: Figure S4B) and a 2.3-fold increase in fibroblast phenotype (Additional file 4: Figure S4C). These results suggest that iPSC-ECs maintain their endothelial phenotypes when cultured on PG73 scaffolds and dedifferentiate back to fibroblast phenotypes on PCL scaffolds.

In-vivo engraftment of transplanted iPSC-ECs and iPSC-EC PG73 scaffolds

Using our bioluminescence standard curve, we quantified 7-day iPSC-EC cell numbers on PG73 scaffolds at concentrations of $\sim 3 \times 10^5$ cells/scaffold. For subsequent in-vivo experiments, we used matched cell concentrations for iPSC-EC alone injections. Bioluminescence was also used to quantify subsequent engraftment and survival of iPSC-ECs in vivo. Within 1 h following implantation, iPSC-ECs alone observed an 11.42-fold decrease in survival compared to iPSC-ECs cultured on PG73 scaffolds (6.69 ± 3.73 vs 76.41 ± 19.56 radiance ratio, $p < 0.001$; Fig. 3b). Area under the curve analysis revealed a 5.25-fold increase in total engraftment of iPSC-ECs seeded on PG73 scaffolds compared to injection alone (210.3 ± 67.22 vs 40.4 ± 16.16 radiance ratio, $p < 0.05$; Fig. 3c). The magnitude and length of engraftment of iPSC-ECs on PG73 scaffolds was significantly increased compared to injection alone.

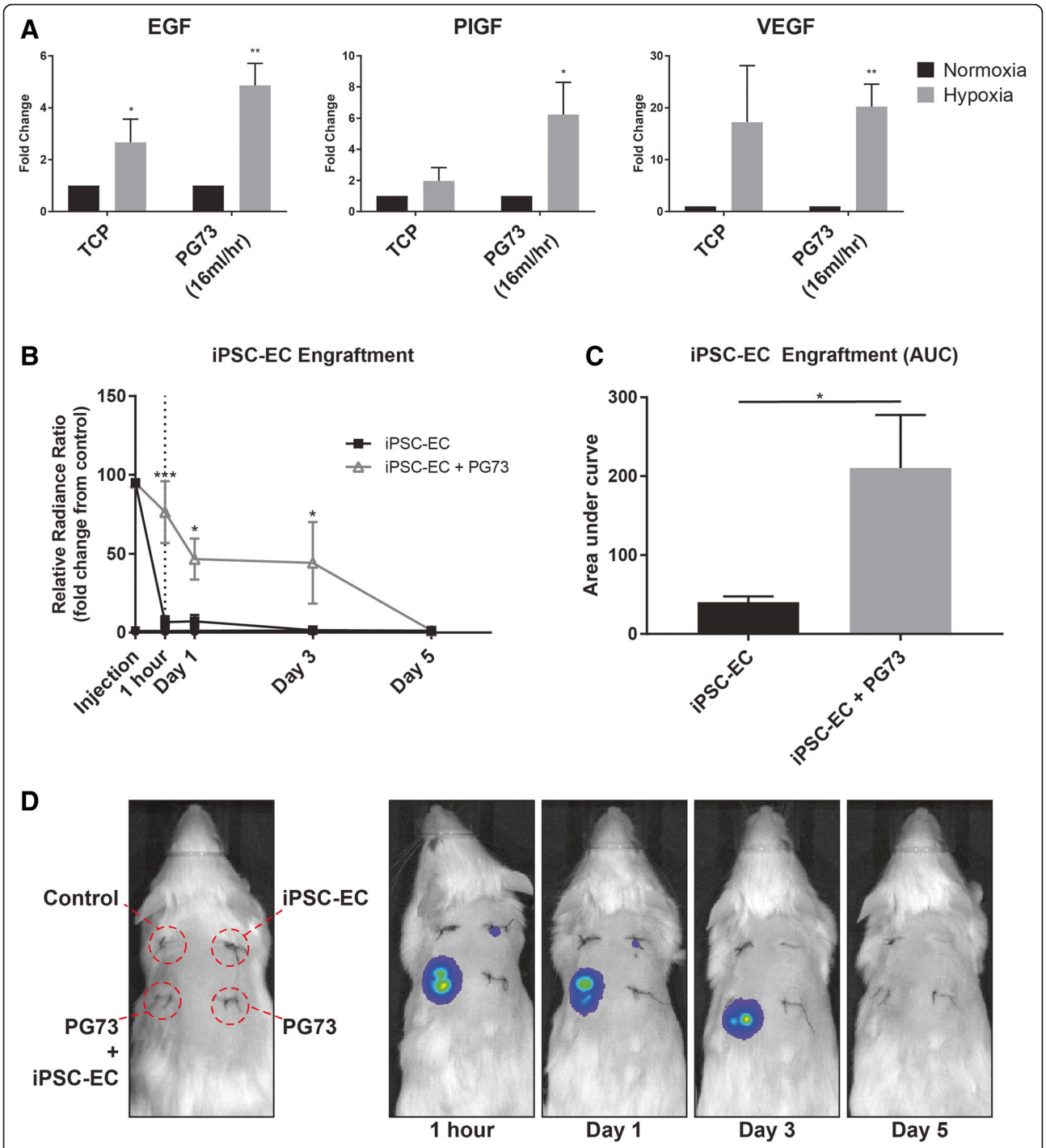

Fig. 3 a Angiogenic cytokine gene expression of iPSC ECs cultured on tissue culture plastic (TCP) and PG73 (16 ml/h scaffolds) in normoxia vs hypoxia. Values presented as fold change normalized to normoxia. *$p < 0.05$, **$p < 0.01$. $n = 5$ samples/group. **b** In vivo engraftment curves measured through IVIS bioluminescence measurement of iPSC ECs and iPSC EC seeded PG73 scaffolds over 5 days. ***$p < 0.001$, *$p < 0.05$. $n = 5$ samples (animals)/group. **c** Area under the curve quantification of engraftment bioluminescence curves. *$p < 0.05$. $n = 5$ samples (animals)/group. **d** Representative bioluminescence photographs of animals implanted with experimental groups over 5 days. EGF epidermal growth factor, PlGF placental growth factor, VEGF vascular endothelial growth factor, PG73 polycaprolactone/gelatin (70:30 ratio), iPSC EC induced pluripotent stem cell derived endothelial cell, AUC area under the curve

Bioluminescence was no longer observed in either group after day 5.

Blood perfusion

Serial Doppler measurements of the implantation sites were taken to non-invasively assess blood reperfusion following tissue injury. Repeated measures analysis of the perfusion curves over 9 days revealed a significant increase in blood perfusion in the tissue surrounding iPSC-EC-seeded PG73 scaffolds compared to control wounds (Fig. 4a). The largest difference in perfusion was observed on day 7 where iPSC-EC-seeded PG73 scaffolds exhibited a 2.04-fold increase compared to control wounds (6.53 ± 0.69 vs 3.20 ± 0.49 × 10^2 flux units, $p < 0.0001$; Fig. 4a). The implantation of PG73 scaffolds alone appeared to also increase wound perfusion, although this was not significant from control wounds.

Wound explants macroscopically appeared to show increased vasculature surrounding both iPSC-EC-seeded and acellular PG73 scaffolds. Increased vascularity was observed contacting iPSC-EC-seeded scaffolds, whereas in PG73 scaffolds the vasculature was localized to the scaffold periphery (Fig. 4b).

Functional angiogenesis

To determine the extent of functional angiogenesis at the implantation site, immunohistochemical analysis was conducted by double staining of SM-α actin (smooth muscle cell) and CD31 (endothelial cell) markers. Quantification of total arteriole density, identified as vessels positive for CD31 and SM-α actin ($CD31^+$/SM-α $actin^+$), revealed a 4.65-fold increase in iPSC-EC-seeded PG73 scaffolds compared to control, iPSC-EC alone, and PG73 alone at day 2 (0.12 ± 0.01 vs 0.03 ± 0.01, 0.03 ± 0.01, and 0.07 ± 0.01 arterioles/mm^2, respectively, $p < 0.05$, $p < 0.001$; Fig. 5a). Arteriole localization analysis showed that this increased arteriole density was localized to the tissue surrounding iPSC-EC-seeded PG73 scaffolds (Fig. 5b). Arteriole analysis at day 9 showed no observable differences amongst all groups. Furthermore, the diameter of arterioles present in both scaffold groups, iPSC-EC-seeded PG73 scaffolds and PG73 scaffolds, were significantly increased compared to control wounds (61.86 ± 4.05 and 56.27 ± 3.49 vs 21.24 ± 2.29 μm, respectively, $p < 0.0001$; Fig. 5c). At day 9, this trend remained; however, arteriole diameters in iPSC-EC-seeded PG73 scaffold groups were even greater than in

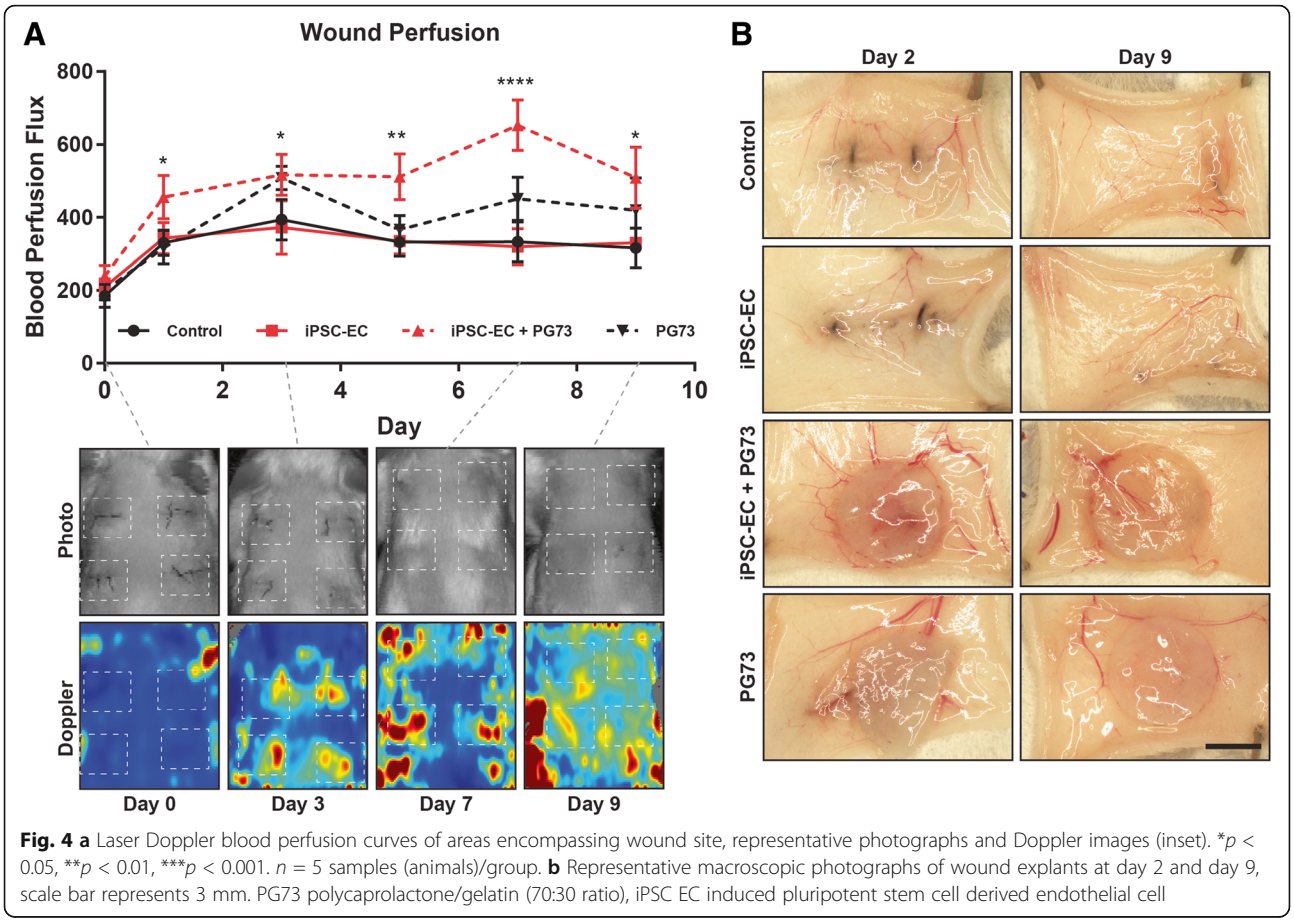

Fig. 4 a Laser Doppler blood perfusion curves of areas encompassing wound site, representative photographs and Doppler images (inset). *$p < 0.05$, **$p < 0.01$, ***$p < 0.001$. $n = 5$ samples (animals)/group. **b** Representative macroscopic photographs of wound explants at day 2 and day 9, scale bar represents 3 mm. PG73 polycaprolactone/gelatin (70:30 ratio), iPSC EC induced pluripotent stem cell derived endothelial cell

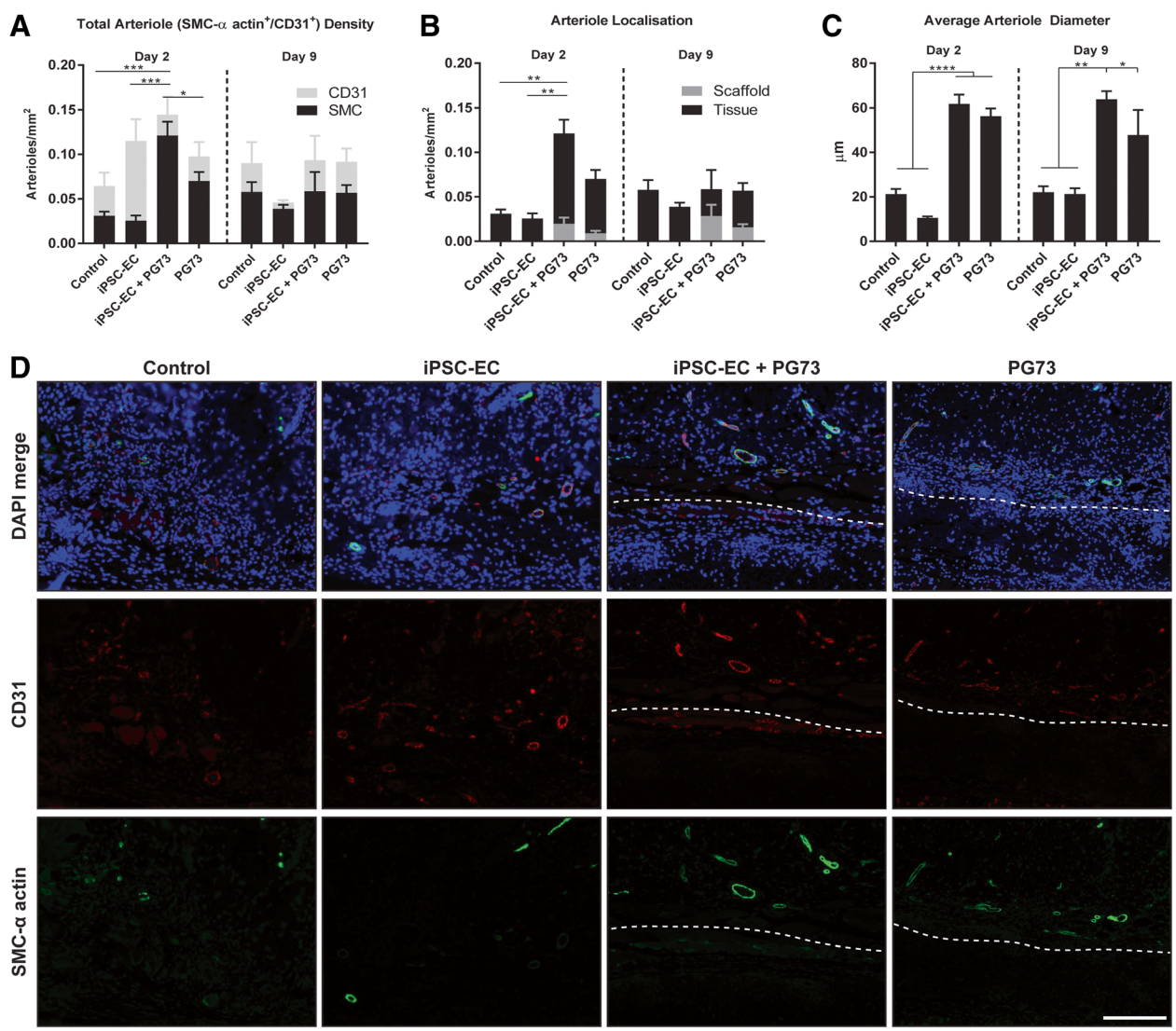

Fig. 5 **a** Functional angiogenesis quantification of arteriole density (vessels double stained for $CD31^+$ and SMC α $actin^+$). *$p < 0.05$, ***$p < 0.001$. $n = 5$ samples/group. **b** Quantification of arteriole location in surrounding tissue vs inside scaffold. **$p < 0.01$. $n = 5$ samples/group. **c** Quantification of average arteriole diameter. ***$p < 0.001$, **$p < 0.01$, *$p < 0.05$. $n = 5$ samples/group. **d** Representative photographs of DAPI/CD31/SMC α actin merge, CD31, and SMC α actin, respectively, at the wound site or tissue implant interface (dotted lines: above represents tissue, below represents scaffold) at day 2, scale bar represents 100 μm. SMC α smooth muscle cell actin, CD31 cluster of differentiation 31 (endothelial marker), PG73 polycaprolactone/gelatin (70:30 ratio), iPSC EC induced pluripotent stem cell derived endothelial cell, DAPI 4',6 diamidino 2 phenylindole

PG7 scaffolds when both were compared to control wounds (63.76 ± 3.68 and 47.86 ± 11.25 vs 22.1 ± 2.7 μm, $p < 0.01$, $p < 0.05$; Fig. 5c).

Local innate immune response

Local innate immune response following implantation was assessed through immunohistochemical analysis of neutrophils and macrophages using the neutrophil-elastase and CD68 markers, respectively. Scaffold implantation (both iPSC-EC-seeded and scaffolds alone) induced a 3.5-fold increase in neutrophil response compared to control wounds 2 days following implantation (~ 0.07 ± 0.01 vs 0.02 ± 0.01 stained area, $p < 0.001$; Fig. 6a). Additionally, iPSC-EC seeding did not further enhance neutrophil responses to PG73 scaffolds (0.07 ± 0.01 vs 0.07 ± 0.02 stained area; Fig. 6b). By day 9, neutrophil levels were equally resolved amongst all groups. Macrophage analysis revealed a 2-fold increase in PG73 scaffolds alone compared to control wounds (1.05 ± 0.05 vs 0.54 ± 0.01 × 10^{-2} stained area, $p < 0.0001$; Fig. 6c). iPSC-EC seeding further enhanced this macrophage response (2.04 ± 0.03 vs 0.54 ± 0.01 × 10^{-2} stained area, $p < 0.0001$; Fig. 6c). Analysis of macrophage localization showed an increased presence of macrophages within iPSC-EC-seeded PG73

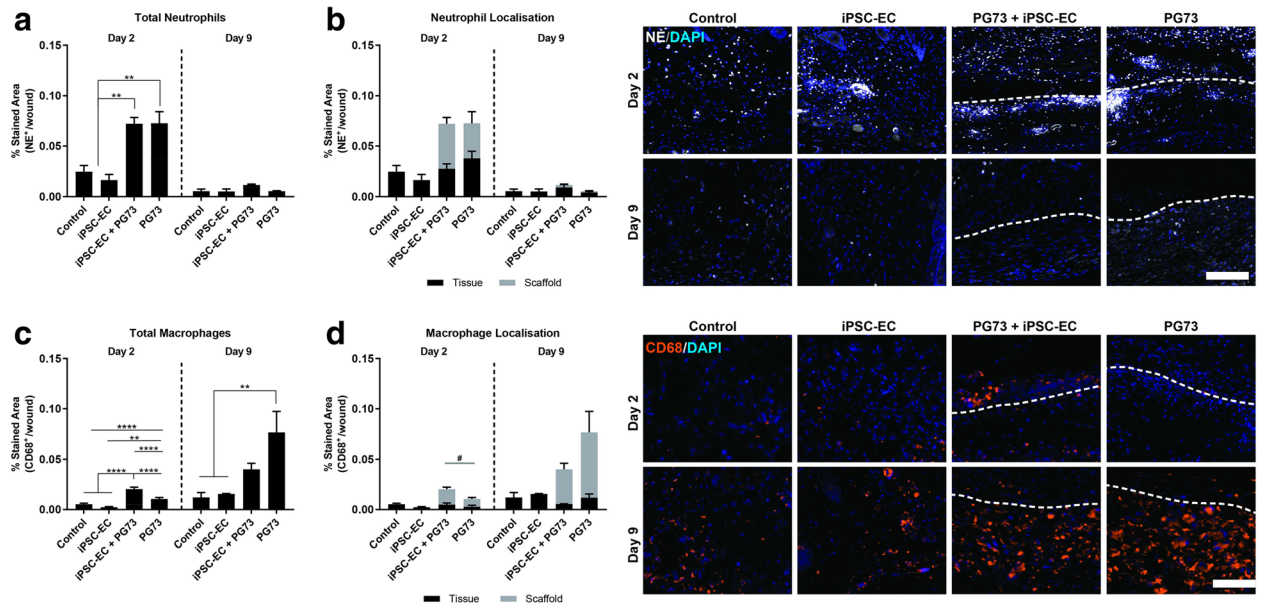

Fig. 6 **a** Quantification of total neutrophil levels at wound site. $^{**}p < 0.01$. $n = 5$ samples/group. **b** Quantification of neutrophil location in surrounding tissue vs within scaffold. **c** Quantification of total macrophage levels at wound site. $^{**}p < 0.01$, $^{****}p < 0.0001$. $n = 5$ samples/group. **d** Quantification of macrophage location in the surrounding tissue vs within the scaffold. $p < 0.05$ comparing macrophages within scaffolds only. $n = 5$ samples/group. Tissue implant interface marked by dotted lines: above represents tissue, below represents scaffold. NE neutrophil elastase, iPSC EC induced pluripotent stem cell derived endothelial cell, PG73 polycaprolactone/gelatin (70:30 ratio), DAPI 4',6 diamidino 2 phenylindole

scaffolds compared to PG73 scaffolds alone (1.5 ± 0.2 vs 0.8 ± 0.2, $p < 0.01$; Fig. 6d). At day 9, macrophage numbers in PG73 scaffolds were increasing, while in iPSC-EC-seeded scaffolds they appeared to be resolving (Fig. 6d).

Angiogenic cytokine modulation and localization

Angiogenic cytokine analysis at the implantation site was determined using immunohistochemical analysis of the classic proangiogenic cytokines placental growth factor (PlGF) and vascular endothelial growth factor (VEGF). At day 2, significant upregulation of total PlGF was observed in iPSC-EC-seeded PG73 scaffolds compared to control, iPSC-EC alone, and PG73 alone (0.11 ± 0.01 vs 0.06 ± 0.01, 0.05 ± 0.01, and 0.03 ± 0.01 stained area, respectively, $p < 0.05$; Fig. 7a). Localization analysis showed that PG73 scaffold implantation alone decreased the baseline levels of PlGF found in control wounds (0.01 ± 0.01 vs 0.06 ± 0.01 stained area, $p < 0.05$; Fig. 7b) At day 9, no differences in PlGF total or localization were observed.

Analysis of VEGF expression at day 2 showed a significant upregulation of VEGF in iPSC-EC-seeded PG73 scaffolds compared to control, iPSC-EC alone, and PG73 alone (0.14 ± 0.01 vs 0.07 ± 0.01, 0.04 ± 0.01, and 0.08 ± 0.01 stained area, respectively, $p < 0.05$, $p < 0.01$, $p < 0.001$; Fig. 8a). Localization analysis revealed that PG73 scaffolds alone resulted in a decrease of VEGF in the surrounding tissue compared to iPSC-EC-seeded PG73 scaffolds and control wounds (0.03 ± 0.01 vs 0.07 ± 0.01 and 0.06 ± 0.01 stained area, $p < 0.05$; Fig. 8b). At day 9, total VEGF expression was significantly increased in PG73 scaffolds alone and iPSC-EC-seeded PG73 scaffolds compared to control wounds (0.17 ± 0.03 and 0.24 ± 0.01 vs 0.03 ± 0.01 stained area, respectively, $p < 0.001$, $p < 0.0001$; Fig. 8a). Between the groups, the highest expression of VEGF was observed in PG73 scaffolds alone. Furthermore, this increased VEGF expression was localized to within PG73 scaffolds (0.19 ± 0.01 vs 0.11 ± 0.03 stained area, $p < 0.05$; Fig. 8b).

Discussion

Induced pluripotent stem cell-derived endothelial cells (iPSC-ECs) have been identified as a promising cell population with potential for increasing therapeutic angiogenesis. Derived from iPSCs possessing unlimited sources and renewal capacity, iPSC-ECs have demonstrated regenerative properties consistent with their stem cell origins. Typically generated from patient-specific cell harvests, iPSC-derived cell therapies mitigate major cell therapy concerns regarding immunogenicity and subsequent cell rejection. Additionally, the advent of iPSC banking has paved the way for the delivery of nonautologous iPSCs without evoking immune rejection [21], thereby reducing the potential time, cost, and invasiveness of iPSC-EC therapy. However, extending the collective

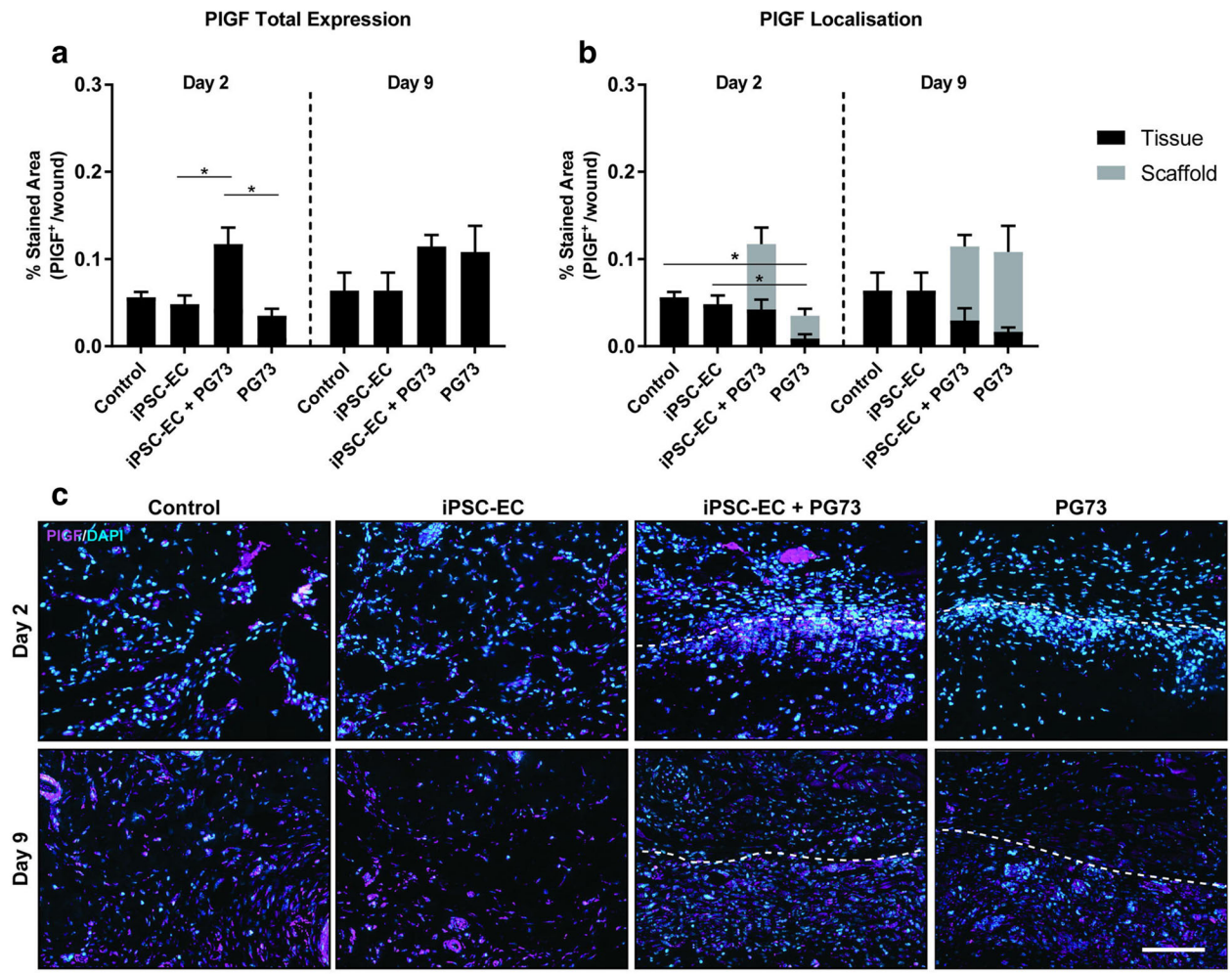

Fig. 7 **a** Quantification of total PlGF expression at the wound site. *$p < 0.05$. $n = 5$ samples/group. **b** Quantification of PlGF expression location in surrounding tissue vs within the scaffold. *$p < 0.05$ comparing PlGF expression within the surrounding tissue only. $n = 5$ samples/group. **c** Representative photographs of PlGF staining with DAPI counterstain, scale bar represents 100 μm. Tissue implant interface marked by dotted lines: above represents tissue, below represents scaffold. PlGF placental growth factor, iPSC EC induced pluripotent stem cell derived endothelial cell, PG73 polycaprolactone/gelatin (70:30 ratio), DAPI 4',6 diamidino 2 phenylindole

translational benefits of iPSC-ECs for therapeutic angiogenesis requires engraftment strategies that can extend their lifetime and maintain their function in vivo.

Using a simple PCL/gelatin composite scaffold system, we assessed the influence of fiber width and gelatin content on iPSC-EC growth and function due to the well-characterized history of these synthetic and natural materials [22, 23]. The stable transfection of luciferase into our iPSC-ECs facilitated both accurate quantification of cell numbers and the capacity for non-invasive imaging in vivo. Using a matrix of conditions including increasing gelatin content and fiber width, we determined that gelatin-containing scaffolds electrospun at high flow rates supported the highest rates of iPSC-EC growth. This is consistent with previous reports of the upregulation of gelatin-binding integrins, such as $\alpha_5\beta_1$, on the surface of ECs differentiated from iPSCs [24]. When combined with increased fiber widths, gelatin-based microfiber scaffolds provided greater cell surface area for integrin-mediated signaling, a key facilitator of growth and proliferation [22]. However, of the two gelatin blends, PG73 promoted higher expression of CD31, suggesting a greater conservation of iPSC-EC endothelial cell phenotype. This effect may have been driven by the inherent structural features of nanofibrous topographies that enable the formation of cellular architectures thought to recapitulate native morphology and phenotype [25]. However, with high concentrations of gelatin the structural integrity of fibers become increasingly compromised due to heightened water solubility and mechanical weakening [23]. Despite the availability of crosslinking methods to resolve this issue, these

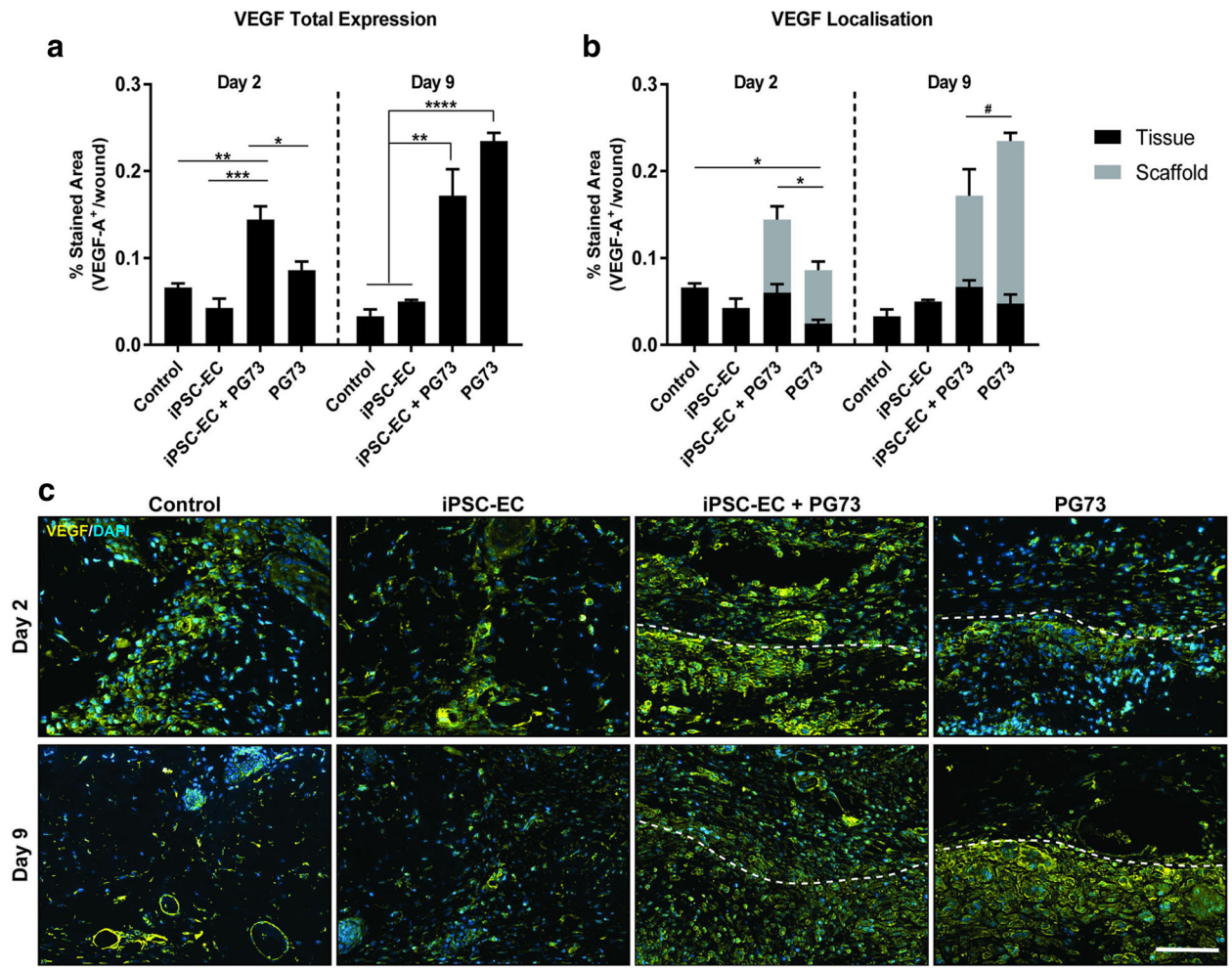

Fig. 8 **a** Quantification of total VEGF expression at the wound site. *$p < 0.05$, **$p < 0.01$, ***$p < 0.001$, ****$p < 0.0001$. $n = 5$ samples/group. **b** Quantification of VEGF expression location in surrounding tissue vs within the scaffold. *$p < 0.05$ comparing VEGF expression within the surrounding tissue only, #$p < 0.05$ comparing VEGF expression within scaffolds only. $n = 5$ samples/group. **c** Representative photographs of VEGF staining with DAPI counterstain, scale bar represents 100 μm. Tissue implant interface marked by dotted lines: above represents tissue, below represents scaffold. VEGF vascular endothelial growth factor, iPSC EC induced pluripotent stem cell derived endothelial cell, PG73 polycaprolactone/gelatin (70:30 ratio), DAPI 4',6 diamidino 2 phenylindole

approaches rely on cytotoxic reagents which impair scaffold function for cell delivery applications [26]. Alternatively, blends with synthetic polymers possessing high mechanical strength and hydrophobicity such as PCL are employed to overcome these structural shortcomings. However, while pure PCL scaffolds may possess greater mechanical stability, they lack the appropriate cell binding domains for optimal cellular interaction. Ideal blends consisting of appropriate amounts of PCL and gelatin, such as those observed in PG73 blends, are often required to effectively balance cell adhesion/proliferation and structural integrity, respectively. While the levels of gelatin content in PG73 scaffolds are capable of supporting iPSC-EC growth, they do not appear to negatively impact the structural integrity or degradation characteristics of the scaffold.

Characterization of iPSC-EC-seeded PG73 scaffolds prior to implantation showed that scaffolds preserved the iPSC-EC phenotype and function after 7 days in culture. The possibility of dedifferentiation to original dermal fibroblast phenotypes appears limited given the lack of fibroblast marker expression [27, 28]. Combined with high CD31 expression, this suggests that the iPSC-EC endothelial cell phenotype is best preserved on PG73 scaffolds. Furthermore, hypoxia-induced gene expression was enhanced on PG73 scaffolds when compared to conventional 2D tissue culture surfaces. This functional response is likely more representative of their in-vivo actions because they assume more native-like in-vivo morphologies on 3D surfaces compared to 2D. This enhanced functional response is highly promising for augmenting in-vivo angiogenesis as the upregulation of

EGF, PlGF, and VEGF is classically associated with underlying host angiogenic mechanisms [29–31]. Taken together, the provision of simple scaffold structural and signaling cues greatly enhanced the growth of iPSC-ECs, while preserving their phenotype and promoting the expression of key proangiogenic factors. This suggests that the development of more nuanced and complex scaffold designs could provide further functional enhancements and cell survival in future studies.

We next examined the functional effects of PG73 scaffolds on iPSC-ECs in vivo, tracking cell survival and retention using non-invasive imaging of the luciferase cell reporter. The administration of iPSC-ECs alone resulted in poor survival consistent with the weight of clinical findings for traditional stem cell therapy [8]. Most cells were lost within 1 h of injection. These results are more closely representative of native engraftment conditions, compared to previous investigations of iPSC-EC function which require the use of severe combined immunodeficient (SCID) mice to enhance cell engraftment [15, 16]. The use of PG73 scaffolds extended the in-vivo lifetime of transplanted iPSC-ECs by improving structural support and providing signaling cues in the wounded area. Nanofibrous scaffolds offer a 3D platform that provides some mimicry of the in-vivo structural environment, increasing the likelihood of iPSC-EC engraftment. While gelatin-based nanofibrous scaffolds extend the in-vivo lifetime of transplanted iPSC-ECs up to 3 days, future biomaterial strategies addressing additional factors impairing cell engraftment, including host inflammatory responses [32] and inadequate nutrient/growth factor cues [33], may help to encourage iPSC-EC in-vivo growth and further enhance engraftment. For example, enhancements in scaffold porosity [34] or the provision of growth factors [35] may prove beneficial.

Indeed, we have determined previously that human iPSC-ECs are sensitive to the diameter and alignment of nanofibrillar collagen scaffolds [16]. Aligned nanofibrillar collagen fibrils (30 nM in diameter) guide cellular organization, modulate endothelial inflammatory response, and enhance cell survival after implantation in normal and ischemic tissues. Human iPSC-ECs cultured on aligned scaffolds persisted for over 28 days, as assessed by bioluminescence imaging, when implanted into the ischemic murine hindlimb of NOD-SCID mice [16, 17]. By contrast, ECs implanted on scaffolds without nanopatterning generated no detectable bioluminescent signal by day 4 in either normal or ischemic tissues [36].

To assess the functional effects of increased cell survival, we first used laser Doppler imaging to non-invasively quantify in-vivo blood perfusion. Perfusion for PG73 scaffolds alone, while not significantly improved compared to controls, showed some improvements, an effect previously demonstrated by other acellular biomaterial platforms [37, 38]. These previous studies suggest that altered tissue remodeling arising from the introduction of foreign materials coupled with the highly invasive nature of native endothelial cells following ischemic injury influence proangiogenic conditions. Our findings demonstrate that further scaffold supplementation with iPSC-ECs significantly augments scaffold-mediated perfusion. Macroscopically, the enhanced Doppler signal appeared to correlate well with the observation of increased vasculature around the scaffolds at explant, particularly for the iPSC-EC-seeded PG73 scaffolds. To confirm this observation, we used immunohistochemistry to examine the density of arteriole vessels as a marker for functional angiogenesis.

Arterioles are more stable blood-carrying vessels compared to capillaries [39] and their diameter is directly connected to the volume of blood flow through the vessel [40]. PG73 scaffolds alone induced the formation of some large-diameter arterioles, explaining the modest increases in perfusion observed through Doppler imaging. The further increase in the density of these large-diameter arterioles at early time points correlated well with the greater perfusion levels of iPSC-EC-seeded PG73 scaffolds. The functional enhancement of angiogenesis in the presence of iPSC-ECs is consistent with previous reports showing acute benefits in a hindlimb ischemia model and *in vitro* [11]. To gain further insights into the mechanisms underpinning this effect, we quantified some of the key angiogenic regulators.

iPSC-EC scaffold-mediated augmentation of host angiogenesis is a complex process regulated by innate immune cells and proangiogenic cytokines. Observed increases in arteriole diameter following implantation surgery arise from vasodilation of nearby blood vessels allowing increased permeability of innate immune cells responding to the material implant [41]. This characteristic foreign body response is hallmarked by the increased presence of neutrophils and macrophages around the implant [42]. While an elevated host-inflammatory response to exogenous cell delivery is common, it does not appear to be the driving force behind increased angiogenic activity surrounding iPSC-EC-seeded scaffolds in this study. Equal levels of neutrophils were observed in both iPSC-EC-seeded scaffolds and control PG73 scaffolds alone [43]. Additionally, macrophage infiltration, typically observed in the later stages of the foreign body response, appeared to resolve more quickly for iPSC-EC-seeded scaffolds compared to scaffolds alone. Instead, the unexpected early increase in macrophages surrounding iPSC-EC-seeded scaffolds following implantation suggests altered tissue remodeling events. Macrophages have the capacity to influence multiple phases of the angiogenic process, including alterations of the local extracellular matrix and

induction of endothelial cell migration and proliferation through angiogenic cytokine release [44].

Increased iPSC-EC engraftment in the first days post implantation coincides with heightened PlGF expression, a potent macrophage chemoattractant [45]. This enhanced macrophage presence at the implantation site, along with elevated expression of the classical angiogenic cytokine VEGF, may account for the increased density of large-diameter arterioles. Localization analysis of these cytokines revealed that these angiogenic factors originate from within the scaffold, possibly from engrafted iPSC-ECs and macrophages responding to the implant. Equally important to the therapeutic translation of these processes is the timing of cytokine release. Although enhanced VEGF expression in scaffolds alone is eventually achieved at similar expression levels to iPSC-EC-seeded scaffolds by day 9, levels at day 2 are significantly improved only in the presence of iPSC-ECs. The benefits of iPSC-EC-mediated increases in angiogenesis arise from this timely augmentation of blood perfusion immediately following implantation, in addition to the longevity of these effects even after iPSC-EC engraftment is no longer observed. Further research into identifying additional factors underlying this function is necessary for optimizing the angiogenic potential of future iPSC-EC scaffold therapies.

Conclusion

The integration of biomaterials with iPSC-ECs is a highly promising and innovative approach for therapeutic angiogenesis. Optimization of these approaches for future therapy requires a comprehensive understanding of cell–material interactions and the resulting effects following implantation of these combined constructs. The findings of this study identify important scaffold design parameters which influence iPSC-EC behavior and function. These initial observations serve as preliminary criteria for developing candidate biomaterial platforms with enhanced capacity to support iPSC-EC engraftment and viability in vivo. Further understanding of the mechanisms underlying the combined effects of iPSC-ECs and their engraftment platforms will more readily lead to the development of enhanced iPSC-EC scaffold designs with clinical applications for therapeutic angiogenesis. The findings of this work help highlight this emerging cell–biomaterial field of regenerative medicine with significant implications for the treatment of ischemic injury.

Additional files

Additional file 1: Figure S1. showing (**A**) representative SEM photographs of PG73 and PG55 scaffolds before and after soaking in PBS for 7 days, scale bar represents 10 μm. (**B**) Scaffold cross section images for porosity analysis. *n* 5 samples/group, scale bar represents 100 μm. (TIFF 19523 kb)

Additional file 2: Figure S2. showing (**A**) analysis of iPSC EC infiltration into scaffolds, representative photographs of scaffold cross sections stained with DAPI. *n* 100 cells/scaffold, scale bar represents 100 μm. (**B**) Young's modulus and (**C**) ultimate tensile strength (UTS) of PG73 scaffolds before and after wetting. *n* 5 samples/group. (**D**) Degradation rate of PG73 scaffolds compared to PCL over 4 days in an accelerated Protease XIV degradation solution. *n* 3 samples/group. (TIFF 12785 kb)

Additional file 3: Figure S3. showing (**A**) bioluminescence standard curve with upper limit of iPSC EC concentration detection before IVIS camera saturation, inset. (**B**) Lower limit of iPSC EC concentration detection after background/noise subtraction. *n* 5 samples/group. (TIFF 44988 kb)

Additional file 4: Figure S4. showing (**A**) dedifferentiation of iPSC ECs seeded on PG73 vs PCL scaffolds after 7 days culture *in vitro*. *Photographs* using (**B**) immunostains for $CD31^+$ for endothelial phenotype and (**C**) $vimentin^+$ for fibroblast phenotype. $*p < 0.05$. *n* 3 samples/group, scale bar represents 40 μm. (TIFF 51787 kb)

Abbreviations

CD31: Cluster of differentiation 31 (endothelial marker); EGF: Epidermal growth factor; iPSC EC: Induced pluripotent stem cell derived endothelial cell; PCL: Polycaprolactone; PG73: PCL/gelatin (70:30 ratio); PlGF: Placental growth factor; SEM: Scanning electron microscopy; SMC α: Smooth muscle cell actin; VEGF: Vascular endothelial growth factor

Acknowledgements

Not applicable.

Funding

This work was supported in part by grants to JPC from the Progeria Research Foundation, the Cullen Trust for Health Care, and the National Institutes of Health (U01 HL100397), in addition to a National Health and Medical Research Council (NHMRC) Early Career Fellowship (grant number GNT0633283) and a grant from the Sydney Medical School Foundation.

Availability of data and materials

The datasets generated during and/or analyzed during the current study are available from the corresponding author on reasonable request.

Authors' contributions

RPT and SGW conceived the overall idea and initial research plan. RPT engineered scaffolds and conducted all subsequent characterizations. JR K conducted all mechanical and tensile testing experiments. RPT and ZEC maintained iPSC EC cultures and conducted cell experiments. RPT and AHPC performed surgical procedures and *in vivo* imaging experiments. RPT and BSLL conducted histological and immunohistochemistry staining on explanted samples. KL and MMM conducted all RNA extractions and subsequent qPCR analysis. RPT and SGW wrote the manuscript. JPC, MKCN, SP, JR K, and SGW all supervised the project. All authors discussed the results and commented on the final version of the manuscript. All authors read and approved the final manuscript.

Ethics approval and consent to participate

Study approval was obtained from Sydney Local Heath District Animal Welfare Committee (protocol number 2013/050). Experiments were conducted in accordance with the Australian Code of Practice for the Care and Use of Animals for Scientific Purpose.

Consent for publication

Not applicable.

Competing interests

The authors declare that they have no competing interests.

Publisher's Note

Author details
[1]The Heart Research Institute, Sydney, NSW 2042, Australia. [2]Sydney Medical School, University of Sydney, Sydney, NSW 2006, Australia. [3]Royal Prince Alfred Hospital, Sydney, NSW 2042, Australia. [4]Department of Cardiovascular Sciences, Houston Methodist Research Institute, Houston, TX 77030, USA. [5]Graduate School of Biomedical Engineering, University of New South Wales, Sydney, NSW 2052, Australia.

Received: 10 January 2018 Revised: 19 February 2018
Accepted: 5 March 2018 Published online: 21 March 2018

References

1. Kalogeris T, Baines CP, Krenz M, Korthuis RJ. Cell biology of ischemia/reperfusion injury. Int Rev Cell Mol Biol. 2012;298:229 317.
2. Kasner SE, Demchuk AM, Berrouschot J, Schmutzhard E, Harms L, Verro P, et al. Predictors of fatal brain edema in massive hemispheric ischemic stroke. Stroke. 2001;32:2117 23.
3. Tibblin G, Wilhelmsen L, Werko L. Risk factors for myocardial infarction and death due to ischemic heart disease and other causes. Am J Cardiol. 1975;35:514 22.
4. Chu H, Wang Y. Therapeutic angiogenesis: controlled delivery of angiogenic factors. Ther Deliv. 2012;3:693 714.
5. Simons M, Ware JA. Therapeutic angiogenesis in cardiovascular disease. Nat Rev Drug Discov. 2003;2:863 72.
6. Patterson C, Runge MS. Therapeutic angiogenesis. Circulation. 1999;99:2614.
7. Grochot Przeczek A, Dulak J, Jozkowicz A. Therapeutic angiogenesis for revascularization in peripheral artery disease. Gene. 2013;525:220 8.
8. Bilic J, JCI B. Concise Review: Induced pluripotent stem cells versus embryonic stem cells: close enough or yet too far apart. Stem Cells. 2012;30:33 41.
9. Rufaihah AJ, Huang NF, Jame S, Lee JC, Nguyen HN, Byers B, et al. Endothelial cells derived from human iPSCS increase capillary density and improve perfusion in a mouse model of peripheral arterial disease. Arterioscler Thromb Vasc Biol. 2011;31:e72 9.
10. Li J, Huang NF, Zou J, Laurent TJ, Lee JC, Okogbaa J, et al. Conversion of human fibroblasts to functional endothelial cells by defined factors. Arterioscler Thromb Vasc Biol. 2013;33:1366 75.
11. Lai WH, Ho JC, Chan YC, Ng JH, Au KW, Wong LY, et al. Attenuation of hind limb ischemia in mice with endothelial like cells derived from different sources of human stem cells. PLoS One. 2013;8:e57876.
12. Laflamme MA, Chen KY, Naumova AV, Muskheli V, Fugate JA, Dupras SK, et al. Cardiomyocytes derived from human embryonic stem cells in pro survival factors enhance function of infarcted rat hearts. Nat Biotech. 2007;25:1015 24.
13. Gu M, Nguyen PK, Lee AS, Xu D, Hu S, Plews JR, et al. Microfluidic single cell analysis show porcine induced pluripotent stem cell derived endothelial cells improve myocardial function by paracrine activation. Circ Res. 2012;111:882 93.
14. Tong Z, Solanki A, Hamilos A, Levy O, Wen K, Yin X, et al. Application of biomaterials to advance induced pluripotent stem cell research and therapy. EMBO J. 2015;34:987 1008.
15. Nakayama KH, Hong G, Lee JC, Patel J, Edwards B, Zaitseva TS, et al. Aligned braided nanofibrillar scaffold with endothelial cells enhances arteriogenesis. ACS Nano. 2015;9:6900 8.
16. Huang NF, Okogbaa J, Lee JC, Jha A, Zaitseva TS, Paukshto MV, et al. The modulation of endothelial cell morphology, function, and survival using anisotropic nanofibrillar collagen scaffolds. Biomaterials. 2013;34:4038 47.
17. Clayton ZE, Yuen GS, Sadeghipour S, Hywood JD, Wong JW, Huang NF, et al. A comparison of the pro angiogenic potential of human induced pluripotent stem cell derived endothelial cells and induced endothelial cells in a murine model of peripheral arterial disease. Int J Cardiol. 2017;234:81 9.
18. Takahashi K, Tanabe K, Ohnuki M, Narita M, Ichisaka T, Tomoda K, et al. Induction of pluripotent stem cells from adult human fibroblasts by defined factors. Cell. 2007;131:861 72.
19. Rufaihah AJ, Huang NF, Kim J, Herold J, Volz KS, Park TS, et al. Human induced pluripotent stem cell derived endothelial cells exhibit functional heterogeneity. Am J Transl Res. 2013;5:21 35.
20. Tan RP, Lee BSL, Chan AHP, Yuen SCG, Hung J, Wise SG, et al. Non invasive tracking of injected bone marrow mononuclear cells to injury and implanted biomaterials. Acta Biomater. 2017;53:378 88.
21. Solomon S, Pitossi F, Rao MS. Banking on iPSC is it doable and is it worthwhile. Stem Cell Rev. 2015;11:1 10.
22. Yao R, He J, Meng G, Jiang B, Wu F. Electrospun PCL/Gelatin composite fibrous scaffolds: mechanical properties and cellular responses. J Biomater Sci Polym Ed. 2016;27:824 38.
23. Gautam S, Dinda AK, Mishra NC. Fabrication and characterization of PCL/gelatin composite nanofibrous scaffold for tissue engineering applications by electrospinning method. Mater Sci Eng C Mater Biol Appl. 2013;33:1228 35.
24. Hou L, Huang N. Extracellular matrix mediated endothelial differentiation of human induced pluripotent stem cells (1152.4). FASEB J. 2014;28:1152 4.
25. Edmondson R, Broglie JJ, Adcock AF, Yang L. Three Cell Culture Systems and Their Applications in Drug Discovery and Cell Based Biosensors. Assay Drug Dev Technol. 2014;12:207 18.
26. Ma B, Wang X, Wu C, Chang J. Crosslinking strategies for preparation of extracellular matrix derived cardiovascular scaffolds. Regen Biomater. 2014;1:81 9.
27. Lareu RR, Subramhanya KH, Peng Y, Benny P, Chen C, Wang Z, et al. Collagen matrix deposition is dramatically enhanced in vitro when crowded with charged macromolecules: the biological relevance of the excluded volume effect. FEBS Lett. 2007;581:2709 14.
28. Bulysheva AA, Bowlin GL, Klingelhutz AJ, Yeudall WA. Low temperature electrospun silk scaffold for in vitro mucosal modeling. J Biomed Mater Res A. 2012;100:757 67.
29. Ribatti D. The discovery of the placental growth factor and its role in angiogenesis: a historical review. Angiogenesis. 2008;11:215 21.
30. Hoeben A, Landuyt B, Highley MS, Wildiers H, Van Oosterom AT, De Bruijn EA. Vascular endothelial growth factor and angiogenesis. Pharmacol Rev. 2004;56:549 80.
31. van Cruijsen H, Giaccone G, Hoekman K. Epidermal growth factor receptor and angiogenesis: opportunities for combined anticancer strategies. Int J Cancer. 2005;117:883 8.
32. Anderson AJ, Haus DL, Hooshmand MJ, Perez H, Sontag CJ, Cummings BJ. Achieving stable human stem cell engraftment and survival in the CNS: is the future of regenerative medicine immunodeficient? Regen Med. 2011;6:367 406.
33. Gobaa S, Hoehnel S, Roccio M, Negro A, Kobel S, Lutolf MP. Artificial niche microarrays for probing single stem cell fate in high throughput. Nat Meth. 2011;8:949 55.
34. Gibly RF, Zhang X, Lowe WL Jr, Shea LD. Porous scaffolds support extrahepatic human islet transplantation, engraftment, and function in mice. Cell Transplant. 2013;22:811 9.
35. Kedem A, Perets A, Gamlieli Bonshtein I, Dvir Ginzberg M, Mizrahi S, Cohen S. Vascular endothelial growth factor releasing scaffolds enhance vascularization and engraftment of hepatocytes transplanted on liver lobes. Tissue Eng. 2005;11:715 22.
36. Huang NF, Lai ES, Ribeiro AJS, Pan S, Pruitt BL, Fuller GG, et al. Spatial patterning of endothelium modulates cell morphology, adhesiveness and transcriptional signature. Biomaterials. 2013;34:2928 37.
37. Patel ZS, Mikos AG. Angiogenesis with biomaterial based drug and cell delivery systems. J Biomater Sci Polym Ed. 2004;15:701 26.
38. Hasan A, Khattab A, Islam MA, Hweij KA, Zeitouny J, Waters R, et al. Injectable hydrogels for cardiac tissue repair after myocardial infarction. Adv Sci (Weinh). 2015;2:1500122.
39. Mac Gabhann F, Peirce SM. Collateral capillary arterialization following arteriolar ligation in murine skeletal muscle. Microcirculation. 2010;17:333 47.
40. Gilmore ED, Hudson C, Preiss D, Fisher J. Retinal arteriolar diameter, blood velocity, and blood flow response to an isocapnic hyperoxic provocation. Am J Physiol Heart Circ Physiol. 2005;288:H2912 7.
41. Newton K, Dixit VM. Signaling in innate immunity and inflammation. Cold Spring Harb Perspect Biol. 2012;4:a006049.
42. Anderson JM, Rodriguez A, Chang DT. Foreign body reaction to biomaterials. Semin Immunol. 2008;20:86 100.
43. Soehnlein O, Steffens S, Hidalgo A, Weber C. Neutrophils as protagonists and targets in chronic inflammation. Nat Rev Immunol. 2017;17:248 61.
44. Nucera S, Biziato D, De Palma M. The interplay between macrophages and angiogenesis in development, tissue injury and regeneration. Int J Dev Biol. 2011;55:495 503.
45. Kim K J, Cho C S, Kim W U. Role of placenta growth factor in cancer and inflammation. Exp Mol Med. 2012;44:10 9.

Chapter 5

Bioactive Materials Facilitating Targeted and Local Modulation of Inflammation

JACC: BASIC TO TRANSLATIONAL SCIENCE VOL. 4, NO. 1, 2019

PRECLINICAL RESEARCH

Bioactive Materials Facilitating Targeted Local Modulation of Inflammation

Richard P. Tan, MSc,[a,b,*] Alex H.P. Chan, BSc,[a,b,*] Simon Wei, PhD,[c] Miguel Santos, PhD,[a,d] Bob S.L. Lee, MSc,[a,b] Elysse C. Filipe, PhD,[b,e] Behnam Akhavan, PhD,[a,d,f] Marcela M. Bilek, PhD, MBA,[d,f,g,h] Martin K.C. Ng, MBBS, PhD,[b,i] Yin Xiao, PhD,[c] Steven G. Wise, PhD[a,b]

VISUAL ABSTRACT

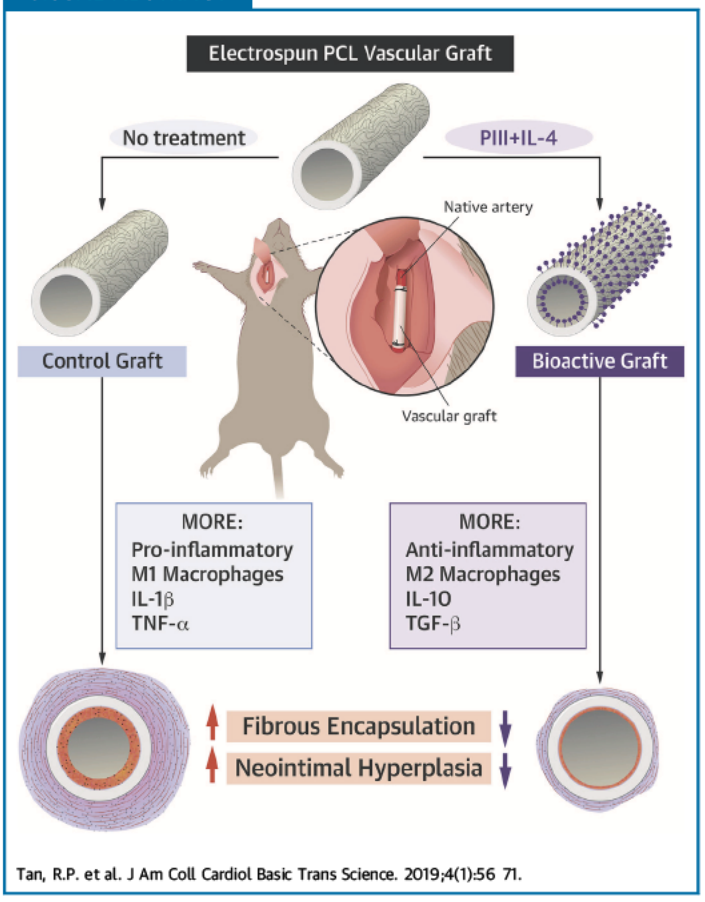

HIGHLIGHTS

- Electrospun polycaprolactone surfaces were immobilized with a monolayer of the cytokine interleukin-4 to create a "bioactive" immunomodulatory surface capable of influencing the phenotype of macrophages responding to the material surface in vivo.
- Bioactive surfaces, evaluated in vitro by using macrophage culture, exhibited upregulation of anti-inflammatory M2 genes and facilitated morphological changes consistent with macrophage activation.
- As a subcutaneous implant in a 14-day model of acute inflammation, bioactive surfaces polarized macrophages from their M1 pro-inflammatory to M2 anti-inflammatory phenotypes, leading to a significant reduction in the local immune-driven foreign body response.
- As vascular grafts in a 28-day mouse carotid interposition model, bioactive grafts maintained their macrophage polarization and immunomodulatory effects, significantly reducing adventitial encapsulation and neointimal hyperplasia development.

From the [a]Heart Research Institute, Sydney, New South Wales, Australia; [b]Sydney Medical School, University of Sydney, Sydney, New South Wales, Australia; [c]Science and Engineering Faculty, Queensland University of Technology, Brisbane, Queensland, Australia; [d]School of Physics, University of Sydney, Sydney, New South Wales, Australia; [e]Garvan Institute of Medical Research, Cancer Division, Sydney, New South Wales, Australia; [f]School of Aerospace, Mechanical and Mechatronic Engineering, University of Sydney, Sydney, New South Wales, Australia; [g]Charles Perkins Centre, University of Sydney, Sydney, New South Wales, Australia; [h]Sydney Nano Institute, University of Sydney, Sydney, New South Wales, Australia; and the [i]Royal Prince Alfred Hospital, Sydney, New South Wales, Australia. *Mr. Tan and Dr. Chan contributed equally to the manuscript and are joint first authors. This work was supported by the Australian Research Council (Dr. Bilek) and the National Health and Medical Research Council (APP1066174; Dr. Ng). Mr. Tan, Mr. Lee, and Dr. Filipe are recipients of an Australian Postgraduate Scholarship, and

ISSN 2452 302X https://doi.org/10.1016/j.jacbts.2018.10.004

SUMMARY

Cardiovascular disease is an inflammatory disorder that may benefit from appropriate modulation of inflammation. Systemic treatments lower cardiac events but have serious adverse effects. Localized modulation of inflammation in current standard treatments such as bypass grafting may more effectively treat CAD. The present study investigated a bioactive vascular graft coated with the macrophage polarizing cytokine interleukin-4. These grafts repolarize macrophages to anti-inflammatory phenotypes, leading to modulation of the pro-inflammatory microenvironment and ultimately to a reduction of foreign body encapsulation and inhibition of neointimal hyperplasia development. These resulting functional improvements have significant implications for the next generation of synthetic vascular grafts.

ABBREVIATIONS AND ACRONYMS

CAD = coronary artery disease

ELISA = enzyme-linked immunoadsorbent assay

IL = interleukin

PCL = polycaprolactone

PIII = plasma immersion ion implantation

qPCR = quantitative polymerase chain reaction

TGF = transforming growth factor

TNF = tumor necrosis factor

The role of inflammation in the genesis and progression of coronary artery disease (CAD) and other manifestations of atherosclerosis has long been established (1). Inflammatory cells drive the initial stages of plaque formation, express growth factors and cytokines that progress disease, and can worsen patient outcomes after an acute coronary syndrome (2). The recent CANTOS (Canakinumab Anti-inflammatory Thrombosis Outcome Study) trial showed that systemic administration of canakinumab, a selective antibody against the inflammatory cytokine interleukin (IL)-1β, significantly lowered the incidence of recurrent cardiovascular events (3). By systemically reducing inflammation while having no effect on lipid levels, CANTOS was a large-scale clinical trial showing that pharmaceutical anti-inflammatory therapy was effective in reducing cardiovascular events. Although these results will have a significant impact on the immediate direction of therapeutic interventions, systemic canakinumab treatment was associated with a higher risk of fatal infection and sepsis, most likely resulting from sustained global immune suppression. Accordingly, future translation of therapies for the treatment of CAD based on anti-inflammatory approaches will benefit from local, targeted modulation of inflammation.

The severity and extent of host foreign body immune responses toward cardiovascular interventional devices significantly affect their long-term performance. The modification of implantable medical devices using anti-inflammatory surface coatings has been previously explored (4). The most effective strategies rely on the controlled release of anti-inflammatory agents to halt local inflammatory responses in the surrounding tissue. Dexamethasone is a commonly used synthetic glucocorticoid hormone shown to reduce the levels of tumor necrosis factor (TNF)-α, IL-1β, IL-6, and interferon gamma. α-Melanocyte-stimulating hormone is a linear peptide shown to reduce TNF-α levels while increasing anti-inflammatory IL-10 levels. Previous controlled-release strategies using anti-inflammatory agents typically involved nonspecific, passive diffusion through polyelectrolyte layers, biodegradable coatings, or swelling coatings. Although these approaches have led to a reduction in some aspects of the foreign body response, including protein adsorption and cell adhesion in vitro, complications such as recurrent inflammatory responses and subsequent device replacement may potentially arise when drug elution is complete. Furthermore, nonspecific blockade of immune cell recruitment after elution of anti-proliferative drugs, as is the case for drug-eluting stents, can impair the resolution of chronic inflammation and hinder long-term device integration and function (5). Improved application of these strategies would therefore aim to better retain the bioactivity, stability, and residence time of locally delivered agents while more selectively modulating the

Mr. Chan and Dr. Santos have received funding support from the Heart Research Institute. The authors acknowledge the financial support of E. Brackenreg. The authors have reported that they have no relationships relevant to the contents of this paper to disclose.

All authors attest they are in compliance with human studies committees and animal welfare regulations of the authors' institutions and Food and Drug Administration guidelines, including patient consent where appropriate. For more information, visit the *JACC: Basic to Translational Science* author instructions page.

Manuscript received August 10, 2018; revised manuscript received October 10, 2018, accepted October 12, 2018.

immune response to facilitate prolonged functional benefits.

We have identified macrophages and their broad spectrum of phenotypes as master effectors of the foreign body response toward implanted materials. At the 2 ends of the spectrum are the M1 (pro-inflammatory) and M2 (anti-inflammatory) phenotypes, which regulate a host of inflammatory cytokines to either propagate or halt innate inflammation, respectively. Modification of the material surface to induce the M2 phenotype of responding macrophages may potentially represent an effective means of mitigating foreign body responses to implanted materials.

In the present study, we developed a novel off-the-shelf bioactive device coating for local and lasting modulation of the inflammatory response to implants. A plasma immersion ion implantation (PIII) surface treatment was used that facilitates the rapid covalent attachment of biomolecules while preserving their bioactivity (6). One of the most well-established and highly documented biomolecules responsible for M2 macrophage phenotype polarization is the cytokine IL-4 (7). Bioactive signaling chemokines such as IL-4 have not previously been immobilized on material surfaces without chemical linkers, representing a fundamentally new off-the-shelf approach to local regulation of inflammation. Herein we examined the in vitro behavior of macrophages in response to bioactive IL-4 surfaces before assessing the in vivo inflammatory responses in 2 distinct mouse models. Comprehensive immunohistochemical analysis of both subcutaneous and carotid arterial graft implants was used to quantitatively assess macrophage phenotype, local cytokine expression, and measures of functional outcome (including fibrous encapsulation and neointimal hyperplasia).

METHODS

PIII SURFACE TREATMENT. Surface modification of electrospun polycaprolactone (PCL) scaffolds was conducted by using PIII as previously described (8). Briefly, nitrogen was admitted into a custom-built vacuum chamber to a working pressure of 2×10^{-3} Torr, and plasma discharges were generated by inductively coupled radiofrequency power at a frequency of 13.56 MHz. Scaffolds were placed on an electrically biased stainless-steel holder. Ion acceleration was achieved through application of -20 kV pulses with a temporal width of 20 μs at a frequency of 50 Hz, drawing a current of 1.3 mA. PIII treatment was run for 800 s, providing ion fluences of 1×10^{16} ions/cm^2. Characterization methods of PIII-treated surfaces can be found in the Supplemental Methods.

BIOACTIVE IL-4 SURFACE CREATION. For in vitro experiments, scaffolds were biopsy punched into 5-mm diameter circular discs and placed into Eppendorf tubes. Recombinant mouse IL-4 (2 μg/ml in sterile phosphate-buffered saline) was added to each scaffold for 1 h at room temperature. To test IL-4 attachment, scaffolds were washed in sodium dodecyl sulfate (5% in phosphate-buffered saline) for 4 h at room temperature before enzyme-linked immunoadsorbent assay (ELISA) using an anti-IL-4 monoclonal antibody (Thermo Fisher Scientific, Waltham, Massachusetts) and horseradish peroxidase-conjugated secondary antibody (Abcam, Cambridge, Massachusetts). For in vivo experiments, both flat scaffolds and PCL conduits (0.5 mm diameter) were incubated in recombinant mouse IL-4 (2 μg/ml in sterile phosphate-buffered saline) for 1 h at room temperature and rinsed in sterile phosphate-buffered saline before implantation.

In vivo performance of bioactive IL-4 subcutaneous implants. Study approval was obtained from the Sydney Local Heath District Animal Welfare Committee (protocol number 2013/050). Experiments were conducted in accordance with the Australian Code of Practice for the Care and Use of Animals for Scientific Purpose. Mice were given four 1.5-cm incisions (two rows side-by-side) on their dorsal surfaces to create subcutaneous pockets, as previously described (9). Scaffolds were then inserted into each pocket (5 mice per time point equaling 5 scaffolds per group per time point) and sutured closed by using 6-0 silk sutures. Explants were taken at 3, 7, and 14 days' post-implantation; analysis is detailed in the Supplemental Methods.

In vivo performance of bioactive IL-4 vascular grafts. Study approval was obtained from the Sydney Local Heath District Animal Welfare Committee (protocol number 2015/016). Experiments were conducted in accordance with the Australian Code of Practice for the Care and Use of Animals for Scientific Purpose. C57/BL6 mice (male, 9 to 10 weeks old, 25 ± 2 g) were purchased from Australian BioResources (Moss Vale, NSW, Australia). Vascular grafts (5 per group) were implanted into the carotid artery by using a previously described technique (10). Briefly, the right common carotid artery was double ligated, and polyimide cuffs (Cole-Parmer North America, Vernon Hills, Illinois) were placed around each end. Overhanging arteries were everted on the plastic cuff, and grafts were then sleeved over each end and secured with 8-0 sutures. Clamps were removed, and blood flow was confirmed with pulsation. After 28 days, mice were perfused with heparinized saline (50 U/ml), and the grafted carotid artery

was isolated and dissected proximal and distal to the graft. Analysis of the vascular cross-sections is detailed in the Supplemental Methods.

RESULTS

CREATION OF A NOVEL IL-4–IMMOBILIZED BIOMATERIAL SURFACE. Control surfaces were PIII treated in nitrogen plasma for a duration of 800 s. Energetic ions accelerated by the 20-kV negative bias penetrate through the scaffold surface, breaking chemical bonds along their path and displacing atoms in the polymer structure. This results in a highly crosslinked, dense, carbonized structure at the surface of the scaffold (**Figure 1A**). The high density of broken bonds and displaced atoms allow for creation of new bonds (**Figure 1B**). The unpaired electrons that remain manifest as reactive radical groups (**Figure 1C**) embedded in the treated layer that gradually diffuse to the surface via thermally activated, local restructuring (Supplemental Results). Radical diffusion leads to surface oxidation, allowing direct covalent immobilization of IL-4 upon contact with the scaffold surface (6). Mechanical testing of scaffolds (n 6 each group) exhibited no significant differences in Young's modulus or strain after PIII treatment (Supplemental Figure 1).

Bioactive IL-4 surfaces were created by incubating the PIII-treated surfaces in an IL-4 solution (2 μg/ml) for 1 h at room temperature (**Figure 1D**). Robust, covalent immobilization was shown by washing surfaces in sodium dodecyl sulfate (5%) for 4 h at room temperature to remove any passively adsorbed molecules (11,12), followed by IL-4 quantification using ELISA (n 3 each group) (**Figure 1E**). Although the PIII-treated scaffolds retained IL-4 (bioactive IL-4), IL-4 was completely removed from the untreated PCL surfaces (passive IL-4).

BIOACTIVE IL-4 SURFACES MODULATE MACROPHAGE PHENOTYPE IN VITRO. RAW264.7 murine macrophages were seeded onto bioactive IL-4 surfaces to evaluate macrophage polarization (**Figure 2A**), as commonly reported (13–15). Macrophage morphology and material interaction were first characterized by using scanning electron microscopy. At 8 h post-seeding, cells cultured on bioactive IL-4 surfaces appeared more spread, with a notably rougher cell surface (**Figure 2B**). Cytoskeletal morphologies, observed by using confocal microscopy, further showed strikingly different morphology. Expression of M2 phenotype genes, arginase-1, CD163, CD206, and IL-10 revealed that passive IL-4 surfaces enhanced the expression of only arginase-1 and IL-10 but had no significant effect on CD163 or CD206. Similarly, PIII-only surfaces significantly increased arginase-1 expression but not the other markers. Only bioactive IL-4 surfaces significantly increased all marker expression at 8 h post-seeding compared with control (**Figure 2C**). These results show that IL-4 covalently immobilized on PIII-treated surfaces robustly polarizes macrophages toward an M2 phenotype and demonstrates that this immobilization approach is necessary for sustained bioactivity.

BIOACTIVE IL-4 SUBCUTANEOUS IMPLANTS REDUCE INFLAMMATORY CYTOKINES AND FIBROUS ENCAPSULATION. A 14-day subcutaneous mouse back model of acute inflammation was initially used to evaluate the in vivo functionality of bioactive IL-4 surfaces (16) (5 scaffolds per group) (**Figure 3A**), before further evaluation in a vascular context. Immunostaining markers for total macrophages ($CD68^+$), M1 (major histocompatibility complex Class II), and M2 (CD206) phenotypes were used to assess macrophage responses (**Figure 3B**). Increasing macrophage recruitment, observed on control surfaces, was reduced by 79 ± 6% and 86 ± 7% on bioactive IL-4 surfaces at days 7 and 14, respectively (**Figure 3B**, top). Bioactive IL-4 surfaces also increased M2 macrophage polarization by 159 ± 11% at day 3, suggesting earlier M2 polarization compared with control (**Figure 3B**, middle). Bioactive IL-4 surfaces also exhibited a 360 ± 15% higher M2/M1 macrophage ratio at day 14 compared with control, indicating a predominantly M2 phenotype residing at the implant surface in the late phases post-implantation (**Figure 3B**, bottom). These results were observed in representative images illustrating a large accumulation of macrophages on control surfaces with a predominantly M1 phenotype. In contrast, bioactive IL-4 surfaces exhibited a significant reduction in total macrophage accumulation and an enhancement of the M2 phenotype (**Figure 3C**).

To corroborate these findings, quantitative polymerase chain reaction (qPCR) and ELISA analysis for classic M1 and M2 markers were conducted at days 3 and 7 post-implantation to assess gene and protein expression changes, respectively. qPCR results revealed that bioactive implants had significantly less TNF-α and inducible nitric oxide synthase at day 3 (Supplemental Figure 2A) and the ELISA results showed significantly reduced IL-1β and IL-6 in bioactive implants at days 3 and 7 (Supplemental Figure 2B). These results were consistent with our immunohistochemistry and validated the presence of a robust anti-inflammatory microenvironment surrounding bioactive subcutaneous implants by independently demonstrating an upregulation of M2 markers and a downregulation of M1 markers.

FIGURE 1 Characterization of PIII Treatment on PCL Control Surfaces

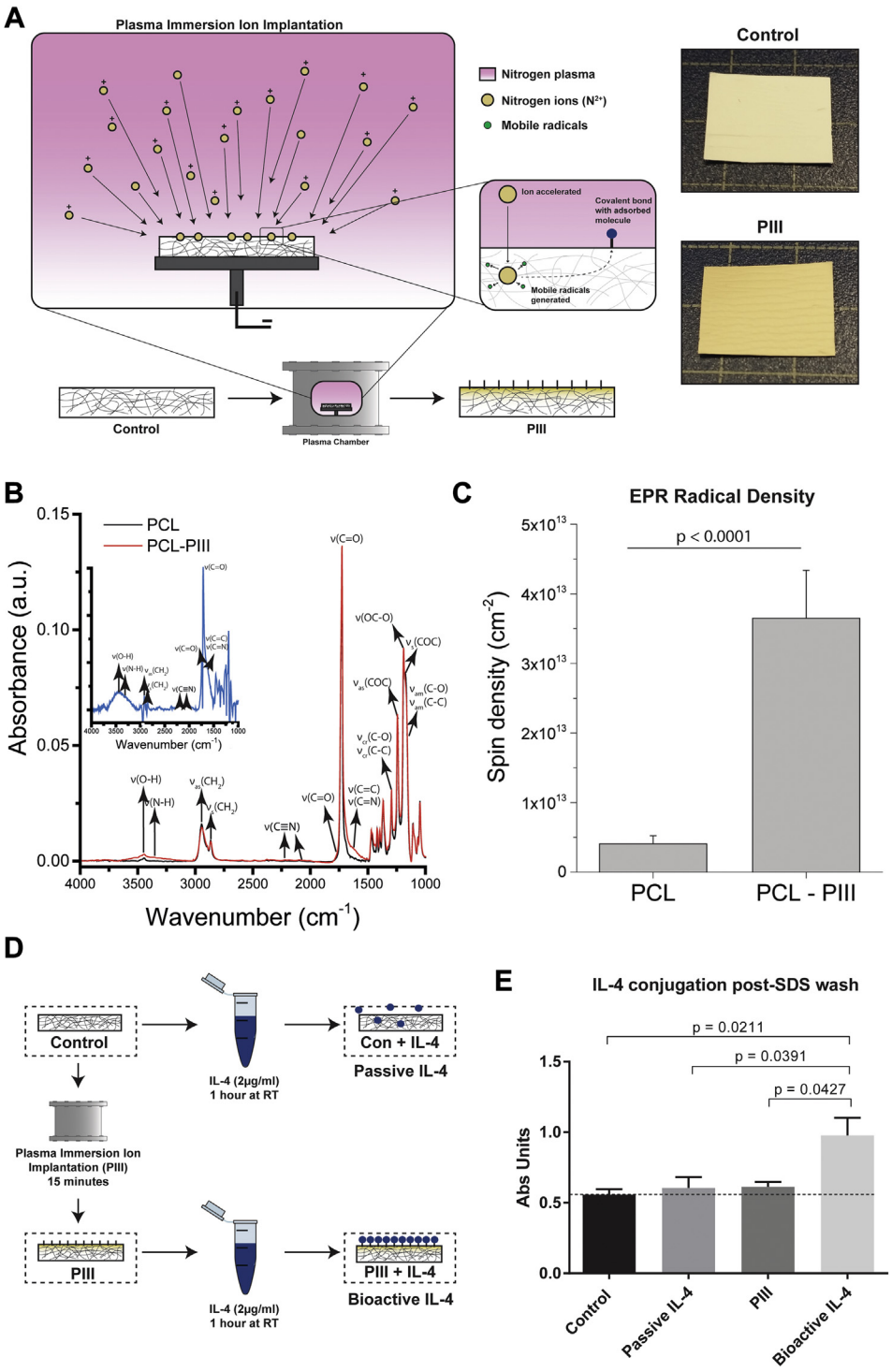

(A) Plasma immersion ion implantation (PIII) schematic with representative images of control surfaces before **(top)** and after **(bottom)** treatment. **(B)** Attenuated total reflectance Fourier transform infrared spectroscopy (ATR FT IR) surface characterization. **(C)** Electron paramagnetic resonance (EPR) characterization. **(D)** Diagram of experimental groups. **(E)** Interleukin 4 (IL 4) retention enzyme linked immunoadsorbent assay (n 3 per group). PCL polycaprolactone; RT room temperature; SDS sodium dodecyl sulfate.

FIGURE 2 **In Vitro Biofunctionality of IL-4 Bioactive Surfaces**

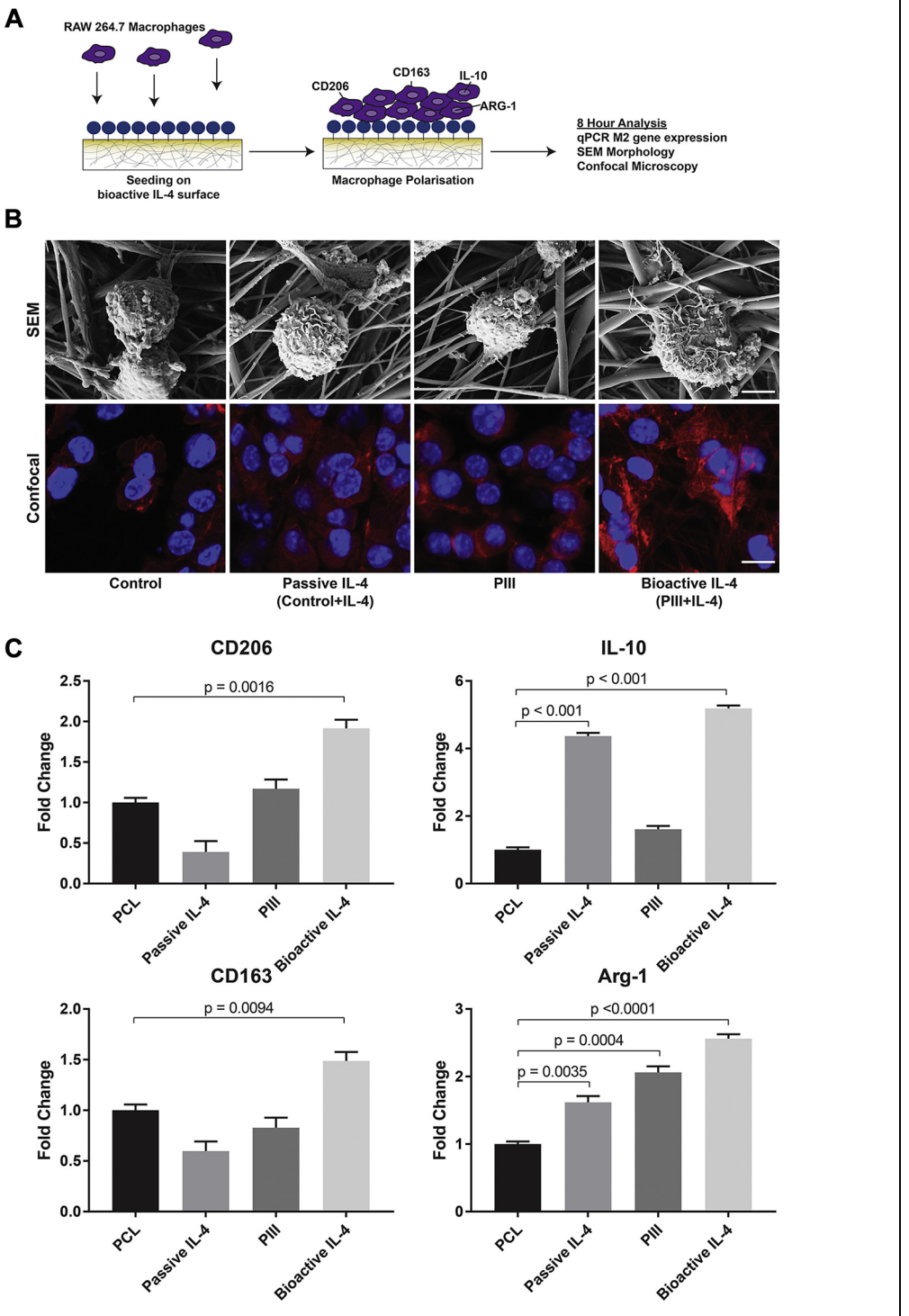

(A) Schematic of experimental design. **(B)** Scanning electron microscopy (SEM) (top row; scale bar represents 50 μm) and confocal micro scopy (bottom row; scale bar represents 5 μm) of cultured macrophages. **(C)** Quantitative polymerase chain reaction (qPCR) of M2 Phenotype genes (n 5 per group). Abbreviations as in Figure 1.

FIGURE 3 Implantation of Bioactive IL-4 Surfaces in Subcutaneous Mouse Model

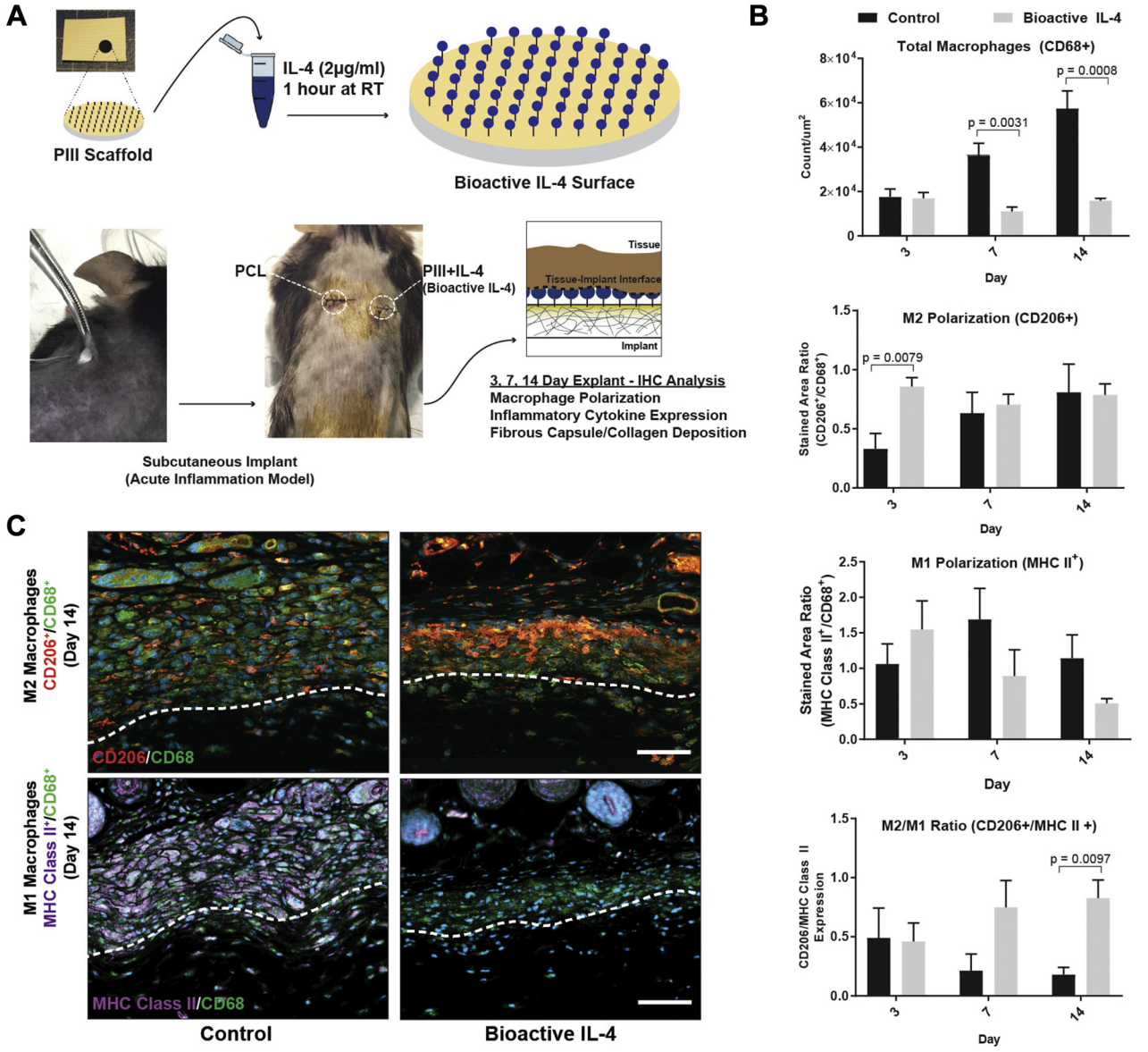

(A) Experimental design schematic. **(B)** Immunohistological quantification of macrophages at the implant surface: total CD68$^+$ macrophages **(top)**, CD206$^+$ M2 polarization **(middle)**, and M2/M1 (CD206$^+$/ major histocompatibility complex (MHC) Class II$^+$) ratio **(bottom)**. **(C)** Representative images of M2 **(top row)** and M1 **(bottom row)** macrophages. CD68 stained in **green**, CD206 stained in **orange**, and MHC Class II stained in **purple**. **Dotted lines** represent the interface between tissue **(above)** and implant **(below)**. Scale bar represents 60μm; n 5 per group. IHC immunohistochemical; other abbreviations as in Figure 1.

Further immunohistochemical analysis was conducted to confirm the expression of inflammatory cytokines (5 scaffolds per group). IL-10 and transforming growth factor (TGF)-β were chosen as classic anti-inflammatory cytokines, whereas IL-1β and TNF-α are well-characterized pro-inflammatory cytokines (17). Bioactive IL-4 surfaces increased IL-10 expression by 432 ± 26% at day 7 compared with controls (Figure 4A). TGF-β expression was also increased 1025 ± 11% at day 7 on bioactive IL-4 surfaces. Representative images show this increased IL-10 and TGF-β present at the scaffold/tissue interface in bioactive surfaces (Figure 4B). Corresponding changes to classically pro-inflammatory cytokines occurred at later time points, with significant differences at day 14. IL-1β and TNF-α

FIGURE 4 **Inflammatory Cytokine Quantification at the Implant Surface In Vivo**

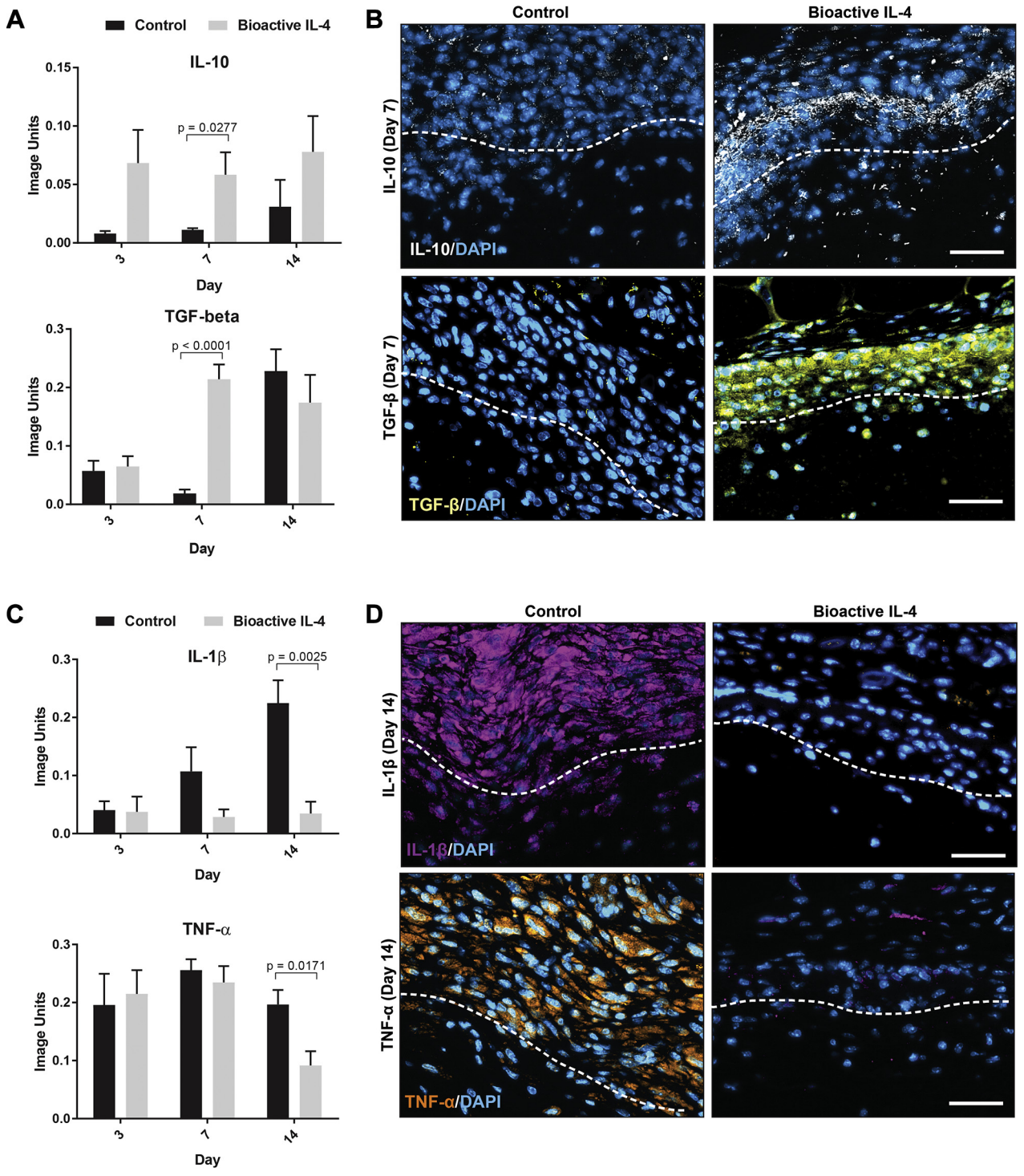

(A) Immunohistological quantification of anti inflammatory cytokines IL 10 **(top)** and transforming growth factor (TGF) β **(bottom)**. **(B)** Representative images of IL 10 **(top)** and TGF β **(bottom)** expression at the implant surface stained in **white** and **yellow** respectively. **(C)** Immunohistological quantification of pro inflammatory cytokines IL 1β **(top)** and tumor necrosis factor (TNF) α **(bottom)**. **(D)** Representative images of IL 1β **(top)** and TNF α **(bottom)** expression at the implant surface stained in **purple** and **orange** respectively. **Dotted lines** represent the interface between tissue **(above)** and implant **(below)**. Scale bar represents 40 μm; n 5 per group. Abbreviations as in Figure 1.

FIGURE 5 Functional Outcomes of Bioactive IL-4 Surfaces In Vivo

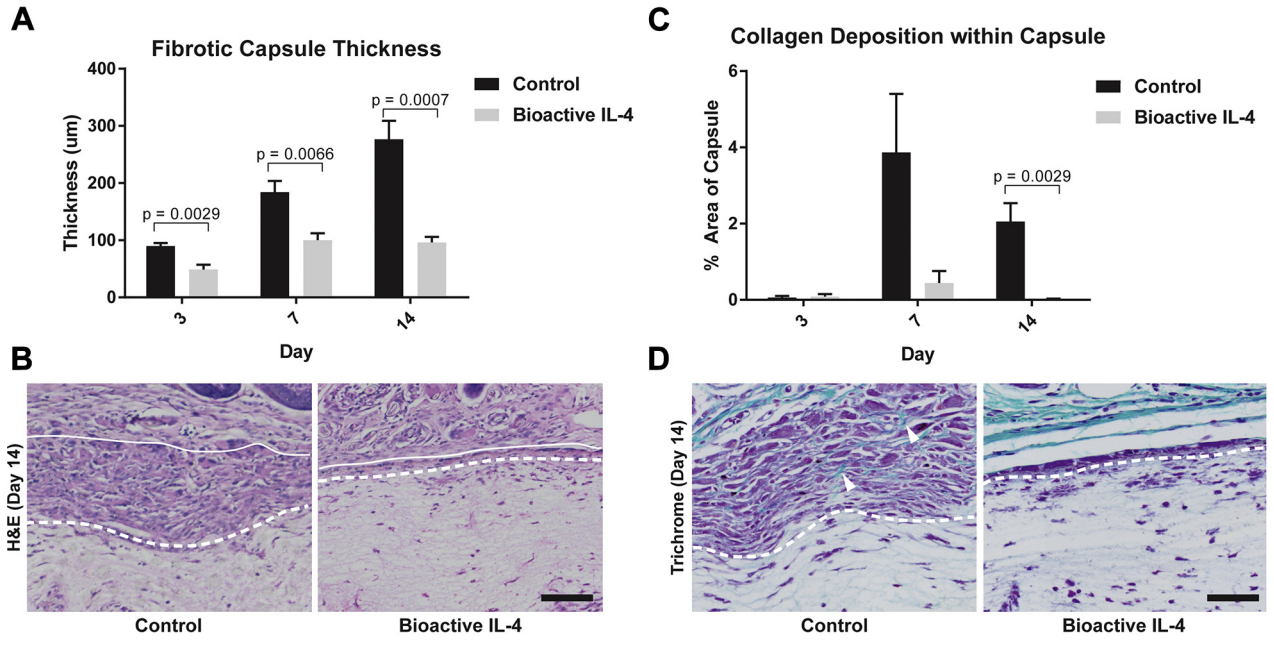

(A) Measurement of fibrotic capsule formation/thickness at the implant surface **(top)**. **(B)** Representative hematoxylin and eosin (H&E) stains of fibrotic capsules. **(C)** Quantification of collagen deposition at the implant surface. **(D)** Representative trichrome stains of collagen **(green)** within the fibrotic capsule, highlighted by **arrows**. **Dotted lines** represent the interface between tissue **(above)** and implant **(below)**. Scale bar represents 50 μm, n 5 per group. IL 4 interleukin 4.

expression was 84 ± 7% and 53 ± 5% less, respectively, on bioactive IL-4 surfaces compared with control (Figure 4C). Again, representative images clearly show these striking changes at the material interface where bioactive IL-4 implants seem to all drastically reduce IL-1β and TNF-α (Figure 4D).

We next sought to characterize functional changes arising from an increased proportion of M2 macrophages and positive regulation of local cytokine production. The fibrotic capsule thickness for the control implants increased steadily over time, as expected, from 90 ± 5.1 μm at day 3 to 276.6 ± 132.1 μm by day 14 (Figure 5A). In contrast, the capsule thickness on bioactive IL-4 surfaces was reduced at all time points with a final reduction of 65 ± 4% at day 14, compared with control, evident in representative images (Figure 5B). Furthermore, peak collagen deposition in PCL controls occurred at day 7 comprising 3.8 ± 2% of the capsule area, with less (2.0 ± 0.7%) by day 14 (Figure 5C). In bioactive IL-4 surfaces, collagen was reduced at day 7 with a significant reduction at day 14, as seen in representative images (Figure 5D). Reductions in collagen deposition over time further suggest significant modulation of the host foreign body response.

BIOACTIVE IL-4 SYNTHETIC ARTERIAL GRAFTS REDUCE LOCAL INFLAMMATION AND NEOINTIMAL HYPERPLASIA. Small diameter vascular grafts were manufactured with bioactive IL-4 surfaces on both the luminal and adventitial surfaces, implanted into an established mouse carotid interposition grafting model, and explanted at 28 days (Figure 6A). Consistent with results from the subcutaneous implant study, IL-4 grafts significantly reduced total macrophages present by 54 ± 6% compared with control (Figure 6B). These macrophages also showed a 47 ± 12% increase in the M2 phenotype and a corresponding decrease in the M1 phenotype by 52 ± 9%, demonstrating similar macrophage polarization effects. This outcome was further supported by a 93 ± 11% increase in the M2/M1 ratio of bioactive IL-4 grafts compared with control. These changes are highlighted in representative images, showing fewer total macrophages and enhanced expression of CD206 with less major histocompatibility complex class II (Figure 6C).

Further examination revealed that anti-inflammatory IL-10 and TGF-β levels were significantly increased by 122 ± 11% and 539 ± 35%, respectively, in bioactive IL-4 grafts compared with controls (Figures 7A and 7B). In addition,

FIGURE 6 **Investigation of IL-4 Bioactive Surfaces for Synthetic Vascular Grafts**

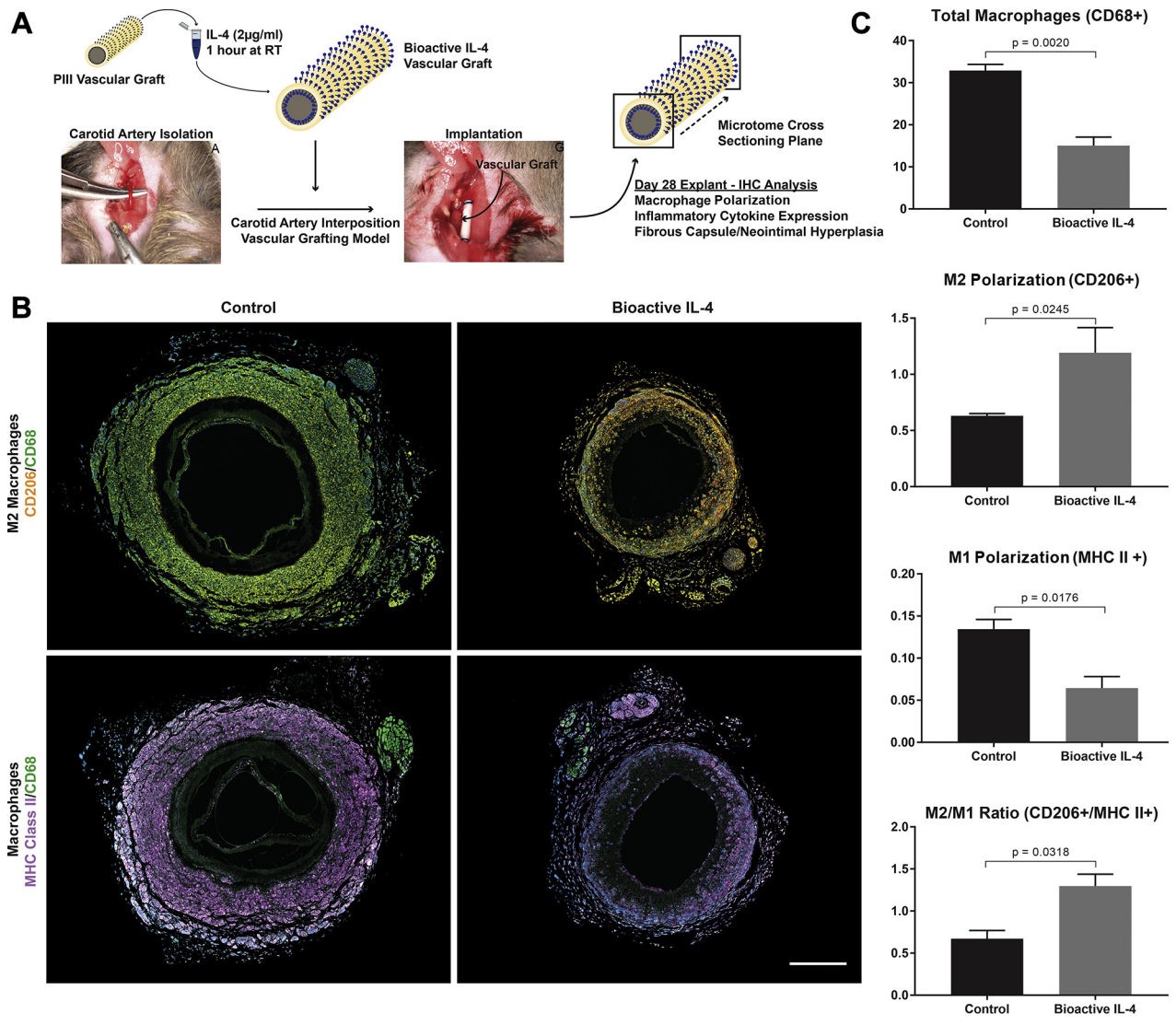

(A) Experimental design schematic; vascular graft dimensions 0.5 mm (inner diameter) × 6 mm length. **(B)** Representative immunostained images of macrophage responses; M2 **(top row)** and M1 **(bottom row)** macrophages. CD68 stained in **green**, CD206 stained in **orange**, and MHC Class II stained in **purple**. Scale bar represents 500 μm. **(C)** Quantification of$CD68^+$ total macrophages **(top)**, $CD206^+$ M2 polarization **(middle)**, MHC Class II^+ M1 polarization, and M2/M1 ($CD206^+$/MHC Class II^+) ratio **(bottom)**. n 3 slides (each region of the graft) per animal, with a total of 5 animals per group. Abbreviations as in **Figures 1 and 3**.

pro-inflammatory IL-1β and TNF-α expression was 43 ± 9% and 50 ± 3% less in bioactive IL-4 grafts (**Figures 7C and 7D**). Representative images of graft cross-sections demonstrate clear increases in levels of IL-10 and TGF-β, as well as corresponding reductions in IL-1β and TNF-α (**Figure 7E**).

To confirm these findings, qPCR and ELISA analyses were conducted on vascular grafts at days 3 and 7 post-implantation. qPCR results showed that the bioactive grafts had significantly less TNF-α and inducible nitric oxide synthase at days 3 and 7, in addition to reduced CD86 at day 7 (Supplemental Figure 3A). ELISA results supported that bioactive grafts had less IL-1β, IL-6, and TNF-α at day 7 (Supplemental Figure 3B). Consistent with the immunohistochemistry data, these additional results further support our proposed immunomodulatory effects of bioactive surfaces.

In a vascular graft context, inflammatory processes drive both fibrous encapsulation and neointimal

FIGURE 7 Immunohistochemical Analysis of Inflammatory Cytokines in Vascular Grafts

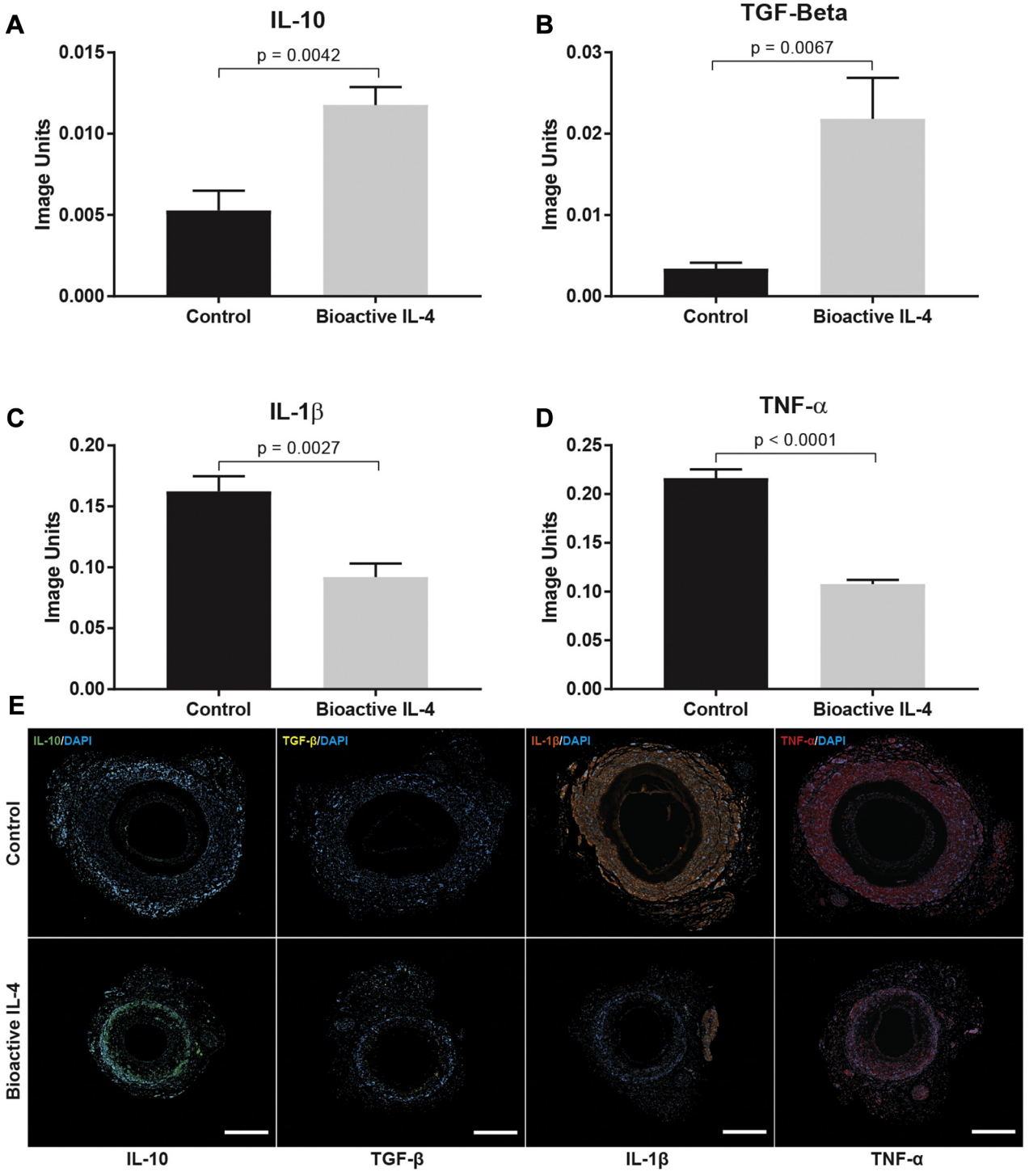

(A) IL 10. **(B)** TGF β. **(C)** IL 1β. **(D)** TNF α. **(E)** Representative images of cytokine expression within vascular graft cross sections: control **(top row)** versus bioactive **(bottom row)**. IL 10 stained in **green**, TGF β stained in **white**, IL 1β stained in **orange**, and TNF α stained in **red**. Scale bar represents 1 mm; n 3 slides (each region of the graft) per animal, with a total of 5 animals per group. Abbreviations as in Figures 1 and 4.

FIGURE 8 Functional Outcomes of Bioactive IL-4 Surfaces for Synthetic Vascular Grafts

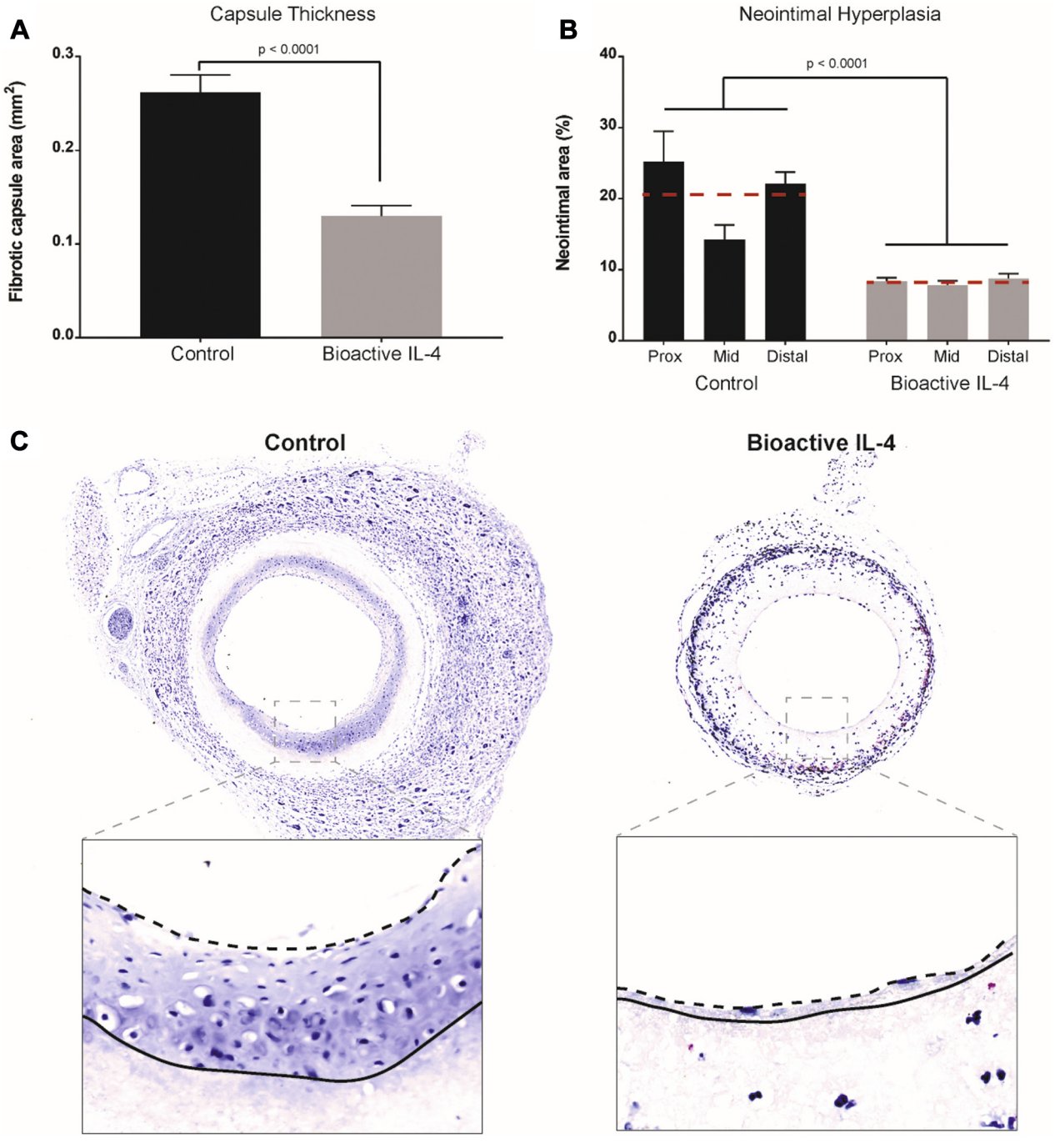

(A) Quantification of adventitia capsule thickness. **(B)** Quantification of neointimal hyperplasia development along 3 segments of vascular graft lumen. **(C)** Repre sentative images of capsule thickness on the adventitia of vascular grafts, scale bar represents 150 μm; representative magnified images of vascular graft lumens **(inset)**. Scale bar represents 40 μm. **Dotted lines** represent the luminal edge of hyperplasia, and **solid lines** represent the luminal graft surface. n 3 slides (each region of the graft) per animal with the average represented as the **red dotted line**; total of n 5 animal averages per group. IL 4 interleukin 4.

hyperplasia leading to graft failure. Adventitial capsule thickness on bioactive IL-4 grafts was 50 ± 1% less than control (**Figure 8A**). In addition, neointimal hyperplasia in bioactive IL-4 grafts was significantly less throughout the length of the graft (**Figure 8B**). The greatest decreases were observed at the proximal and distal anastomoses, with a reduction of 69 ± 6.7% and 61 ± 6.1%, respectively, relative to control. The midsection of the graft also saw significantly less hyperplasia (51 ± 9.6%) compared with control (**Figure 8C**). No significant changes to re-endothelialization were observed between the grafts (Supplemental Figure 4). Further characterization of the neointima observed increases in smooth muscle cells and proliferating cells compared to control while the elastin in the neointima was not significantly different (Supplemental Figure 5). Collectively, these results suggest that local modulation of macrophage phenotypes and cytokine profiles were responsible for significant reductions in neointimal hyperplasia.

DISCUSSION

CAD has become increasingly characterized as a chronic inflammatory disorder, prompting consideration of new anti-inflammatory therapeutic interventions. An overabundance of immune cells is common to atherosclerosis progression and neointimal hyperplasia development. The underlying immune cell presence arises from a complex interplay of inflammatory cytokines, which act to coordinate, propagate, and sustain inflammatory responses. Clinical evidence highlights the therapeutic potential of inhibiting cytokine expression to reduce inflammation and improve outcomes. Although the deployment of cardiovascular materials and devices in high-risk areas is an established treatment for CAD, accelerated inflammatory responses are a major cause of failure (18). In search of the next generation of CAD therapies, there remains an unmet need for cardiovascular devices fabricated from materials capable of modulating local inflammatory responses.

The present study describes rapid resolution of the inflammatory response to implanted materials in 2 separate mouse models, leading to durable functional improvements. Previous studies have shown the feasibility of local modulation of inflammation, using drug release or direct injection approaches to influence cell populations and chemokine profiles (19). Together, these studies have highlighted the limitation of using nonspecific suppressive drugs and the transient effects of these approaches, with most studies showing changes only in the first few days after implantation. Our results show that electrospun PCL scaffolds and conduits can be robustly functionalized with bioactive IL-4 to drive rapid polarization of macrophages to an anti-inflammatory M2 phenotype.

Multiple studies have now reported that implanted materials that promote an early shift to more M2-like macrophages at the material interface have an improved host response. The “alternatively activated” M2 phenotype is driven by signaling from M2-polarizing cytokines, including IL-4 (20). Previous research on IL-4-mediated regulation of the local response to materials has been limited to short-term elution from flat scaffolds. Examples include release from silk scaffolds over 24 h successfully polarizing macrophages in vitro (21) and microsphere-mediated release from poly(lactic-co-glycolic acid) scaffolds that increased the proportion of $CD206^{+}$ macrophages after 1 day in vivo, but local gene expression changes beyond this time were inconsistent (20). Similarly, release of IL-4 from polypropylene meshes showed no change to the number of local macrophages but a shift toward M2 phenotype at 14 days in a mouse subcutaneous implant model (22). Together, these studies illustrate the promise of early-stage macrophage polarization at the tissue implant interface toward an M2 phenotype. However, the applicability of this approach to any functional application, such as in a high-blood flow environment, has yet to be performed.

Robust immobilization of IL-4 onto the surface of PCL substrates was consistent with previous use of PIII surface activation of polymers to immobilize other biomolecules, including fibrillin-1 to polytetrafluoroethylene (PTFE) (23) and tropoelastin to expanded polytetrafluoroethylene (ePTFE) (24) and polyurethane conduits (6). In vitro macrophage interactions with bioactive IL-4 surfaces provided evidence of retained IL-4 bioactivity. The effects of IL-4 immobilization through PIII are consistent with the transient and variable effects on gene expression previously described for eluted IL-4 (20,21). PIII treatment is also well suited to the modification of implanted materials due to the established benefits of a long shelf-life post-treatment and the rapid covalent binding of a range of biomolecules during solution incubation (6). At the bedside, these off-the-shelf features would allow for the preparation of bioactive surfaces by simply taking pre-treated PIII materials/devices off the shelf and immersing them in IL-4

solutions, ready for transplant into patients with minimal time and cost expenditures.

The findings of the present study suggest that simultaneous changes to the local expression of both pro- and anti-inflammatory cytokines may be a more suitable approach to achieve rapid and comprehensive resolution of inflammation. Modulating macrophage phenotype and behavior is potentially an effective way of accomplishing this goal, demonstrating a preferable immunomodulatory strategy in the context of materials for vascular repair. Furthermore, these changes led to functional reductions in fibrous encapsulation sustained for at least 14 days. In contrast, studies using passive release of IL-4 commonly report upregulation of M2 macrophages surrounding implants but typically no significant differences in total cell accumulation (20) or macrophages (22) at the implant interface. In fact, M2 macrophage polarization is greatest at distances farthest from the surface of drug elution, accentuating the disadvantage of passive release strategies in which IL-4 diffuses away from the implant site. Significant reductions in cell accumulation and fibrous encapsulation seen on bioactive IL-4 surfaces demonstrate improved functional outcomes compared with passive release strategies. More broadly, our findings suggest the potential utility for a diverse range of tissue repair applications. Previous studies have highlighted benefits for regulating the inflammatory response to scaffolds in the context of soft tissue and wound repair, as well as potentially in cardiac patches to treat myocardial infarction in which the role of macrophage polarization has recently been highlighted (25). Studies thus far share the limitation of being restricted to analysis in tissue, with none to date modulating inflammation in flowing blood.

The present study reports sustained effectiveness in a vascular graft context with direct implications for vascular materials and devices deployed in contact with circulation. Regulating fibrotic encapsulation is important for limiting compliance mismatch between the graft and adjacent native vasculature, which has long been correlated with poor patency in small-diameter applications (26). Restenosis, the main source of long-term graft occlusion, is caused by neointimal hyperplasia and widely accepted to be inflammation driven. Previous studies have clearly reported this link observing reduced neointima formation after inhibition of leukocyte trafficking (27), release of dexamethasone (28), the cytotoxic drugs paclitaxel and sirolimus (29), and specific anti-inflammatory CX_3CR1 antagonists (30). Although these strategies have collectively shown promising in vitro results, beneficial long-term outcomes in vivo have not been reported, with efficacy often limited to the period of drug elution. In addition to the benefit of immobilization to address these issues, bioactive IL-4 surfaces drive a rapid shift of the native immune response that would be expected to have lasting effects long after the IL-4 biomolecules are removed from the surface. By elevating M2 macrophage populations, yielding favorable modulation of the inflammatory response through regulation of both pro- and anti-inflammatory cytokines, the foreign body response is more quickly resolved. Our research has significant implications for improving the inflammatory response to all implants, with potential applications for cardiovascular devices in contact with flowing blood such as the prevention of foreign body encapsulation and neointimal hyperplasia in small diameter conduits.

STUDY LIMITATIONS. Limitations to this study include the use of a small animal model of grafting, with a nondiseased phenotype, and a short-time frame of neointimal hyperplasia assessment. While the mouse grafting model used in this study facilitates quantification of clinically relevant endpoints such as neointimal hyperplasia and re-endothelialization, the established pre-clinical pathway includes larger animals including sheep. The sheep model more closely resembles human pathology and incorporates additional considerations of graft efficacy including thrombogenicity and longer-term graft performance. The wild-type mice used in this study have a healthy vasculature, lacking the persistent inflammatory environment commonly present in atherosclerosis and CAD. Use of fat-fed or transgenic animals may potentially benefit future studies investigating bioactive vascular grafts in cardiovascular disease phenotypes. The findings of this study justify the further assessment of bioactive IL-4 surfaces in the context of atherosclerosis and in larger animal models with implications for improving the efficacy of all implants, including small diameter vascular grafts.

CONCLUSIONS

The present study evaluated a novel bioactive device coating that modulates macrophage phenotype and extensively suppresses local inflammatory responses. The bioactivity of our surfaces relies on a covalently immobilized layer of IL-4, a key regulator of macrophage recruitment and anti-inflammatory polarization, to provide comprehensive suppression of

inflammation. As a subcutaneous implant, bioactive IL-4 surfaces exhibited increased polarization of macrophages to their anti-inflammatory M2 phenotype, reducing the overall recruitment of macrophages. This finding also correlates with the favorable regulation of inflammatory cytokine production that led to striking reductions in the formation of the foreign body fibrotic capsule at 2 weeks after implantation. Using these materials as vascular grafts, we observed the same striking effects on macrophage reduction, M2 polarization, and positive regulation of the local cytokine environment, which translate to important functional outcomes, most notably a significant reduction in foreign body encapsulation and neointimal hyperplasia development after 1 month in vivo. The collective findings of our 2 models have significant implications for improving the inflammatory response and the long-term performance of medical implants, with demonstrated potential for cardiovascular devices in contact with flowing blood.

ACKNOWLEDGMENTS The authors acknowledge the facilities as well as scientific and technical assistance at the Australian Center for Microscopy and Microanalysis, The University of Sydney.

ADDRESS FOR CORRESPONDENCE: Mr. Richard P. Tan, Applied Materials Group, The Heart Research Institute, 7 Eliza Street, Newtown NSW 2042, Australia. E-mail: richard.tan@hri.org.au.

PERSPECTIVES

COMPETENCY IN MEDICAL KNOWLEDGE: CAD and other manifestations of atherosclerosis have become increasingly characterized as inflammatory disorders. The success of future interventional therapies for CAD requires effective delivery of anti-inflammatory agents that can provide localized and sustained suppression of inflammation while avoiding the adverse effects of systemic administration, including infection. Representing an alternative approach to systemic treatment, this study investigates the targeted delivery of the anti-inflammatory cytokine IL-4 through bioactive coatings on materials capable of being implanted into the vasculature.

TRANSLATIONAL OUTLOOK: Given their roles as major effectors of innate immunity, targeting macrophage phenotype and behavior may represent a more focused and comprehensive approach to immunomodulation, with potentially greater impact on improved cardiac outcomes for implanted vascular materials. Bioactive surfaces with immobilized IL-4 can modulate local inflammation in a sustained and robust manner. These have numerous applications for implants and devices being implanted into high-risk cardiovascular areas, with the immediate benefits of improving device performance as well as the long-term advantages of mitigating chronic inflammation that drive CAD pathology.

REFERENCES

1. Hansson GK. Inflammation, atherosclerosis, and coronary artery disease. N Engl J Med 2005;352:1685 95.

2. Mulvihill NT, Foley JB. Inflammation in acute coronary syndromes. Heart 2002;87:201 4.

3. Ridker PM, Everett BM, Thuren T, et al. Antiin flammatory therapy with canakinumab for atherosclerotic disease. N Engl J Med 2017;377:1119 31.

4. Bridges AW, García AJ. Anti Inflammatory polymeric coatings for implantable biomaterials and devices. J Diabetes Sci Technol 2008;2:984 94.

5. Hiroyuki O, Tsutomu T, Kiyoshi Y. Therapies targeting inflammation after stent implantation. Curr Vasc Pharmacol 2013;11:399 406.

6. Bilek MM. Biofunctionalization of surfaces by energetic ion implantation: review of progress on applications in implantable biomedical devices and antibody microarrays. Appl Surf Sci 2014;310:3 10.

7. Pajarinen J, Tamaki Y, Antonios JK, et al. Mod ulation of mouse macrophage polarization in vitro using IL 4 delivery by osmotic pumps. J Biomed Mater Res A 2015;103:1339 45.

8. Kondyurin A, Bilek M. 10 Protection in an aggressive environment. Ion Beam Treatment of Polymers. Amsterdam, the Netherlands: Elsevier, 2008:243 60.

9. Liu H, Wise SG, Rnjak Kovacina J, et al. Biocompatibility of silk tropoelastin protein poly mers. Biomaterials 2014;35:5138 47.

10. Chan AH, Tan RP, Michael PL, et al. Evaluation of synthetic vascular grafts in a mouse carotid grafting model. PLoS One 2017;12:e0174773.

11. Bilek MM, McKenzie DR. Plasma modified sur faces for covalent immobilization of functional biomolecules in the absence of chemical linkers: towards better biosensors and a new generation of medical implants. Biophysical Reviews 2010;2:55 65.

12. Bilek MM, Bax DV, Kondyurin A, et al. Free radical functionalization of surfaces to prevent adverse responses to biomedical devices. Proc Natl Acad Sci U S A 2011;108:14405 10.

13. Liu CP, Zhang X, Tan QL, et al. NF κB pathways are involved in M1 polarization of RAW 264.7 macrophage by polyporus polysaccharide in the tu mor microenvironment. PLoS One 2017;12:e0188317.

14. Liu CY, Xu JY, Shi XY, et al. M2 polarized tumor associated macrophages promoted epithelial mesenchymal transition in pancreatic cancer cells, partially through TLR4/IL 10 signaling pathway. Lab Invest 2013;93:844 54.

15. Li B, Cao H, Zhao Y, et al. In vitro and in vivo responses of macrophages to magnesium doped titanium. Sci Rep 2017;7:42707.

16. Tan RP, Lee BSL, Chan AH, et al. Non invasive tracking of injected bone marrow mononuclear cells to injury and implanted biomaterials. Acta Biomater 2017;53:378 88.

17. Anderson JM, Rodriguez A, Chang DT. Foreign body reaction to biomaterials. Semin Immunol 2008;20:86 100.

18. Inoue T, Croce K, Morooka T, Sakuma M, Node K, Simon DI. Vascular inflammation and repair: implications for reendothelialization,

restenosis, and stent thrombosis. J Am Coll Cardiol Intv 2011;4:1057–66.

19. Browne S, Pandit A. Biomaterial-mediated modification of the local inflammatory environment. Front Bioeng Biotechnol 2015;3:67.

20. Minardi S, Corradetti B, Taraballi F, et al. IL-4 release from a biomimetic scaffold for the temporally controlled modulation of macrophage response. Ann Biomed Eng 2016;44:2008–19.

21. Reeves AR, Spiller KL, Freytes DO, Vunjak-Novakovic G, Kaplan DL. Controlled release of cytokines using silk biomaterials for macrophage polarization. Biomaterials 2015;73:272–83.

22. Hachim D, LoPresti ST, Yates CC, Brown BN. Shifts in macrophage phenotype at the biomaterial interface via IL-4 eluting coatings are associated with improved implant integration. Biomaterials 2017;112:95–107.

23. Hajian H, Wise SG, Bax DV, et al. Immobilisation of a fibrillin-1 fragment enhances the biocompatibility of PTFE. Colloids Surf B Biointerfaces 2014;116:544–52.

24. Wise SG, Liu H, Kondyurin A, et al. Plasma-ion activated expanded polytetrafluoroethylene vascular grafts with a covalently immobilized recombinant human tropoelastin coating reducing neointimal hyperplasia. ACS Biomaterials Sci Eng 2016;2:1286–97.

25. Mongue-Din H, Patel AS, Looi YH, et al. NADPH oxidase-4 driven cardiac macrophage polarization protects against myocardial infarction-induced remodeling. J Am Coll Cardiol Basic Trans Science 2017;2:688.

26. Baird RN, Abbott WM. Pulsatile blood flow in arterial grafts. Lancet 1976;308:948–50.

27. Lavin B, Gomez M, Pello OM, et al. Nitric oxide prevents aortic neointimal hyperplasia by controlling macrophage polarization. Arterioscler Thromb Vasc Biol 2014;34:1739–46.

28. Liu X, De Scheerder I, Desmet W. Dexamethasone-eluting stent: an anti-inflammatory approach to inhibit coronary restenosis. Expert Rev Cardiovasc Ther 2004;2:653–60.

29. Wessely R, Schömig A, Kastrati A. Sirolimus and paclitaxel on polymer-based drug-eluting stents: similar but different. J Am Coll Cardiol 2006;47:708–14.

30. Ali MT, Martin K, Kumar AH, et al. A novel CX3CR1 antagonist-eluting stent reduces stenosis by targeting inflammation. Biomaterials 2015;69:22–9.

KEY WORDS covalent biomolecule immobilization, inflammation, interleukin-4, neointimal hyperplasia, plasma-based ion implantation, radical functionalized surface, vascular graft

APPENDIX For supplemental figures, results, and methods, please see the online version of this paper.

Chapter 6

Discussion and Conclusion

General Conclusion

The challenges of developing efficacious tissue engineering solutions are compounded by the requirements from the various fields of study which are incorporated into a single multi-disciplinary approach. Information from various areas of biology and medicine must successfully integrate with knowledge in materials synthesis and manufacturing in order to develop a tissue engineering solution that is both efficacious and translational. As a result, the field of tissue engineering has generated a limited number of clinical successes so far, and the future development of solutions is viewed as long and arduous. However, the outlook of the field is still bright given that advancements in technologies across the various stages of scaffold/construct development continue to progress. In particular, low-throughput methodology in scaffold/construct development combined with a lack of consideration for their translational challenges continue to remain the limitations of tissue engineering solutions for clinical use in regenerative medicine. Developing the necessary tools to stream-line the scaffold/construct design process while incorporating strategies that utilize translationally relevant components have the potential to redefine numerous areas of the tissue engineering research field with significant implications for real-world regenerative medicine therapies.

The findings of this thesis contribute novel solutions to the scaffold design problem by redefining the methodology through which scaffolds and constructs are fabricated. The utilization of the bioluminescence imaging modality has been a cornerstone to these studies by allowing for non-invasive and real-time reporting of cellular behaviour both *in vitro* and *in vivo*. Incorporation of bioluminescence imaging can increase both the efficiency and accuracy of identifying optimal scaffolds and constructs for a given tissue engineering application. Cell responses toward scaffolds can be measured over time on a single scaffold, eliminating the need for multiple samples to account for time points along the cell growth curve. Additionally, by reporting real-time measurements, we are able to observe time-dependent changes in cellular behaviour, giving us more informed insight into the scaffold features which may enhance or impair cell function. This information helps to

eliminate the current methodology of trial-and-error fabrication by offering more suitable and accessible late-stage development testing.

Tissue engineering product development conventionally starts with *in vitro* biological assays which then progress from small animal (rodent) models, large animal models and finally clinical trials in humans. While the great advantage of *in vitro* testing is that it allows a large degree of automation and high throughput screening of biomaterials, they are mostly limited to investigation at the cellular level and do not effectively mimic the complexity of tissue formation *in vivo*. Although more biologically and clinically relevant testing environments for biomaterial screening are implantation into the tissue itself, *in vivo* testing becomes generally expensive from excessive animal usage for evaluation at different time intervals, in addition to being time-consuming for histological analysis. These issues are more prevalent during the early phases of scaffold design where ideal cellular interactions with scaffold parameters are still unknown. While the use of bioluminescence imaging has revolutionized the field of stem cell biology, the potential benefits to the field of tissue engineering have not yet been fully explored, and the incorporation of bioluminescent reporters into tissue engineering strategies is still a recently developed concept. For example, bioluminescence reporters can be encoded into IL-1β promoter regions to more closely examine host inflammatory responses towards implanted scaffolds [121]. The incorporation of bioluminescence imaging both *in vitro* and *in vivo* combined with endpoint molecular analysis techniques such as immunostaining and/or qPCR will enable the more rapid identification of scaffolds that exhibit the most favourable interaction with desired cell types for an intended tissue engineering application, greatly expediting the scaffold design process.

Extending the functionality of this imaging approach will also undoubtedly allow for high-throughput investigations of scaffolds with novel cell types, paving the way for novel constructs with key translational features and high therapeutic potential. This concept is explored throughout this thesis with the investigation of the regenerative properties of iPSCs and their integration with tissue

engineering scaffolds. As previously discussed, one of the main translational challenges underlying stem-cell based tissue engineering and regenerative medicine approaches are stem cell sources capable of providing clinically relevant stem cell numbers. The advent of iPSC technology has revolutionised the stem cell biology field by providing an indefinite stem cell source that are void of the ethical concerns of previous approaches with embryonic stem cells. However, investigation of their numerous lineages and their respective regenerative properties are lacking, placing them merely as a potential stem cell source for tissue engineering. Developing iPSCs as a main stay element of the cellular component of the tissue engineering paradigm is a large endeavour requiring the investigation of multiple iPSC lineages. The investigation of iPSC-ECs in this thesis shows the tissue regeneration potential of this cell type, and more importantly, highlight their improved effectiveness when integrated with biomaterial scaffolds. These findings contribute to the notion that iPSCs may be the future cell source for tissue engineering constructs given their known translational qualities and recently growing demonstration of their regenerative effects. While the research field investigating iPSC laden tissue engineering constructs continues to expand, iPSC safety remains an ongoing issue preventing their clinical use in regenerative medicine. However, advances in iPSC technology are continually making them safer for use. For example, universal iPSC banking systems are currently being developed with genetically matched human leukocyte antigens (HLAs) which almost eliminates the likelihood of immune rejection and drastically improves their therapeutic potential. Additionally, while there is still no accepted method for large scale derivation and characterisation of iPSCs, numerous approaches have been reported focusing on reduced costs and high-throughput characterisation, which have been demonstrated to yield sizeable numbers of patient-specific iPSCs in clinically relevant time scales. Given the rapidly approaching future of iPSC seeded scaffolds in tissue engineering, solutions improving the integration of these novel constructs with the body will be essential. Seamless integration of iPSC constructs has the potential of achieving some of tissue engineering's largest outstanding goals, including the regeneration of whole organs and tissues.

To meet these demands, the large gap that exists within the tissue engineering field between research findings and translational applicability must first be bridged. The fundamental concepts of tissue engineered scaffolds to enhance stem cell survival and function have been widely demonstrated, however application of these strategies within the body presents another range of challenges. The longevity of any beneficial effect arising from these constructs are determined by the degree of host integration. Foreign body responses largely decide the success of any implanted construct or device. Although mitigating this host response to improve efficacy and safety is not a novel concept, current approaches employed typically rely on the view of the foreign body response as a binary biological process. Anti-inflammatory or anti-proliferative drugs are the most common approaches that aim to halt inflammation entirely through the inhibition of immune signalling or elimination immune cells, respectively. However, it is increasingly apparent that the immune response is a very dynamic response that facilitates numerous biological processes that may in fact assist in device integration. With this revamped perspective of the immune response, the studies within this thesis examine strategies that utilize, manipulate, and augment the body's endogenous mechanisms to achieve more robust and long-lasting biological responses. This is exemplified in our bioactive coating functionalisation studies that target macrophage polarisation to facilitate a chain reaction of immune resolution. The demonstration of covalently immobilised monolayers of IL-4 represents the creation a biological barrier comprising of anti-inflammatory M2 macrophages that are resistant to chronic inflammation and instead enhance integration. Additionally, macrophages also participate in a host of tissue regeneration mechanisms in a variety of M2 sub-phenotypes. The ideal use of macrophage phenotype would be to first halt inflammation that is detrimental to implant acceptance of cell survival, while also simultaneously stimulating the body's own capacity for tissue repair. Given their numerous roles and integral functions in many biological processes, the appropriate control over macrophages will only continue to grow as a central theme of tissue engineering solutions. However, having the appropriate control over the right functionalisation methods and biomolecules that are

capable of modulating macrophage phenotype will be equally crucial to the success of these future approaches.

Scaffold functionalisation is an inevitable step in the fabrication process that is crucial to scaffold function, longevity, and safety. The incorporation of many growth factors, cytokines, drugs, and other biomolecules have been widely demonstrated with a wide range of beneficial effects. However, while these findings typically show promise within the confounds of research settings, the development of these approaches often fail to consider the translational requirements needed for clinical relevancy. The most notable of which being time, cost, and safety constraints of the manufacturing processes as previously discussed. The findings of this thesis largely address these considerations through the employment of PIII functionalisation methodology. As shown in our findings, PIII allows for robust immobilisation of biomolecules in clinically relevant time frames and this binding capacity possesses extended shelf-life, which opens up the translational possibilities of numerous tissue engineering solutions, while also potentially allowing for a revisit of the past research findings that have relied on the functionalisation of biomolecules but utilized non-translatable fabrication techniques. With the ongoing development and optimisation of these translational approaches, a change in the future landscape of the tissue engineering paradigm, in favour of solutions possessing more off-the-shelf versatility, may be imminent. When closely examining the paradigm, cellular components currently exhibit very low off-the-shelf properties due to the current lack of high-throughput derivation methods. With the availability of extended storage methods for biomolecules and non-degradable materials for scaffold manufacturing, these two components of the paradigm may instead highlight the future focus of the tissue engineering paradigm. Utilizing these two components, investigation of functionalisation technologies such as PIIII represents a method through which scaffolds can be functionalised with the necessary biomolecules with minimal preparation, prior to implantation in the body. These approaches hit upon the consistent themes of this thesis which are stimulating and enhancing innate biological processes through biomolecules, while also taking into consideration the

translational challenges that can hinder their development. Until there are advancements in the rapid derivation of stem cells and other cell sources, functionalised scaffolds pose as the most promising tissue engineering strategies with the highest likelihood of success in the short future. However, utilizing all components of the paradigm will still benefit research studies with crucial knowledge of the mechanisms underlying tissue repair and bring to light new strategies and targets which can augment these processes.

Combining these essential research findings with clinically relevant development methods are represented as the cumulative findings of this thesis which impart both tools and lessons for the future development of translational biomaterials and tissue engineering solutions for regenerative medicine. The future of whole organ regeneration and functional restoration will undoubtedly lie in the form of combined research approaches incorporating the rapid identification of functional biomaterials, novel stem cell sources with enhance regenerative capacity, manipulation of the body's innate biological mechanisms, and utilization of translational fabrication techniques. Incorporating the findings of these studies help to build the ongoing path towards accomplishing the outstanding goals of tissue engineering and regenerative medicine. With continued research, the allure of curing diseases once thought to be incurable comes even closer to reality.

Thesis References

1. Mao, A.S.; Mooney, D.J., Regenerative medicine: Current therapies and future directions, *Proceedings of the National Academy of Sciences of the United States of America* **2015**, *112*, 14452-14459.

2. Sampogna, G.; Guraya, S.Y.; Forgione, A., Regenerative medicine: Historical roots and potential strategies in modern medicine, *Journal of Microscopy and Ultrastructure* **2015**, *3*, 101-107.

3. Nadig, R.R., Stem cell therapy – Hype or hope? A review, *Journal of Conservative Dentistry : JCD* **2009**, *12*, 131-138.

4. Zhao, Q.; Ren, H.; Han, Z., Mesenchymal stem cells: Immunomodulatory capability and clinical potential in immune diseases, *Journal of Cellular Immunotherapy* **2016**, *2*, 3-20.

5. Berthiaume, F.; Maguire, T.J.; Yarmush, M.L., Tissue Engineering and Regenerative Medicine: History, Progress, and Challenges, *Annual Review of Chemical and Biomolecular Engineering* **2011**, *2*, 403-430.

6. Eming, S.A.; Martin, P.; Tomic-Canic, M., Wound repair and regeneration: Mechanisms, signaling, and translation, *Science translational medicine* **2014**, *6*, 265sr6-265sr6.

7. Michalopoulos, G.K., Liver Regeneration, *Journal of cellular physiology* **2007**, *213*, 286-300.

8. Gargett, C.E.; Nguyen, H.P.; Ye, L., Endometrial regeneration and endometrial stem/progenitor cells, *Rev Endocr Metab Disord* **2012**, *13*, 235-51.

9. Land, W.G., The Role of Damage-Associated Molecular Patterns (DAMPs) in Human Diseases: Part II: DAMPs as diagnostics, prognostics and therapeutics in clinical medicine, *Sultan Qaboos University Medical Journal* **2015**, *15*, e157-e170.

10. Lipid leads the way in wound healing, *Development* **2013**, *140*, e402.

11. Dunnill, C.; Patton, T.; Brennan, J.; Barrett, J.; Dryden, M.; Cooke, J.; Leaper, D.; Georgopoulos Nikolaos, T., Reactive oxygen species (ROS) and wound healing: the functional role of ROS and emerging ROS-modulating technologies for augmentation of the healing process, *International Wound Journal* **2015**, *14*, 89-96.

12. Behm, B.; Babilas, P.; Landthaler, M.; Schreml, S., Cytokines, chemokines and growth factors in wound healing, *Journal of the European Academy of Dermatology and Venereology* **2011**, *26*, 812-820.

13. Koh, T.J.; DiPietro, L.A., Inflammation and wound healing: The role of the macrophage, *Expert reviews in molecular medicine* **2011**, *13*, e23-e23.

14. Ayala, A.; Chung, C.-S.; Grutkoski, P.S.; Song, G.Y., Mechanisms of immune resolution, *Critical care medicine* **2003**, *31*, S558-S571.

15. Straub, R.H.; Schradin, C., Chronic inflammatory systemic diseases: An evolutionary trade-off between acutely beneficial but chronically harmful programs, *Evolution, Medicine, and Public Health* **2016**, *2016*, 37-51.

16. Nuyttens, B.P.; Thijs, T.; Deckmyn, H.; Broos, K., Platelet adhesion to collagen, *Thrombosis Research* **2011**, *127*, S26-S29.

17. Engels, E.A.; Jennings, L.; Kemp, T.J.; Chaturvedi, A.K.; Pinto, L.A.; Pfeiffer, R.M.; Trotter, J.F.; Acker, M.; Onaca, N.; Klintmalm, G.B., Circulating TGF-β1 and VEGF and risk of cancer among liver transplant recipients, *Cancer Medicine* **2015**, *4*, 1252-1257.

18. Patan, S., Vasculogenesis and angiogenesis, *Cancer Treat Res* **2004**, *117*, 3-32.

19. Deveza, L.; Choi, J.; Yang, F., Therapeutic Angiogenesis for Treating Cardiovascular Diseases, *Theranostics* **2012**, *2*, 801-814.

20. Caley, M.P.; Martins, V.L.C.; O'Toole, E.A., Metalloproteinases and Wound Healing, *Advances in Wound Care* **2015**, *4*, 225-234.

21. Bainbridge, P., Wound healing and the role of fibroblasts, *J Wound Care* **2013**, *22*, 407-8, 410-12.

22. van Zuijlen, P.P.; Ruurda, J.J.; van Veen, H.A.; van Marle, J.; van Trier, A.J.; Groenevelt, F.; Kreis, R.W.; Middelkoop, E., Collagen morphology in human skin and scar tissue: no adaptations in response to mechanical loading at joints, *Burns* **2003**, *29*, 423-31.

23. Atala, A.; Irvine, D.J.; Moses, M.; Shaunak, S., Wound Healing Versus Regeneration: Role of the Tissue Environment in Regenerative Medicine, *MRS bulletin / Materials Research Society* **2010**, *35*, 10.1557/mrs2010.528.

24. Martínez-Garza, D.M.; Cantú-Rodríguez, O.G.; Jaime-Pérez, J.C.; Gutiérrez-Aguirre, C.H.; Góngora-Rivera, J.F.; Gómez-Almaguer, D., Current state and perspectives of stem cell therapy for stroke, *Medicina Universitaria* **2016**, *18*, 169-180.

25. Jezierska-Wozniak, K.; Mystkowska, D.; Tutas, A.; Jurkowski, M.K., Stem cells as therapy for cardiac disease - a review, *Folia Histochem Cytobiol* **2011**, *49*, 13-25.

26. Sheik Abdulazeez, S., Diabetes treatment: A rapid review of the current and future scope of stem cell research, *Saudi Pharmaceutical Journal* **2015**, *23*, 333-340.

27. Sakthiswary, R.; Raymond, A.A., Stem cell therapy in neurodegenerative diseases: From principles to practice, *Neural Regeneration Research* **2012**, *7*, 1822-1831.

28. Biehl, J.K.; Russell, B., Introduction to Stem Cell Therapy, *The Journal of cardiovascular nursing* **2009**, *24*, 98-105.

29. Ahmed, A.S.I.; Sheng, M.H.C.; Wasnik, S.; Baylink, D.J.; Lau, K.-H.W., Effect of aging on stem cells, *World Journal of Experimental Medicine* **2017**, *7*, 1-10.

30. Oh, J.; Lee, Y.D.; Wagers, A.J., Stem cell aging: mechanisms, regulators and therapeutic opportunities, *Nature medicine* **2014**, *20*, 870-880.

31. Behrens, A.; van Deursen, J.M.; Rudolph, K.L.; Schumacher, B., Impact of genomic damage and ageing on stem cell function, *Nature cell biology* **2014**, *16*, 201-207.

32. Wagers, A.J.; Weissman, I.L., Plasticity of Adult Stem Cells, *Cell 116*, 639-648.

33. Zhao, Y.; Ling, F.; Wang, H.-C.; Sun, X.-H., Understanding the Impact of Inflammation on Hematopoietic Stem Cells, *Blood* **2010**, *116*, 2629.

34. Ko, I.K.; Lee, S.J.; Atala, A.; Yoo, J.J., In situ tissue regeneration through host stem cell recruitment, *Experimental & Molecular Medicine* **2013**, *45*, e57.

35. Lennard, A.L.; Jackson, G.H., Stem cell transplantation, *Western Journal of Medicine* **2001**, *175*, 42-46.

36. Martello, G.; Smith, A., The nature of embryonic stem cells, *Annu Rev Cell Dev Biol* **2014**, *30*, 647-75.

37. Vazin, T.; Freed, W.J., Human embryonic stem cells: derivation, culture, and differentiation: a review, *Restor Neurol Neurosci* **2010**, *28*, 589-603.

38. Ilic, D.; Ogilvie, C., Concise Review: Human Embryonic Stem Cells—What Have We Done? What Are We Doing? Where Are We Going?, *STEM CELLS* **2016**, *35*, 17-25.

39. Hamazaki, T.; El Rouby, N.; Fredette, N.C.; Santostefano, K.E.; Terada, N., Concise Review: Induced Pluripotent Stem Cell Research in the Era of Precision Medicine, *Stem Cells* **2017**, *35*, 545-550.

40. Soldner, F.; Jaenisch, R., iPSC Disease Modeling, *Science* **2012**, *338*, 1155.

41. Szablowska-Gadomska, I.; Gorska, A.; Malecki, M., Induced pluripotent stem cells (iPSc) for gene therapy, *Med Wieku Rozwoj* **2013**, *17*, 191-5.

42. Krabbe, C.; Zimmer, J.; Meyer, M., Neural transdifferentiation of mesenchymal stem cells--a critical review, *Apmis* **2005**, *113*, 831-44.

43. Graf, T., Historical Origins of Transdifferentiation and Reprogramming, *Cell Stem Cell 9*, 504-516.

44. Fu, Y.; Huang, C.; Xu, X.; Gu, H.; Ye, Y.; Jiang, C.; Qiu, Z.; Xie, X., Direct reprogramming of mouse fibroblasts into cardiomyocytes with chemical cocktails, *Cell Research* **2015**, *25*, 1013.

45. Lee, C.H.; Shah, B.; Moioli, E.K.; Mao, J.J., CTGF directs fibroblast differentiation from human mesenchymal stem/stromal cells and defines connective tissue healing in a rodent injury model, *The Journal of Clinical Investigation* **2010**, *120*, 3340-3349.

46. Ikehara, S., Grand challenges in stem cell treatments, *Frontiers in Cell and Developmental Biology* **2013**, *1*, 2.

47. Pikula, M.; Langa, P.; Kosikowska, P.; Trzonkowski, P., [Stem cells and growth factors in wound healing], *Postepy Hig Med Dosw (Online)* **2015**, *69*, 874-85.

48. Kyurkchiev, D.; Bochev, I.; Ivanova-Todorova, E.; Mourdjeva, M.; Oreshkova, T.; Belemezova, K.; Kyurkchiev, S., Secretion of immunoregulatory cytokines by mesenchymal stem cells, *World Journal of Stem Cells* **2014**, *6*, 552-570.

49. Nagareddy, P.R.; Asfour, A.; Klyachkin, Y.M.; Abdel-Latif, A., A novel role for bioactive lipids in stem cell mobilization during cardiac ischemia: new paradigms in thrombosis: novel mediators and biomarkers, *J Thromb Thrombolysis* **2014**, *37*, 24-31.

50. Baraniak, P.R.; McDevitt, T.C., Stem cell paracrine actions and tissue regeneration, *Regen Med* **2010**, *5*, 121-43.

51. Anthony, D.F.; Shiels, P.G., Exploiting paracrine mechanisms of tissue regeneration to repair damaged organs, *Transplantation Research* **2013**, *2*, 10-10.

52. Kay, A.G.; Long, G.; Tyler, G.; Stefan, A.; Broadfoot, S.J.; Piccinini, A.M.; Middleton, J.; Kehoe, O., Mesenchymal Stem Cell-Conditioned Medium Reduces Disease Severity and Immune Responses in Inflammatory Arthritis, *Scientific Reports* **2017**, *7*, 18019.

53. Chen, Y.; Tang, Y.; Long, W.; Zhang, C., Stem Cell-Released Microvesicles and Exosomes as Novel Biomarkers and Treatments of Diseases, *Stem Cells International* **2016**, *2016*, 2.

54. Aliotta, J.M.; Pereira, M.; Johnson, K.W.; de Paz, N.; Dooner, M.S.; Puente, N.; Ayala, C.; Brilliant, K.; Berz, D.; Lee, D.; Ramratnam, B.; McMillan, P.N.; Hixson, D.C.; Josic, D.; Quesenberry, P.J., Microvesicle entry into marrow cells mediates tissue-specific changes in mRNA by direct delivery of mRNA and induction of transcription, *Exp Hematol* **2010**, *38*, 233-45.

55. Trounson, A.; McDonald, C., Stem Cell Therapies in Clinical Trials: Progress and Challenges, *Cell Stem Cell 17*, 11-22.

56. Ito, K.; Frenette, P.S., HSC Contribution in Making Steady-State Blood, *Immunity* **2016**, *45*, 464-466.

57. Squillaro, T.; Peluso, G.; Galderisi, U., Clinical Trials With Mesenchymal Stem Cells: An Update, *Cell Transplant* **2016**, *25*, 829-48.

58. Wang, C.-H.; Huang, P.-H.; Chen, J.-W.; Lin, S.-J.; Lee, M.-F.; Yang, N.-I.; Cherng, W.-J., Clinical Application of Endothelial Progenitor Cell: Are We Ready?, *Acta Cardiologica Sinica* **2013**, *29*, 479-487.

59. Trounson, A.; McDonald, C., Stem Cell Therapies in Clinical Trials: Progress and Challenges, *Cell Stem Cell* **2015**, *17*, 11-22.

60. Zhang, J.; Huang, X.; Wang, H.; Liu, X.; Zhang, T.; Wang, Y.; Hu, D., The challenges and promises of allogeneic mesenchymal stem cells for use as a cell-based therapy, *Stem Cell Research & Therapy* **2015**, *6*, 234.

61. Baraniak, P.R.; McDevitt, T.C., Scaffold-free culture of mesenchymal stem cell spheroids in suspension preserves multilineage potential, *Cell and tissue research* **2012**, *347*, 701-711.

62. Sun, L.; Reagan, M.R.; Kaplan, D.L., Role of Cartilage Forming Cells in Regenerative Medicine for Cartilage Repair, *Orthopedic research and reviews* **2010**, *2010*, 85-94.

63. Chen, M.; Przyborowski, M.; Berthiaume, F., Stem Cells for Skin Tissue Engineering and Wound Healing, *Critical reviews in biomedical engineering* **2009**, *37*, 399-421.

64. Katari, R.; Peloso, A.; Orlando, G., Tissue Engineering and Regenerative Medicine: Semantic Considerations for an Evolving Paradigm, *Frontiers in Bioengineering and Biotechnology* **2014**, *2*, 57.

65. Lu, T.; Li, Y.; Chen, T., Techniques for fabrication and construction of three-dimensional scaffolds for tissue engineering, *International Journal of Nanomedicine* **2013**, *8*, 337-350.

66. Bryers, J.D.; Giachelli, C.M.; Ratner, B.D., Engineering Biomaterials to Integrate and Heal: The Biocompatibility Paradigm Shifts, *Biotechnology and bioengineering* **2012**, *109*, 1898-1911.

67. Ghasemi-Mobarakeh, L.; Prabhakaran, M.P.; Tian, L.; Shamirzaei-Jeshvaghani, E.; Dehghani, L.; Ramakrishna, S., Structural properties of scaffolds: Crucial parameters towards stem cells differentiation, *World Journal of Stem Cells* **2015**, *7*, 728-744.

68. Bružauskaitė, I.; Bironaitė, D.; Bagdonas, E.; Bernotienė, E., Scaffolds and cells for tissue regeneration: different scaffold pore sizes—different cell effects, *Cytotechnology* **2016**, *68*, 355-369.

69. O'Brien, F.J., Biomaterials & scaffolds for tissue engineering, *Materials Today* **2011**, *14*, 88-95.

70. López-Álvarez, M.; Rodríguez-Valencia, C.; Serra, J.; González, P., Bio-inspired Ceramics: Promising Scaffolds for Bone Tissue Engineering, *Procedia Engineering* **2013**, *59*, 51-58.

71. Amini, A.R.; Laurencin, C.T.; Nukavarapu, S.P., Bone Tissue Engineering: Recent Advances and Challenges, *Critical reviews in biomedical engineering* **2012**, *40*, 363-408.

72. Polymeric Scaffolds in Tissue Engineering Application: A Review, *International Journal of Polymer Science* **2011**, *2011*.

73. Thevenot, P.; Nair, A.; Shen, J.; Lotfi, P.; Ko, C.Y.; Tang, L., The Effect of Incorporation of SDF-1α into PLGA Scaffolds on Stem Cell Recruitment and the Inflammatory Response, *Biomaterials* **2010**, *31*, 3997-4008.

74. Hajian, H.; Wise, S.G.; Bax, D.V.; Kondyurin, A.; Waterhouse, A.; Dunn, L.L.; Kielty, C.M.; Yu, Y.; Weiss, A.S.; Bilek, M.M.M.; Bannon, P.G.; Ng, M.K.C., Immobilisation of a fibrillin-1 fragment enhances the biocompatibility of PTFE, *Colloids and Surfaces B: Biointerfaces* **2014**, *116*, 544-552.

75. Felding-Habermann, B.; Cheresh, D.A., Vitronectin and its receptors, *Curr Opin Cell Biol* **1993**, *5*, 864-8.

76. Gomes, M.; Azevedo, H.; Malafaya, P.; Silva, S.; Oliveira, J.; Silva, G.; João Mano, R.S.; Reis, R., 16 - Natural Polymers in Tissue Engineering Applications, in: S. Ebnesajjad (Ed.), Handbook of Biopolymers and Biodegradable Plastics, William Andrew Publishing, Boston, 2013, pp. 385-425.

77. Dang, J.M.; Leong, K.W., Natural polymers for gene delivery and tissue engineering, *Advanced Drug Delivery Reviews* **2006**, *58*, 487-499.

78. Kim, P.-H.; Cho, J.-Y., Myocardial tissue engineering using electrospun nanofiber composites, *BMB Reports* **2016**, *49*, 26-36.

79. Glicklis, R.; Shapiro, L.; Agbaria, R.; Merchuk, J.C.; Cohen, S., Hepatocyte behavior within three-dimensional porous alginate scaffolds, *Biotechnol Bioeng* **2000**, *67*, 344-53.

80. Szymańska, E.; Winnicka, K., Stability of Chitosan—A Challenge for Pharmaceutical and Biomedical Applications, *Marine Drugs* **2015**, *13*, 1819-1846.

81. Gloria, A.; De Santis, R.; Ambrosio, L., Polymer-based Composite Scaffolds for Tissue Engineering, *Journal of Applied Biomaterials and Biomechanics* **2010**, *8*, 57-67.

82. Fu, W.; Liu, Z.; Feng, B.; Hu, R.; He, X.; Wang, H.; Yin, M.; Huang, H.; Zhang, H.; Wang, W., Electrospun gelatin/PCL and collagen/PLCL scaffolds for vascular tissue engineering, *International Journal of Nanomedicine* **2014**, *9*, 2335-2344.

83. Turco, G.; Marsich, E.; Bellomo, F.; Semeraro, S.; Donati, I.; Brun, F.; Grandolfo, M.; Accardo, A.; Paoletti, S., Alginate/Hydroxyapatite Biocomposite For Bone Ingrowth: A Trabecular Structure With High And Isotropic Connectivity, *Biomacromolecules* **2009**, *10*, 1575-1583.

84. Brodbeck, W.G.; Shive, M.S.; Colton, E.; Nakayama, Y.; Matsuda, T.; Anderson, J.M., Influence of biomaterial surface chemistry on the apoptosis of adherent cells, *J Biomed Mater Res* **2001**, *55*, 661-8.

85. Vashist, S.K., Comparison of 1-Ethyl-3-(3-Dimethylaminopropyl) Carbodiimide Based Strategies to Crosslink Antibodies on Amine-Functionalized Platforms for Immunodiagnostic Applications, *Diagnostics* **2012**, *2*, 23-33.

86. Neves-Petersen, M.T.; Snabe, T.; Klitgaard, S.; Duroux, M.; Petersen, S.B., Photonic activation of disulfide bridges achieves oriented protein immobilization on biosensor surfaces, *Protein Sci* **2006**, *15*, 343-51.

87. Bilek, M.M.M., Biofunctionalization of surfaces by energetic ion implantation: Review of progress on applications in implantable biomedical devices and antibody microarrays, *Applied Surface Science* **2014**, *310*, 3-10.

88. Pathi, P.; Ma, T.; Locke Bruce, R., Role of nutrient supply on cell growth in bioreactor design for tissue engineering of hematopoietic cells, *Biotechnology and Bioengineering* **2005**, *89*, 743-758.

89. Yamamoto, M.; Ikada, Y.; Tabata, Y., Controlled release of growth factors based on biodegradation of gelatin hydrogel, *Journal of Biomaterials Science, Polymer Edition* **2001**, *12*, 77-88.

90. Kohane Daniel, S., Microparticles and nanoparticles for drug delivery, *Biotechnology and Bioengineering* **2006**, *96*, 203-209.

91. Aoki, J.; Serruys, P.W.; van Beusekom, H.; Ong, A.T.; McFadden, E.P.; Sianos, G.; van der Giessen, W.J.; Regar, E.; de Feyter, P.J.; Davis, H.R.; Rowland, S.; Kutryk, M.J., Endothelial progenitor cell capture by stents coated with antibody against CD34: the HEALING-FIM (Healthy Endothelial Accelerated Lining Inhibits Neointimal Growth-First In Man) Registry, *J Am Coll Cardiol* **2005**, *45*, 1574-9.

92. Braghirolli, D.I.; Steffens, D.; Pranke, P., Electrospinning for regenerative medicine: a review of the main topics, *Drug Discovery Today* **2014**, *19*, 743-753.

93. Haider, A.; Haider, S.; Kang, I.-K., A comprehensive review summarizing the effect of electrospinning parameters and potential applications of nanofibers in biomedical and biotechnology, *Arabian Journal of Chemistry* **2015**.

94. Fong, H.; Chun, I.; Reneker, D.H., Beaded nanofibers formed during electrospinning, *Polymer* **1999**, *40*, 4585-4592.

95. Oyama, H.T.T.; Cortella, L.R.X.; Rosa, I.N.S.; Filho, L.E.R.; Hui, W.S.; Cestari, I.N.; Cestari, I.A., Assessment of the Biocompatibility of the PLLA-PLCL Scaffold Obtained by Electrospinning, *Procedia Engineering* **2015**, *110*, 135-142.

96. Wang, S.-D.; Ma, Q.; Wang, K.; Chen, H.-W., Improving Antibacterial Activity and Biocompatibility of Bioinspired Electrospinning Silk Fibroin Nanofibers Modified by Graphene Oxide, *ACS Omega* **2018**, *3*, 406-413.

97. Rodríguez, K.; Gatenholm, P.; Renneckar, S., Electrospinning cellulosic nanofibers for biomedical applications: structure and in vitro biocompatibility, *Cellulose* **2012**, *19*, 1583-1598.

98. Horner, C.B.; Low, K.; Nam, J., 10 - Electrospun scaffolds for cartilage regeneration A2 - Liu, Huinan, Nanocomposites for Musculoskeletal Tissue Regeneration, Woodhead Publishing, Oxford, 2016, pp. 213-240.

99. Norouzi, M.; Boroujeni, S.M.; Omidvarkordshouli, N.; Soleimani, M., Advances in skin regeneration: application of electrospun scaffolds, *Adv Healthc Mater* **2015**, *4*, 1114-33.

100. Punnakitikashem, P.; Truong, D.; Menon, J.U.; Nguyen, K.T.; Hong, Y., Electrospun biodegradable elastic polyurethane scaffolds with dipyridamole release for small diameter vascular grafts, *Acta Biomaterialia* **2014**, *10*, 4618-4628.

101. Kitsara, M.; Joanne, P.; Boitard, S.E.; Ben Dhiab, I.; Poinard, B.; Menasché, P.; Gagnieu, C.; Forest, P.; Agbulut, O.; Chen, Y., Fabrication of cardiac patch by using electrospun collagen fibers, *Microelectronic Engineering* **2015**, *144*, 46-50.

102. Ena, B.-L.; Cristina, M.-R.; Manuel, M.-P.; Wilberth, H.-K.; Juan, V.C.-R.; José, M.C.-U., Electrospun polycaprolactone/chitosan scaffolds for nerve tissue engineering: physicochemical characterization and Schwann cell biocompatibility, *Biomedical Materials* **2017**, *12*, 015008.

103. Cipitria, A.; Skelton, A.; Dargaville, T.R.; Dalton, P.D.; Hutmacher, D.W., Design, fabrication and characterization of PCL electrospun scaffolds-a review, *Journal of Materials Chemistry* **2011**, *21*, 9419-9453.

104. Qi, C.; Yan, X.; Huang, C.; Melerzanov, A.; Du, Y., Biomaterials as carrier, barrier and reactor for cell-based regenerative medicine, *Protein & Cell* **2015**, *6*, 638-653.

105. Villalona, G.A.; Udelsman, B.; Duncan, D.R.; McGillicuddy, E.; Sawh-Martinez, R.F.; Hibino, N.; Painter, C.; Mirensky, T.; Erickson, B.; Shinoka, T.; Breuer, C.K., Cell-Seeding Techniques in Vascular Tissue Engineering, *Tissue Engineering. Part B, Reviews* **2010**, *16*, 341-350.

106. Jabbarzadeh, E.; Starnes, T.; Khan, Y.M.; Jiang, T.; Wirtel, A.J.; Deng, M.; Lv, Q.; Nair, L.S.; Doty, S.B.; Laurencin, C.T., Induction of angiogenesis in tissue-engineered scaffolds designed for bone repair: A combined gene therapy–cell transplantation approach, *Proceedings of the National Academy of Sciences of the United States of America* **2008**, *105*, 11099-11104.

107. Li, X.; Dai, Y.; Shen, T.; Gao, C., Induced migration of endothelial cells into 3D scaffolds by chemoattractants secreted by pro-inflammatory macrophages in situ, *Regenerative Biomaterials* **2017**, *4*, 139-148.

108. Anderson, J.M.; Rodriguez, A.; Chang, D.T., FOREIGN BODY REACTION TO BIOMATERIALS, *Seminars in immunology* **2008**, *20*, 86-100.

109. Yu, T.; Tutwiler, V.J.; Spiller, K., The Role of Macrophages in the Foreign Body Response to Implanted Biomaterials, in: L. Santambrogio (Ed.), Biomaterials in Regenerative Medicine and the Immune System, Springer International Publishing, Cham, 2015, pp. 17-34.

110. Wang, Y.; Vaddiraju, S.; Gu, B.; Papadimitrakopoulos, F.; Burgess, D.J., Foreign Body Reaction to Implantable Biosensors: Effects of Tissue Trauma and Implant Size, *Journal of Diabetes Science and Technology* **2015**, *9*, 966-977.

111. Martinez, F.O.; Gordon, S., The M1 and M2 paradigm of macrophage activation: time for reassessment, *F1000Prime Reports* **2014**, *6*, 13.

112. Martinez, F.O.; Sica, A.; Mantovani, A.; Locati, M., Macrophage activation and polarization, Frontiers in bioscience : a journal and virtual library, 2008, pp. 453-461.

113. Rodrigues, C.A.V.; Fernandes, T.G.; Diogo, M.M.; da Silva, C.L.; Cabral, J.M.S., Stem cell cultivation in bioreactors, *Biotechnology Advances* **2011**, *29*, 815-829.

114. Turinetto, V.; Vitale, E.; Giachino, C., Senescence in Human Mesenchymal Stem Cells: Functional Changes and Implications in Stem Cell-Based Therapy, *International Journal of Molecular Sciences* **2016**, *17*, 1164.

115. Tuğba İnanç, H.; Belibağlı, K.B., Production of electrospun gelatin nanofibers: an optimization study by using Taguchi's methodology, *Materials Research Express* **2017**, *4*, 015023.

116. Bulte, J.W.M., In Vivo MRI Cell Tracking: Clinical Studies, *AJR. American journal of roentgenology* **2009**, *193*, 314-325.

117. MacAskill, M.G.; Tavares, A.S.; Wu, J.; Lucatelli, C.; Mountford, J.C.; Baker, A.H.; Newby, D.E.; Hadoke, P.W.F., PET Cell Tracking Using 18F-FLT is Not Limited by Local Reuptake of Free Radiotracer, *Scientific Reports* **2017**, *7*, 44233.

118. Malide, D., In Vivo Cell Tracking Using Two-Photon Microscopy, *Methods Mol Biol* **2016**, *1444*, 109-22.

119. Youn, H.; Hong, K.-J., In vivo Noninvasive Small Animal Molecular Imaging, *Osong Public Health and Research Perspectives* **2012**, *3*, 48-59.

120. Lee, A.S.; Inayathullah, M.; Lijkwan, M.A.; Zhao, X.; Sun, W.; Park, S.; Hong, W.X.; Parekh, M.B.; Malkovskiy, A.V.; Lau, E.; Qin, X.; Pothineni, V.R.; Sanchez-Freire, V.; Zhang, W.Y.; Kooreman, N.G.; Ebert, A.D.; Chan, C.K.F.; Nguyen, P.K.; Rajadas, J.; Wu, J.C., Prolonged survival of transplanted stem cells after ischaemic injury via the slow release of pro-survival peptides from a collagen matrix, *Nature Biomedical Engineering* **2018**, *2*, 104-113.

121. Liu, H.; Wise, S.G.; Rnjak-Kovacina, J.; Kaplan, D.L.; Bilek, M.M.; Weiss, A.S.; Fei, J.; Bao, S., Biocompatibility of silk-tropoelastin protein polymers, *Biomaterials* **2014**, *35*, 5138-47.